Sediment transport
& beach morphodynamics

Institut des Mathématiques pour la Planète Terre

November 25th 2021

Julien CHAUCHAT

Associate Professor
Grenoble Institute of Technology
LEGI - ENSE3
Grenoble, France

PARCOURS

2018	Habilitation à diriger des recherches in Environmental Science
2015-2016	Sabbatical at University of Delaware (USA) - Prof. Tom HSU
2009-pres.	Associate Professor GINP ENSE3/LEGI
2008-2009	Postdoc at IUSTI Aix-Marseille University
2003-2007	PhD at University of Caen-Basse Normandie
2001-2002	High-School teacher - Nobody is perfect ;-)
2000-2001	Master 2 at Ecole Centrale de Nantes - Naval Hydrodynamics and Ocean Engineering

Mechanical engineering

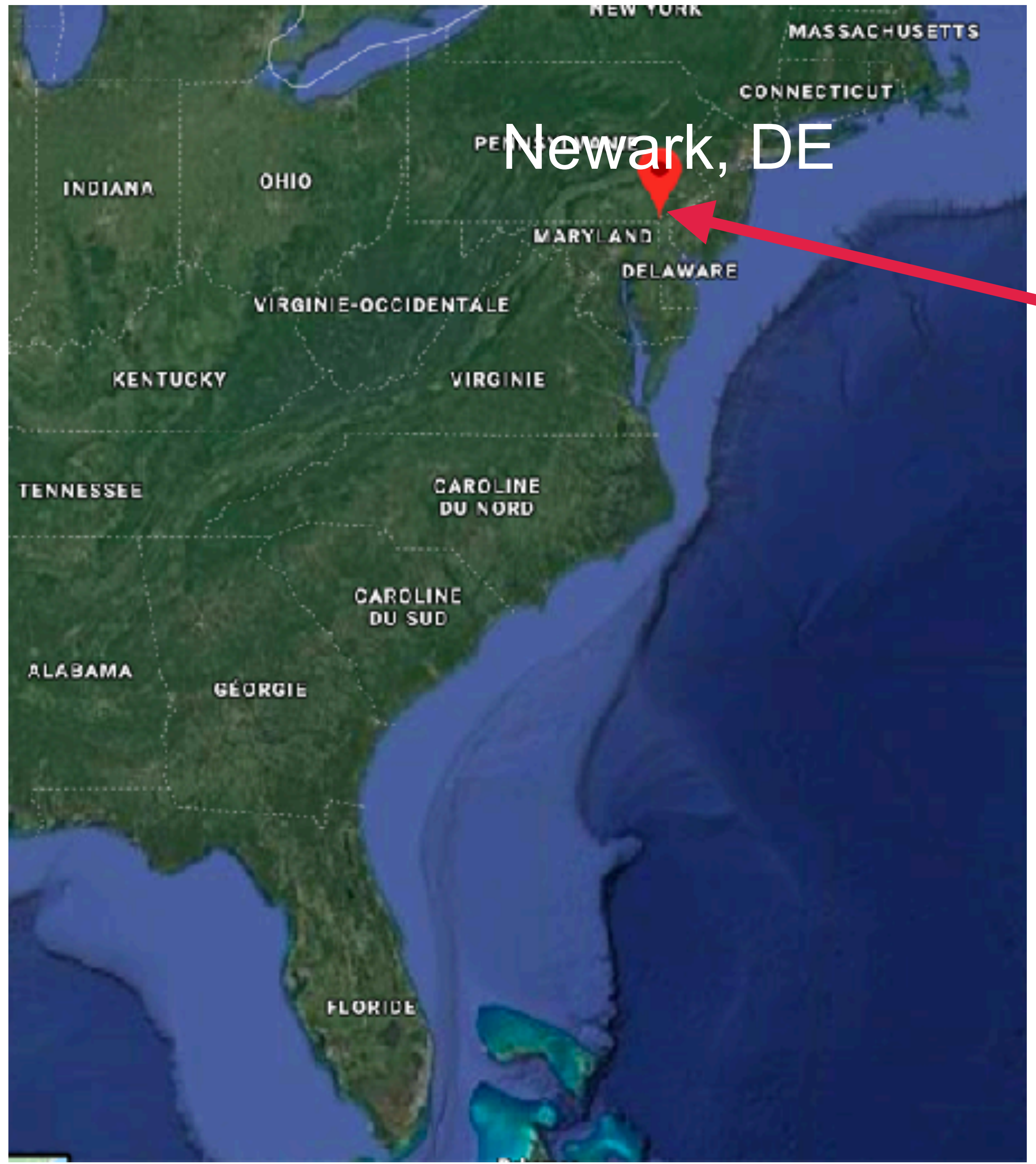

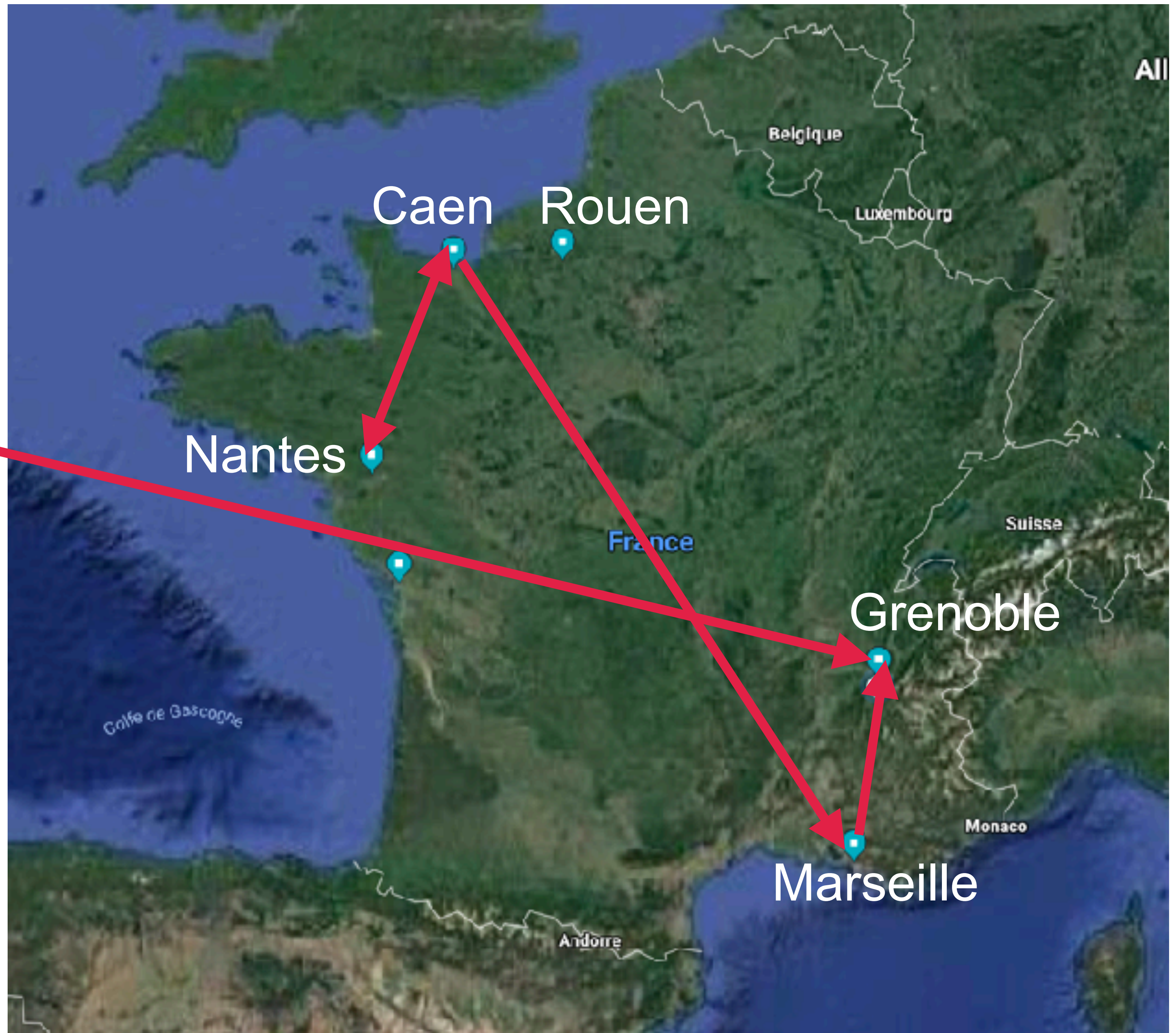

LEGI: Geophysical and Industrial Flows Lab

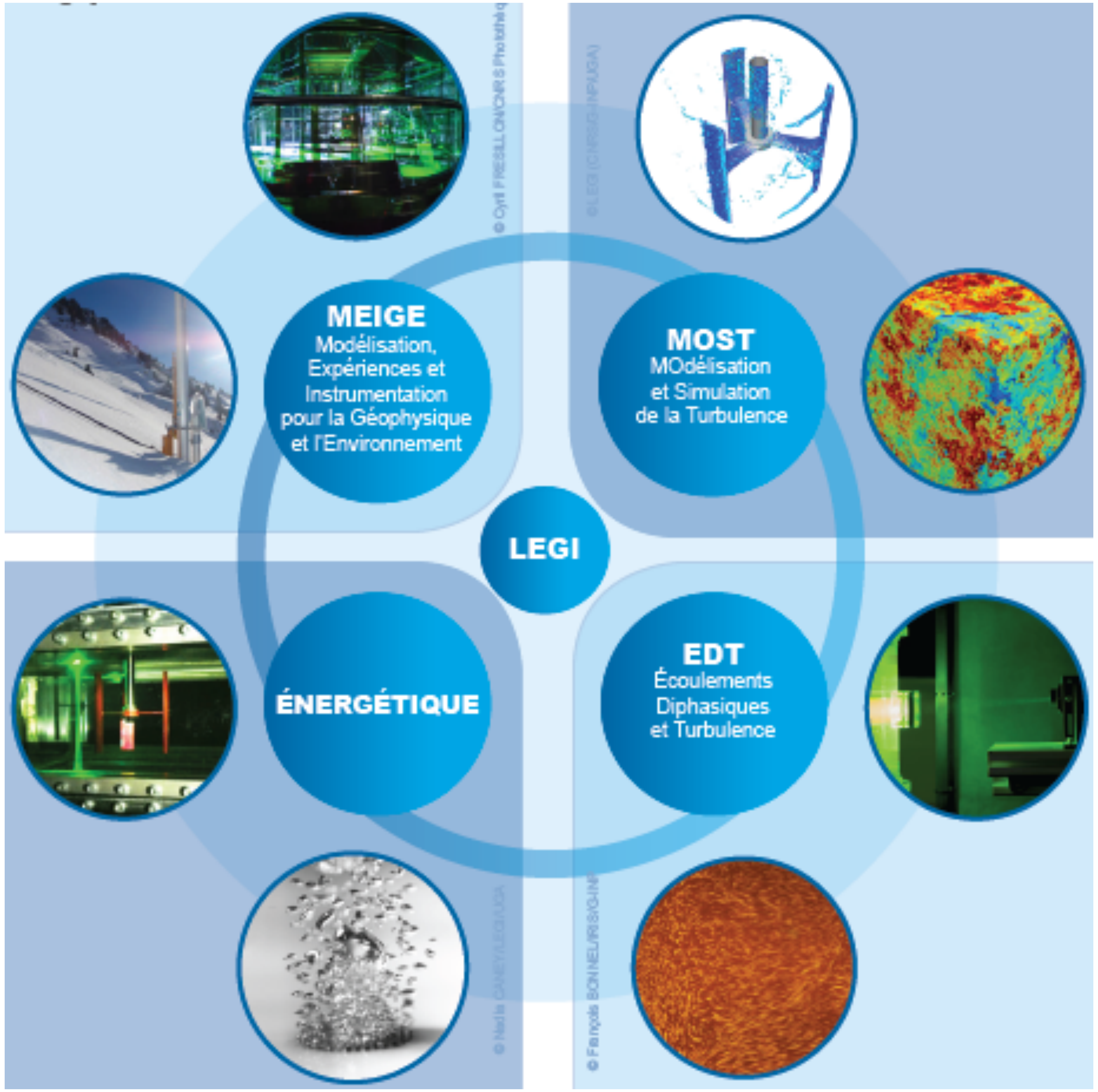

Human Ressources ≈ 110 people

Permanent staff ~ 40 people
PhD & Postdocs ~ 50 people

CORIOLIS platform

The largest rotating hydraulic basin in the world

D = 13m ; m=350T

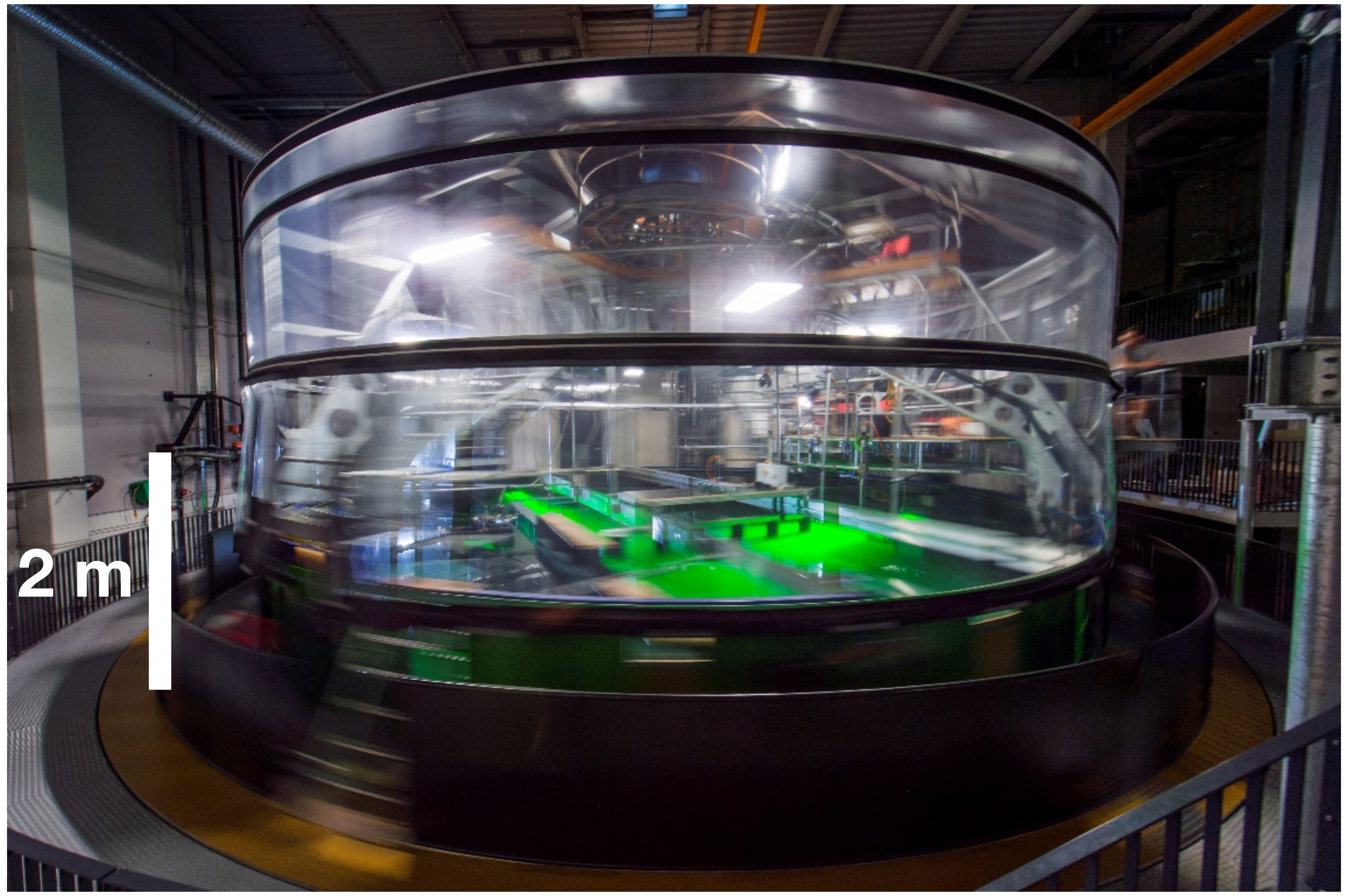

Collaborations

- **LEGI, Grenoble:** T. Revil-Baudard, T. Nagel, A. Mathieu, H. Shafiei, D. Hurther, C. Bonamy, G. Fromant, A. Wirth, G. Balarac, E. Barthélémy, H. Michallet, J.-M. Barnoud, S. Mercier, P.-A. Barraud
- **INRAE, Grenoble:** G. Richard, P. Frey, *R. Chassagne, H. Rousseau*
- **3S-R, Grenoble:** B. Chareyre, D. Marzougui
- **IMFT, Toulouse:** R. Maurin
- **LEGOS, Toulouse:** P. Marchesiello
- **SHOM, Brest:** T. Garlan
- **ARTELIA Group, Grenoble:** O. Bertrand
- **IUSTI, Marseille:** M. Médale, P. Aussillous, E. Guazzelli, M. Paihla, Y. Forterre, O. Pouliquen
- **University of Delaware, USA:** T.-J. Hsu, Z. Cheng, Y. Kim, J. Puleo, R. Mieras
- **NRL:** J. Calantoni
- **KIT, Germany:** O. Eiff, Y. Akutina
- **Pennsylvania State Univ., USA:** X. Liu

Motivations

Soulac-sur-mer, France (source: twitter, L. Theillet Sud-Ouest)

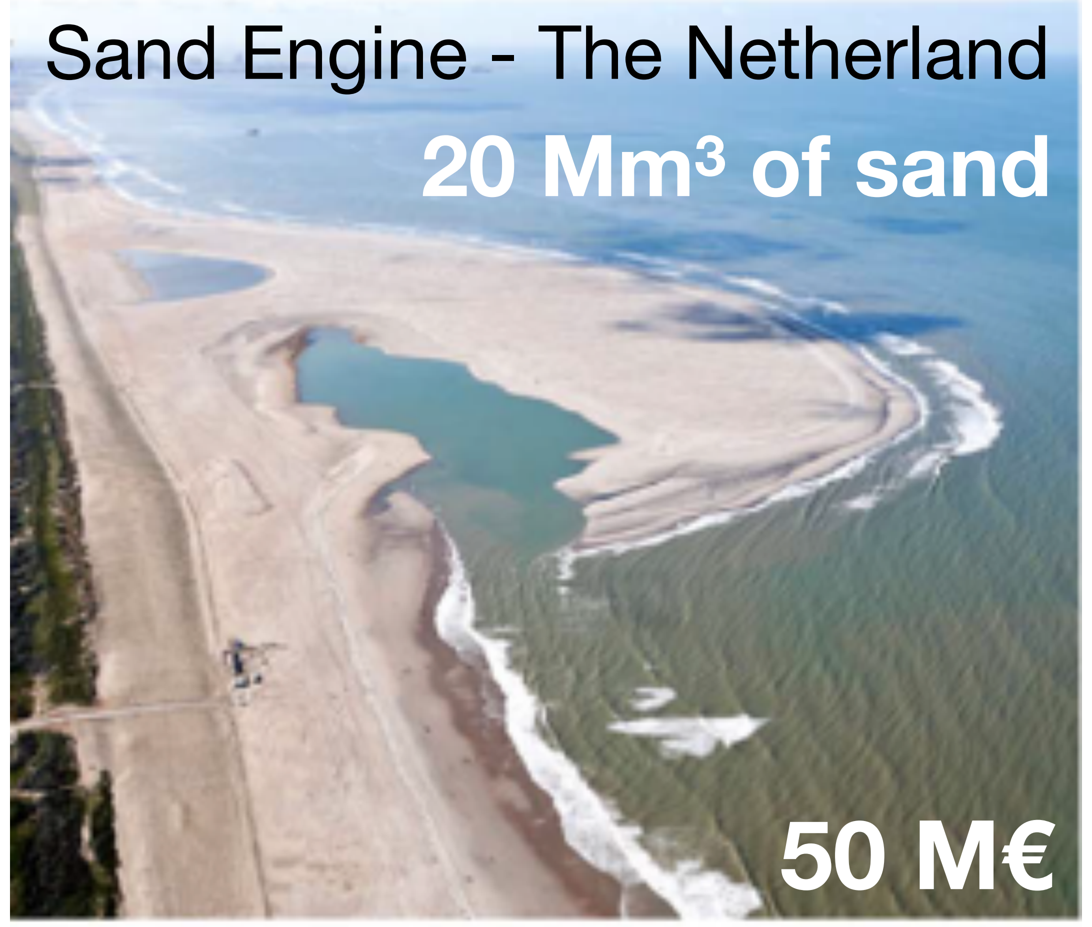

Observation after 1 year **Prediction after 1 year**

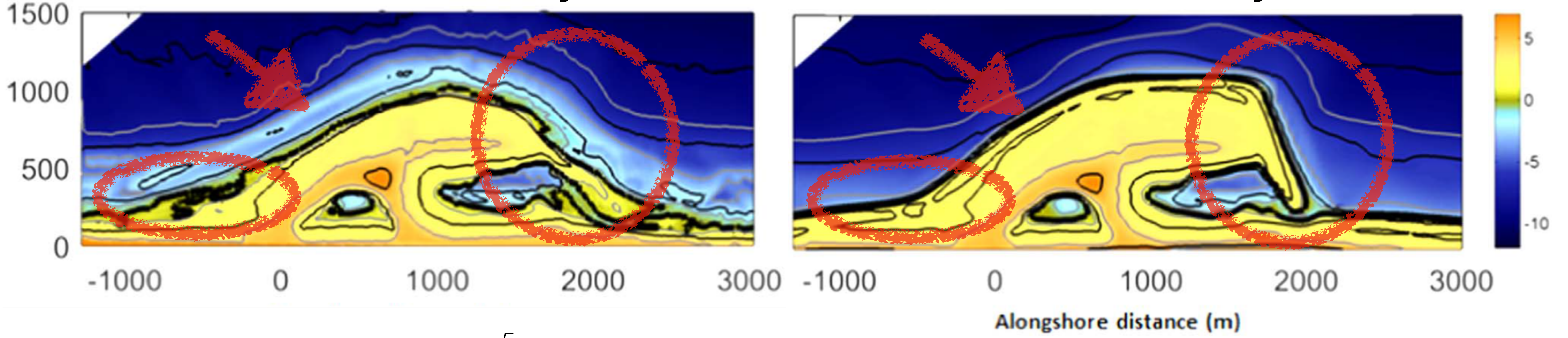

Luijendijk et al. CE (2017)

Motivations

At the European scale

1. 20% of European coasts are in erosion - 15 km² / year
2. Sandy beaches are mostly in erosion
3. Coastal marshes are mostly in accretion

Majority of European coasts are at moderate to high risk of erosion

The focus of this lecture is on sandy beaches

Tendances	Types géomorphologiques					
	Côtes rocheuses		Plages		Rivages limono-vaseux	
	%	km	%	km	%	km
Engraissement	NS	34	10,4	232	48,6	119
Stabilité	64,4	1216	45,8	1022	35,1	86
Erosion	23	436	41,4	924	11,8	29
Pas de données	10,6	200	2,3	52	4,5	11
Total	**100**	**1886**	**100**	**2230**	**100**	**245**

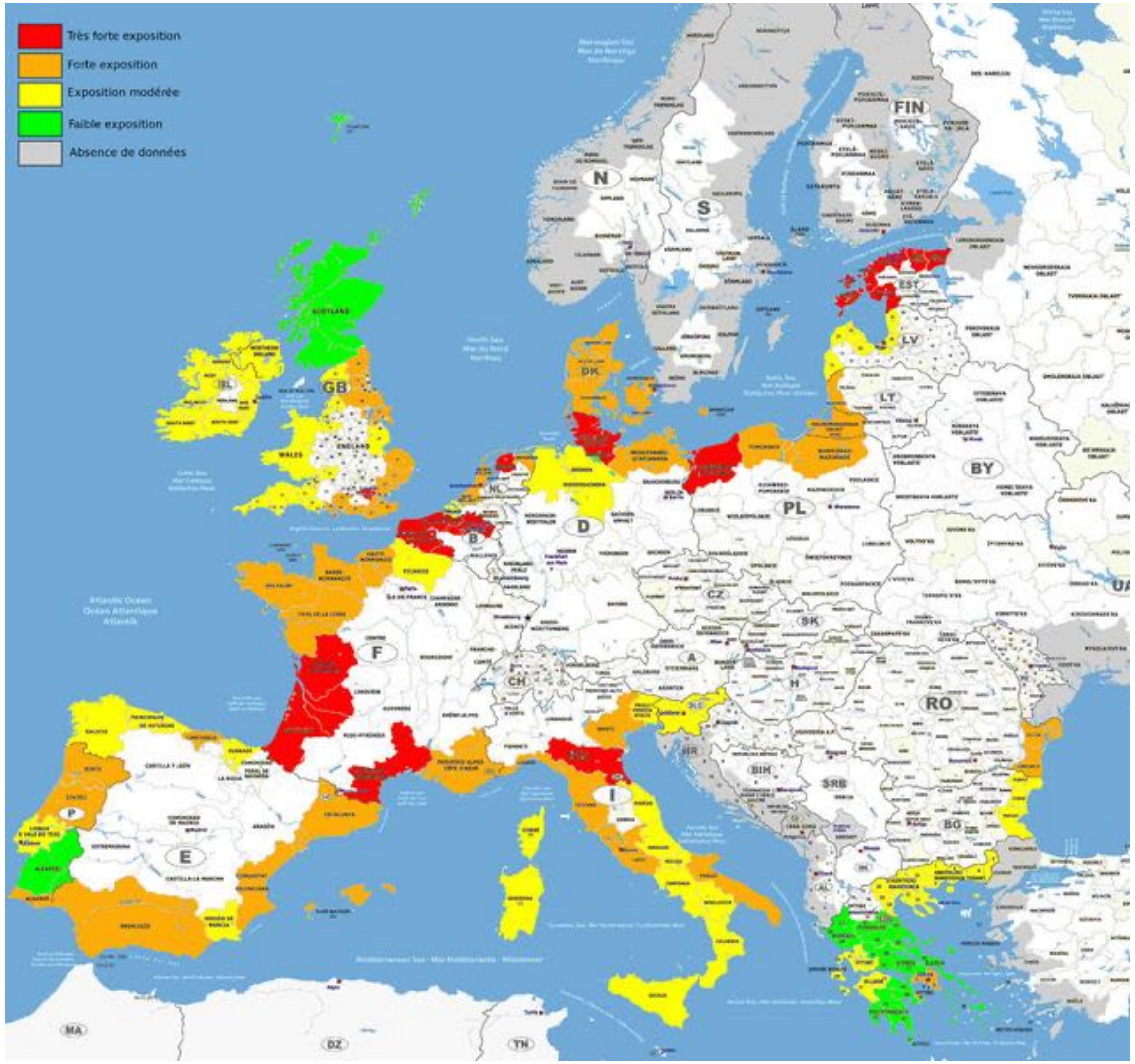

Le climat de la France au XXIè siècle - Volume 3 - Evolution du niveau de la mer - février 2012

Philosophy of this lecture

In coastal morphydynamics there are mainly 2 approaches:

◉ Reductionism: Process-based modeling

« Reductionism is the modeling methodology whereby the development and behavior of large (pattern)-scale features are reduced entirely to their underlying fundamental processes. »

Werner (2015)

◉ Universality: Reduced-complexity modeling

« Universality is the modeling methodology whereby the overall characteristics of behaviors and patterns are modeled with the simplest system within a class of systems sharing these same behaviors and characteristics, despite being composed of very different building blocks »

Werner (2015)

In what follows, I present you my personal vision of coastal erosion which rely on process-based modeling

and not reduced-complexity modeling

Morphodynamics: a multi-scale problem

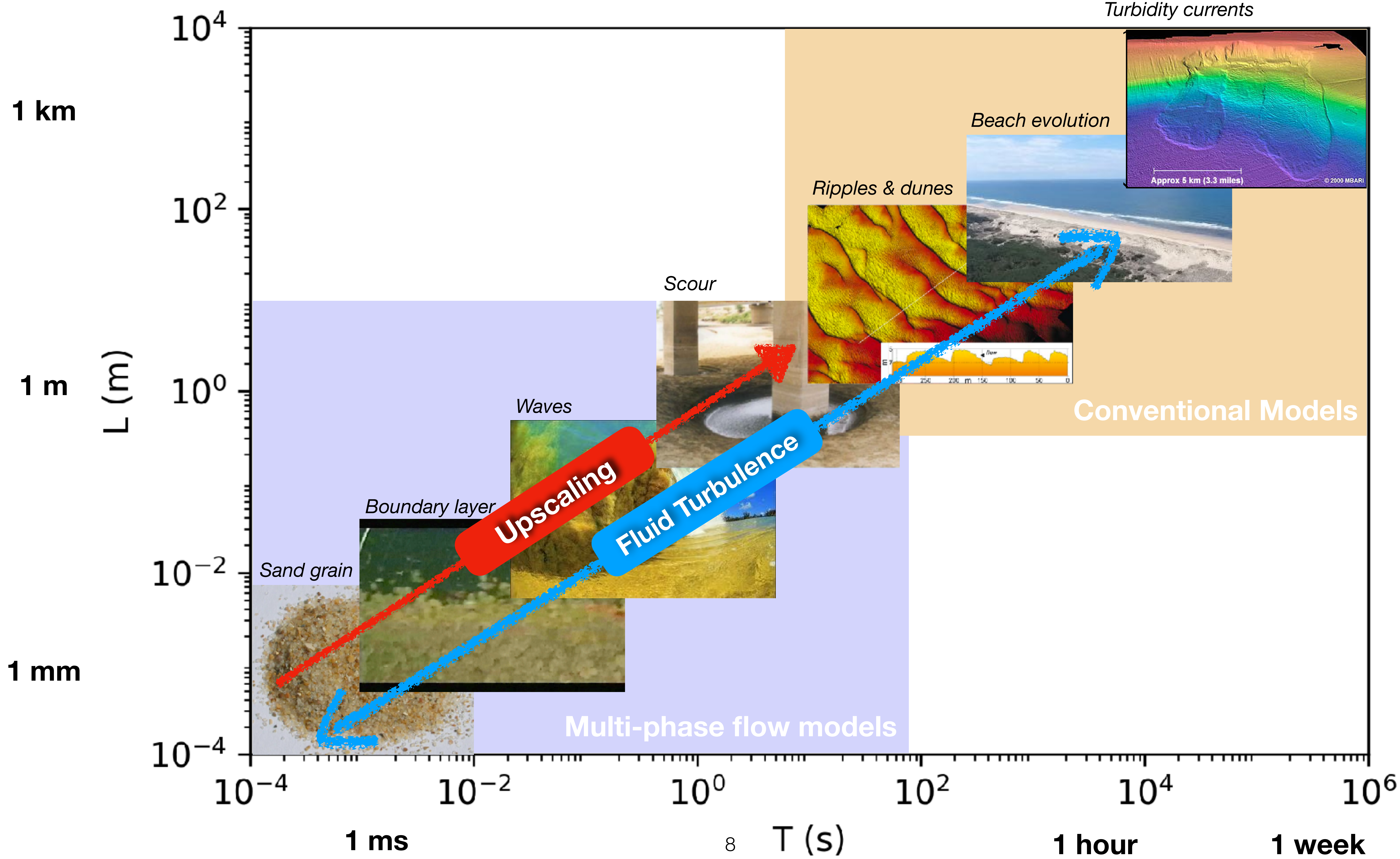

Outline

1. Coastal modeling at « large scale »

2. Sediment transport modeling at the grain scale : turbulent and granular processes

3. Upscaling of fine-scale processes at intermediate scales

Outline

1. Coastal modeling at « large scale »

2. Sediment transport modeling at the grain scale : turbulent and granular processes

3. Upscaling of fine-scale processes at intermediate scales

Wave energy spectrum in the ocean

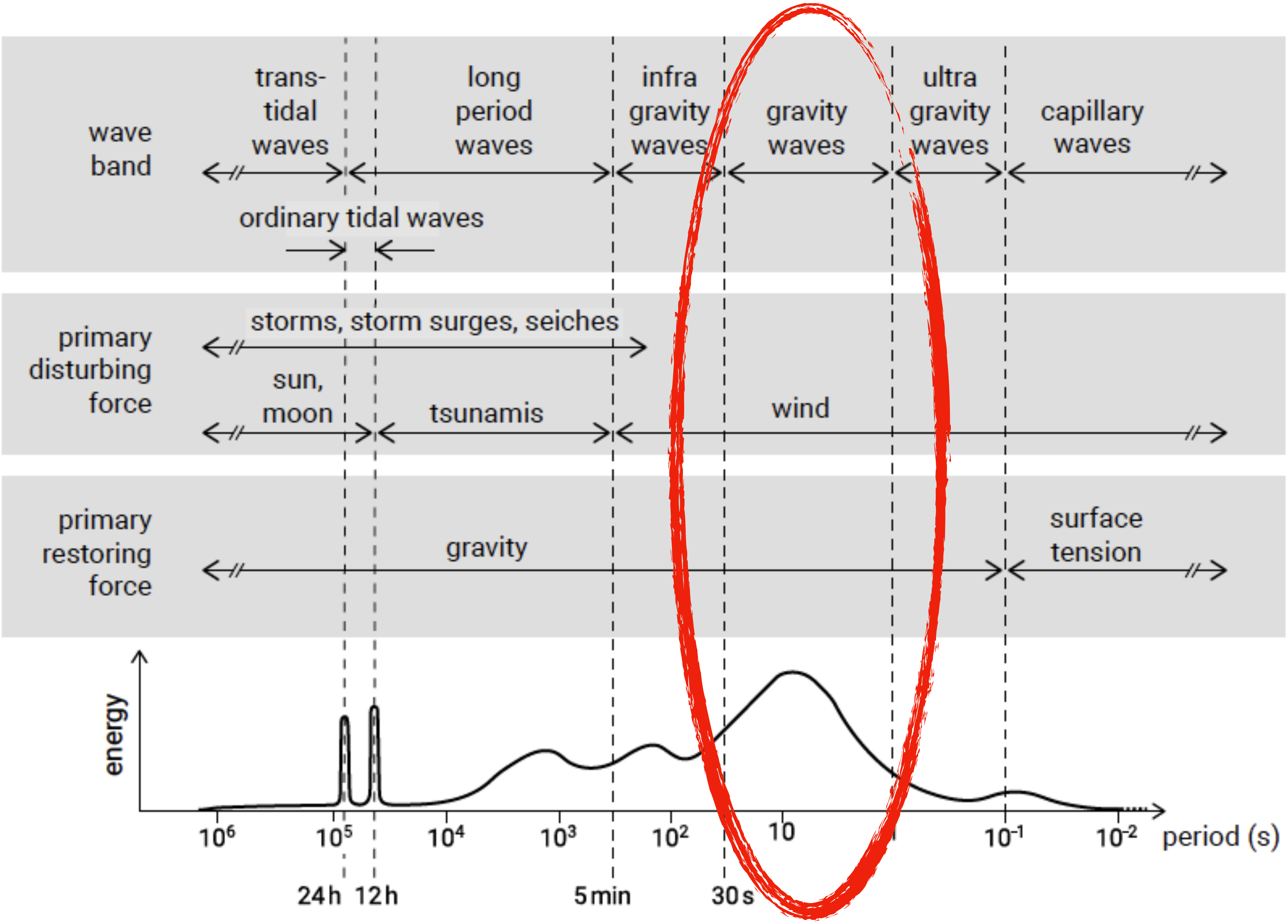

Figure 3.2: Sketch of the relative amounts of energy as a function of wave period in ocean waves. The top line gives the classification based on wavelength, the line below the classification based on the wave-generating force, and the bottom line the classification based on the restoring force. After Munk (1950) and Kinsman (1965).

Bosboom & Stive (2020)

Stokes wave model

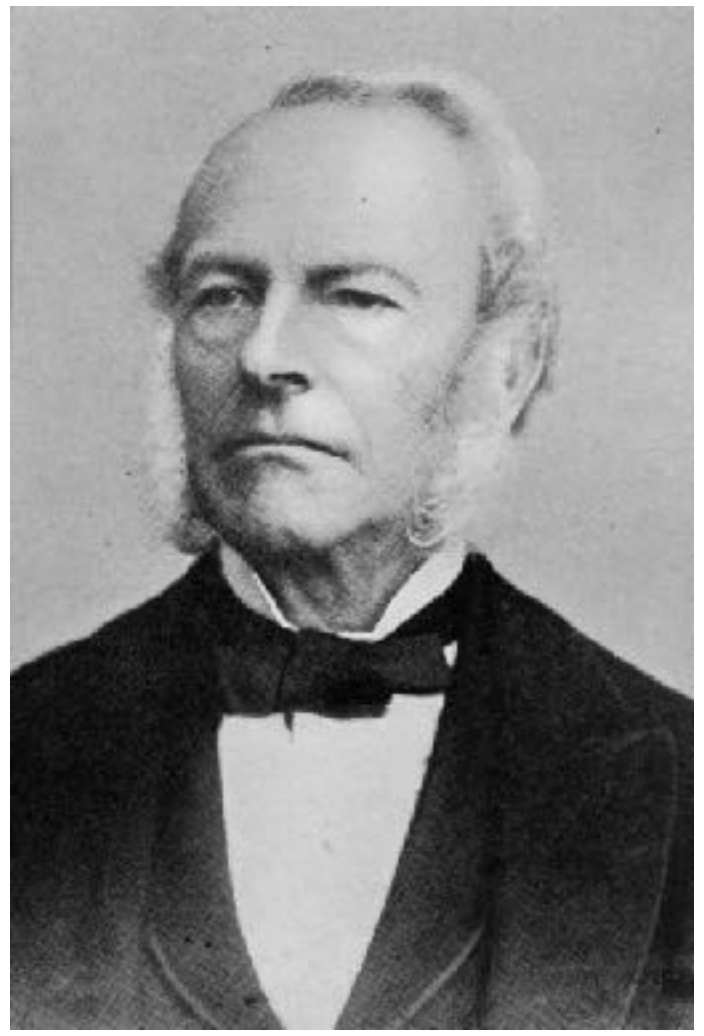

Sir G. Stokes (1819-1903)

For a perfect irrotational fluid flow, a velocity potential ϕ exists such that

$$\vec{u} = \vec{\nabla} \phi$$

and the Navier-Stokes equations reduces to:

$$\Delta\phi(x, z, t) = 0, \quad \forall (x, z) \in \mathbb{R}^2, \forall t \in \mathbb{R}^+$$

$$\frac{\partial \phi}{\partial t} + \frac{(\nabla \phi)^2}{2} + \frac{p}{\rho} + gz = C(t)$$

Asymptotic expansion in wave steepness: $\epsilon = \dfrac{H}{L}$:

$$\phi(x, z, t) = \phi_0 + \epsilon \ \phi_1(x, z, t) + \epsilon^2 \ \phi_2(x, z, t) + \epsilon^3 \ \phi_3(x, z, t) + \ldots$$

$$\eta(x, t) = \eta_0 + \epsilon \ \eta_1(x, t) + \epsilon^2 \ \eta_2(x, t) + \epsilon^3 \ \eta_3(x, t) + \ldots$$

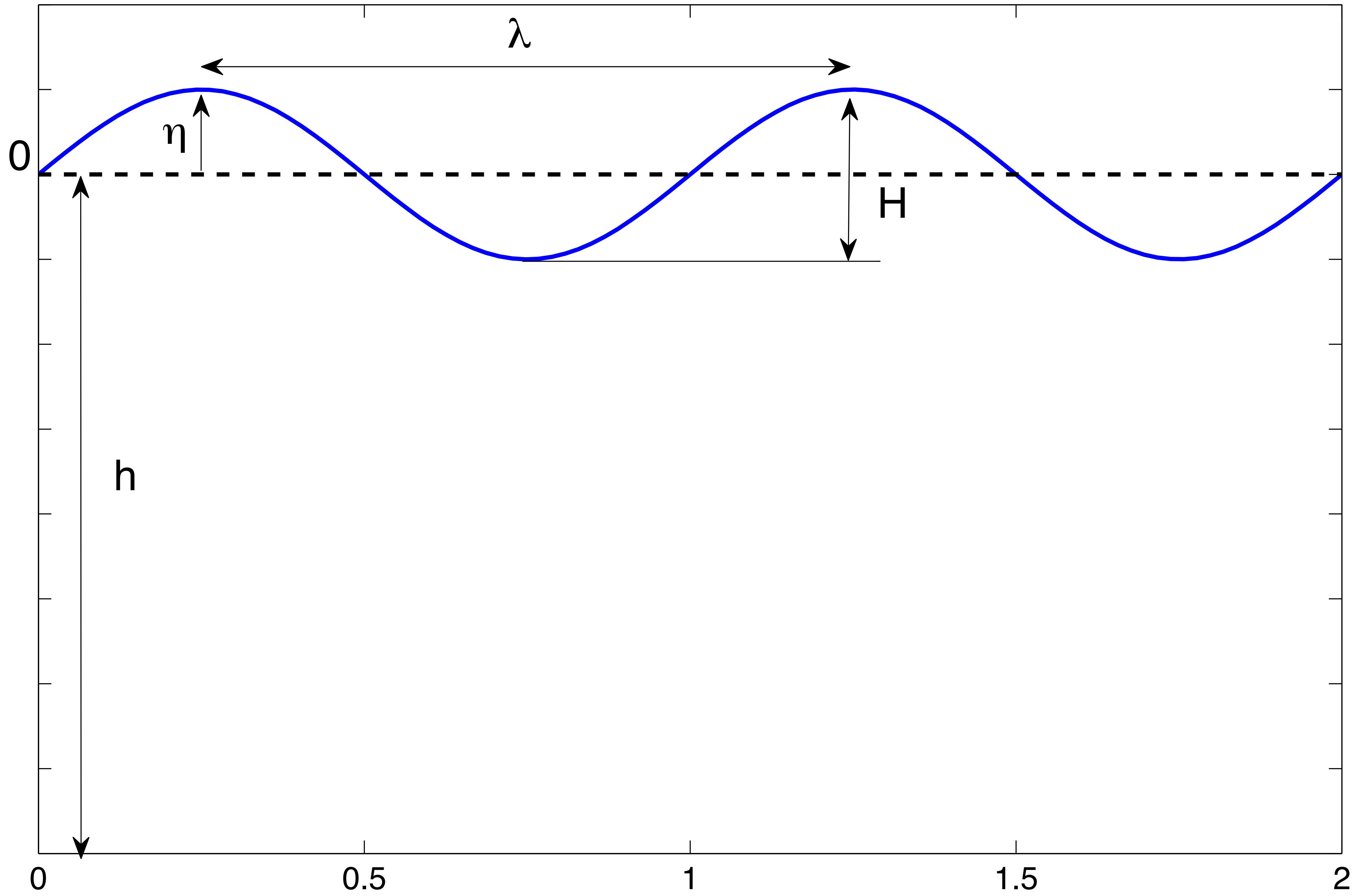

Stokes (1847)

More advanced lecture by G. Richard tomorrow

Stokes wave model: linear theory

First order solution:

- Potential: $\phi(x,z,t) = \dfrac{a\ g}{\omega}\dfrac{\cosh(k(z+h))}{\cosh(kh)}\cos(kx-\omega t)$
- Free surface: $\eta_1 = a\sin(kx-\omega t)$
- Dispersion relation: $\omega^2 = g\ k\tanh(kh)$

Also known as Airy wave theory

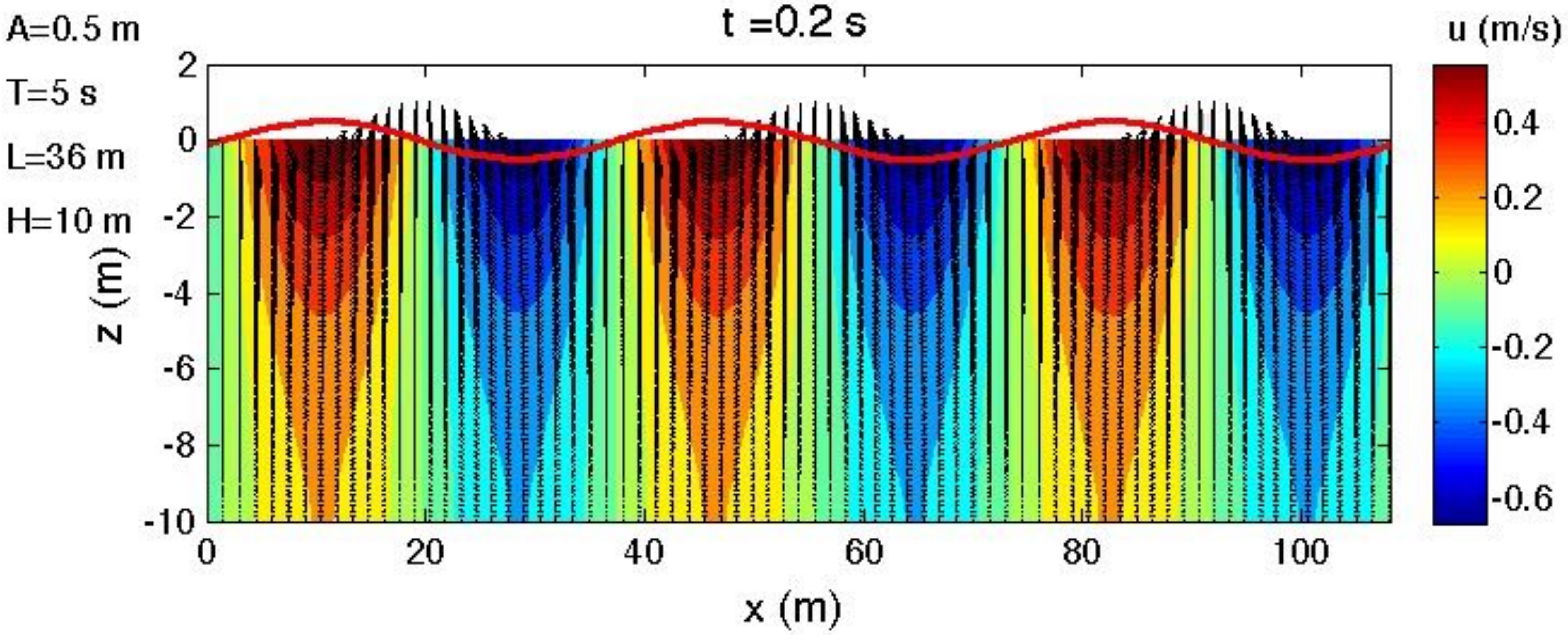

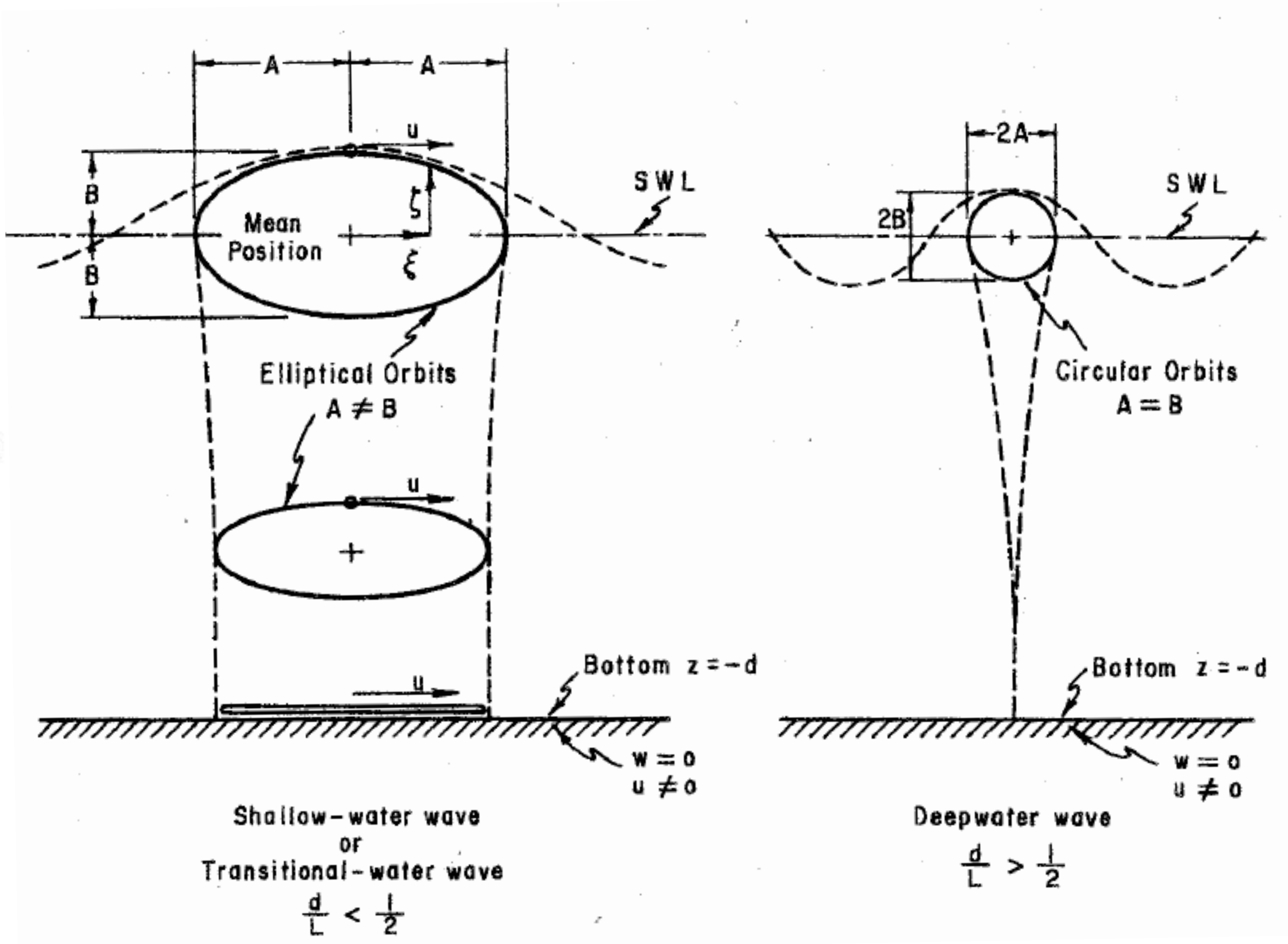

Shallow water **Deep water**

Closed trajectories of « fluid particles » implies no mass flux (first order model)

Stokes (1847)

Stokes wave model: limits of the linear theory

Linear theory valid for

- Small steepness: $\epsilon = \dfrac{H}{L} << 1$
- Large relative depth: $\dfrac{h}{L} >> 1$

Limit of the linear theory is given by the Ursell number:

$$U_r = \frac{H}{L}\left(\frac{L}{h}\right)^3 \propto \frac{\phi_2}{\phi_1} << 1$$

Not very relevant for beach morphodynamics

but still very useful

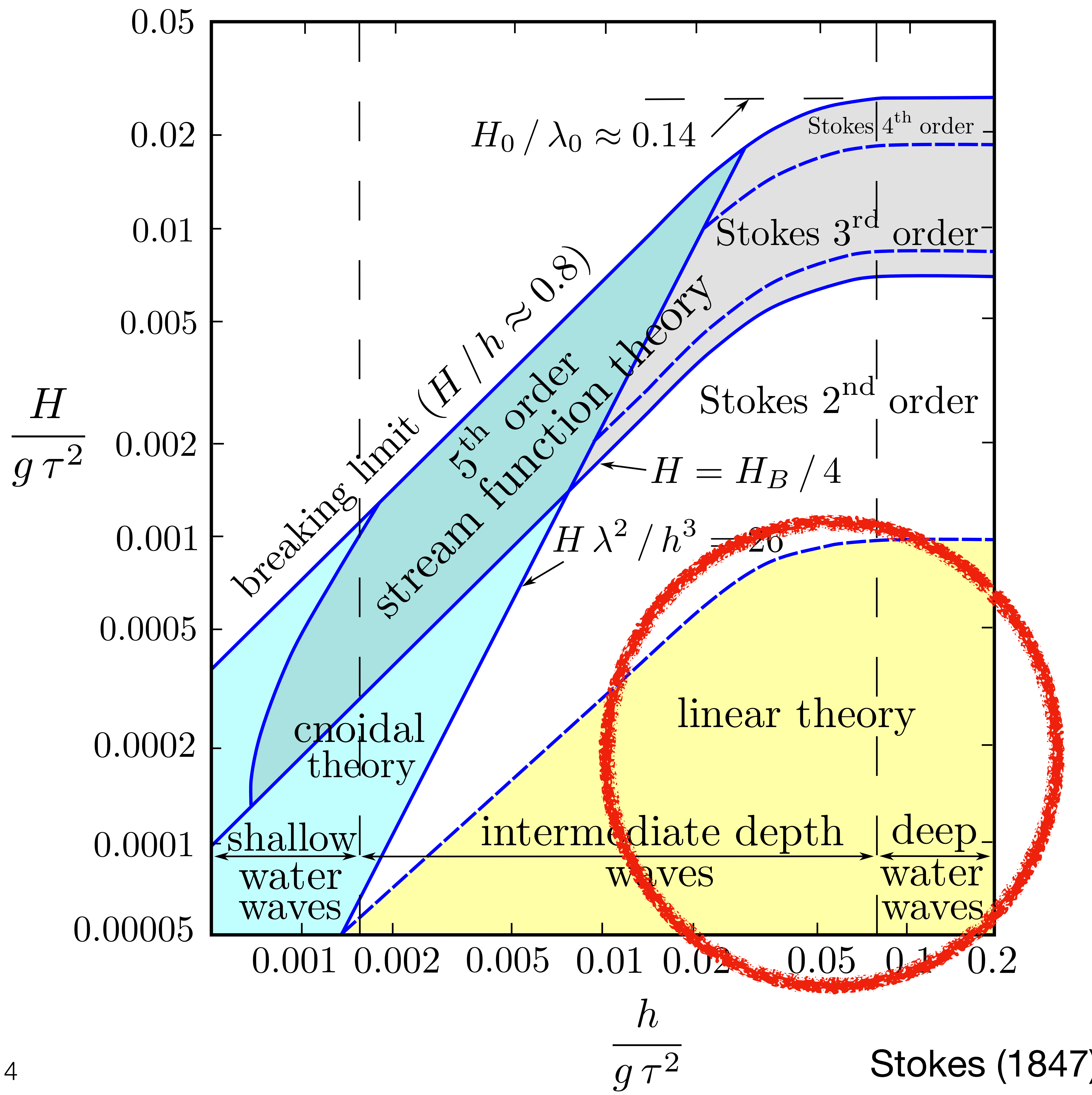

Stokes (1847)

Stokes wave model: non-linear effects

2nd order velocity potential:

$$\phi_2(x,z,t) = -\frac{3}{8}\frac{a^2\ \omega}{sinh^4(kh)}\ \frac{cosh(2\ k(z+h))}{cosh(kh)}\cos[2\ (kx-\omega t)] + \ldots$$

$$\eta_2(x,z,t) = \frac{a^2\ k}{4}(cotanh^3(kh) - cotanh(kh))\ cos[2\ (kx-\omega t)] + \ldots$$

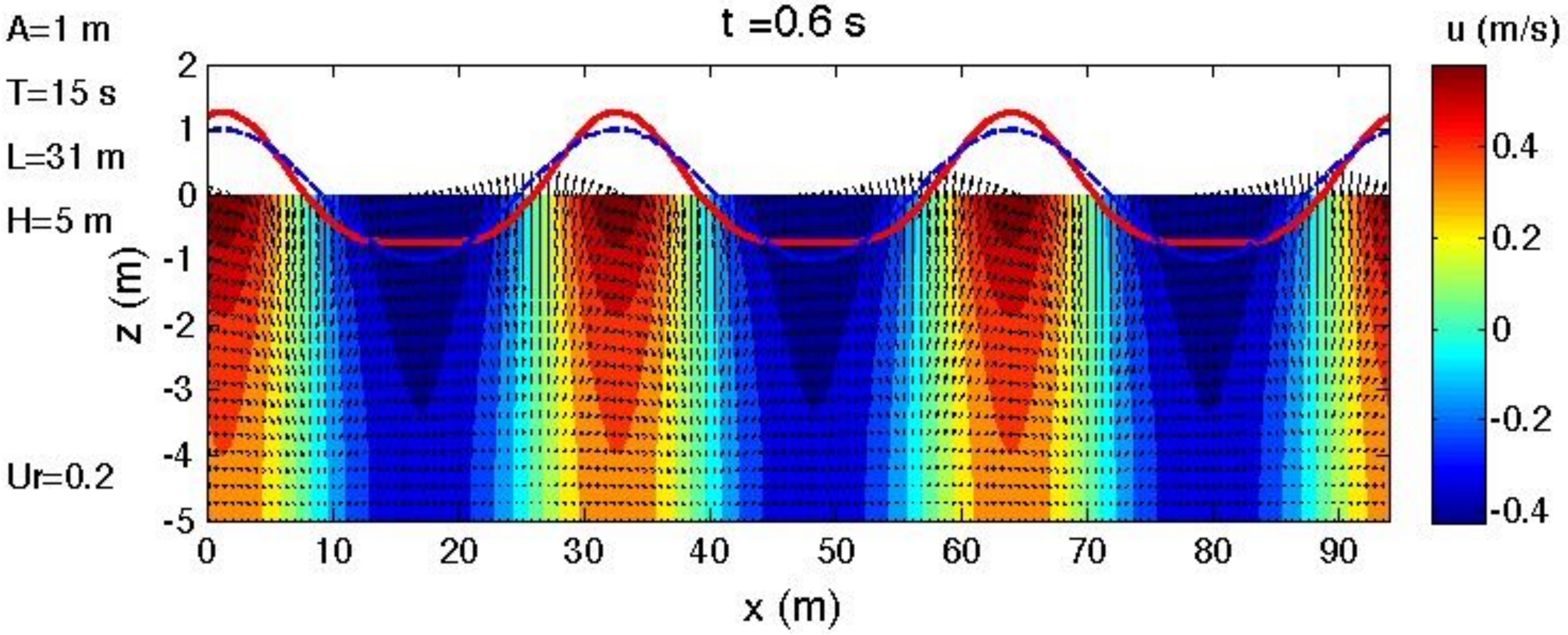

- Non-linear waves are velocity skewed: peak crest velocity is larger than trough velocity
- Mean water level is not zero
- Non-closed trajectories of « fluid particles » implies mass flux toward the coast = Stokes drift

Stokes (1847)

Stokes wave model: Wave energy

Total wave energy: $E_w = E_P + E_C$

- Potential energy contained in one wavelength: *associated with wave motion*

$$E_P = \frac{1}{L}\int_0^L \int_0^\eta \rho g \ z dz \ dx = \frac{1}{L}\int_0^L \frac{1}{2}\rho g \ \eta^2 dx = \frac{1}{L}\int_0^L \frac{1}{2}\rho g \ a^2 \ sin^2(kx)dx = \frac{1}{4}\rho \ g \ a^2$$

- Kinetic energy contained in one wavelength:

$$E_C = \frac{1}{L}\int_0^L \int_{-h}^\eta \frac{1}{2}\rho \left(u^2 + w^2\right) dz \ dx = \frac{1}{L}\int_0^L \int_{-h}^0 \frac{1}{2}\rho \left(u^2 + w^2\right) dz \ dx + o(\epsilon) = \frac{1}{4}\rho \ g \ a^2$$

- Equipartition between potential and kinetic energy: $E_C = E_P$

Total energy : $E_w = \frac{1}{2}\rho \ g \ a^2 = \frac{1}{8}\rho \ g \ H^2$

Wave height: $H = 2a$

- Wave power: $P = E_w \ C_g$ with group celerity: $C_g = \frac{C}{2}\left(1 + \frac{2kh}{\sinh(2kh)}\right)$

Stokes wave model: wave groups

Superposition of 2 linear solutions: bi-chromatic waves

- 2 wave frequency: ω_1 and ω_2 ($\omega_1 \approx \omega_2$)
- If $\exists(n;m) \in \mathbb{N}^2$ such that $\omega_g = n\omega_1 = m\omega_2$
  Then smallest value of ω_g = wave group frequency

- Free surface elevation:

$$\eta^T = A_1 \left(sin(k_1 x - \omega_1 t) + sin(k_2 x - \omega_2 t) \right)$$

$$\eta^T = A_1 \ 2 \ \sin\left(\frac{(k_1 + k_2)x - (\omega_1 + \omega_2)t}{2}\right) \cos\left(\frac{(k_1 - k_2)x - (\omega_1 - \omega_2)t}{2}\right)$$

with $\omega_1 - \omega_2 << \omega_1 + \omega_2$

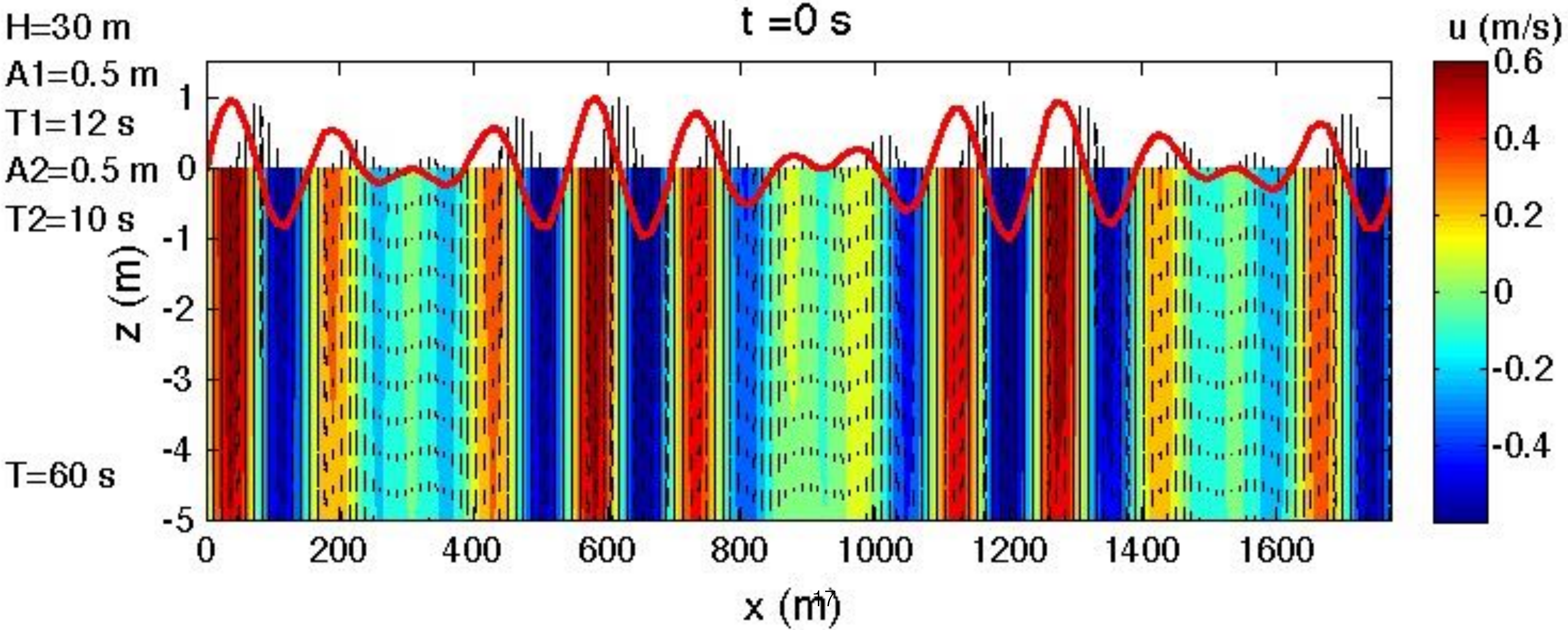

Stokes wave model: wave groups

Credits: Nate Lawrence

https://www.surfline.com/surf-news/city-surf-changing-lives-san-francisco/41874

Irregular waves modeling

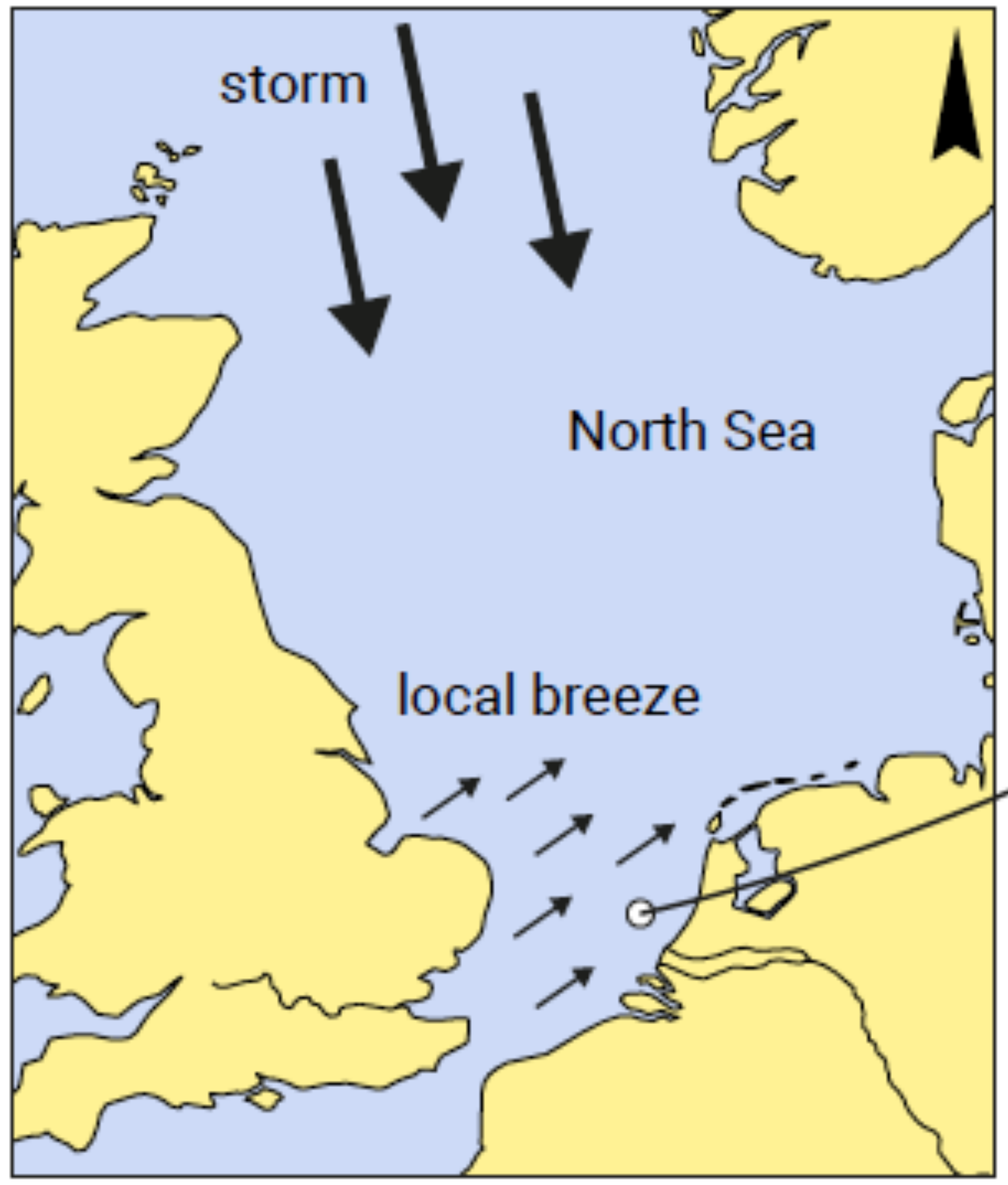

2 peaks in the spectrum one for the swell and one for the wind-sea

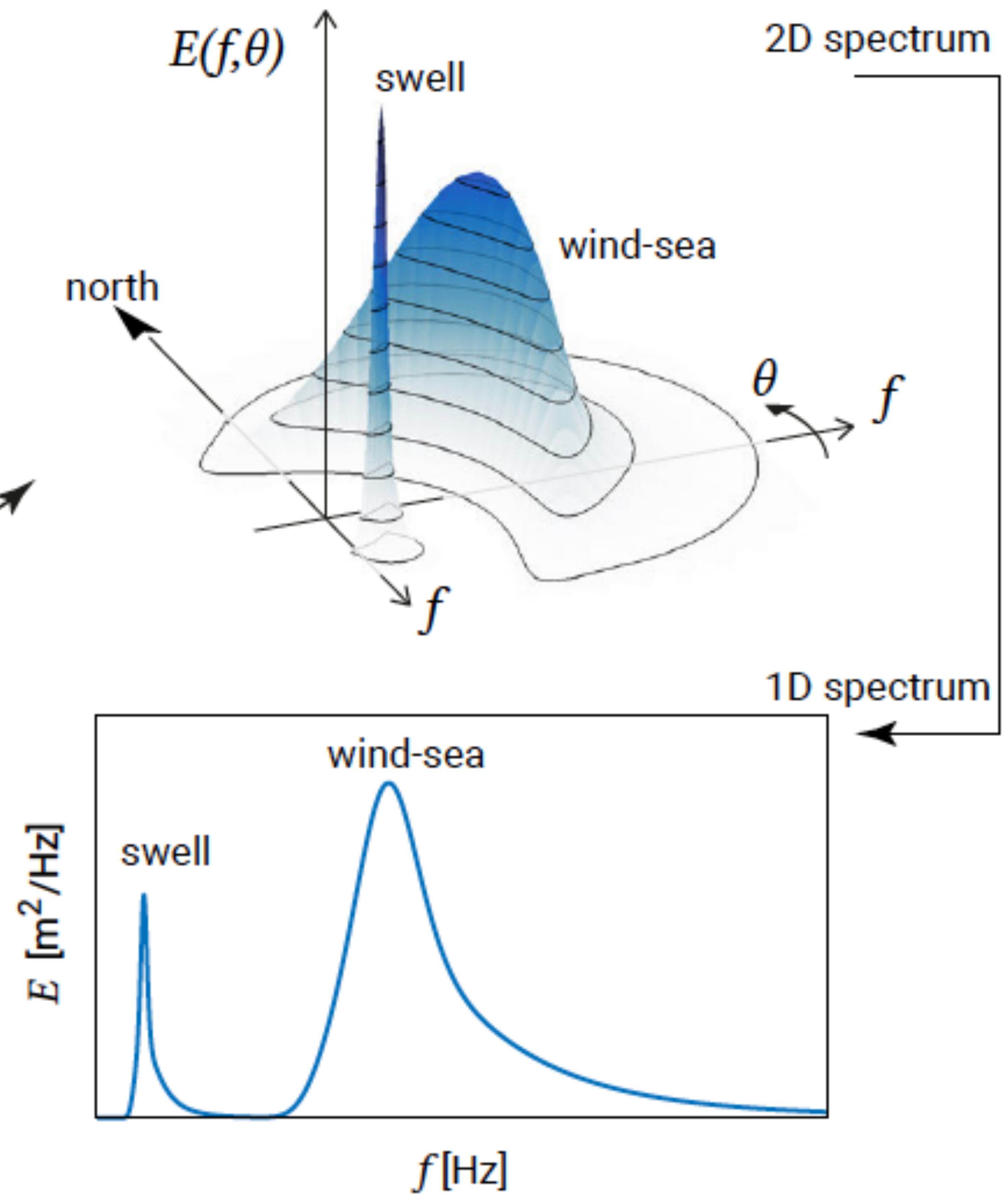

Wave Spectrum: $E_w = \rho g \int_0^{\infty} \int_{-\pi}^{\pi} E(f,\theta)\ d\theta\ df$

Significant wave height: $H_s \approx 4\sqrt{\dfrac{E_w}{\rho g}}$

Wave spectrum depends on frequency & direction

$$E(f) = \frac{\alpha\ g^2}{(2\pi)^4\ f^5}\ e^{-1.25\left(\frac{f_m}{f}\right)^4}\ \gamma^{exp(-(f-f_m)^2/2\ (\sigma\ f_m)^2)}$$

JONSWAP (Hasselman et al., 1973) : North Sea

Bosboom & Stive (2020)

Irregular waves modeling

Transport equation for wave action spectral density:

$$\frac{\partial N}{\partial t} + \frac{\partial c_{gx} N}{\partial x} + \frac{\partial c_{gy} N}{\partial y} + \frac{\partial c_{\theta} N}{\partial \theta} + \frac{\partial c_{\omega} N}{\partial \omega_r} = \frac{S_{in} + S_d + S_{nl}}{\omega_r}$$

Large number of DoF per node: $N_\theta \times N_\omega$

Community models: WW3 (USA), SWAN (Dutch), TOMAWAC (French)

with $N(\omega_r, \theta) = \dfrac{E(\omega_r, \theta)}{\omega_r}$ $\qquad \omega_r = 2\pi f$

S_{in} : wind

S_d : wave breaking and bottom friction

S_{nl} : non-linear wave interactions

Data predicted by Fleet Numerical Meteorology and Oceanography Center (FNMOC) for now

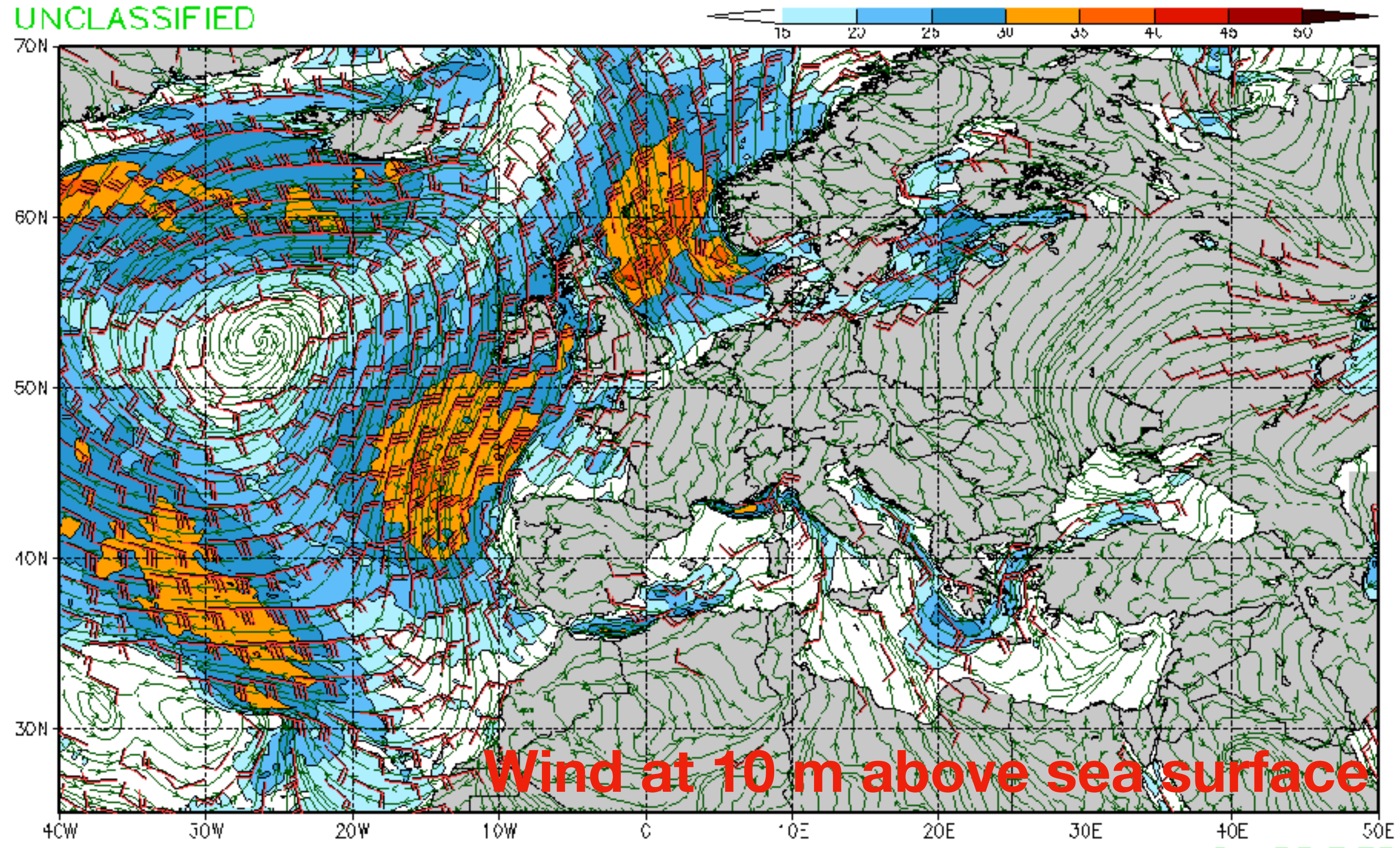

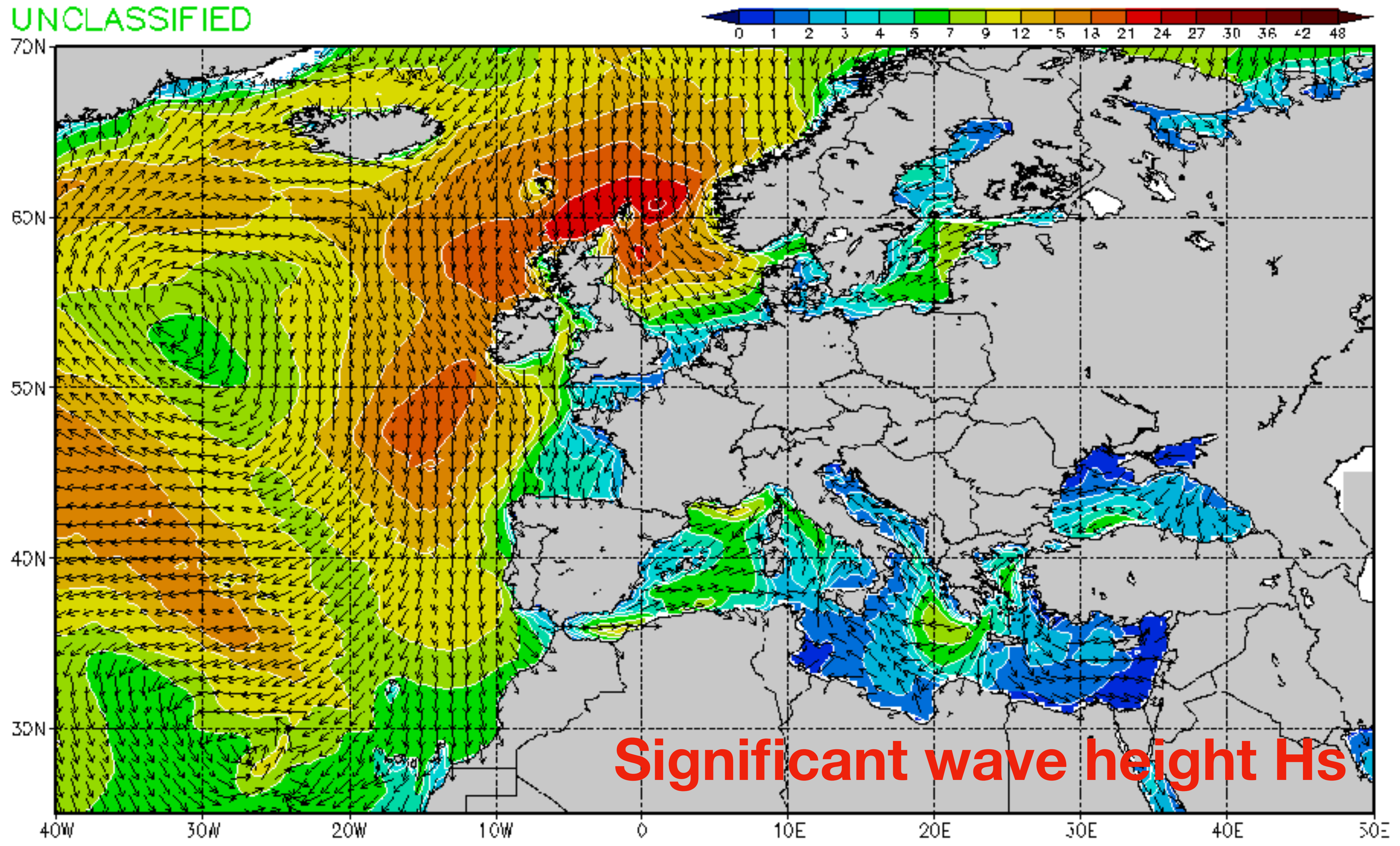

Irregular waves nearshore

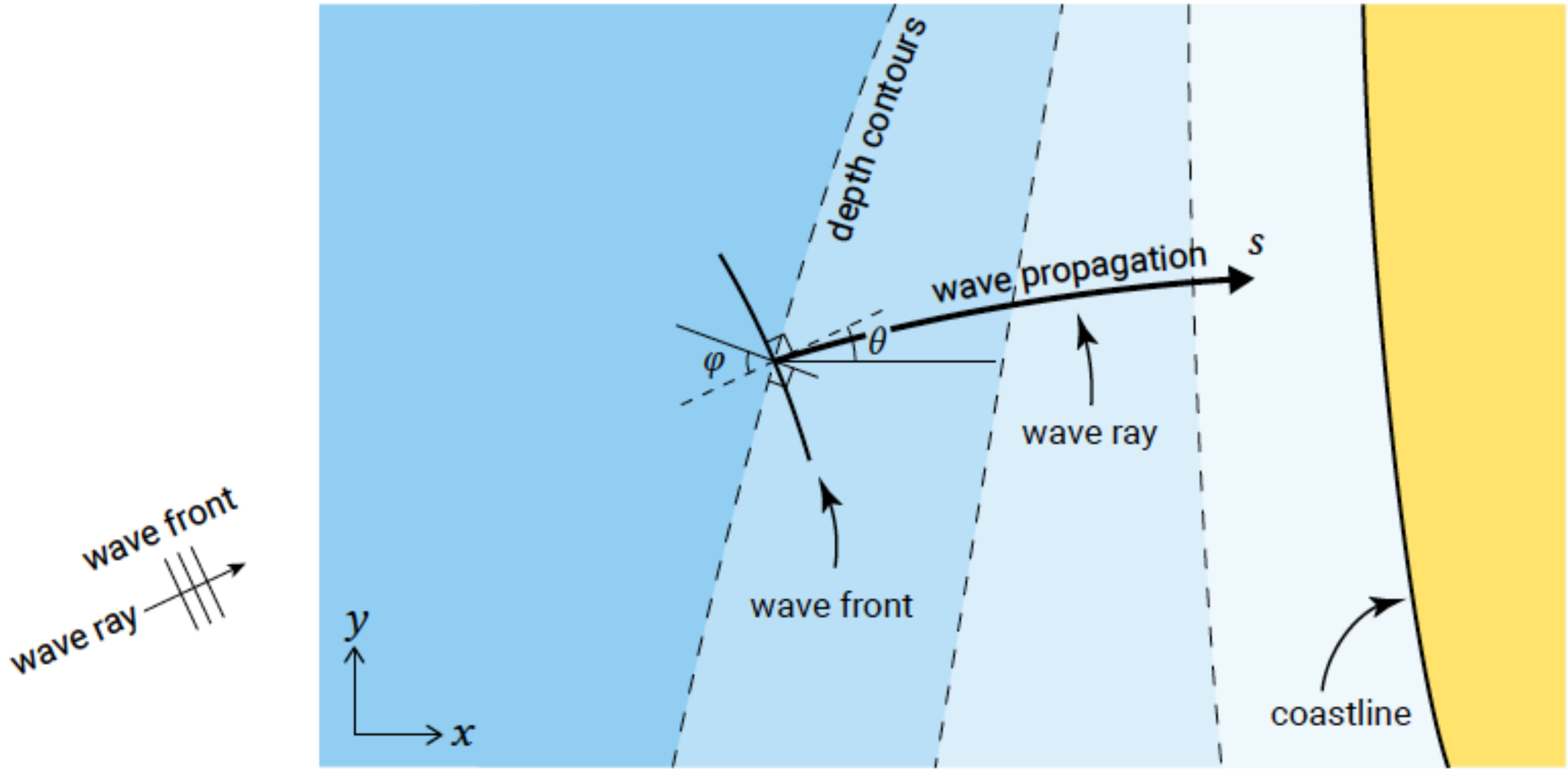

Integrated wave energy over frequency and directions

$$\frac{\partial A}{\partial t} + \frac{\partial c_{gx} A}{\partial x} + \frac{\partial c_{gy} A}{\partial y} + \frac{\partial c_{\theta} A}{\partial \theta} = -\frac{D_w + D_f}{\omega_r}$$

$A(\theta) = \int N(\omega, \theta)\, \mathrm{d}\omega$: Wave action density

C_g : Wave group celerity

D_f : Wave dissipation due to bottom friction $\quad D_f = \frac{1}{2\sqrt{\pi}} \rho f_w \, |u_{orb}|^3 \quad$ f_w = friction factor and u_{orb} = orbital wave velocity

D_w : Wave dissipation due to breaking $\quad D_w = \frac{3\sqrt{\pi}}{16} \rho g \frac{B_b^3}{\gamma^4 h^5} f_p H_{rms}^7 \quad$ $\gamma_b = \frac{H_{rms}}{h} \approx 0.3 - 0.8$: wave breaking parameter

Thornton and Guza (1986)

Bosboom & Stive (2020)

Irregular waves nearshore

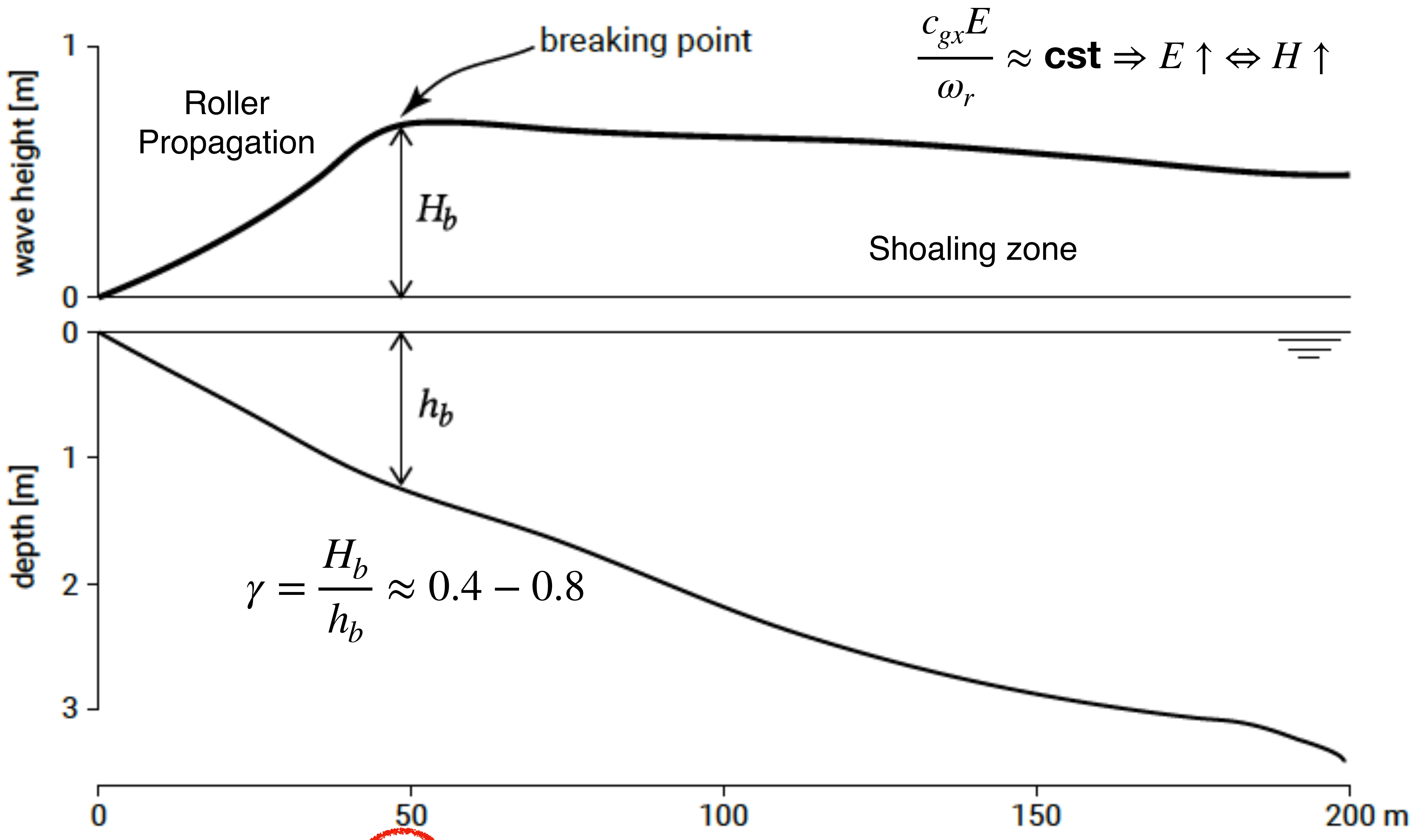

$$\frac{c_{gx}E}{\omega_r} \approx \textbf{cst} \Rightarrow E\uparrow \Leftrightarrow H\uparrow$$

$$C_g \approx C = \sqrt{gh}$$

Steady-state: $$\frac{\partial C_g A}{\partial x} = -\frac{D_w + D_f}{\omega_r}$$

Roller energy equation: $$\frac{\partial C\,E_r}{\partial x} = D_w - D_r$$

Bosboom & Stive (2020)

Wave induced mass flux: Stokes drift

Cross shore currents

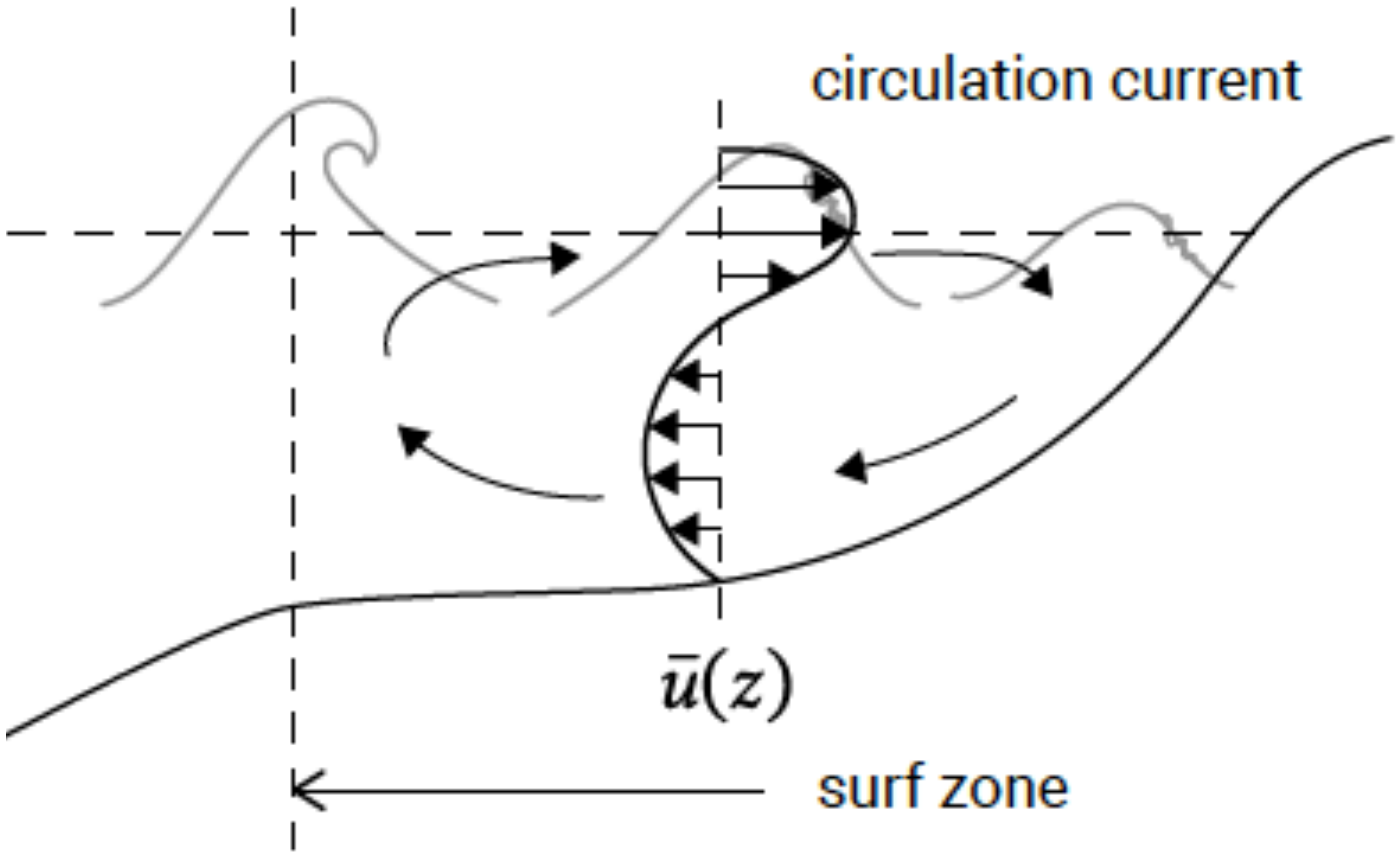

Undertow

=

Return current that compensate the onshore mass flux due to breaking waves

From Stokes 2nd order theory:

$$M = \rho \int_{-h}^{\eta} u(x,z)dz = E\frac{C_g}{C}$$

The mass flux is

- Proportional to energy flux
- Preferentially located near the surface
- Oriented toward the beach (wave propagation direction)
- May be on the order of 0.5 m/s

Stokes drift

Mass conservation implies a return current: undertow

- Located near the bottom
- Oriented offshore

Ardhuin (2006)

Bosboom & Stive (2020)

Wave effects on currents

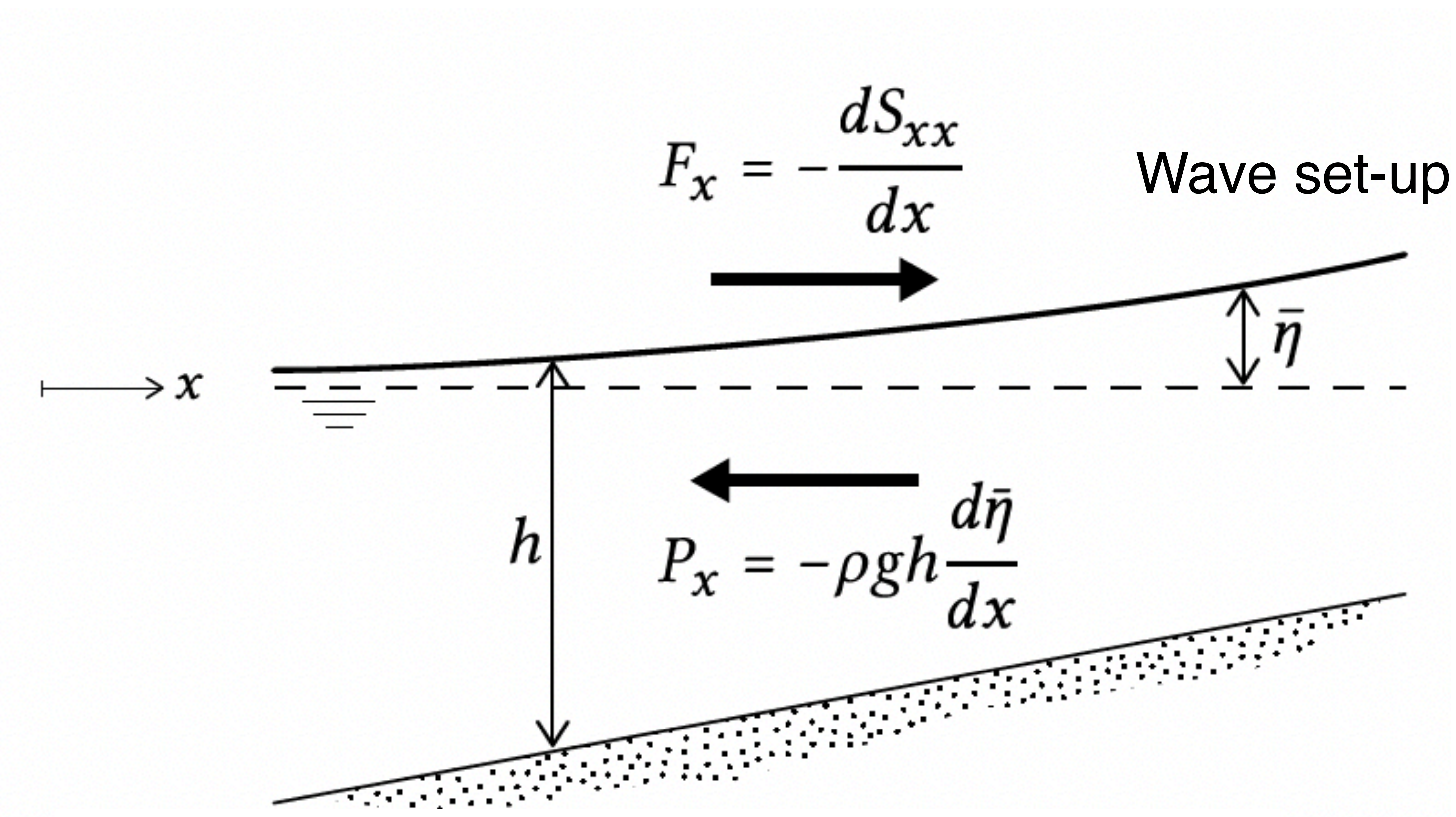

$$S_{xx} = \underbrace{\overline{\int_{-h_0}^{\eta} (\rho u_x)\, u_x \, dz}}_{\text{part due to advection by horizontal particle velocity}} + \underbrace{\overline{\int_{-h_0}^{\eta} p_{\text{wave}} \, dz}}_{\text{pressure part}}$$

$$S_{xx} = \rho g E \left(\frac{C_g}{C} + \frac{1}{2} \frac{2kh}{\sinh(2kh)} \right)$$

Bosboom & Stive (2020)

Radiation stress

=

depth-integrated and wave-averaged flux of momentum due to waves

(Longuet-Higgins and Stewart, 1964)

- Raises the mean water level in the surf zone (set-up);
- Drives a longshore current (oblique waves).

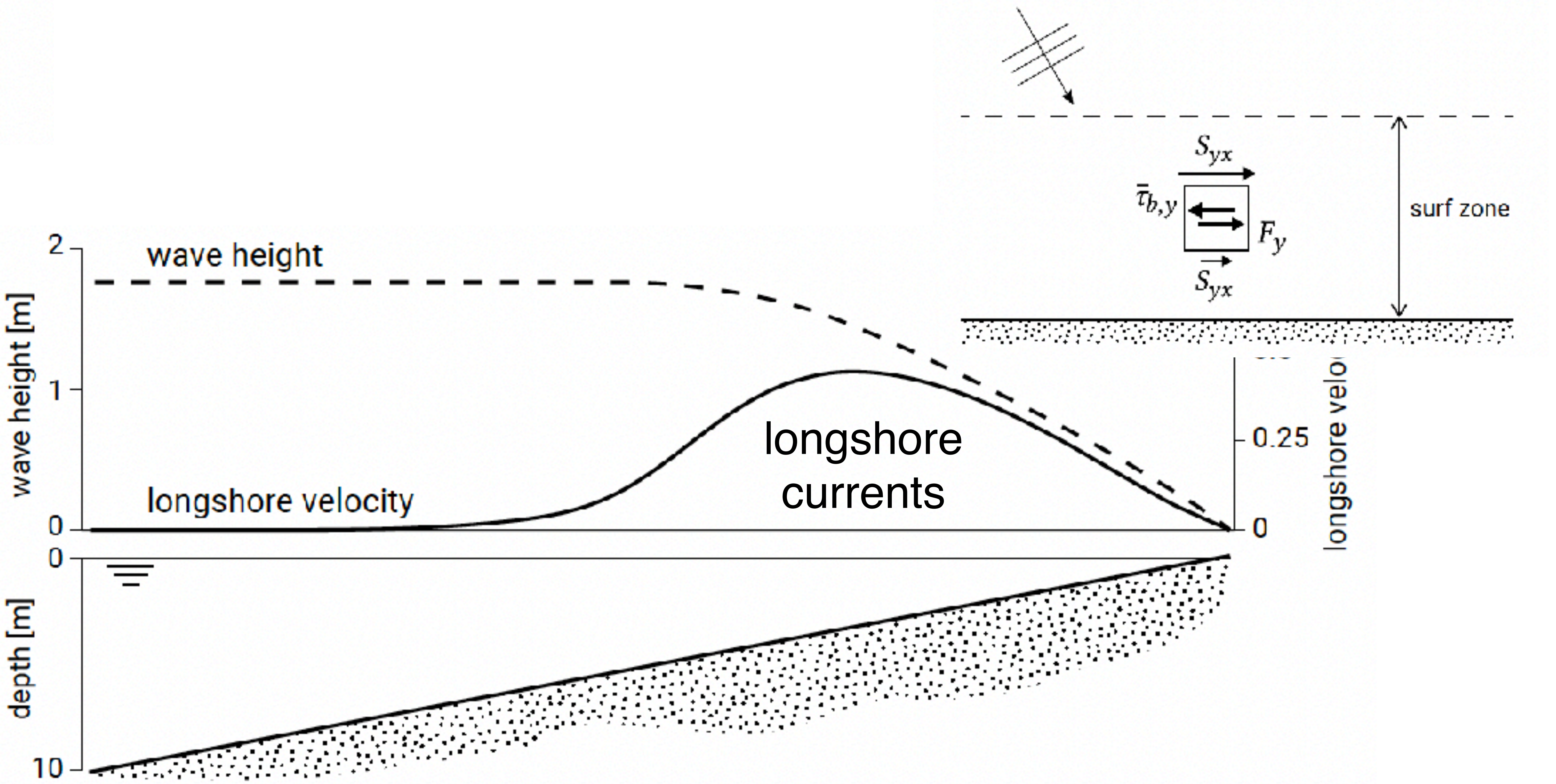

Coastal flooding in the context of climate change

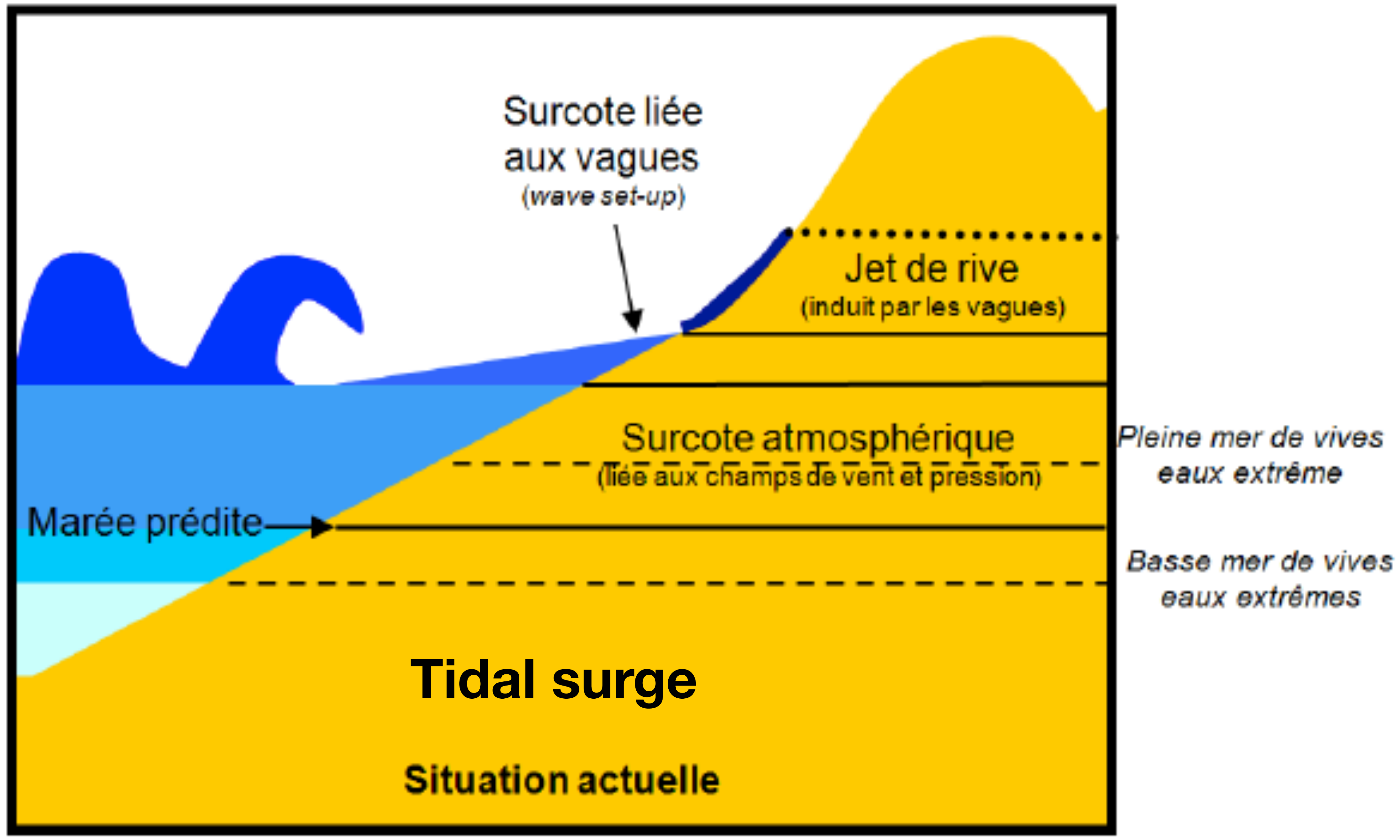

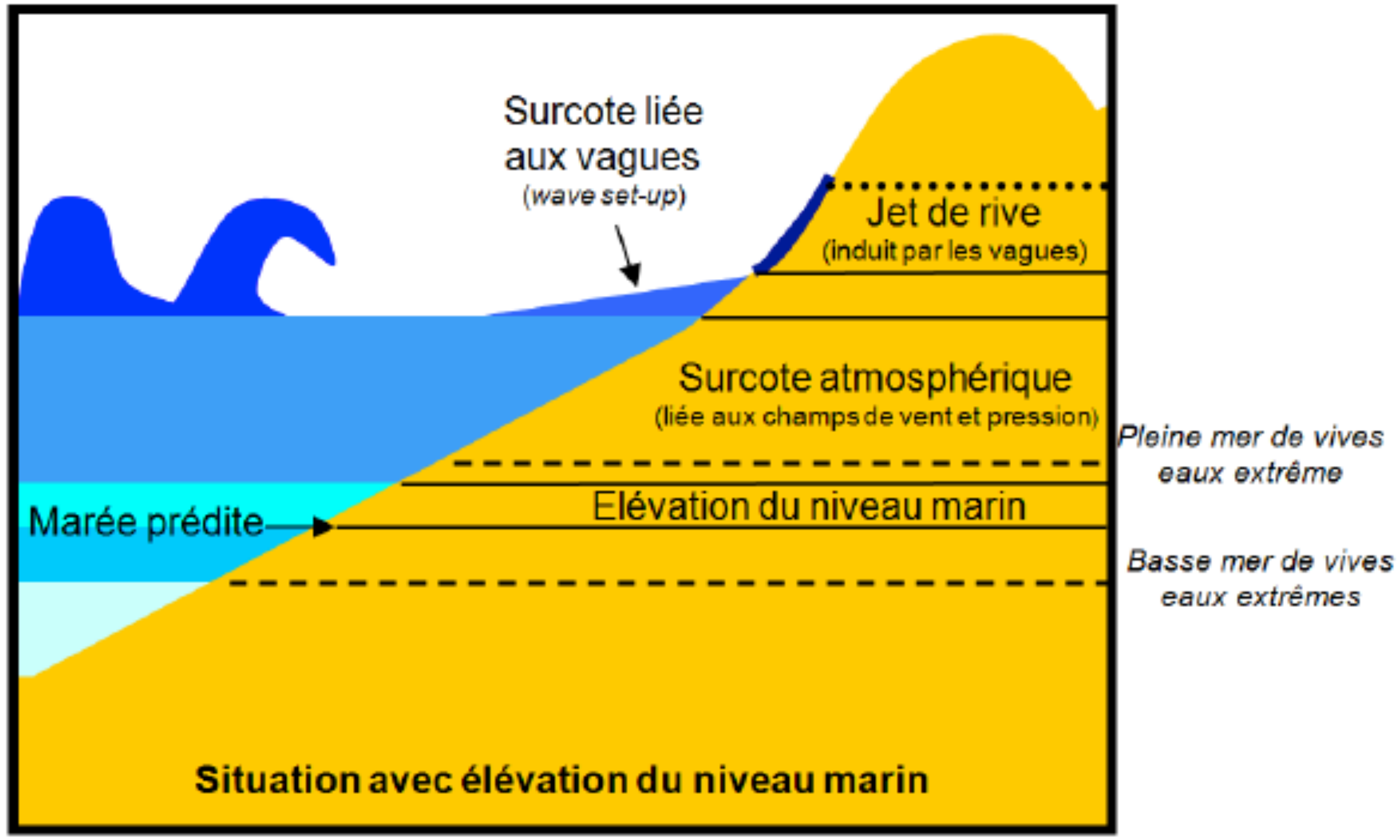

Yates-Michelin et al. (2011)

Atmospheric contributions

- Pressure: $\Delta P_{atm} = 10\ hPa \leftrightarrow \Delta h = 0.1\ m$
- Winds: dynamical effects

Wave contributions

- Wave set-up
- Swash

Possible non-linear interactions between sea level rise, wave propagation and coastal bathymetric evolution but these processes have not been addressed so far…

Open question ?

Le climat de la France au XXIè siècle - Volume 3 - Evolution du niveau de la mer - février 2012

Links with sediment transport and morphodynamics

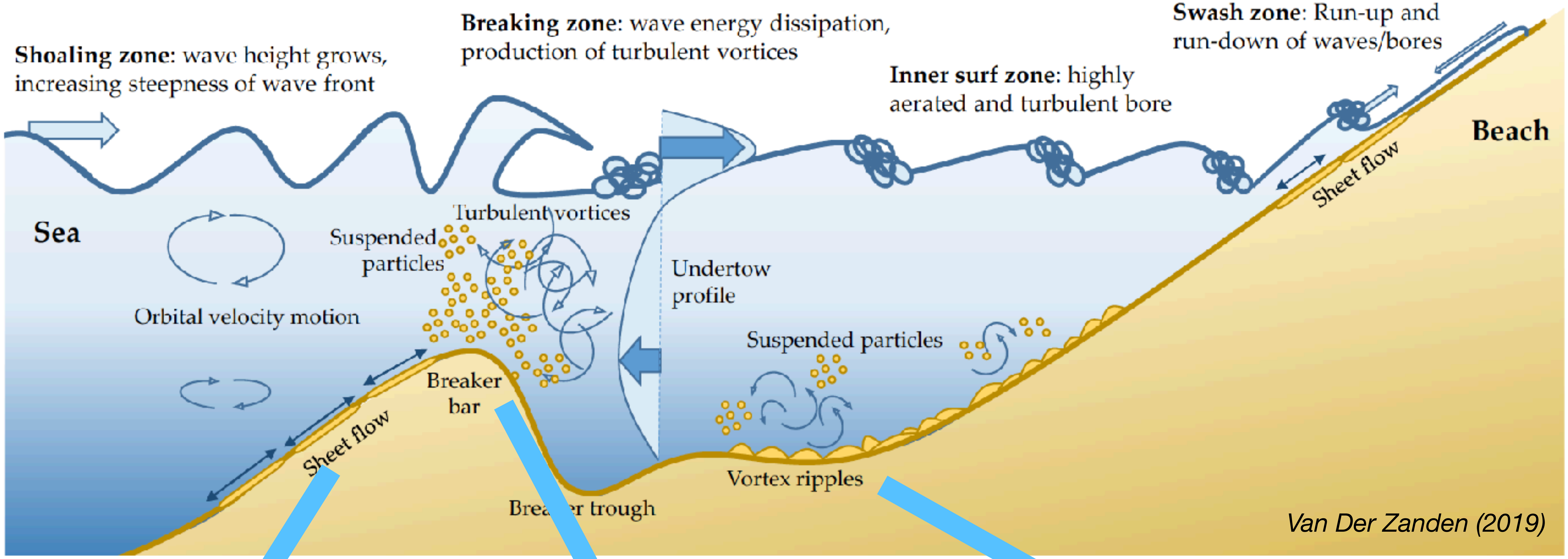

Van Der Zanden (2019)

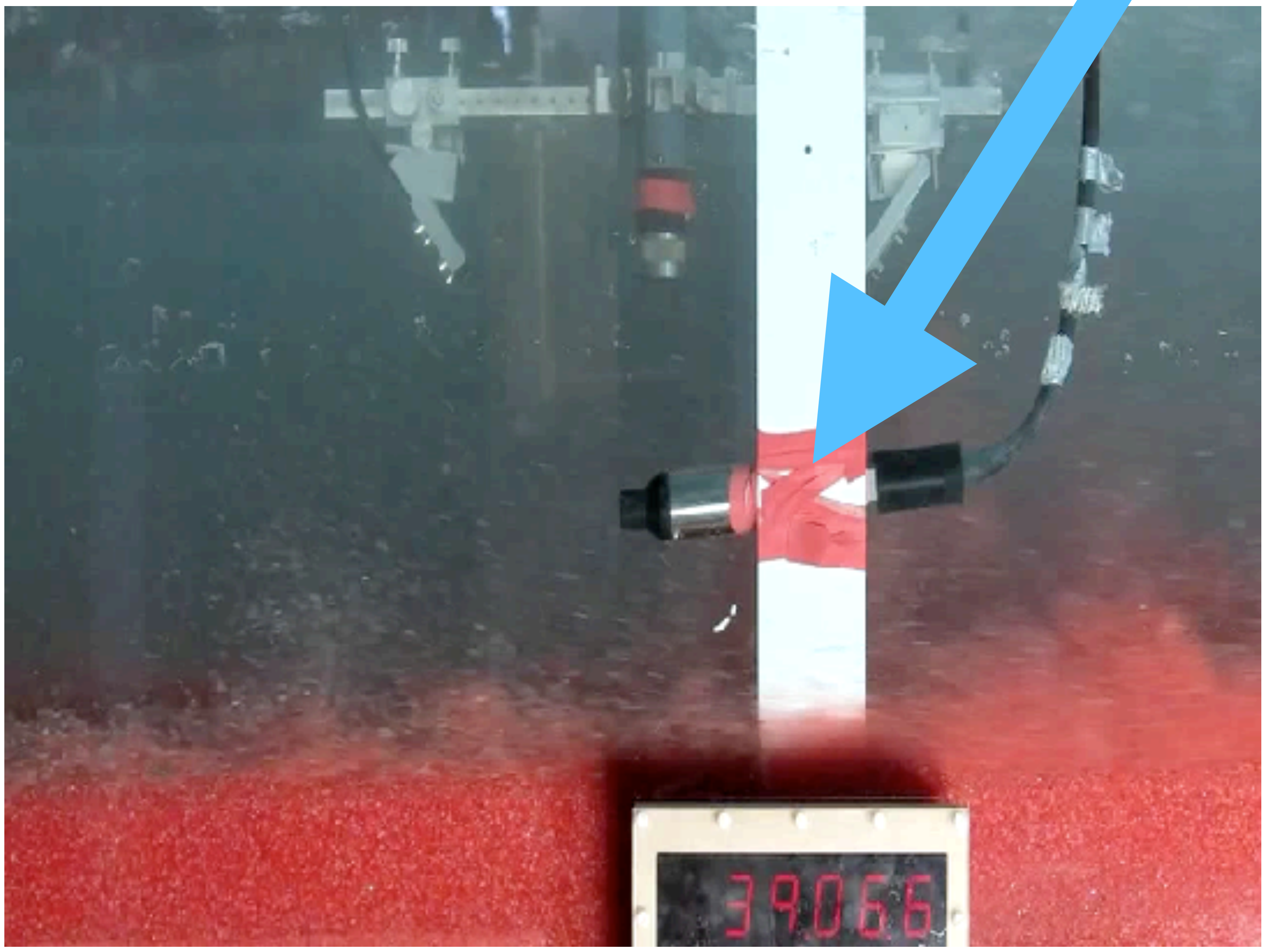

PhD F.X. Chassagneux (2010)

PhD F. Grasso (2009)

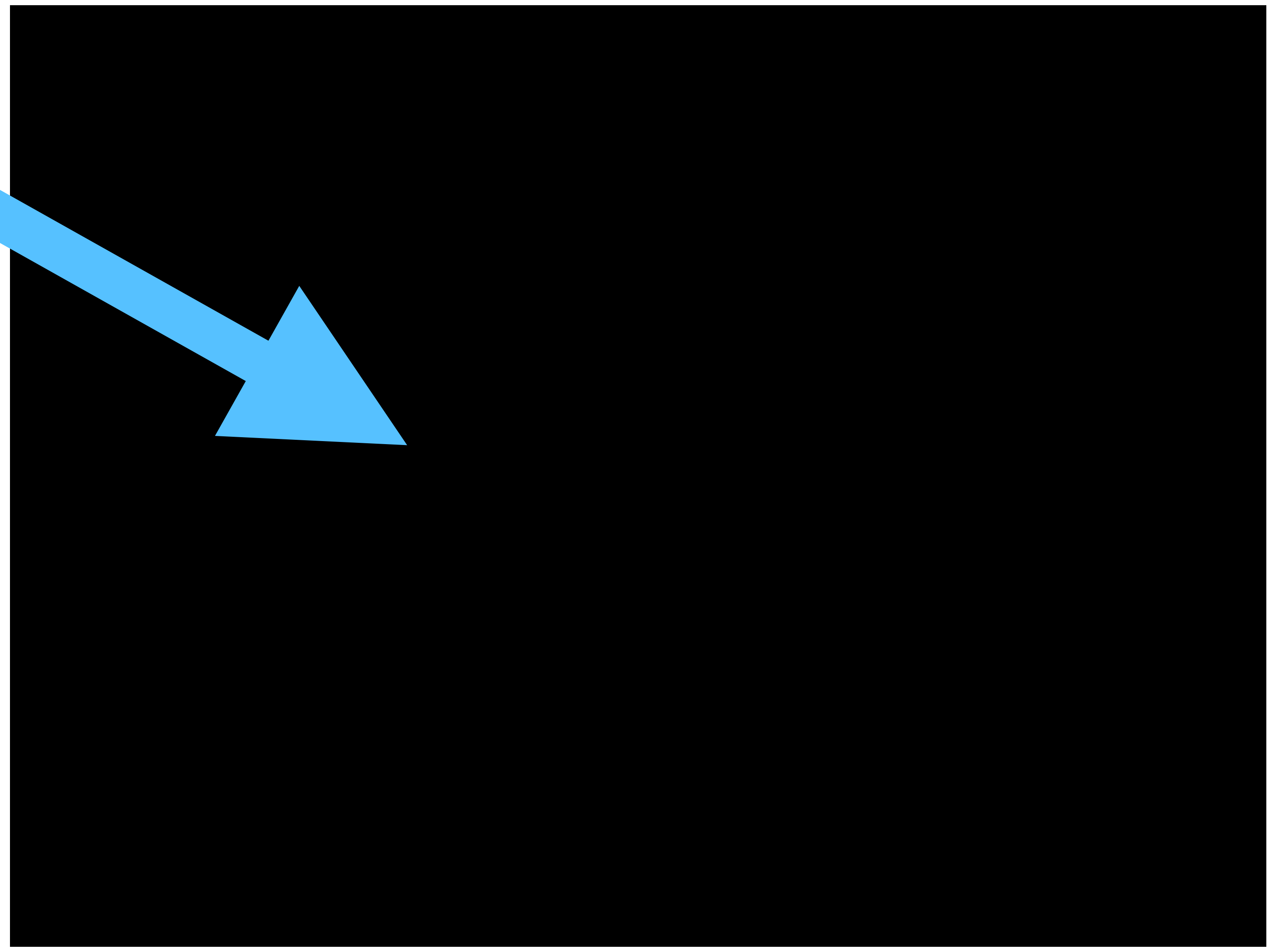

PhD F. Grasso (2009)

Sediment transport regimes

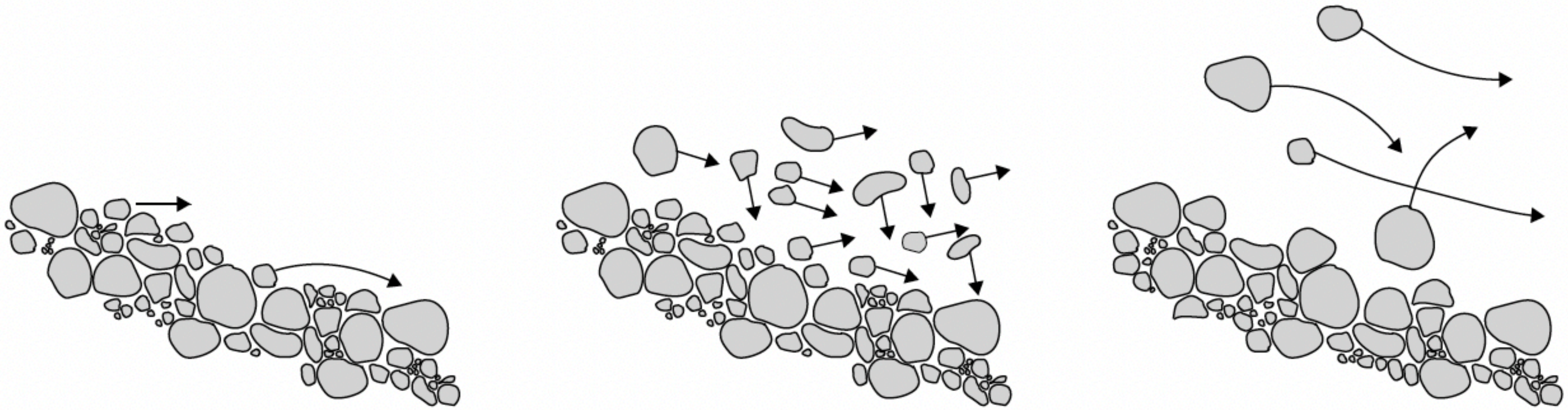

Bed-load	Sheet-Flow	Suspended-load
$\theta \approx \theta_c$	$\theta > 0.3$	S <1

Dimensionless numbers

Shields number: $\theta = \dfrac{\rho^f u_*^2}{\Delta\rho g d_p}$

Suspension number: $S = \dfrac{W_s}{u_*}$

Sediment transport modeling

Pros

- Simple
- Applicable at large-scale

Cons

- Empirical formulas
  - Especially bed-load
  - Large scatter (~100%)
  - Missing physics
- Arbitrary separation between bed-load and suspended-load

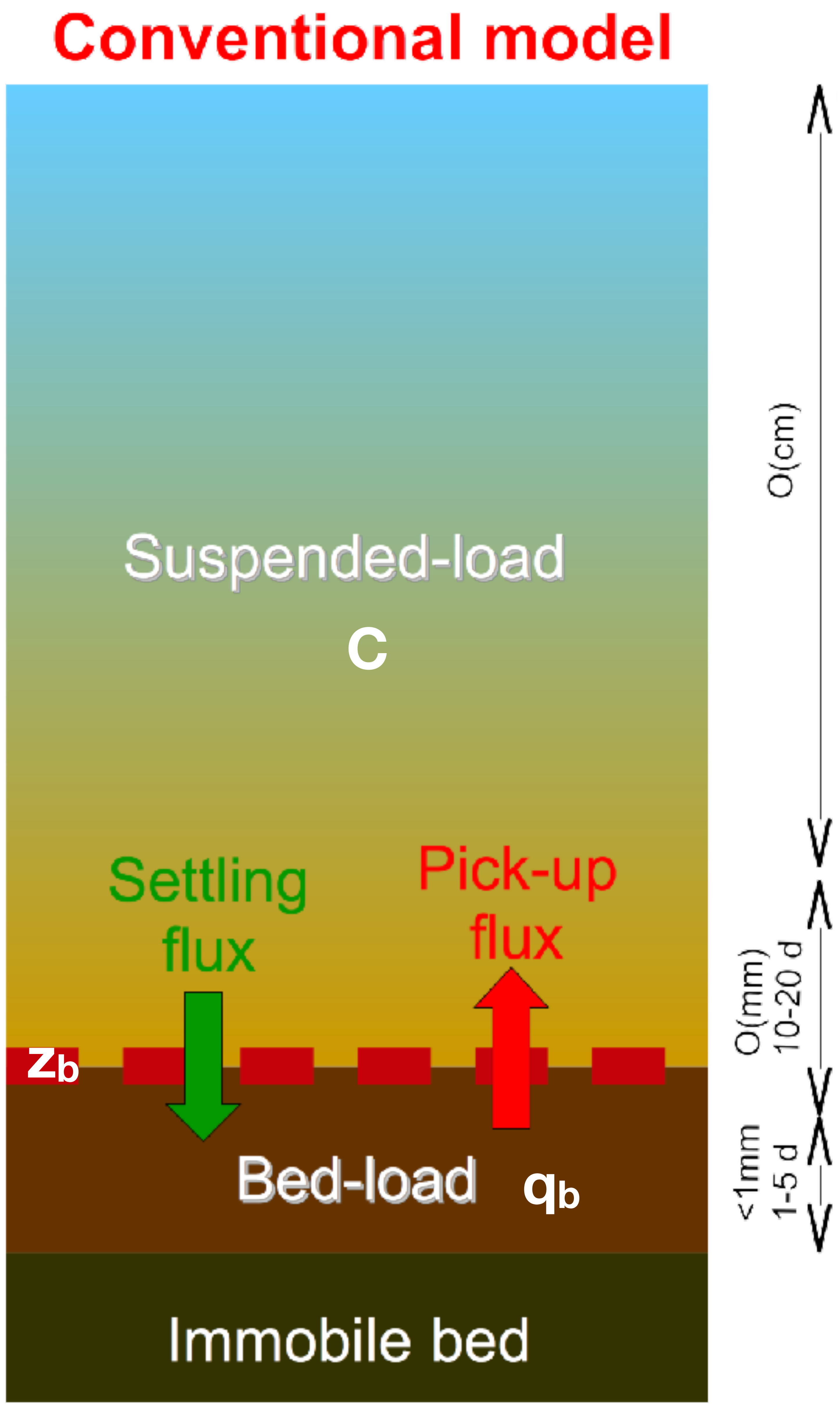

Hydrodynamic model for currents: U, V, W, h

Spectral wave model: $A(\theta)$, U_{Stokes}, V_{Stokes}

Sediment transport model: C, q_b, z_b

Jenkins and Hanes JFM (1998)

Bed-load transport

Bed-load formula: $\vec{\Phi} = \dfrac{\vec{q_b}}{\sqrt{(s-1)gd_{50}^3}}$

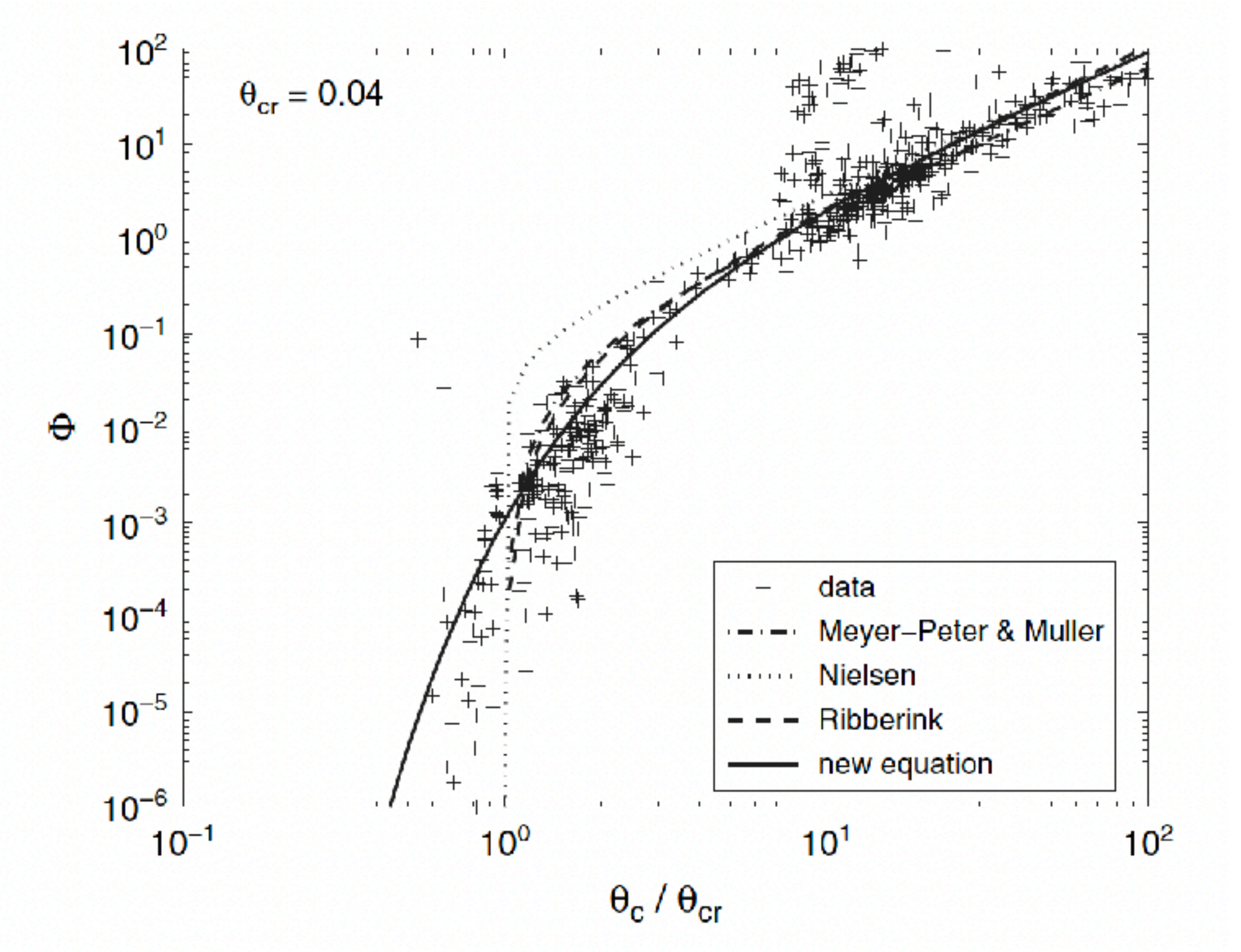

Current: $\vec{\Phi_c} = \max\left[K(\theta_c - \theta_{cr})^n; 0\right] \dfrac{\vec{\tau_c}}{\tau_c}$

Waves: $\vec{\Phi_w} = \dfrac{1}{T}\int_0^T \max\left[K(\theta_w(t) - \theta_{cr})^n; 0\right] \dfrac{\vec{\tau_w}}{|\tau_w|} dt$

$\vec{\Phi_w} \approx \max\left[K(\tilde{\theta}_w - \theta_{cr})^n; 0\right] \dfrac{\vec{\tau_w}}{|\tau_w|}$ sinusoidal waves = no sand-flux

Waves + current:

complex problem - no simple solution

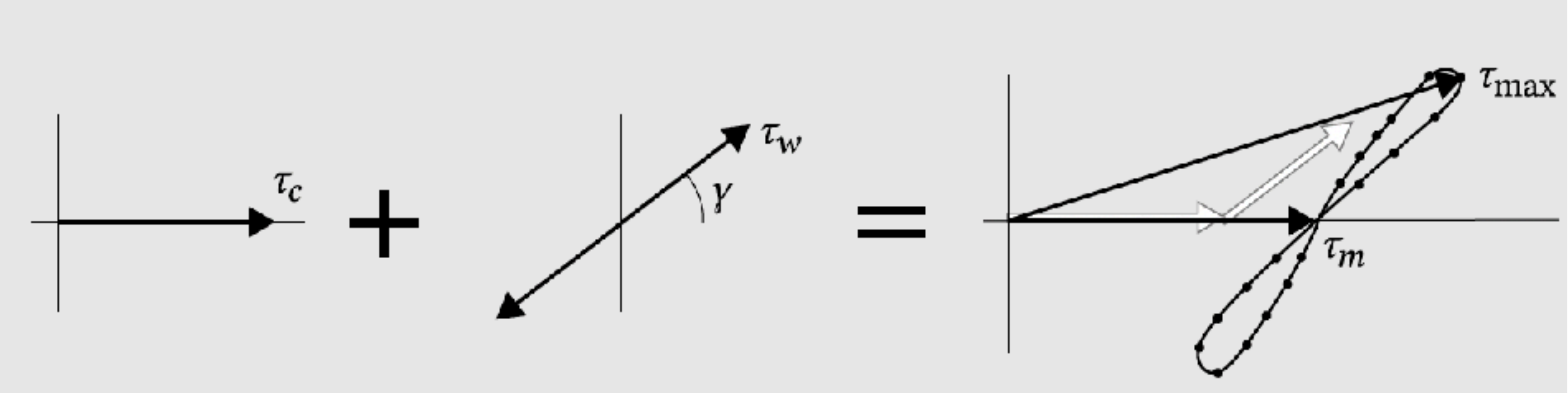

Bosboom & Stive (2020)

Bed-load transport

Bed-load formula for wave and currents

$$\vec{\Phi} = \frac{q_b}{\sqrt{(s-1)gd_{50}^3}} = \max\left[12\theta^{1/2}(\theta_{sf} - \theta_c); 0\right] \frac{\vec{\tau_{sf}}}{\tau_{sf}}$$

Dirty kitchen of coastal engineering

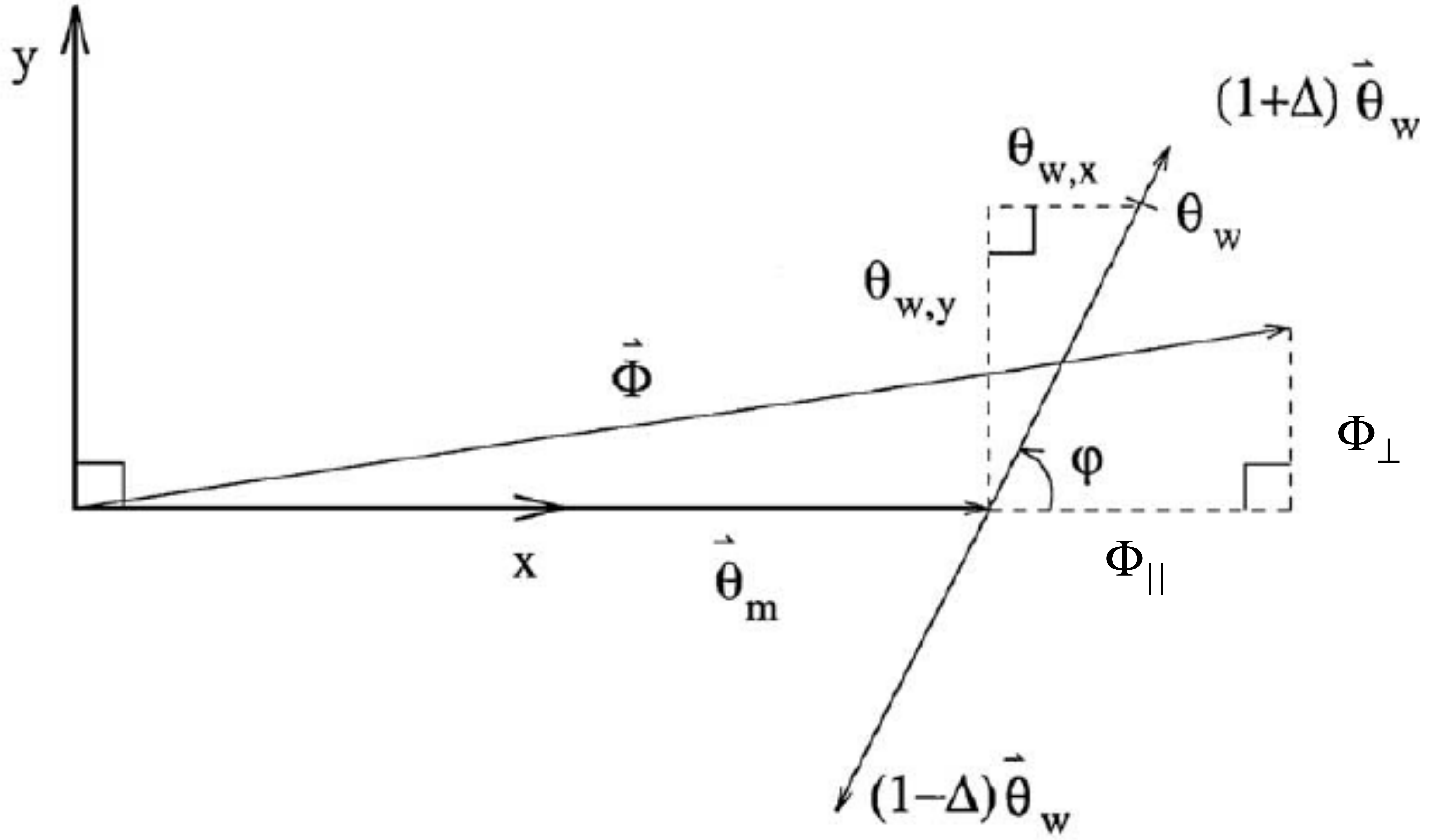

$\vec{\Phi} = \left(\Phi_{||}; \Phi_\perp\right)^T$ with $\Phi_{||}$ = transport in direction of current and $\Phi_\perp$ = transport perpendicular to the current

$\Phi_{||} = \max\left[\Phi_{||1}; \Phi_{||2}\right]$ with $\Phi_{||1} = 12\theta_m^{1/2}(\theta_m - \theta_c)$ and $\Phi_{||2} = 12\left((0.9534 + 0.1907\cos(2\phi_w))\theta_w^{1/2}\theta_m + 0.229\gamma_w\cos(\phi_w)\theta_w^{3/2}\right)$

$$\Phi_\perp = 12\frac{0.1907\theta_w^2}{\theta_x^{3/2} + 3/2\theta_m^{3/2}}\left(\theta_m\sin(2\phi) + 1.2\gamma_w\theta_w\sin(\phi_w)\right)$$

γ_w: wave asymmetry factor

Empirical formula providing (very) limited success to predict sandbar migration

(Soulsby and Damgaard, 2005)

Bed-load transport

Half-wave cycle concept (Dibajnia and Watanabe, 1992)

- Asymmetric transport by non-linear waves
- Effect of phase lag between mobilization and transport

Dohmen-janssen et al. (2002)

Sediment load

- On-going wave-cycle: $\Omega_i = \max\left(11\left(\left|\theta_i\right| - \theta_{cr}\right)^{1.2}, 0\right)$
- Previous wave-cycle: $\Omega_{tc/ct}$ phase-lag/unsteady contributions

Velocity scale: Based on friction velocity: $\sqrt{\theta_i}$

Direction: Aligned with the shear stress direction: $\dfrac{\vec{\theta_i}}{\left|\theta_i\right|}$

where *i* stands for crest or trough

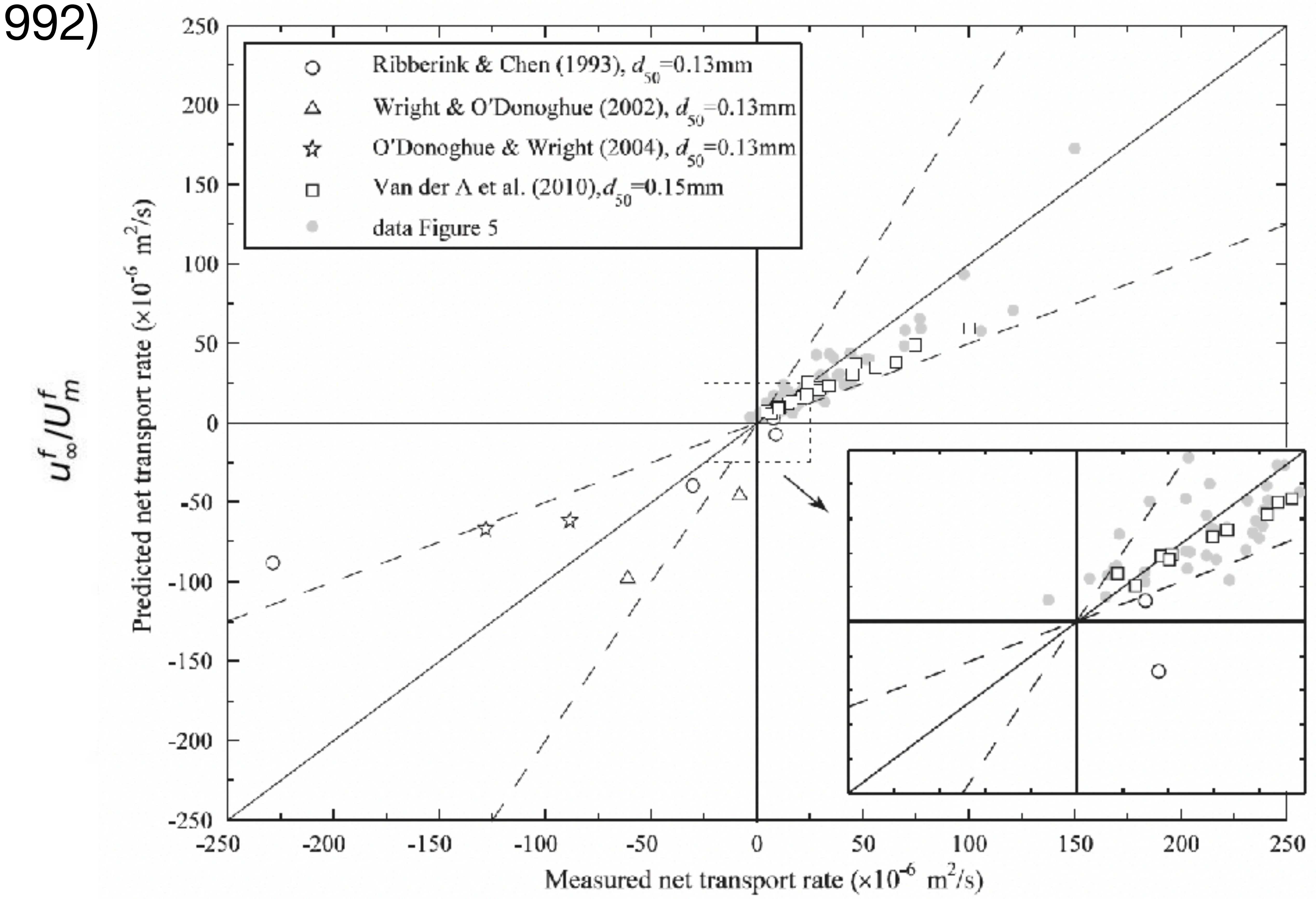

$$\vec{\Phi} = \frac{1}{T}\left[\sqrt{\theta_c}\, T_c\left(\Omega_{cc} + \frac{T_c}{2T_{cu}}\Omega_{tc}\right)\frac{\vec{\theta_c}}{\left|\theta_c\right|} + \sqrt{\theta_t}\, T_t\left(\Omega_{tt} + \frac{T_t}{2T_{tu}}\Omega_{ct}\right)\frac{\vec{\theta_t}}{\left|\theta_t\right|}\right]$$

Camenen and Larson (2007)

Van Der A et al. (2013)

Suspended-load and bed evolution

Adv.-Diff equation for C: $$\frac{\partial C}{\partial t} + \vec{\nabla} \cdot \left(\vec{U} C\right) - \frac{\partial W^c C}{\partial z} = \vec{\nabla}_h \left(K_h^C \vec{\nabla} C\right) + \frac{\partial}{\partial z}\left(K_z^C \frac{\partial C}{\partial z}\right)$$

Settling velocity : W^c

Bed morphological evolution: $$\frac{\partial z_b}{\partial t} + \frac{f_{mor}}{1-p} \vec{\nabla}_h \cdot \vec{q_b} = \frac{1}{1-p}(E - D)$$

= Hyperbolic equation

Erosion flux : $E = E_0 \ \max(\tau_{sf}/\tau_{ce} - 1; 0)$

Morphological factor : f_{mor} (may be up to 100)

Morphological time scales >> Hydrodynamic time scales

=> Speed-up morphodynamics effects

Useful in practice but questionable from a mathematical perspective…

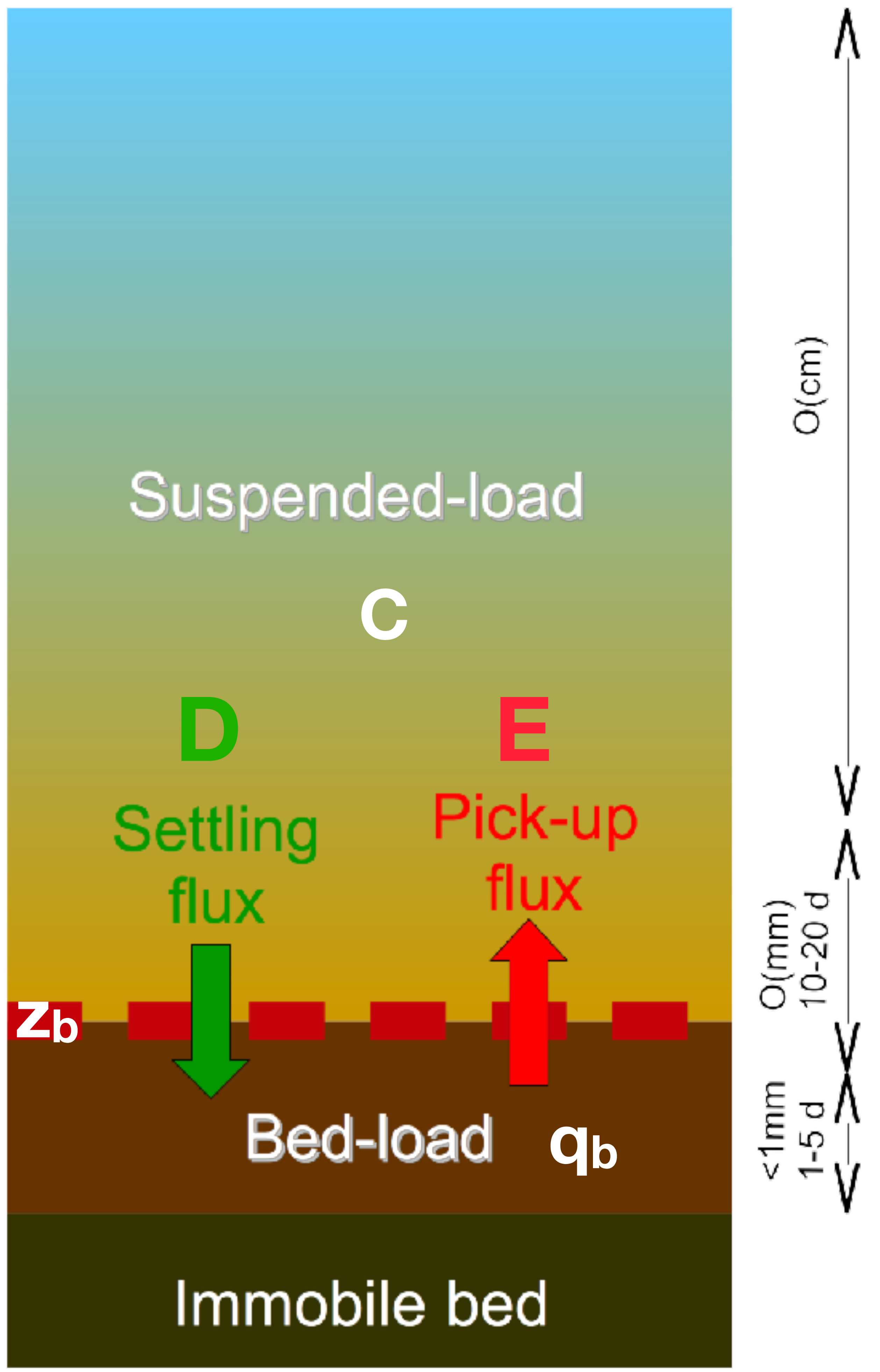

Summary of nearshore model equations

$$\frac{\partial \zeta}{\partial t} + \frac{\partial hu}{\partial x} + \frac{\partial hv}{\partial y} + \frac{\partial w^*}{\partial \sigma} = 0$$

$$\frac{\partial u}{\partial t} + u\frac{\partial u}{\partial x} + v\frac{\partial u}{\partial y} + \frac{w^*}{h}\frac{\partial u}{\partial \sigma} = fv - \frac{1}{\rho_0}\frac{\partial P}{\partial x} + F_x + M_x + \frac{1}{h^2}\frac{\partial}{\partial \sigma}\left(\nu_V \frac{\partial u}{\partial \sigma}\right)$$ … same for v+w

HYDRO

$$\frac{\partial A}{\partial t} + \frac{\partial C_{gx}A}{\partial x} + \frac{\partial C_{gy}A}{\partial y} + \frac{\partial C_{g\theta}A}{\partial \theta} = -\frac{D_w + D_f}{\omega}$$ **Wave action**

$$\frac{\partial S_r}{\partial t} + \frac{\partial c_x S_r}{\partial x} + \frac{\partial c_y S_r}{\partial y} + \frac{\partial c_\theta S_r}{\partial \theta} = D_w - D_r$$ **Roller energy**

WAVES

$$\frac{\partial C}{\partial t} + \vec{\nabla} \cdot \left(\vec{U} C\right) - \frac{\partial W^c C}{\partial z} = \vec{\nabla}_h \left(K_h^C \vec{\nabla} C\right) + \frac{\partial}{\partial z}\left(K_z^C \frac{\partial C}{\partial z}\right)$$

$$\frac{\partial z_b}{\partial t} + \frac{f_{mor}}{1-p}\vec{\nabla}_h \cdot \vec{q_b} = E - D$$

SEDIMENT

8 non-linearly coupled PDEs

Numerical simulation of sandbar migration

- CROCO with spectral wave model
- Bedload: van Der A *et al.* (2013)
- Domaine size : 200 m cross-shore
- Grid resolution : 1.5 m ; time step: 0.1s
- Measurements:
  - Wave height
  - Current profiles
  - Sediment concentration profiles
  - Bathymetry
- 2 Wave conditions

	Hs (m)	Tp (s)	Duration (h)
LIP1B	1.4	5	18
LIP1C	0.6	8	13

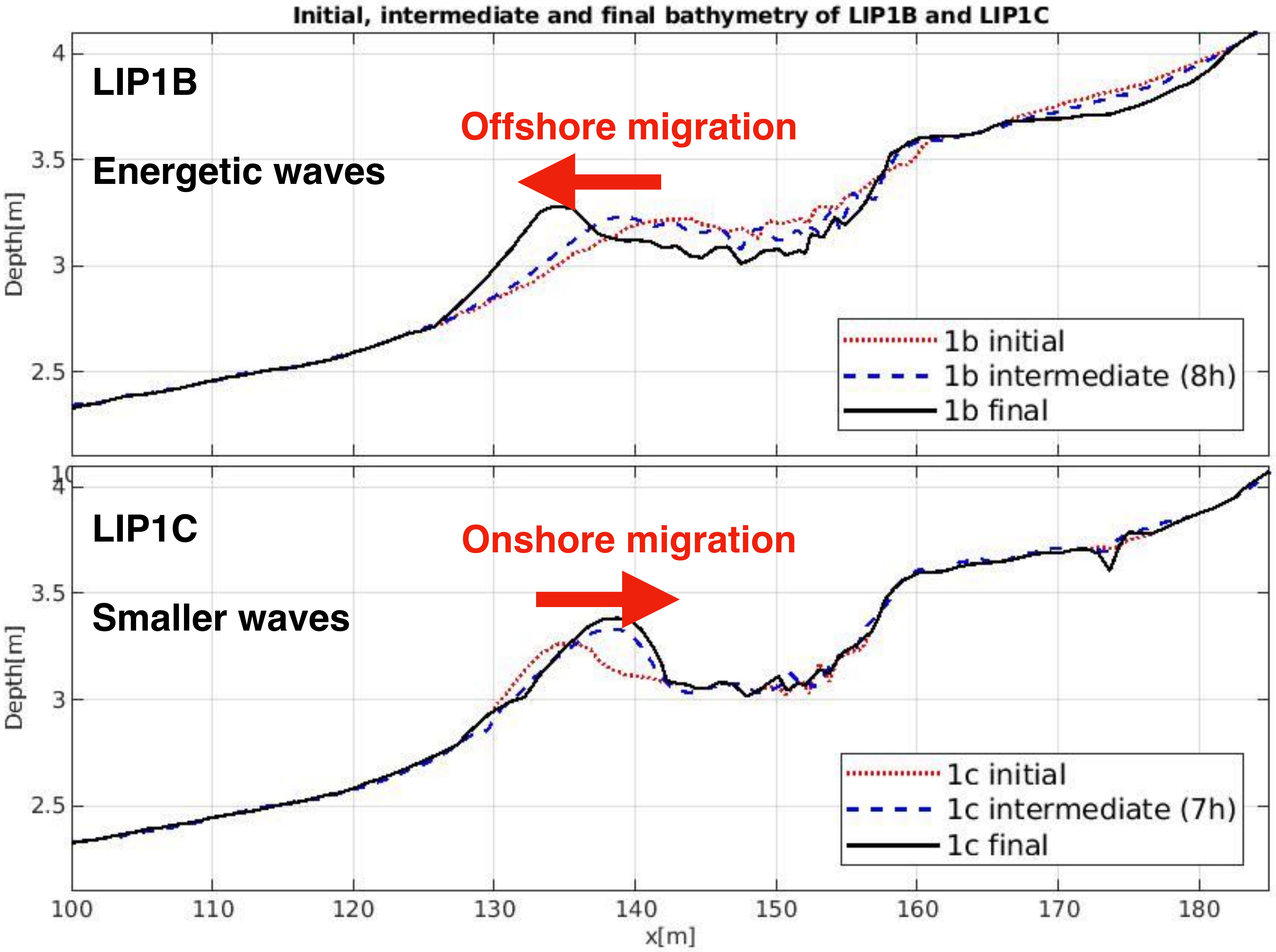

Roelvink and Reniers (1995)

Hydrodynamic calibration

Hs = 1.4 m - Tp = 5 s

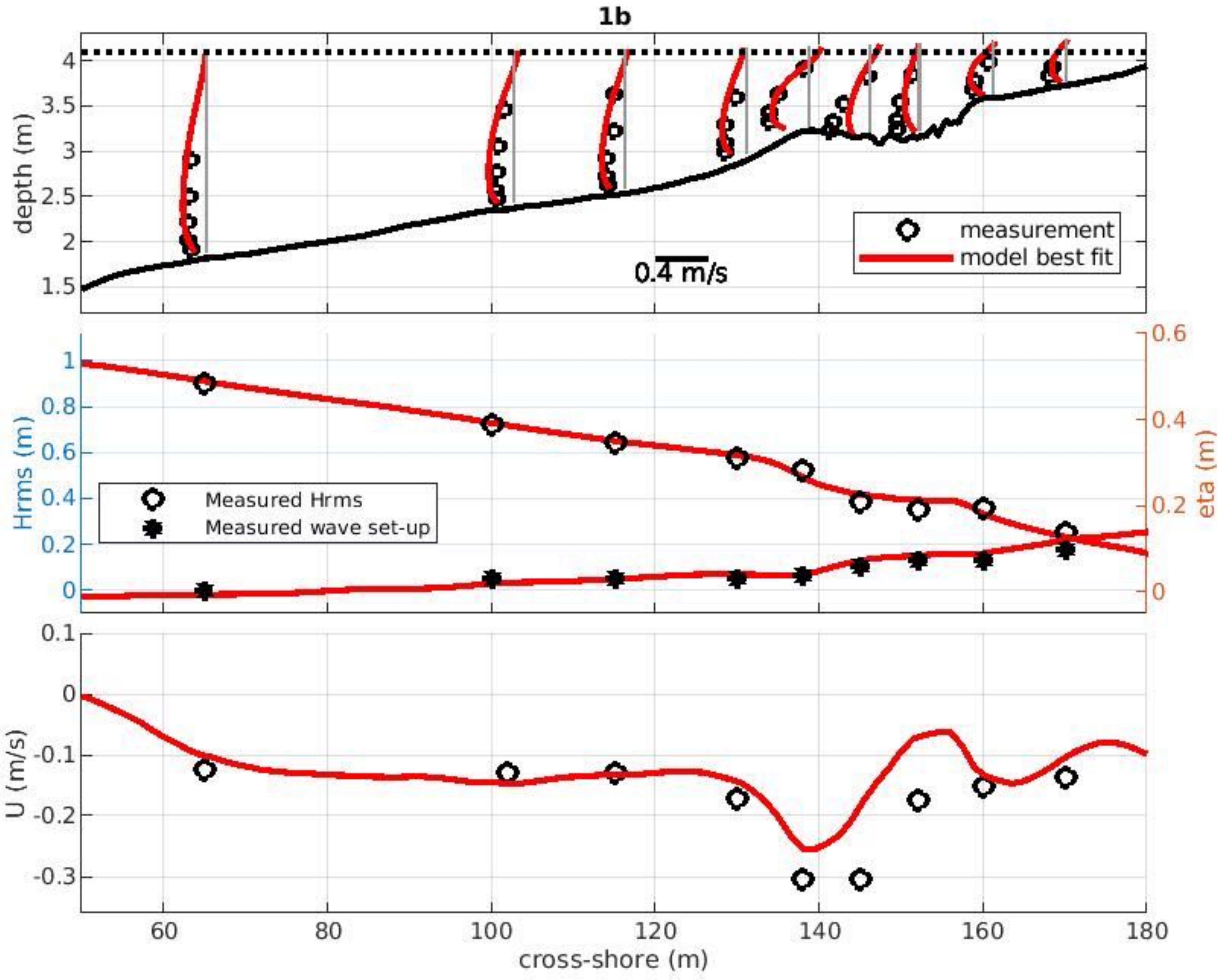

Hs = 0.6 m - Tp = 8 s

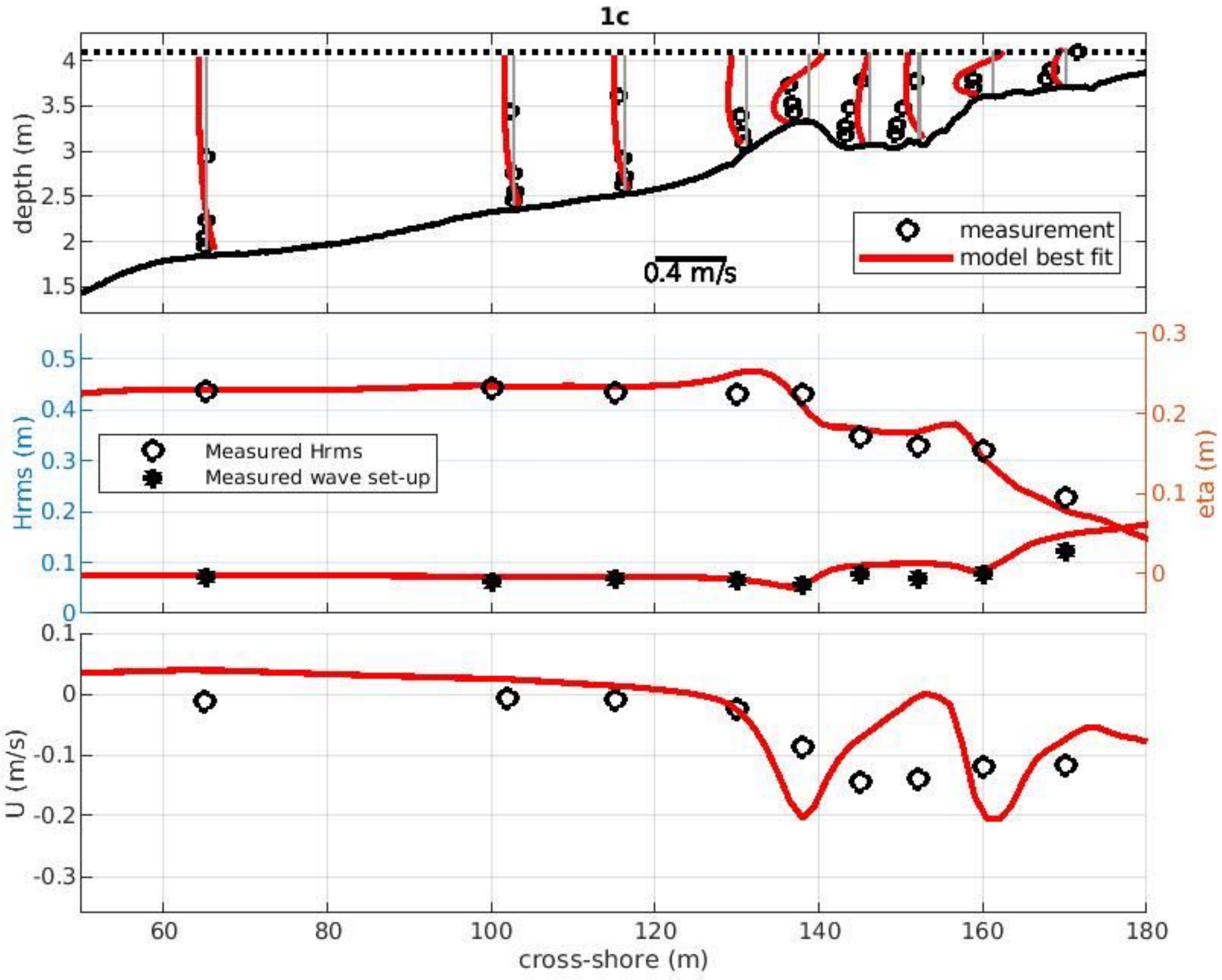

Friction coefficient, breaking parameter and roller coefficients are tuned (same parameters for both configurations)

Shafiei et al. (submitted to ocean modeling)

Morphodynamic simulations

Hs = 1.4 m - Tp = 5 s **Hs = 0.6 m - Tp = 8 s**

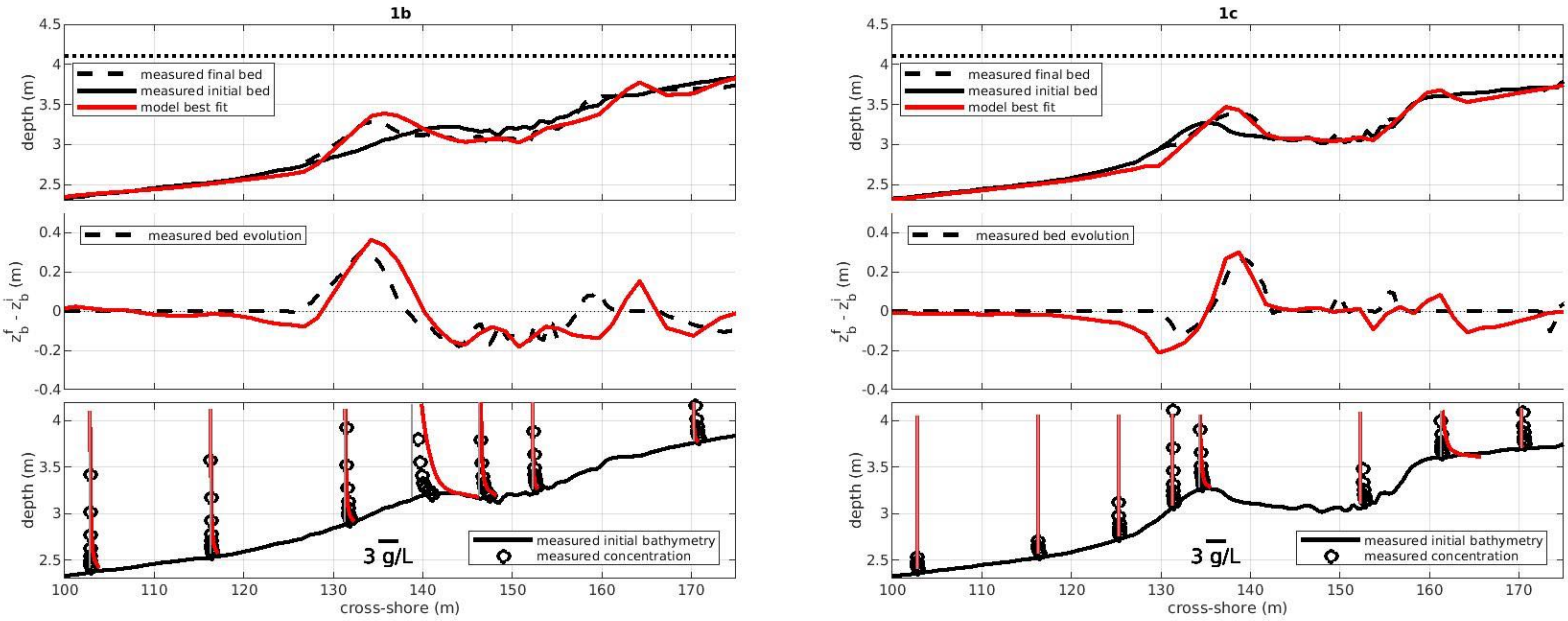

Onshore/offshore sandbar migration reproduced for varying wave conditions

Shafiei et al. (submitted to ocean modeling)

Morphodynamic simulations

Hs = 1.4 m - Tp = 5 s

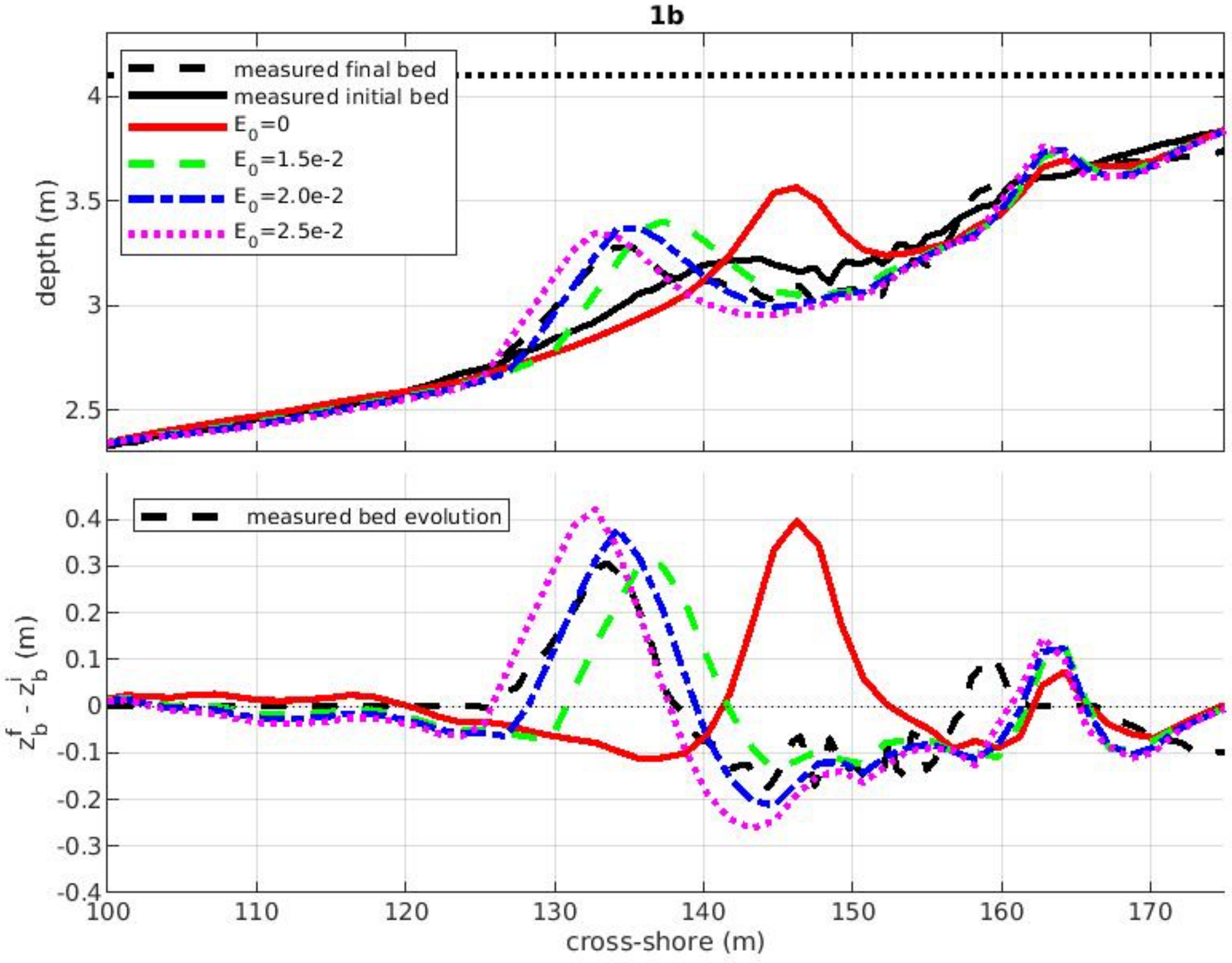

Offshore sandbar migration is due to suspended load undertow driven sand transport

Hs = 0.6 m - Tp = 8 s

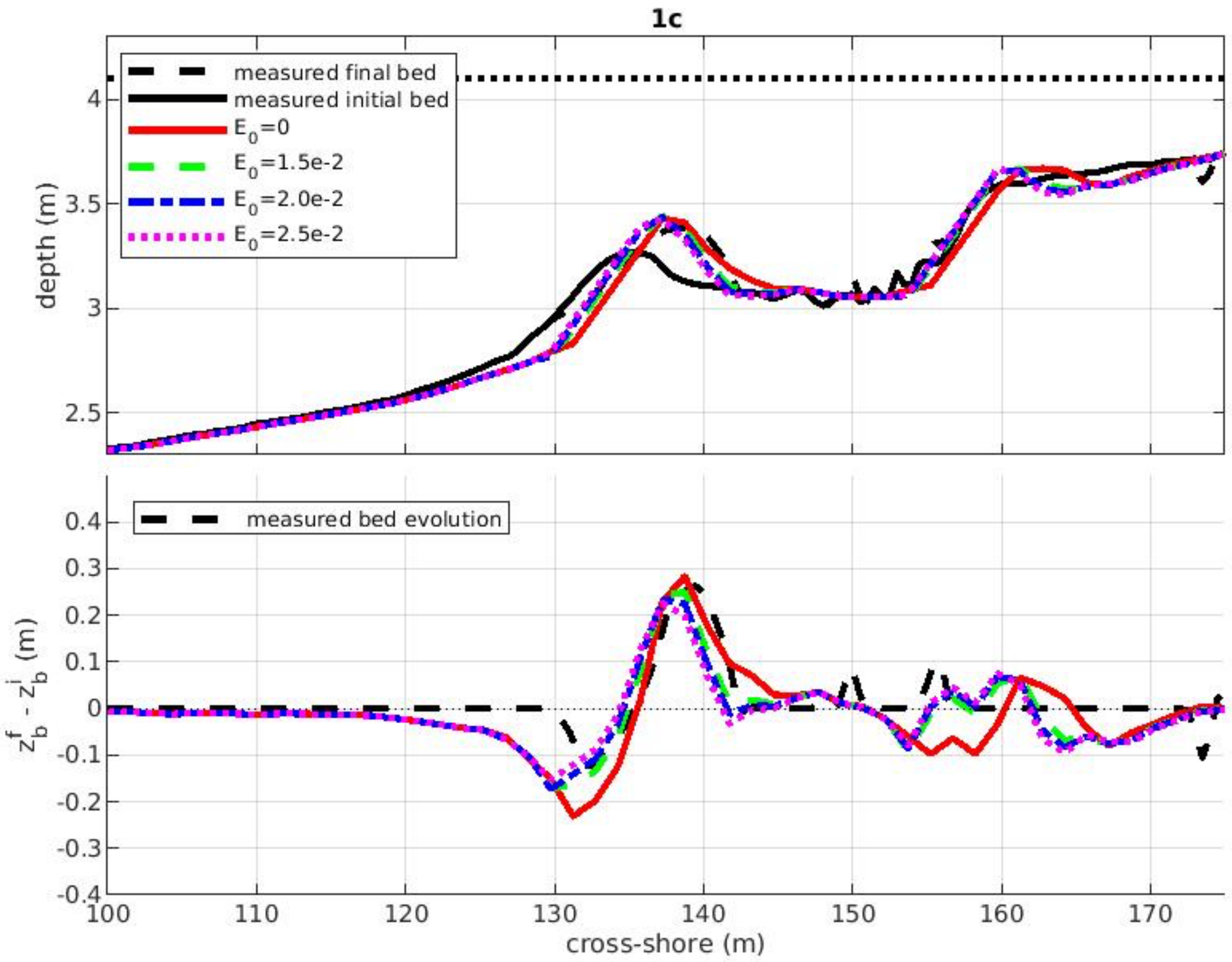

Onshore sandbar migration is due to wave skewness effect on sand transport

Shafiei et al. (submitted to ocean modeling)

1st open question

Open question: What are the stability conditions for the coupled system of equations ?

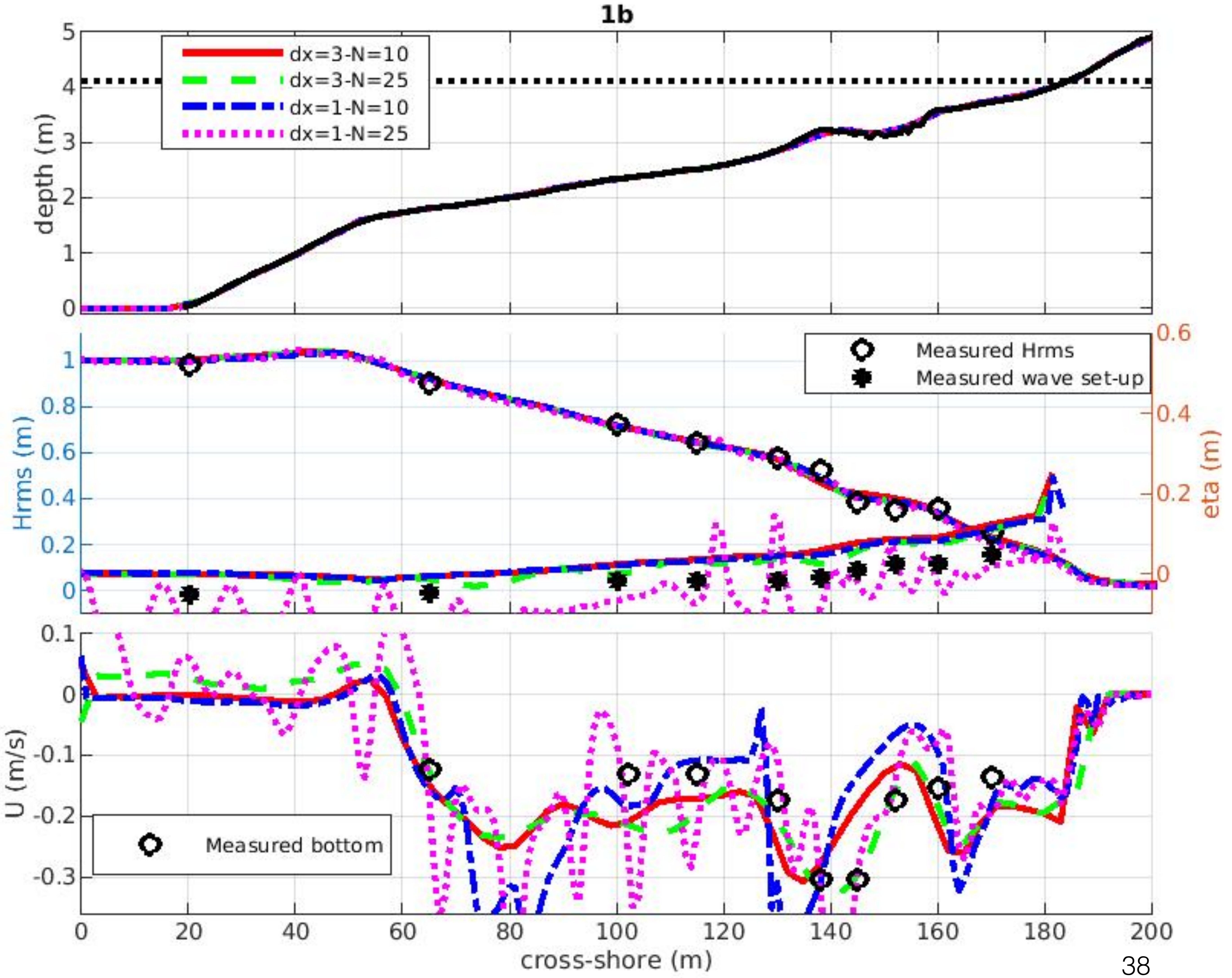

- Coupling between the spectral wave and the hydrodynamics models
- Coupling between morphodynamics and wave-current model
- Stability associated with morphological acceleration?

This is just an example but we have observed instabilities in other situations

Numerical simulation of the Truc vert ECORS 2008 field campaign

- Simulation period: February to April 2008 - 4 Storms
- CROCO with spectral wave model
- Bedload: Soulsby & Daamgard (2005)
- Domaine size: 2 km longshore / 1.5 km cross-shore
- Grid resolution: 10-20 m ; Time step: 0.5-1 s

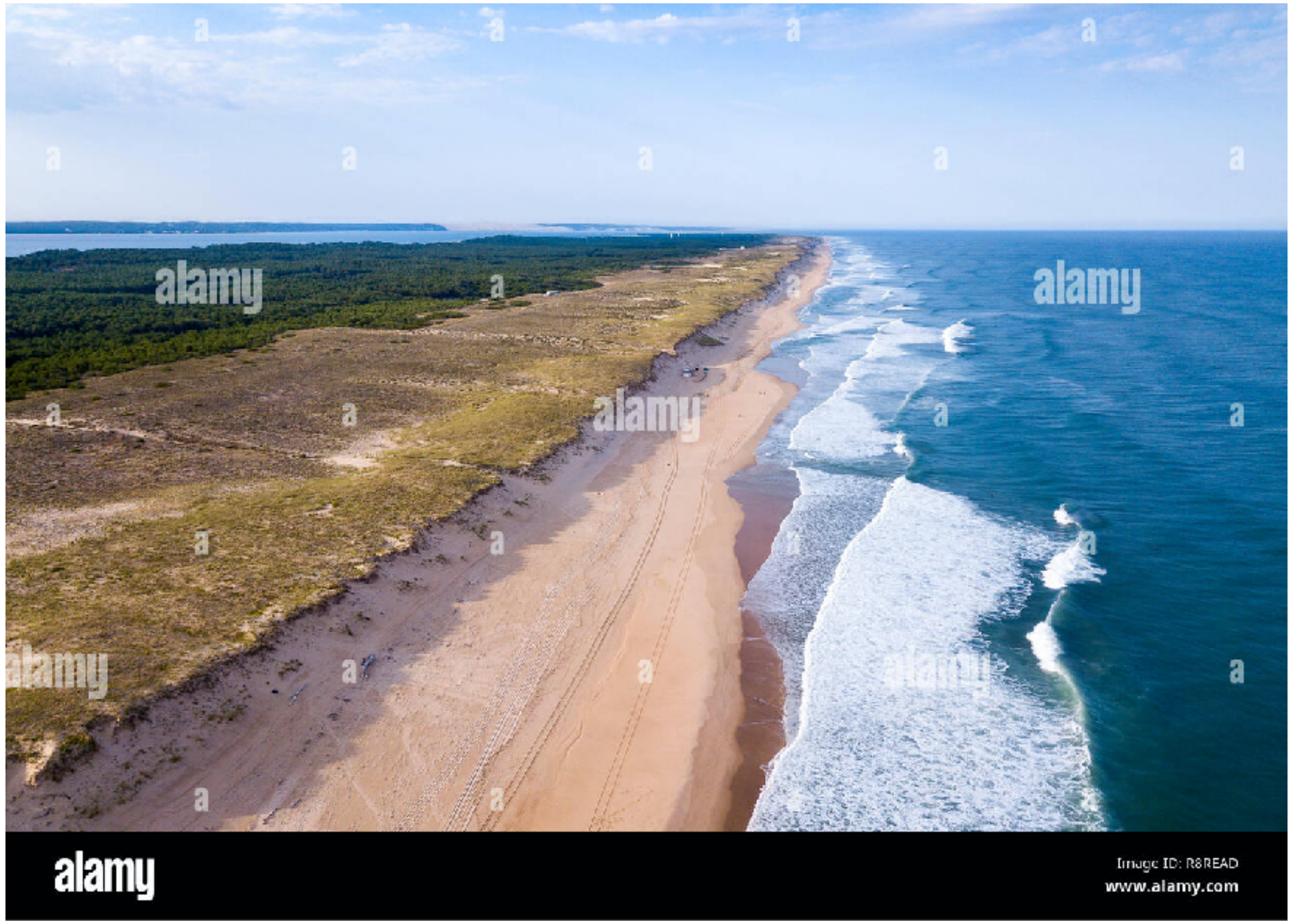

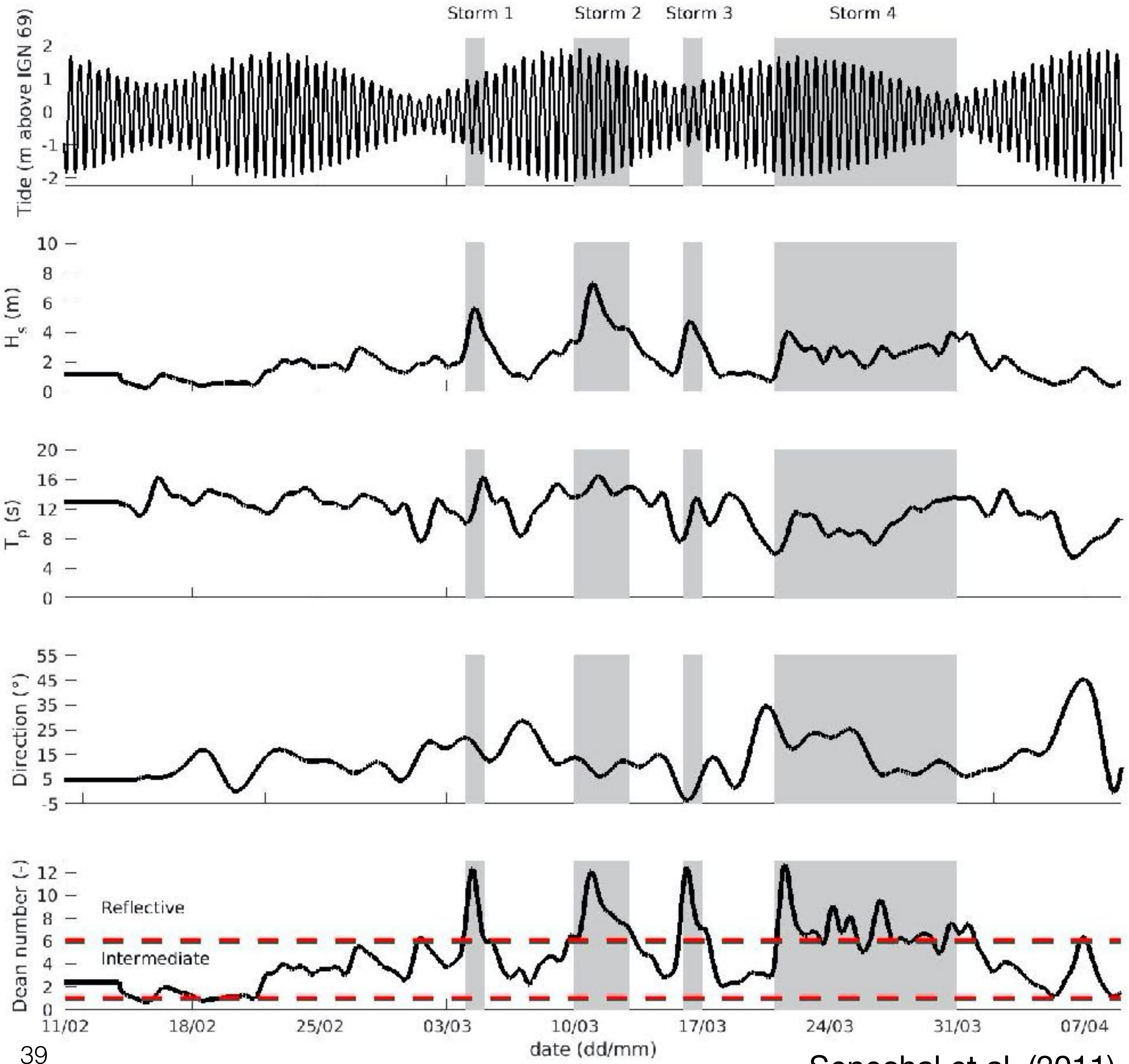

Senechal et al. (2011)

Measured bathymetries Truc vert ECORS 2008 field campaign

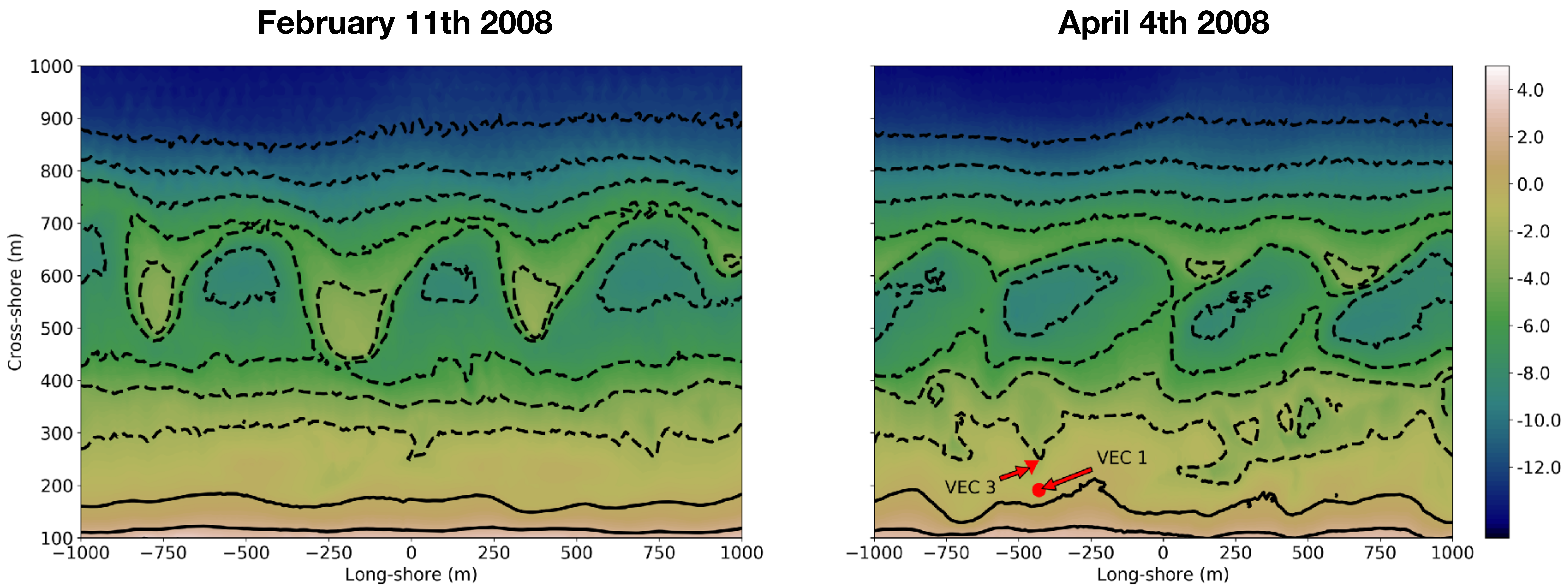

Senechal et al. (2011)

Morphodynamic simulations: bar positions & quantification

Brier Skill Score :

$$BSS = 1 - \frac{Var(Zp) - Var(Zm)}{Var(Zm) - Var(Zi)}$$

with :

- Zp predicted bathymetry
- Zm measured bathymetry
- Zi initial bathymetry

BSS	classification
0	Mauvaise
0,0-0,3	Pauvre
0,3-0,6	Raisonnable
0,6-0,8	Bonne
0,8-1,0	Excellente

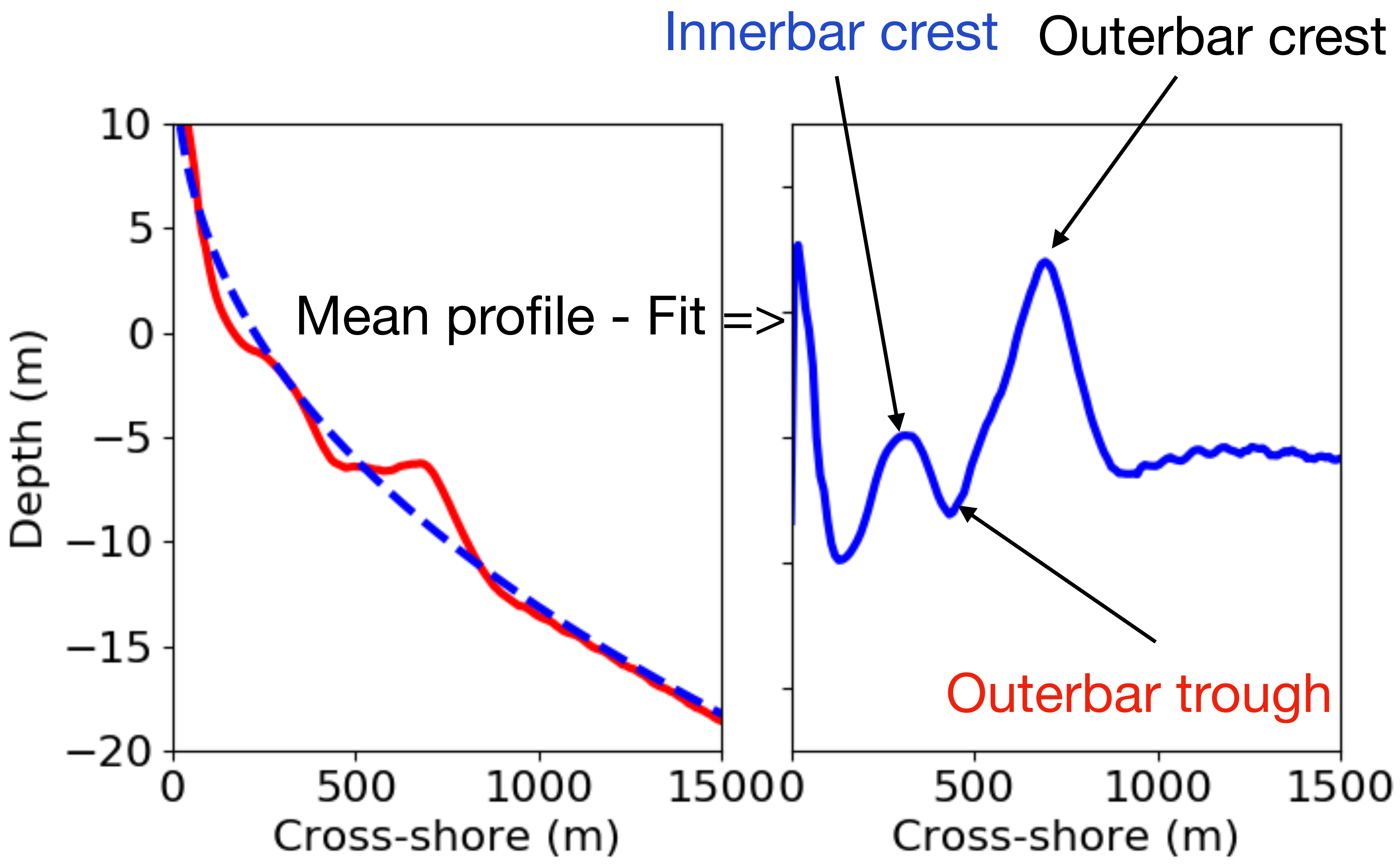

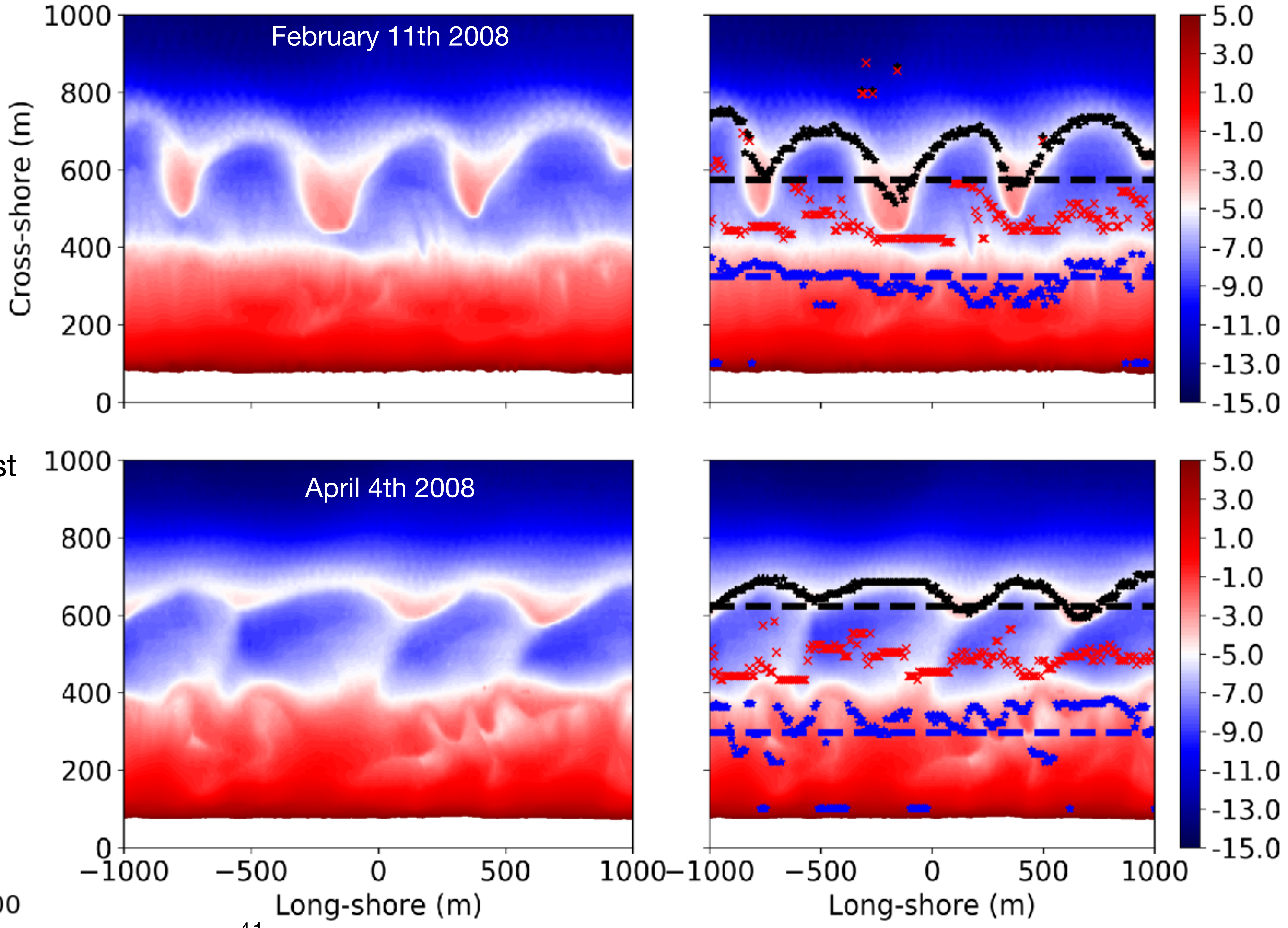

Vidéos

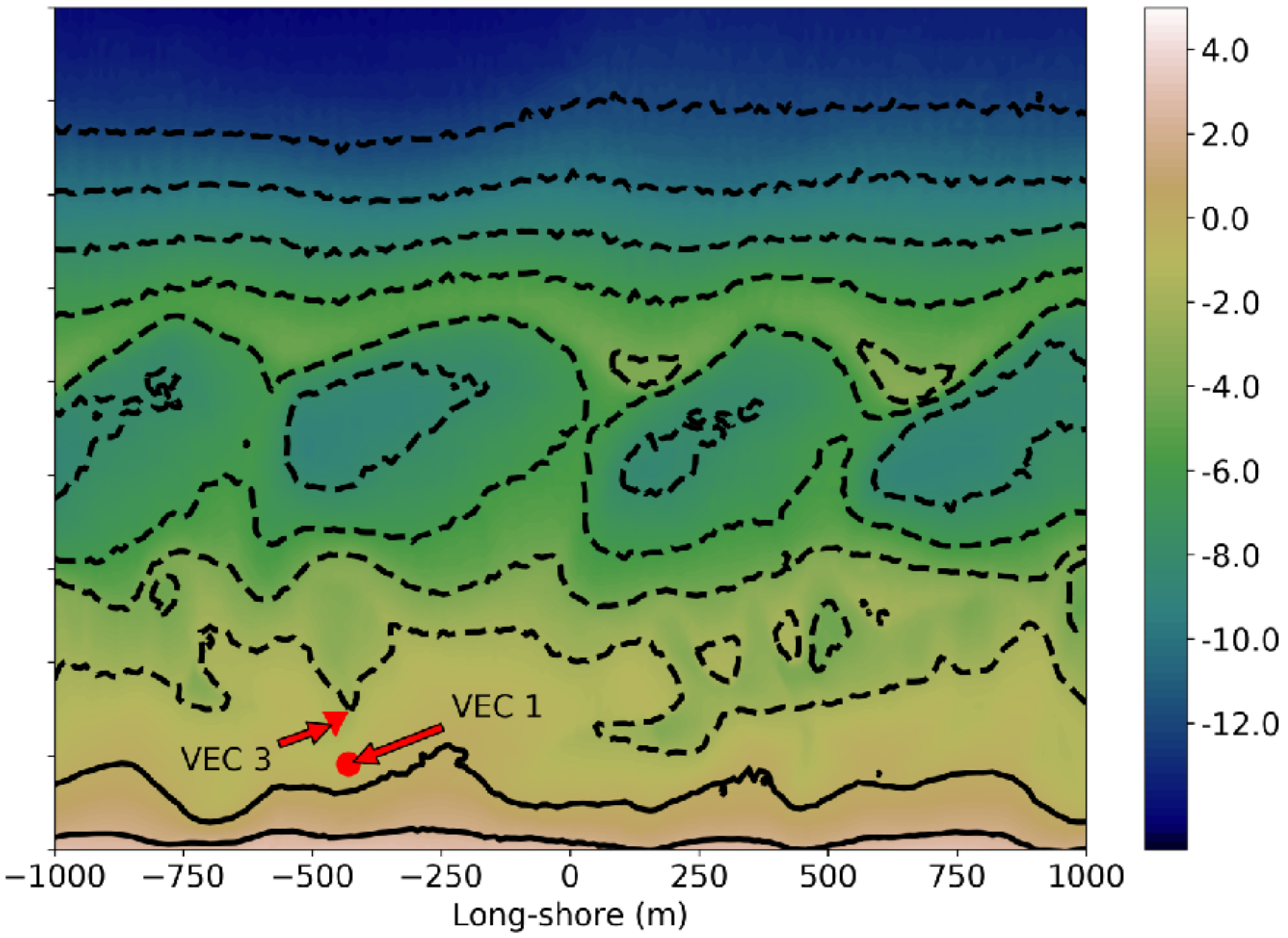

Measured in-situ

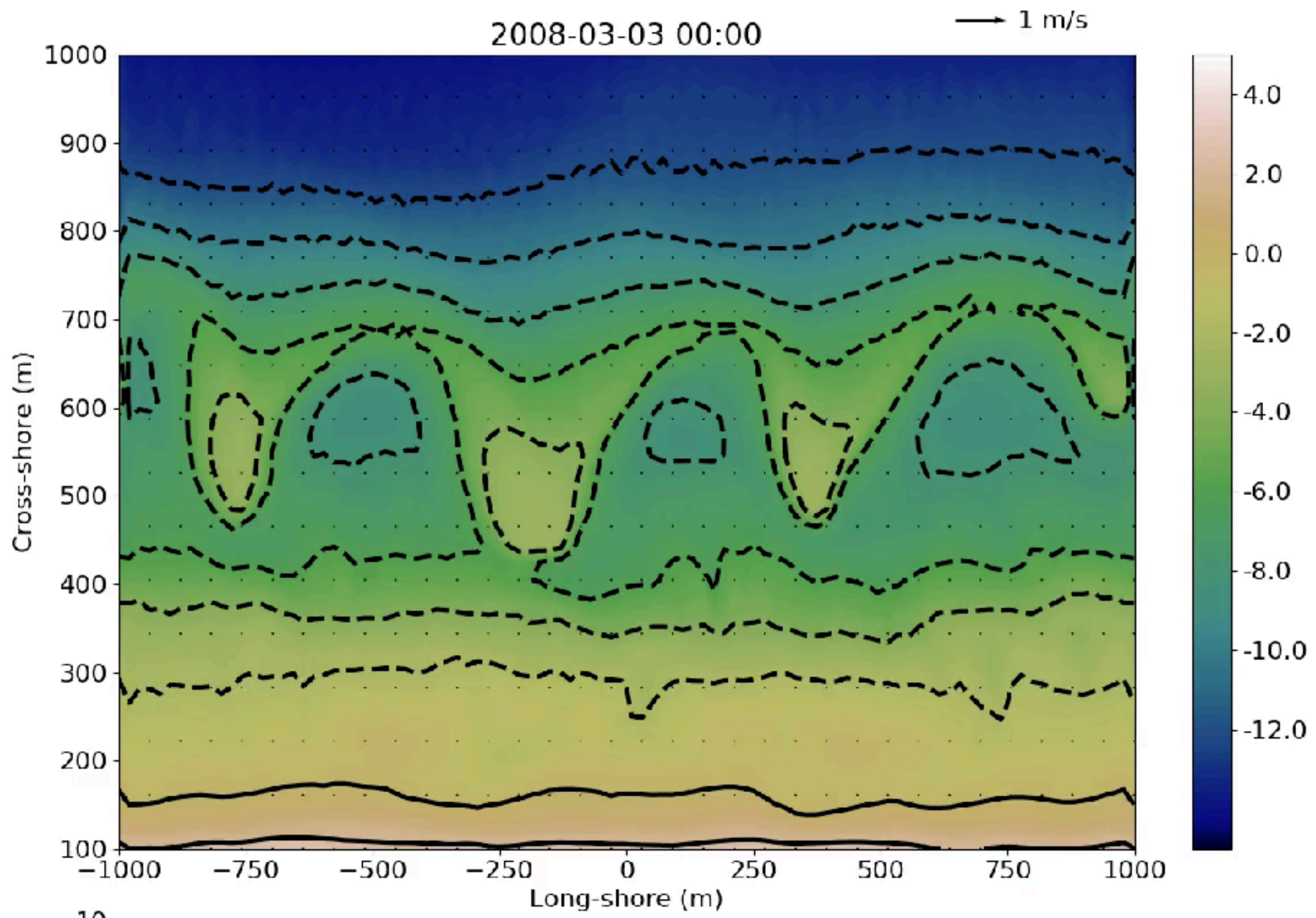

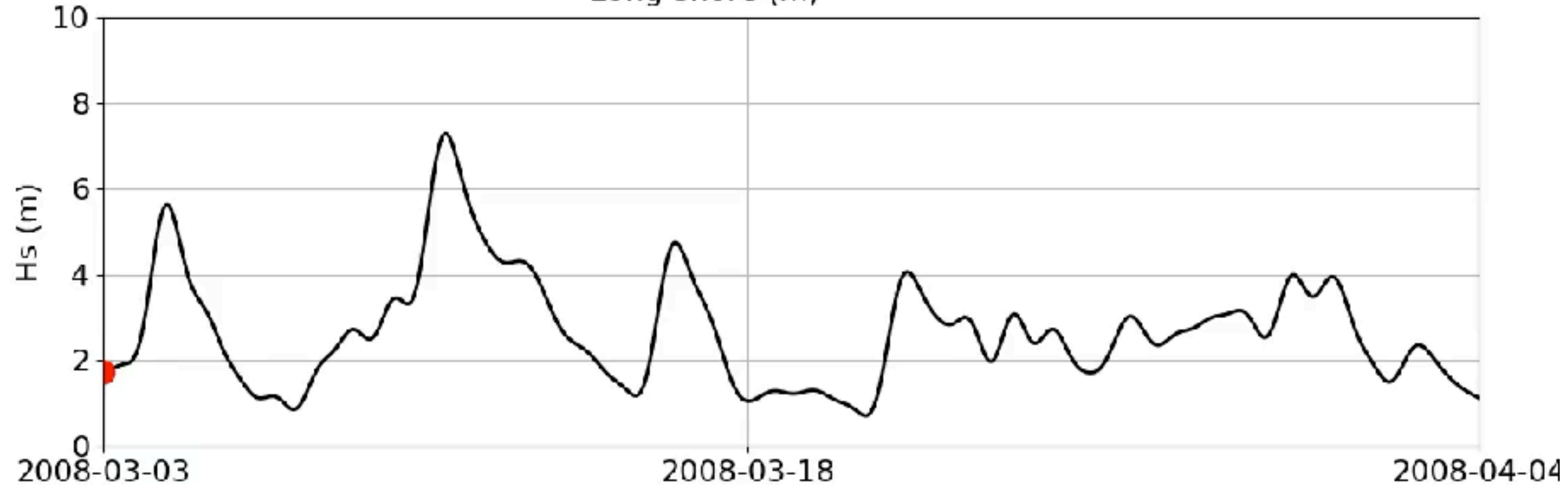

CROCO

Best BSS with CROCO

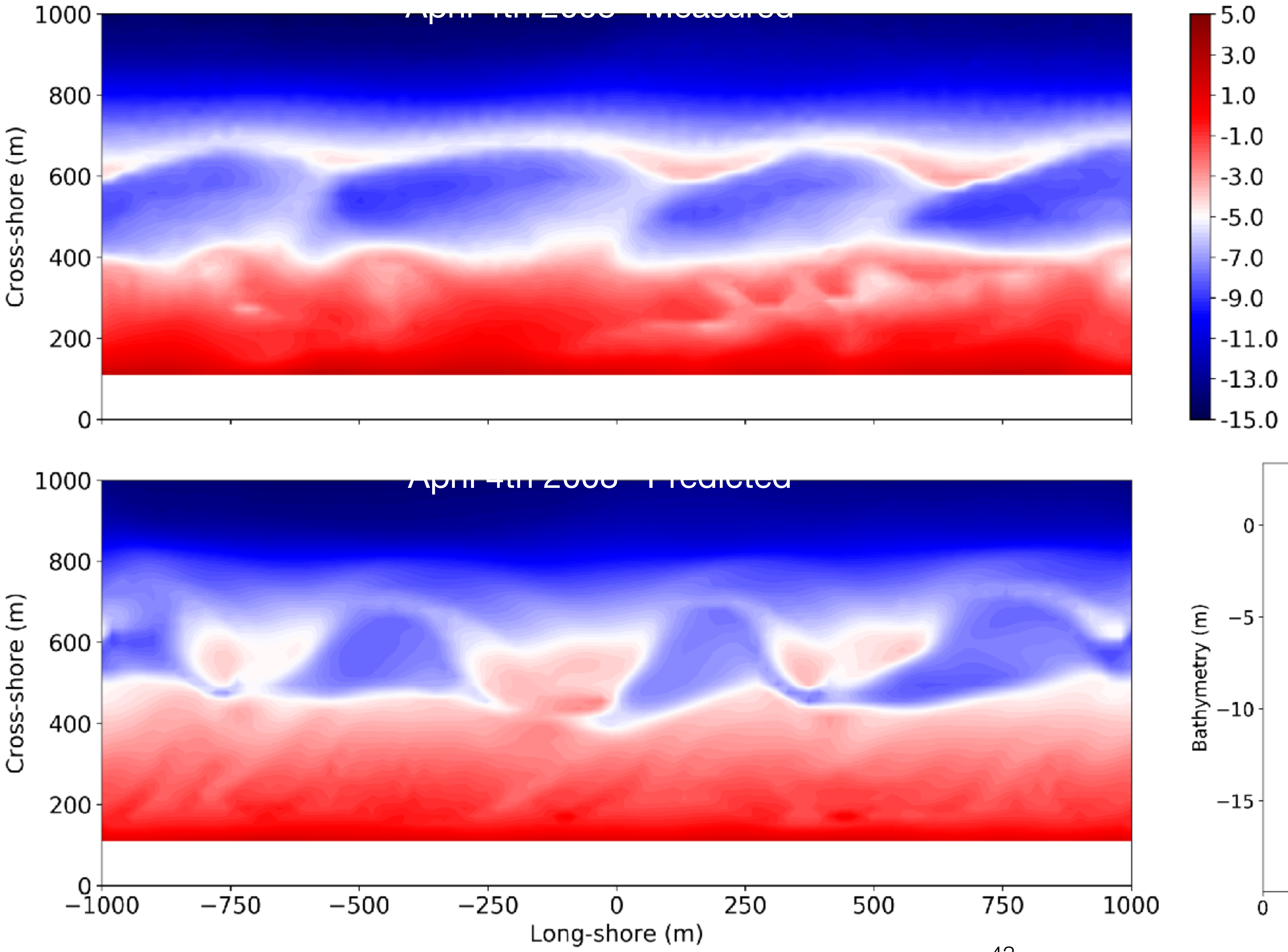

BSS = 0.11

Poor predictions of morphodynamics

- Improvement of wave and current modeling
- Improvement of sand transport modeling

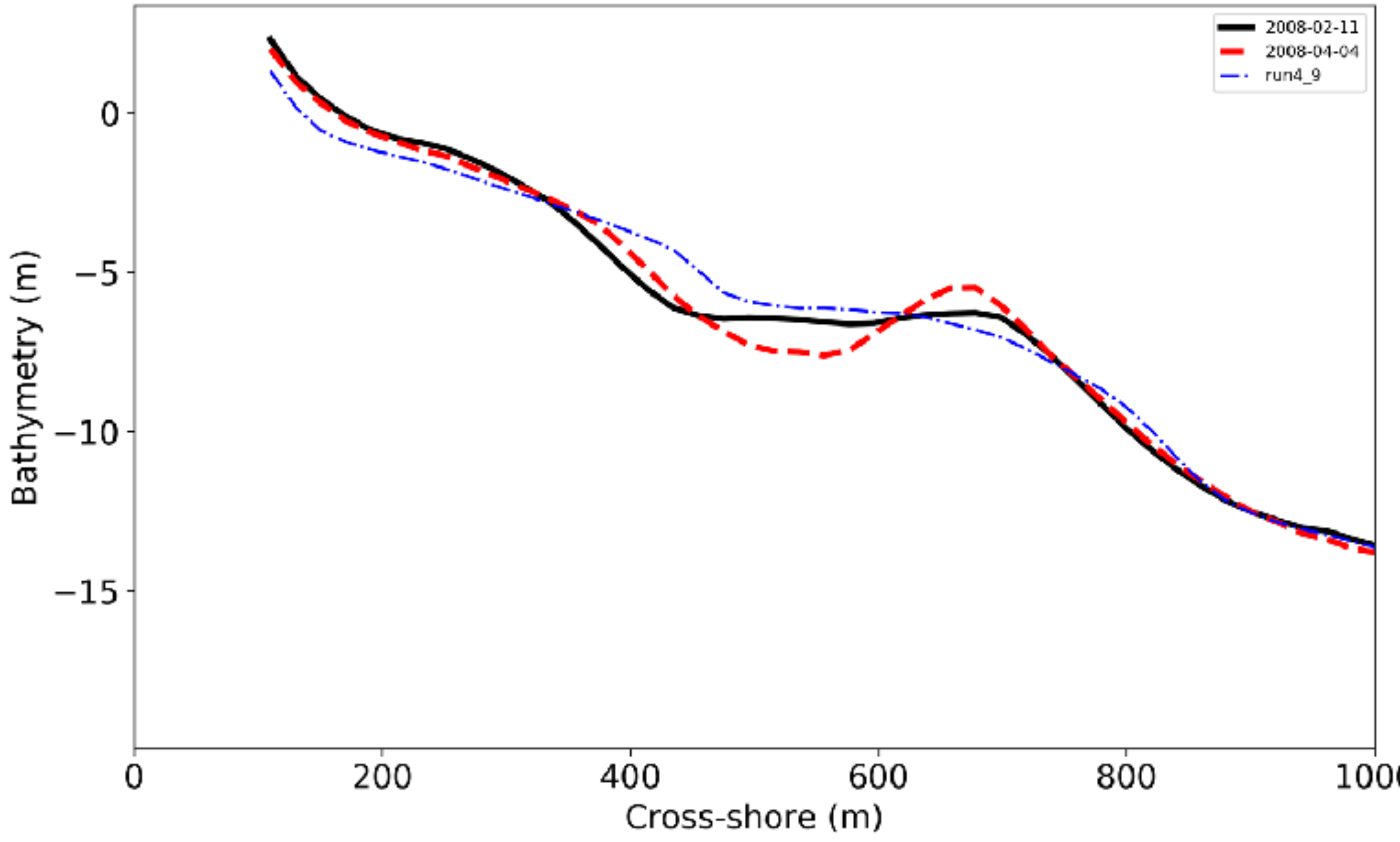

Conclusion on coastal modeling at « large scale »

- **Summary**
  - Coupled hydrodynamic-spectral wave-sediment transport equations models allows to simulate nearshore morphodynamics at time-scales of storm events
  - Predictability of nearshore morphodynamics is still poor and highly sensitive to empirical coefficients of the model
  - Main sources of errors:
    - Wave-current interactions
    - Wave propagation in shallow coastal zones (H ~ L/2)
    - Sediment transport modeling
- **Perspectives**
  - Use wave-resolving models for beach morphodynamics

    P. Marchesiello LEGOS is developing the non-hydrostatic version of CROCO

    PhD of Hung funded by IMPT at LAMA/LEGI, co-supervised by M. Kazakhova
  - Improve sand transport formula *(Camenen and Larson, 2007 ; van Der A et al., 2013)*

    Active research field in coastal engineering

    Use multi-phase flow approaches to infer the fine-scale processes and improve parametrizations (collab. with T. Hsu UD)

Open question: What are the stability conditions of nearshore numerical models when Δx and Δt tends to zero ?

What is the role of sandy beaches morphodynamical evolution on coastal flooding risks ?

Perspectives

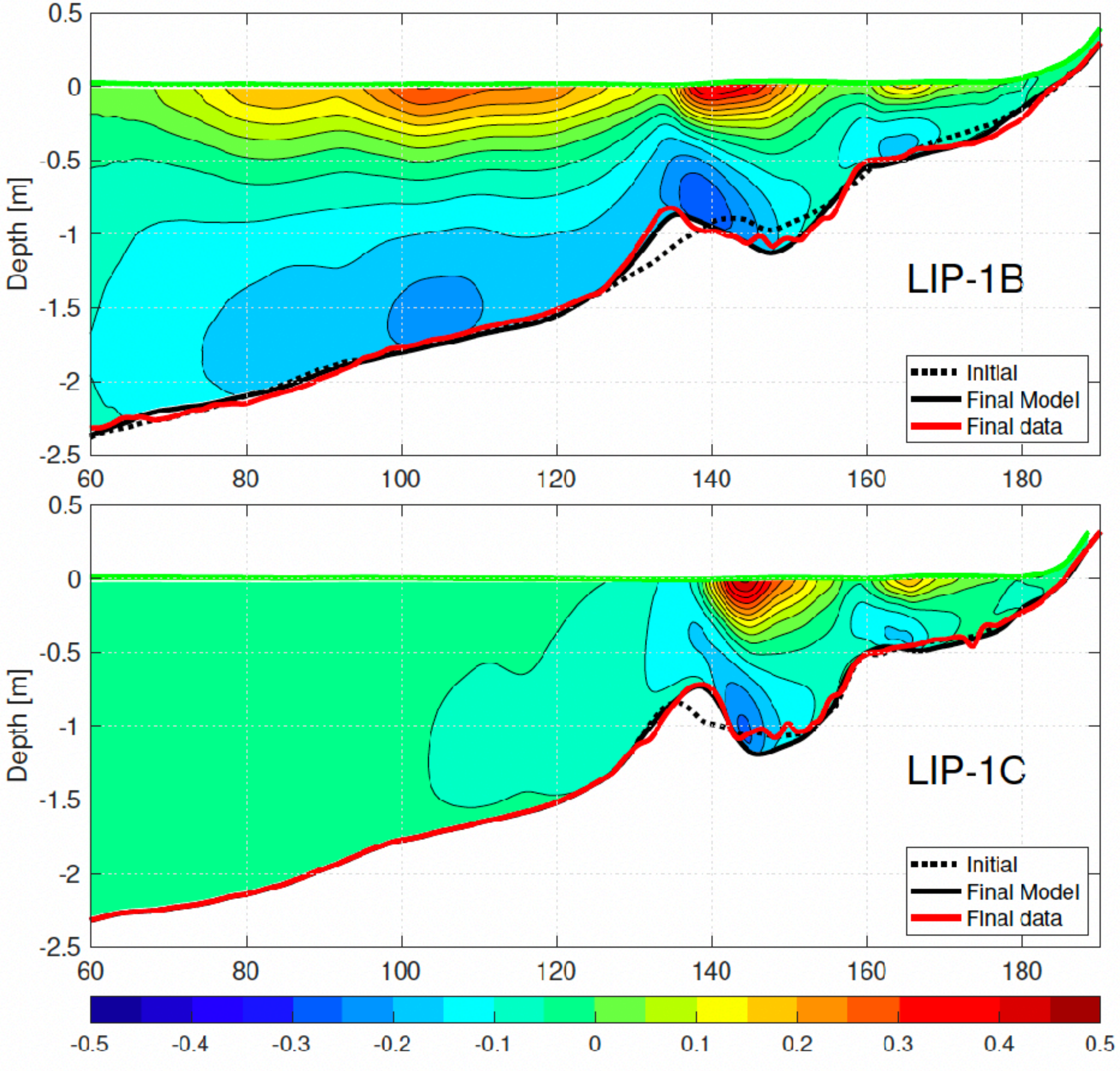

Wave-resolving models coupled with sediment transport

- CROCO model - P. Marchesiello (LEGOS, Toulouse)
  - 3D non-hydrostatic model
  - suspended-load and bed evolution
- Less modeling hypothesis but limited to shorter time-scales

Marchesiello et al. (submitted to ocean modeling)

Outline

1. Coastal modeling at « large scale »

2. Sediment transport modeling at the grain scale : turbulent and granular processes

3. Upscaling of fine-scale processes at intermediate scales

Motivations

Pros
- Simple
- Applicable at large-scale

Cons
- Empirical formulas
  - Especially bed-load
  - Large scatter (~100%)
  - Missing physics
- Arbitrary separation between bed-load and suspended-load

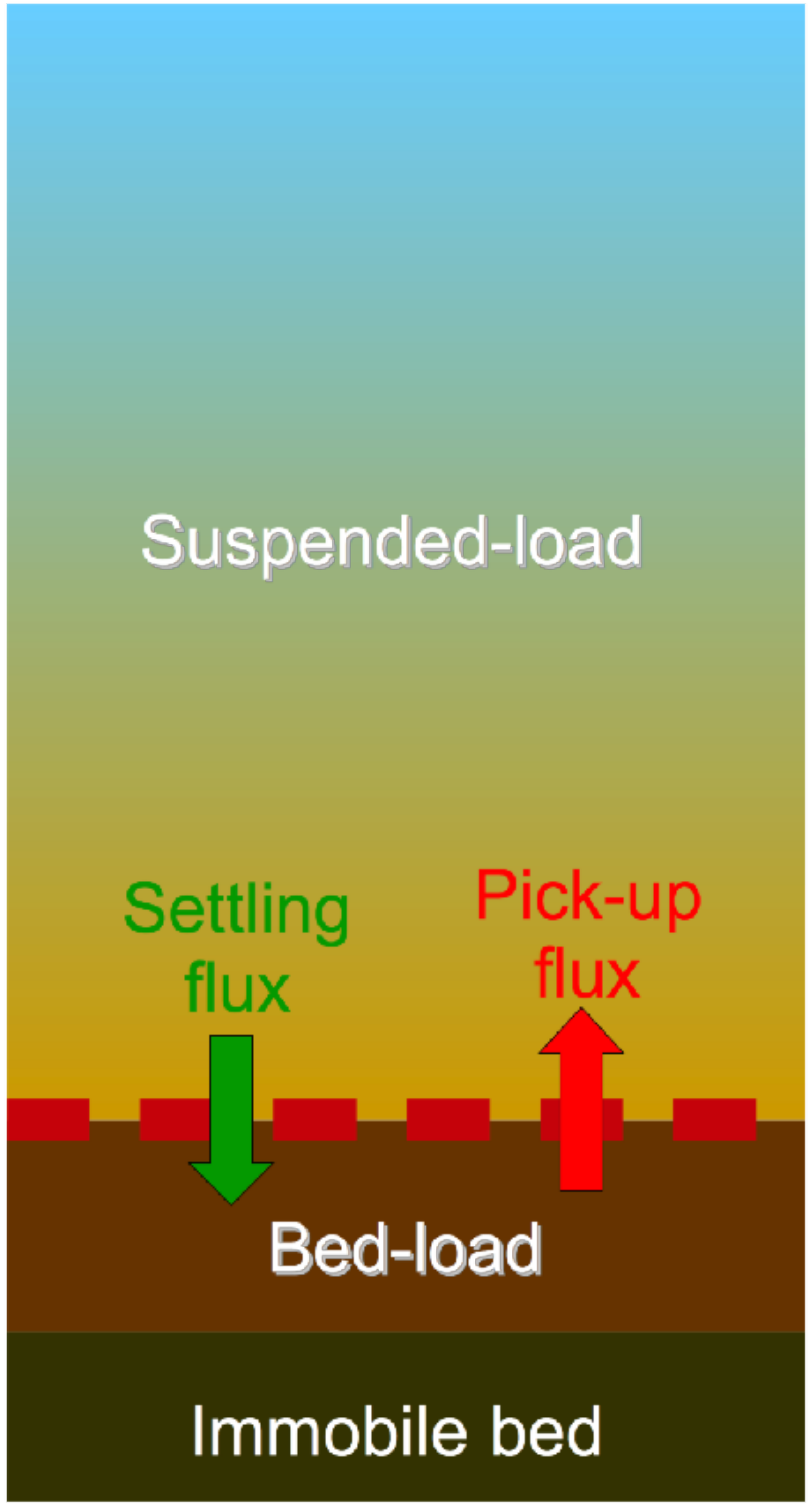

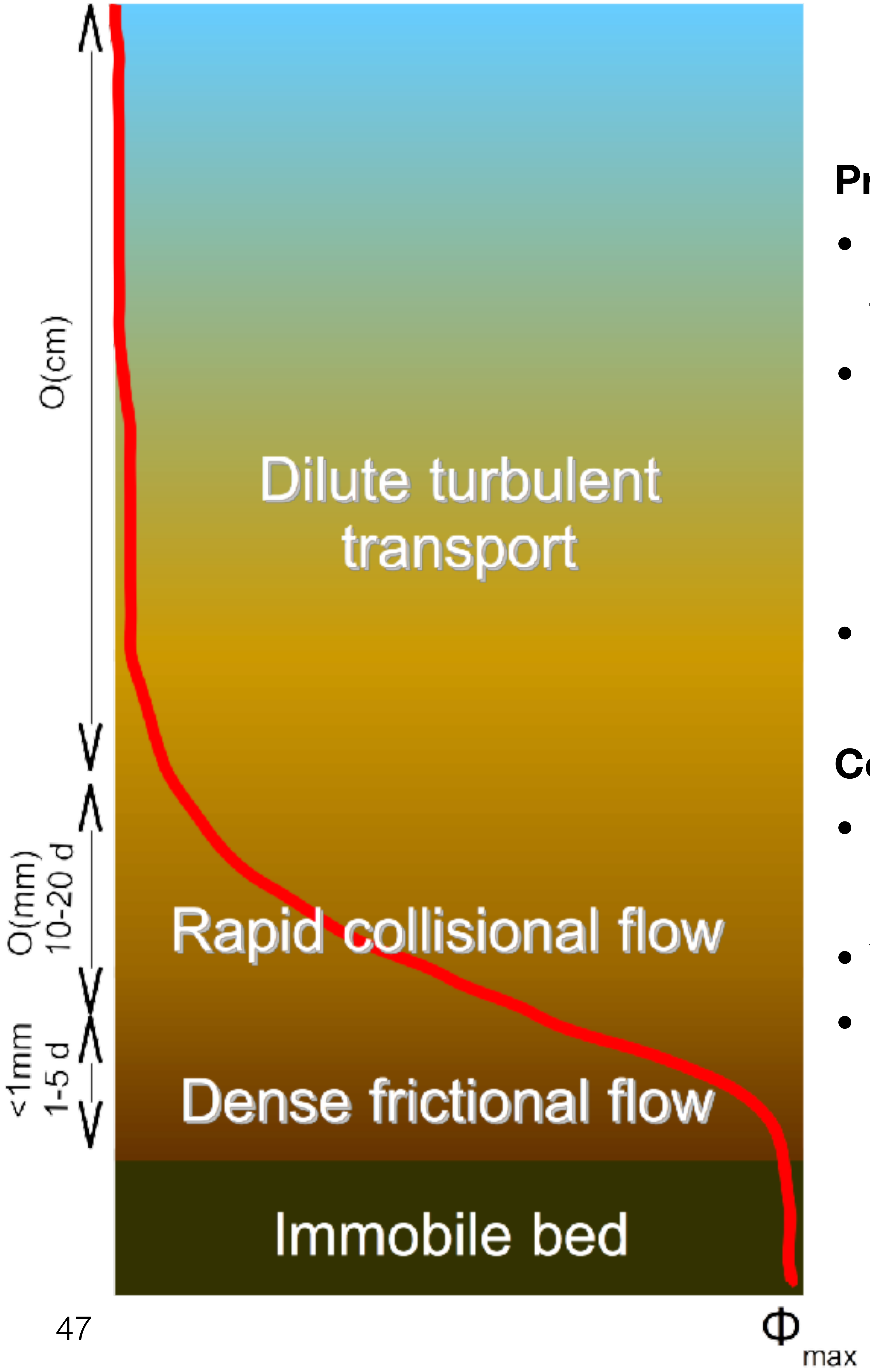

Pros
- Resolve continuously sediment transport profile
- Incorporate fine-scale processes:
  - Turbulence
  - Turbulence-particle interactions
  - Particle-particle interactions
- No arbitrary separation

Cons
- Complexity of the processes to be modeled
- Very expensive
- Limited to 'small scale' applications

Jenkins and Hanes JFM (1998)

The role of granular interactions & fluid turbulence

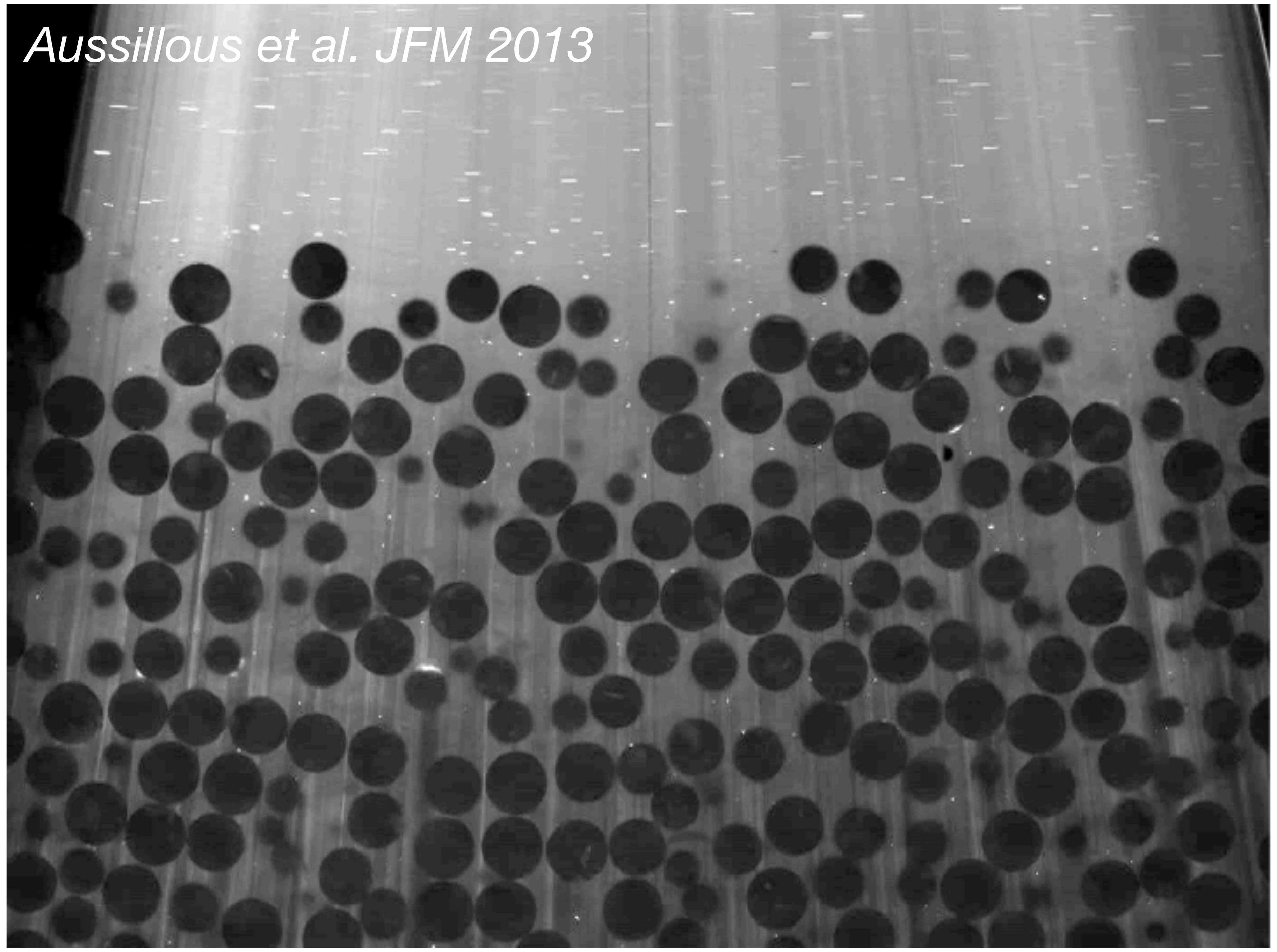

$$d_p = 2 \text{ mm} \;\; ; \;\; \frac{\rho^p}{\rho^f} = 1.19$$

$$Re \approx 1 \;\; ; \;\; \theta \approx 0.5 \;\; ; \;\; S \approx \infty$$

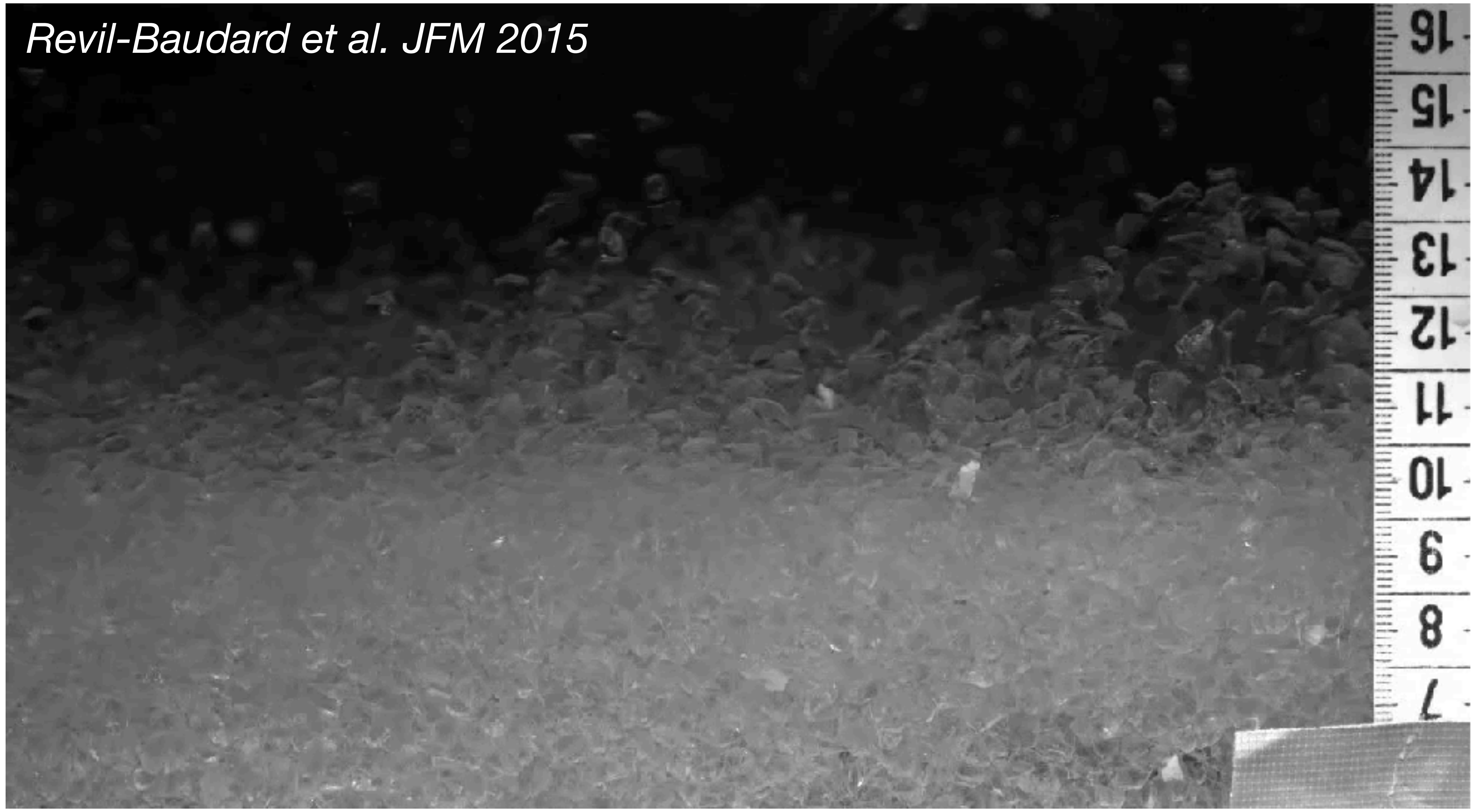

$$d_p = 3 \text{ mm} \;\; ; \;\; \frac{\rho^p}{\rho^f} = 1.19$$

$$Re \approx 10^5 \;\; ; \;\; \theta \approx 0.5 \;\; ; \;\; S \approx 1$$

Dimensionless numbers

Shields number: $\theta = \dfrac{\rho^f u_*^2}{\Delta\rho g d_p} > 0.3$

Stokes number: $St = \dfrac{t_p}{t_f}$

Suspension number: $S = \dfrac{W_s}{u_*}$

Reynolds number: $Re = \dfrac{UH}{\nu^f}$

Granular interactions

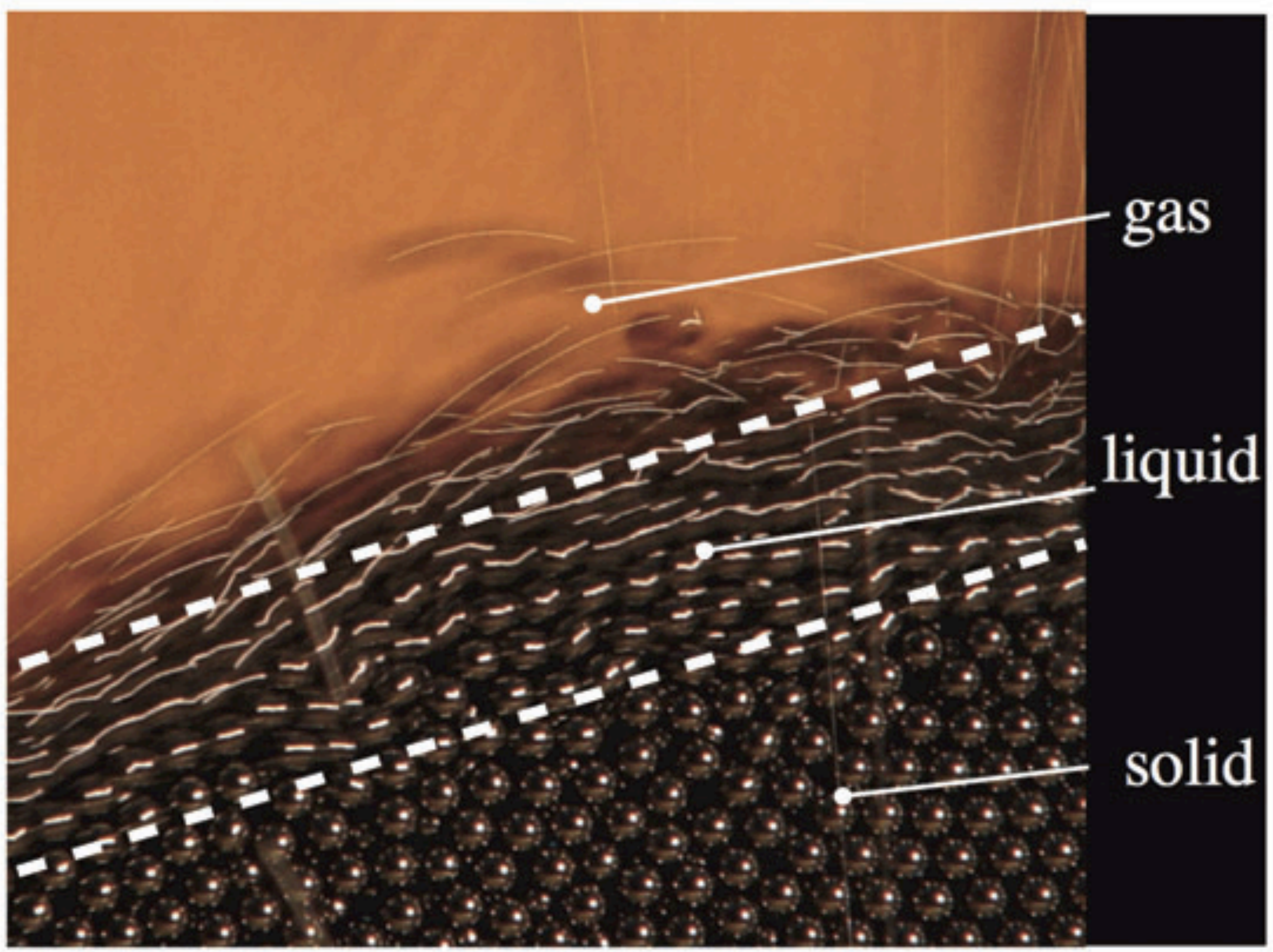

Gaseous regime <—> kinetic theory of granular flows

- Dilute and rapid flow
- Particles interact by collision

Liquid regime <—> μ(I) - ϕ(I) rheology

- Dense granular media flows like a liquid
- particles interact through both collision and frictional contacts

Dense quasi-static regime <—> elasto-plastic model

- Very slow deformation
- Particles interact through frictional contacts

GDR Midi (2004), Forterre and Pouliquen (2008)

Kinetic theory of dense granular flows

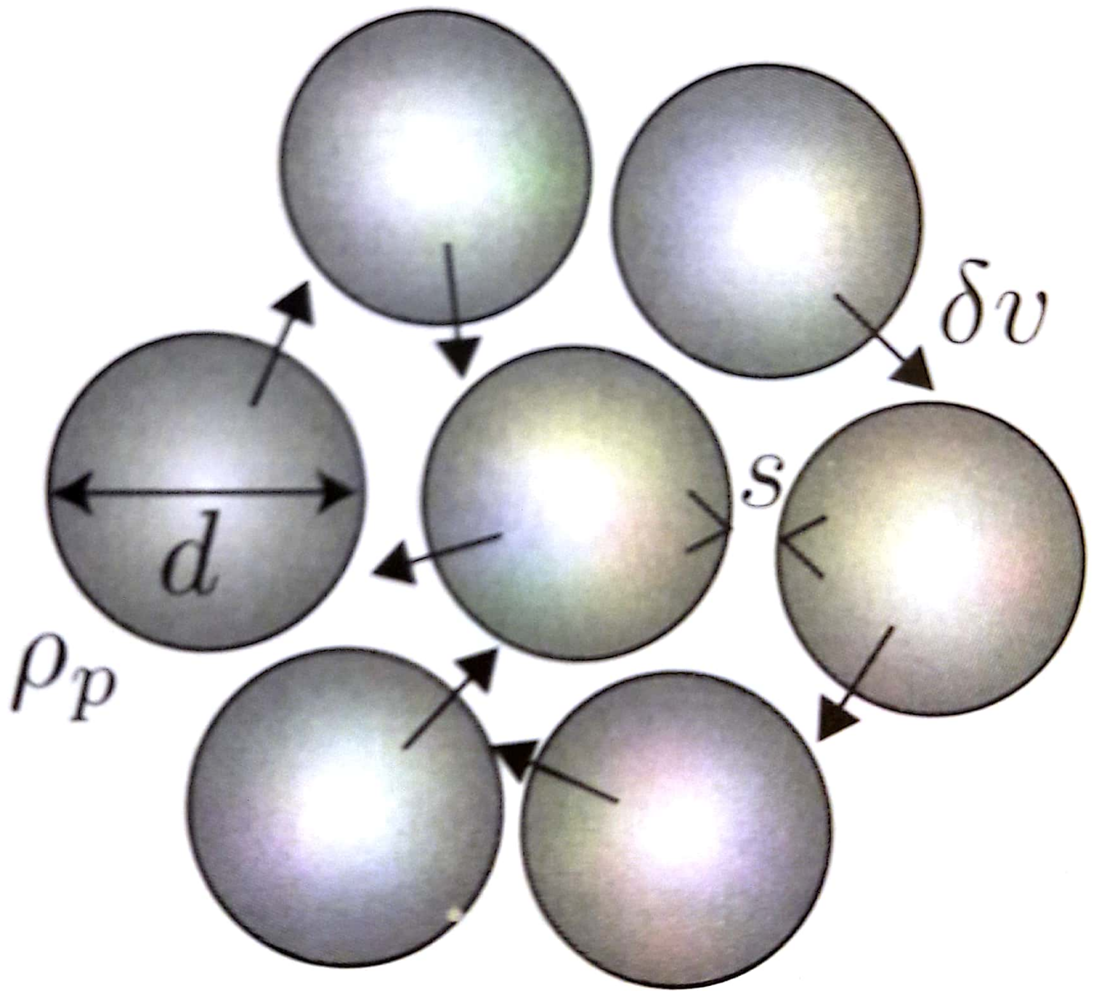

- Particles interact through binary and instantaneous collisions only
- The granular media is dense: ϕ is close to ϕ_m or $s << d$
- Granular temperature: $\Theta = <\delta v^2>$ (Ogawa, 1978)

The granular gas may be described using Navier-Stokes equations:

$$\nabla \cdot \overrightarrow{u^p} = 0$$

$$\phi \rho_p \left(\frac{\partial \overrightarrow{u^p}}{\partial t} + \overrightarrow{u} \cdot \nabla \overrightarrow{u^p} \right) = \phi \rho_p \overrightarrow{g} - \nabla P^p + \nabla \left(2\eta^p \bar{\bar{\dot{\epsilon}}} \right)$$

$$\frac{1}{2} \phi \rho_p \left(\frac{\partial \Theta}{\partial t} + \overrightarrow{u^p} \cdot \nabla \Theta \right) = 2\eta^p \bar{\bar{\dot{\epsilon}}} : \bar{\bar{\dot{\epsilon}}} + \nabla (K \nabla \Theta) - \Gamma$$

Radial distribution function:

$$g_0(\phi) = \frac{2 - \phi}{2(1 - \phi)^3}$$

with

Granular pressure: $P^P = \rho_p \, \phi \left(1 + 2 \, (1 + e) \, \phi \, g_0(\phi)\right) \, \Theta$

e: restitution coefficient for binary collisions

Granular viscosity: $\eta^P = f_2(\phi) \, \rho_p \, d \, \Theta^{1/2}$

Collisional dissipation: $\Gamma = f(\phi) \, \frac{\rho_p}{d} \, (1 - e^2) \, \Theta^{3/2}$

Haff (1983) ; Andreotti, Forterre and Pouliquen (2013)

Granular interactions: μ(I) rheology

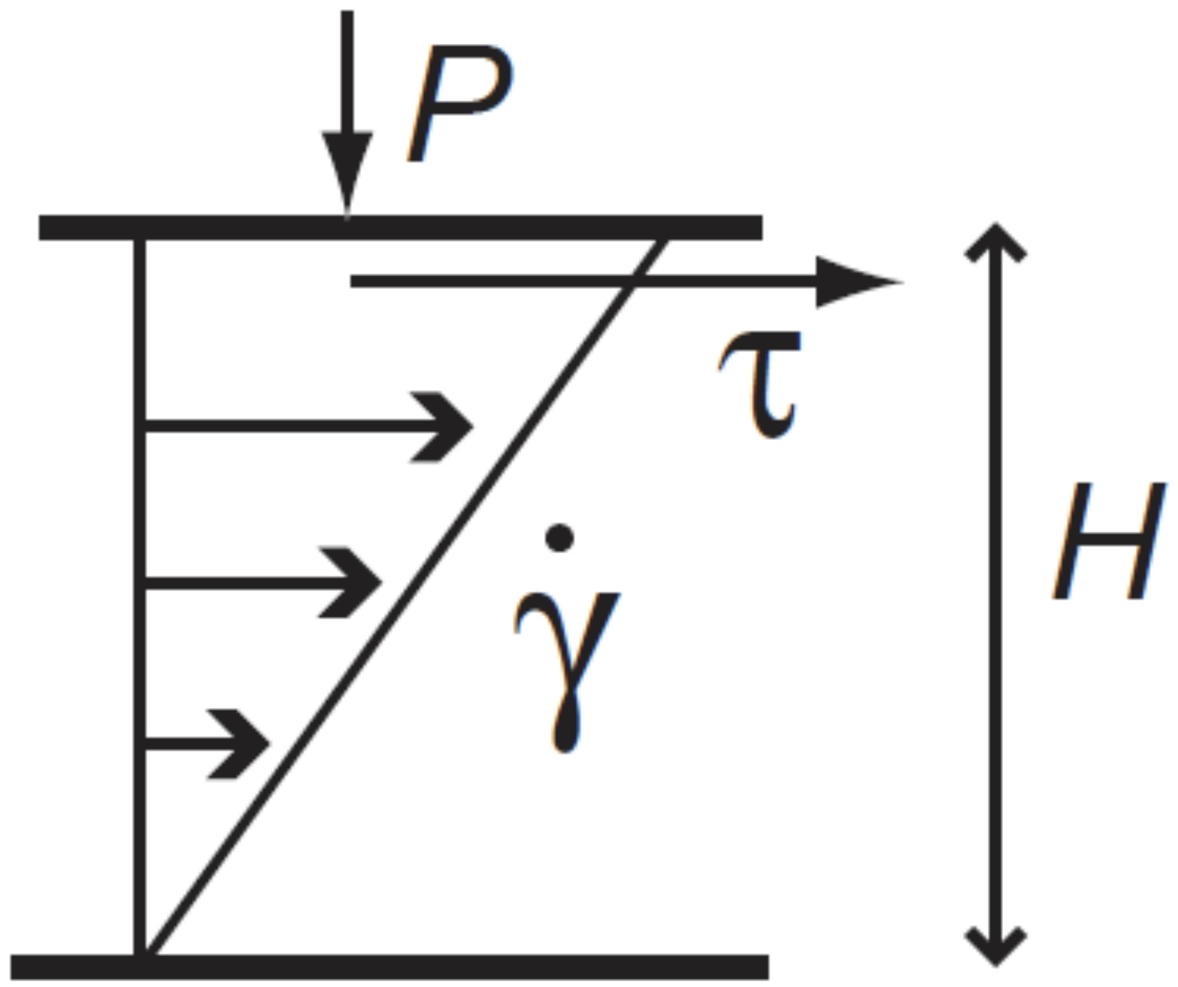

- Monodisperse spherical particles with density ρ_p and diameter d
- Imposed pressure P and velocity V on the top plate $\Rightarrow \dot{\gamma} = \dfrac{V}{H}$
- Measure the shear stress τ that develops on the top plate

For large system H>>d a single dimensionless number control the system: $I = \dfrac{\dot{\gamma}\, d}{\sqrt{P/\rho_p}}$

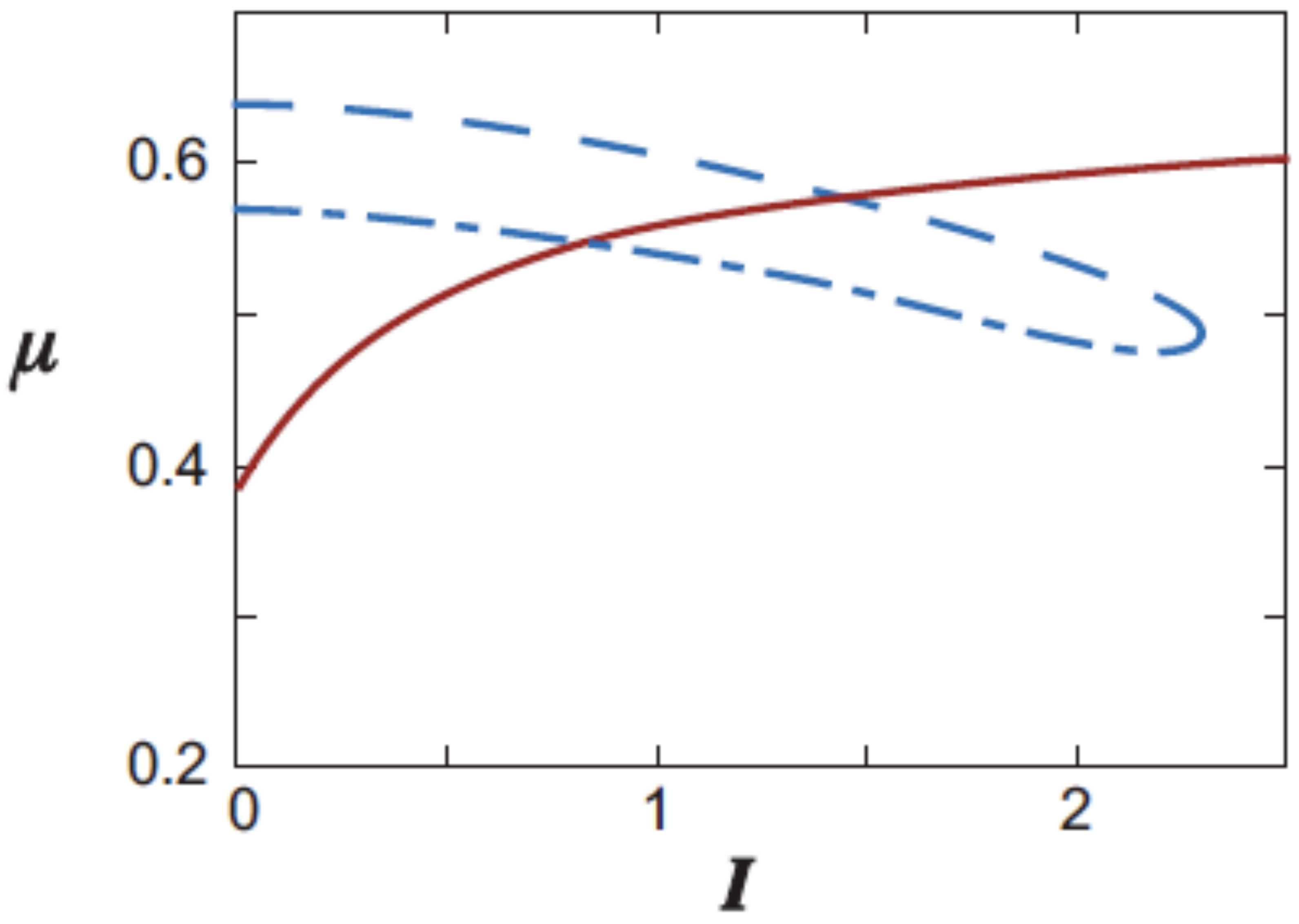

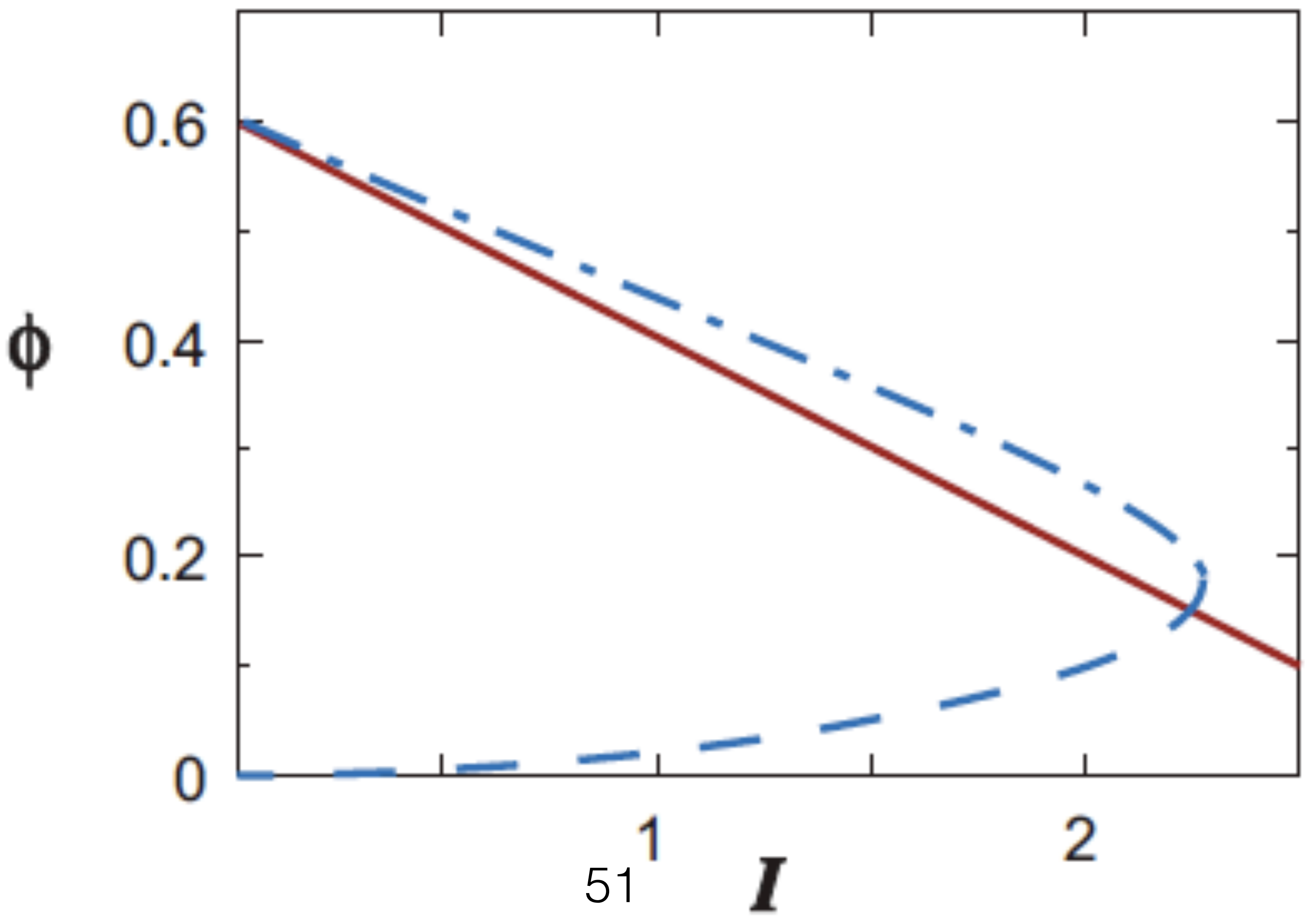

$$\boxed{\begin{aligned}\mu(I) &= \mu_s + \frac{\mu_2 - \mu_s}{I_0/I + 1} \\ \phi(I) &= \phi_{max} + (\phi_{min} - \phi_{max})\, I\end{aligned}}$$

$$\tau = \mu(I)\ P$$

Da Cruz et al. (2004), Lois et al. (2005)

Eulerian-Lagrangian model derivation

Local mass & momentum conservation for a fluid-particle mixture

$$\nabla.\vec{u} = 0 \quad \text{and} \quad \frac{d\rho\vec{u}}{dt} + \nabla.(\rho\vec{u}\otimes\vec{u}) = \nabla.\overline{\overline{\sigma}} + \rho\vec{g}$$

Maurin (2015) ; Maurin et al. (2015)

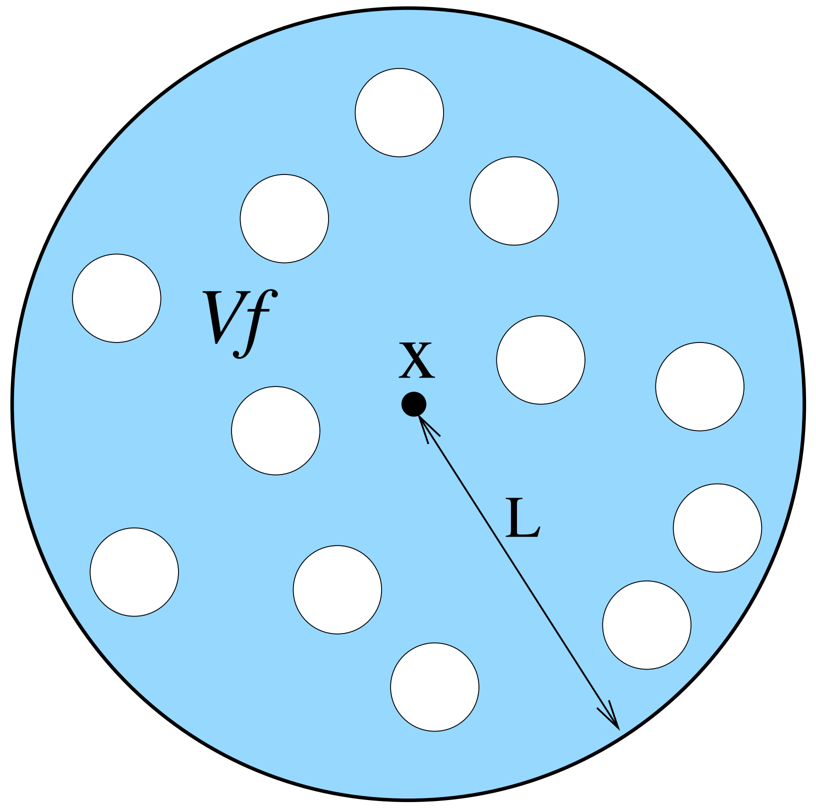

Local spatial averaging

Jackson (2000)

$$\langle f\rangle^f(\vec{x},t) = \frac{1}{\epsilon}\int_{V_f(t)} f(\vec{y},t)G_L(|\vec{x}-\vec{y}|)dV_y$$

Discrete Element Modeling

Newton's eq.: $m_p\frac{\mathrm{d}\overrightarrow{v^p}}{\mathrm{d}t} = \overrightarrow{f_c^p} + \overrightarrow{f_g^p} + \overrightarrow{f_f^p}$ + angular mom.

Contact forces: $\overrightarrow{f_c^p} = \sum_{k\in\mathcal{N}} \overrightarrow{f_c^{pk}}$ *(spring-dashpot model)*

Gravity force: $\overrightarrow{f_g^p} = (\pi/6)\ d^3\ \rho^p\ \overrightarrow{g}$

Fluid phase mass and momentum equations

$$\frac{\partial\epsilon}{\partial t} + \nabla\left(\epsilon\langle\overrightarrow{u}\rangle^f\right) = 0$$

$$\rho^f\left[\frac{\partial\epsilon\langle\overrightarrow{u}\rangle^f}{\partial t} + \nabla\left(\epsilon\langle\overrightarrow{u}\rangle^f\otimes\langle\overrightarrow{u}\rangle^f\right)\right] = \nabla\sigma^f - n\vec{f} + \epsilon\rho^f g$$

Fluid-particle coupling forces

Buoyancy force: $\overrightarrow{f_b^p} = -\pi d_p^3/6\,\nabla p$

Drag force: $\overrightarrow{f_d^p} = \frac{1}{2}\ \rho^f\ C_D\ \frac{\pi d_p^2}{4}\left|\overrightarrow{u^f} - \overrightarrow{v^p}\right|\left(\overrightarrow{u^f} - \overrightarrow{v^p}\right)$

Eulerian-Lagrangian bed-load simulations (Maurin PhD, 2015)

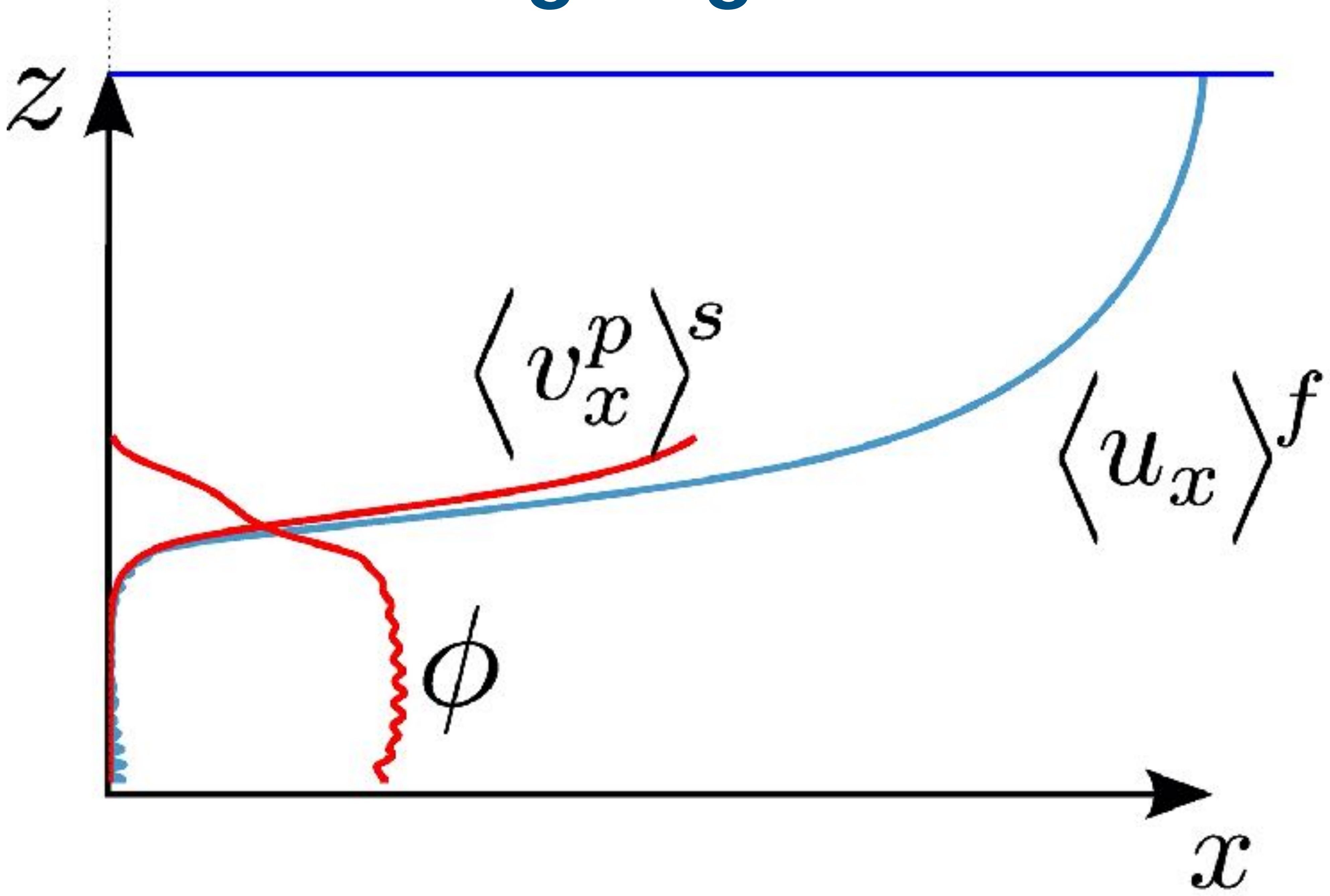

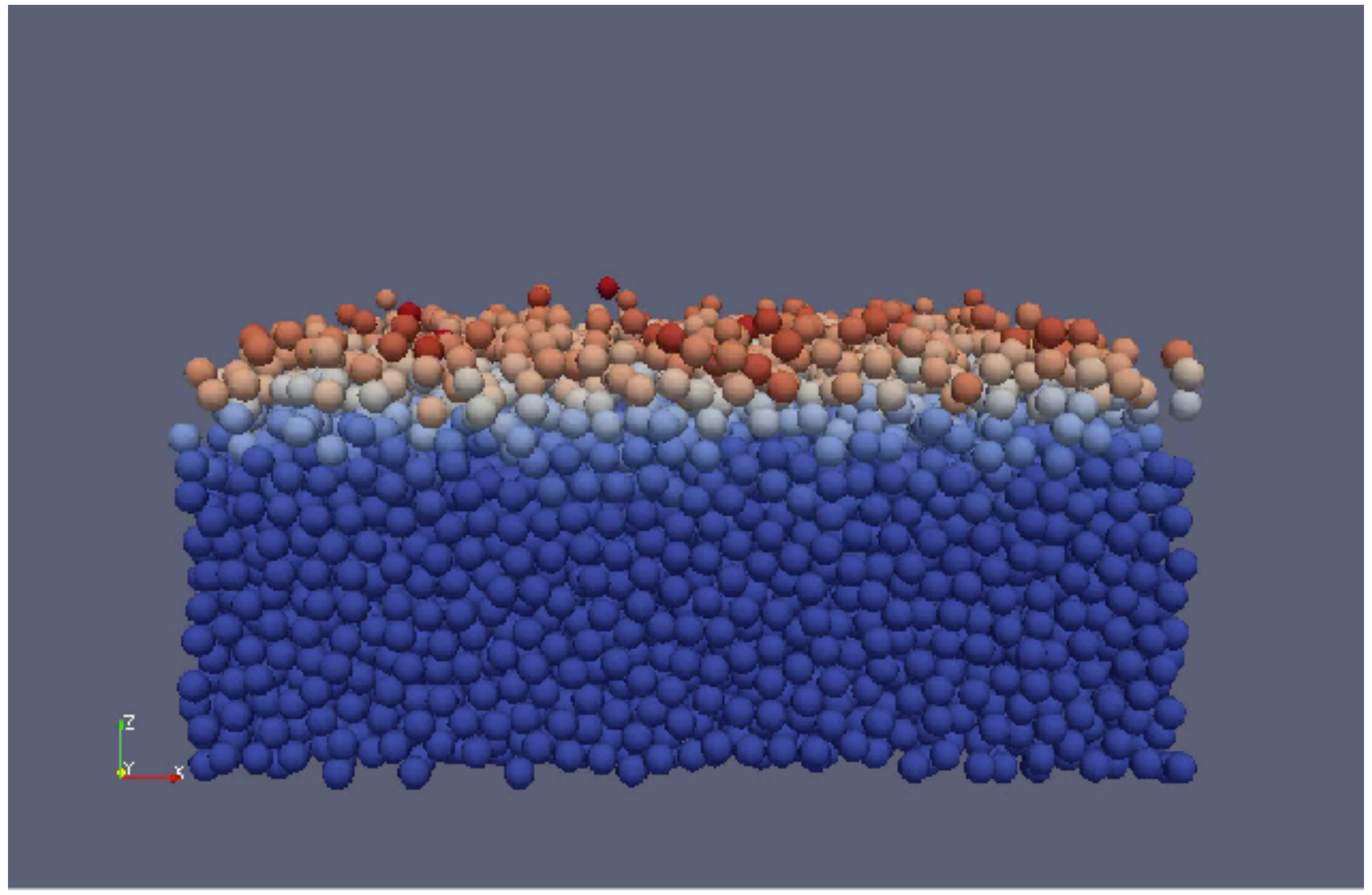

$$(1-\phi)\rho^f \frac{\partial < u_x^f >}{\partial t} = \underbrace{\frac{\partial R_{xz}^f}{\partial z}}_{Turb.\ stress} + \underbrace{\frac{\partial \tau_{xz}^f}{\partial z}}_{Visc.\ stress} + \underbrace{(1-\phi)\ \rho^f\ g\ S_0}_{Gravity} - \underbrace{n \langle f_{D_x} \rangle^s}_{Drag}$$

coupling

Newton's law

$$m_p \frac{\mathrm{d}\mathbf{v}^p}{\mathrm{d}t} = \underbrace{\mathbf{f}_c^p}_{Contact} + \underbrace{\mathbf{f}_g^p}_{Gravity} + \underbrace{\mathbf{f}_b^p}_{Buoyancy} + \underbrace{\mathbf{f}_D^p}_{Drag}$$

1DV Fluid model *(chauchat et al. 2013)*

DEM model (YADE)

- Turbulence model = Mixing length $\nu_t^f = l_m^2 \left| \frac{d\langle u_x^f \rangle}{dz} \right|$ with $l_m = \kappa \int_{-\infty}^{z} \frac{\phi_m - \phi}{\phi_m} dz$

Revil-Baudard and Chauchat (2013)

- Validation on Frey (2014) experiments (not shown here)

Maurin PhD (2015) ; Maurin et al. PoF (2015)

Dense granular flow rheology in bed-load transport

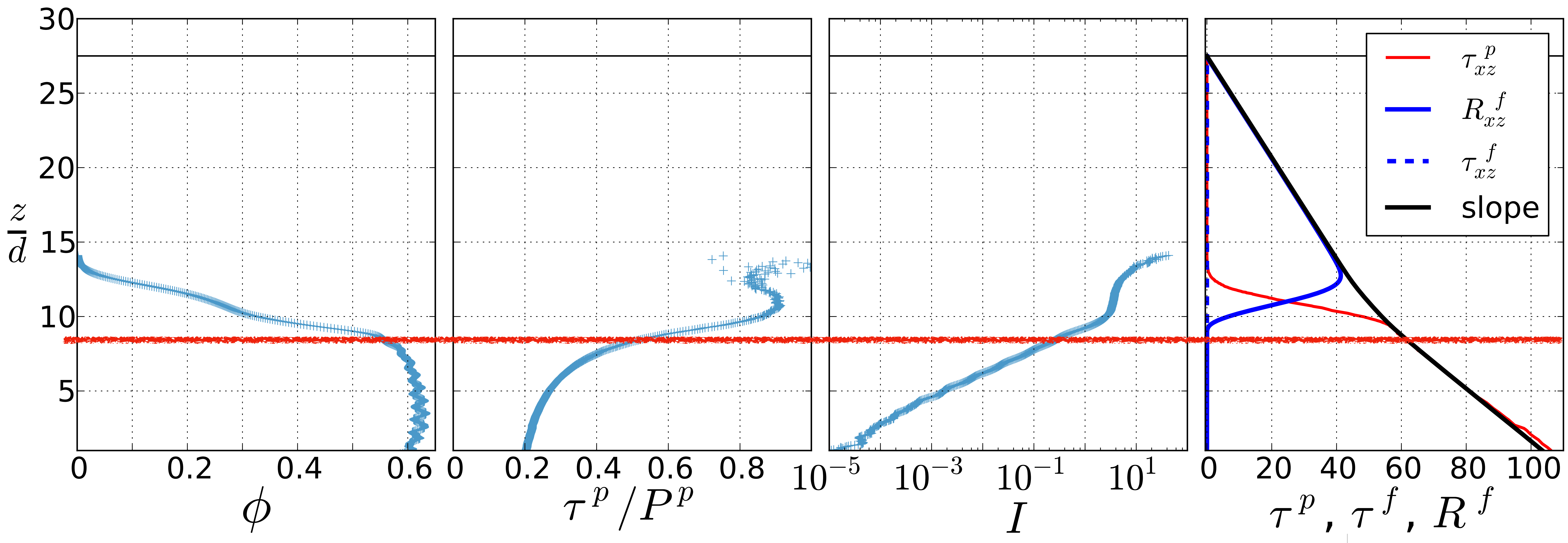

Stress tensor from contact forces and velocity fluctuations

$$\langle \sigma_{ij}^p \rangle (z) = -\frac{1}{V(z)} \sum_{\alpha \in V(z)} m^\alpha v_i'^\alpha v_j'^\alpha - \frac{1}{V(z)} \sum_{c \in V(z)} f_i^c b_j^c$$

Shear and Normal stresses: $\tau^p(z_i), P^p(z_i) \longrightarrow \mu = \frac{\tau^p}{P^p}$ **Friction coefficient**

Velocity shear rate: $\dot{\gamma}^p(z_i) = dv^p/dz \longrightarrow I(z_i) = \frac{\dot{\gamma}^p \, d}{\sqrt{P^p/\rho^p}}$ **Inertial number**

Maurin et al. JFM (2016)

Dense granular flow rheology in bed-load transport

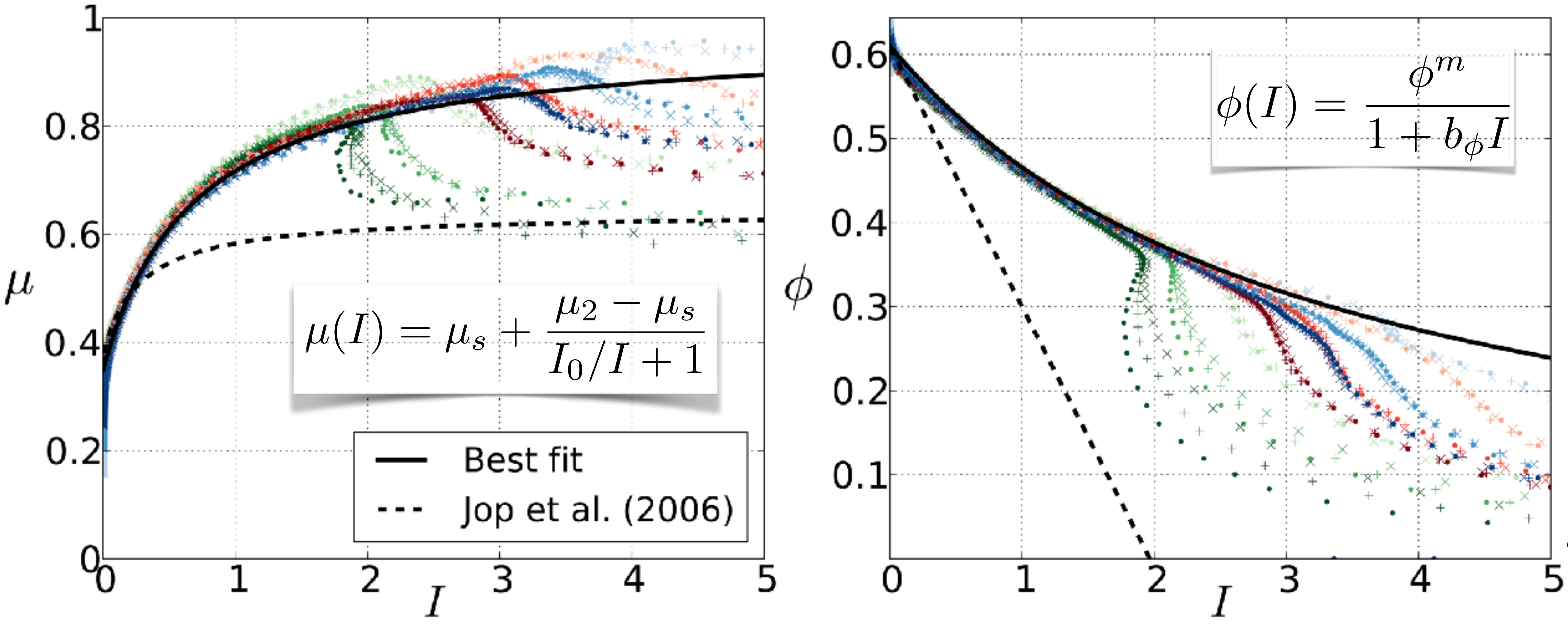

Maurin et al. JFM (2016)

- 27 simulations

  ➡ 3 diameters (d=3, 6, 12 mm), 3 density ratio (s=1.375, 1.75, 2.5), 3 Shields numbers (0.1, 0.3, 0.6)

- Collapse for I < 2 => the inertial number is the control parameter of the granular flow rheology

- **Granular rheology for Eulerian model:**

$$\phi(I) = \frac{\phi_m}{1 + b_\phi I} \iff P^p = \left(\frac{b_\phi \phi}{\phi_m - \phi}\right)^2 \rho^p d^2 \dot{\gamma}^{p\,2}$$

$$\mu(I) = \frac{\tau^p}{P^p} \iff \tau^p = \mu(I) P^p \propto \dot{\gamma}^{p\,2}$$

with

$$\mu_s = 0.35 \ ; \ \mu_2 = 0.97 \ ; \ I_0 = 0.69 \ ; \ \phi^m = 0.61 \ ; \ b_\phi = 0.31$$

Frictional kinetic theory of granular flow in bed-load transport

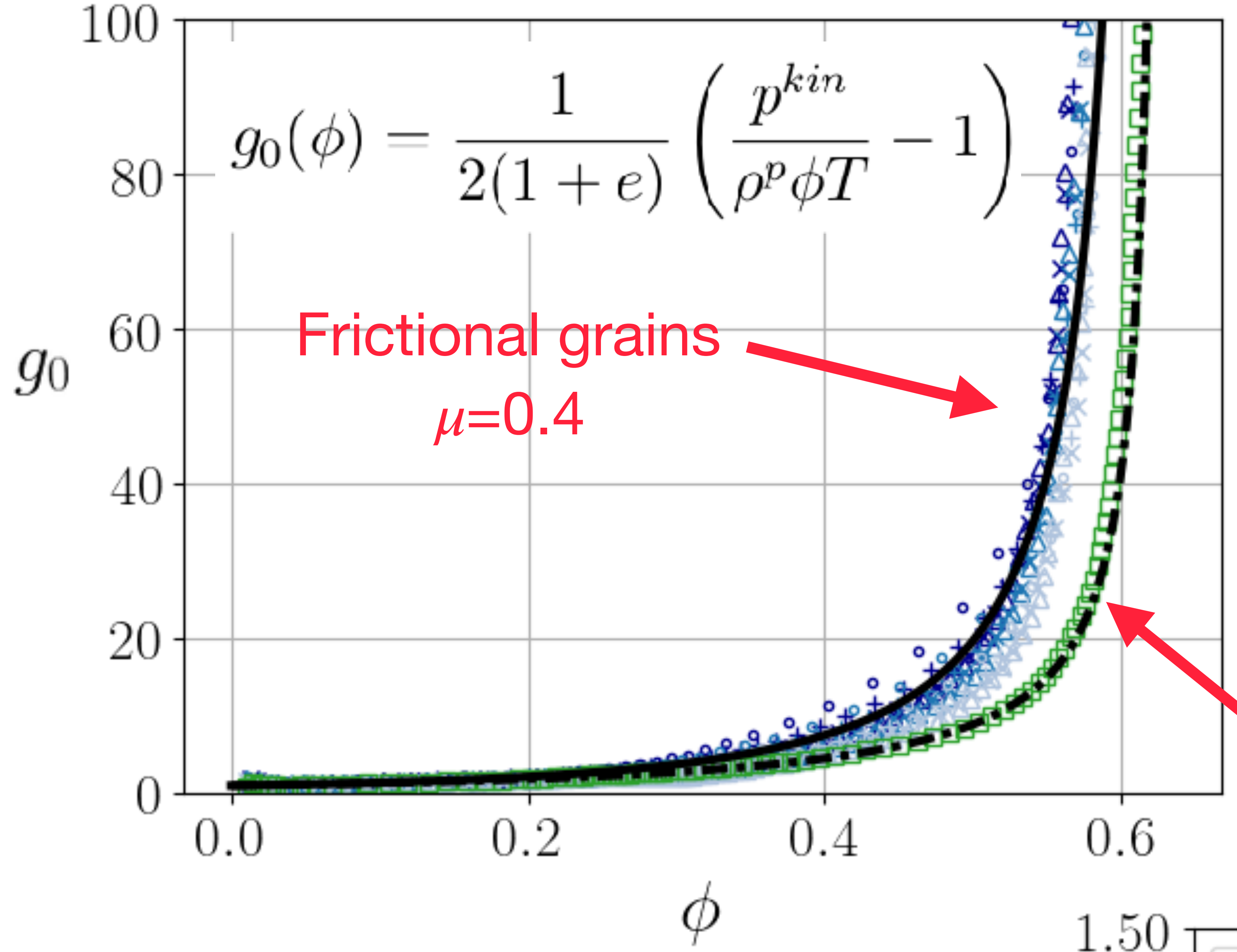

Radial distribution function fitted from DEM results

$$g_0(\phi) = \frac{2-\phi}{2(1-\phi)^3} + \frac{2.71\phi^2}{(\phi_m - \phi)^{3/2}}$$

Chialvo and Sundaresan (2013) ; Chassagne et al. (submitted to PRF)

+ modifications of viscosity, pseudo-heat diffusion, and restitution coefficient

- Captures dense regime as μ(I)
- Avoid unrealistic behavior at I~1
- Better predict dilute transition
  - Especially ϕ(I) *i.e. particle pressure*

Chassagne et al. (submitted to PRF)

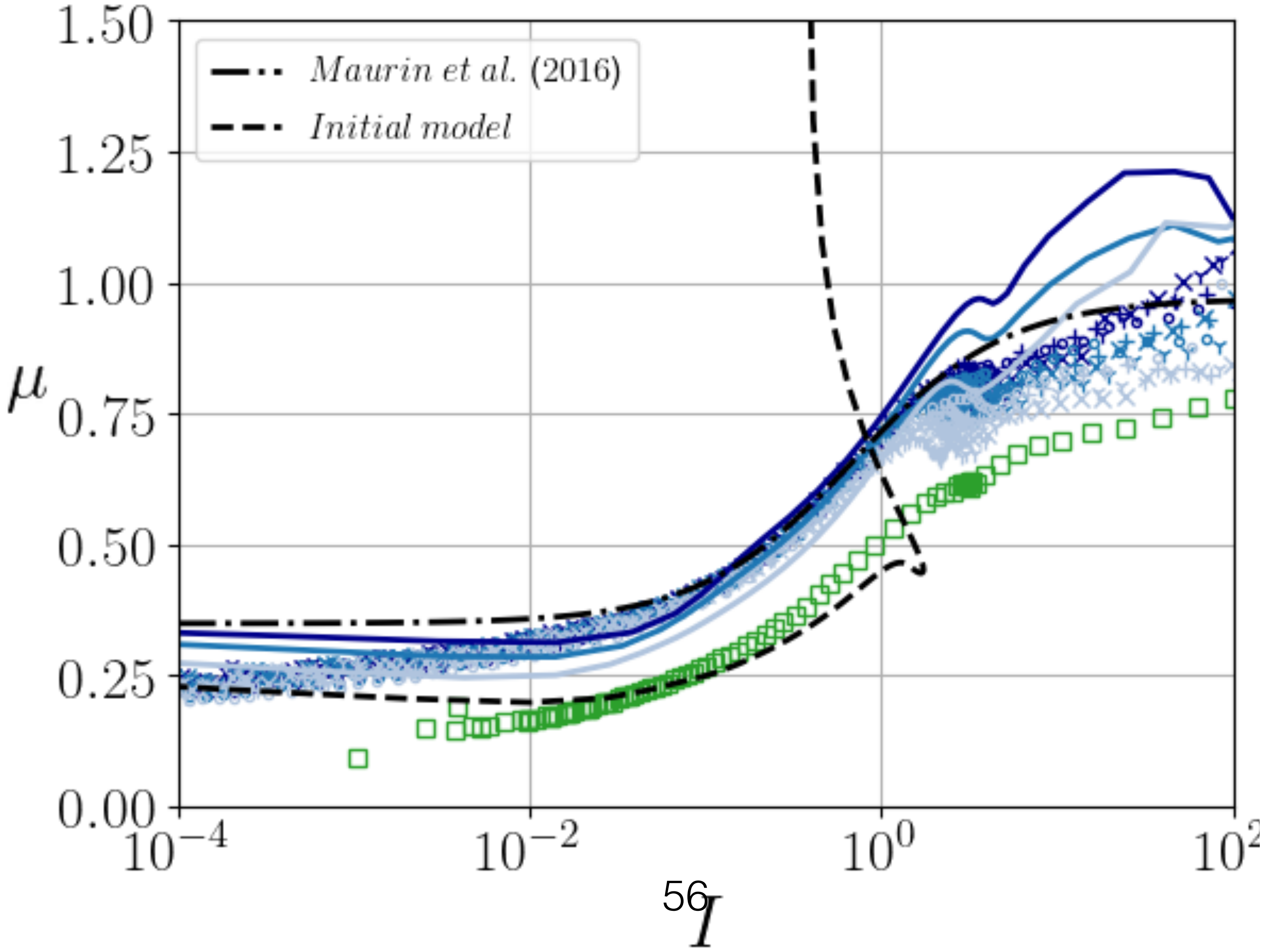

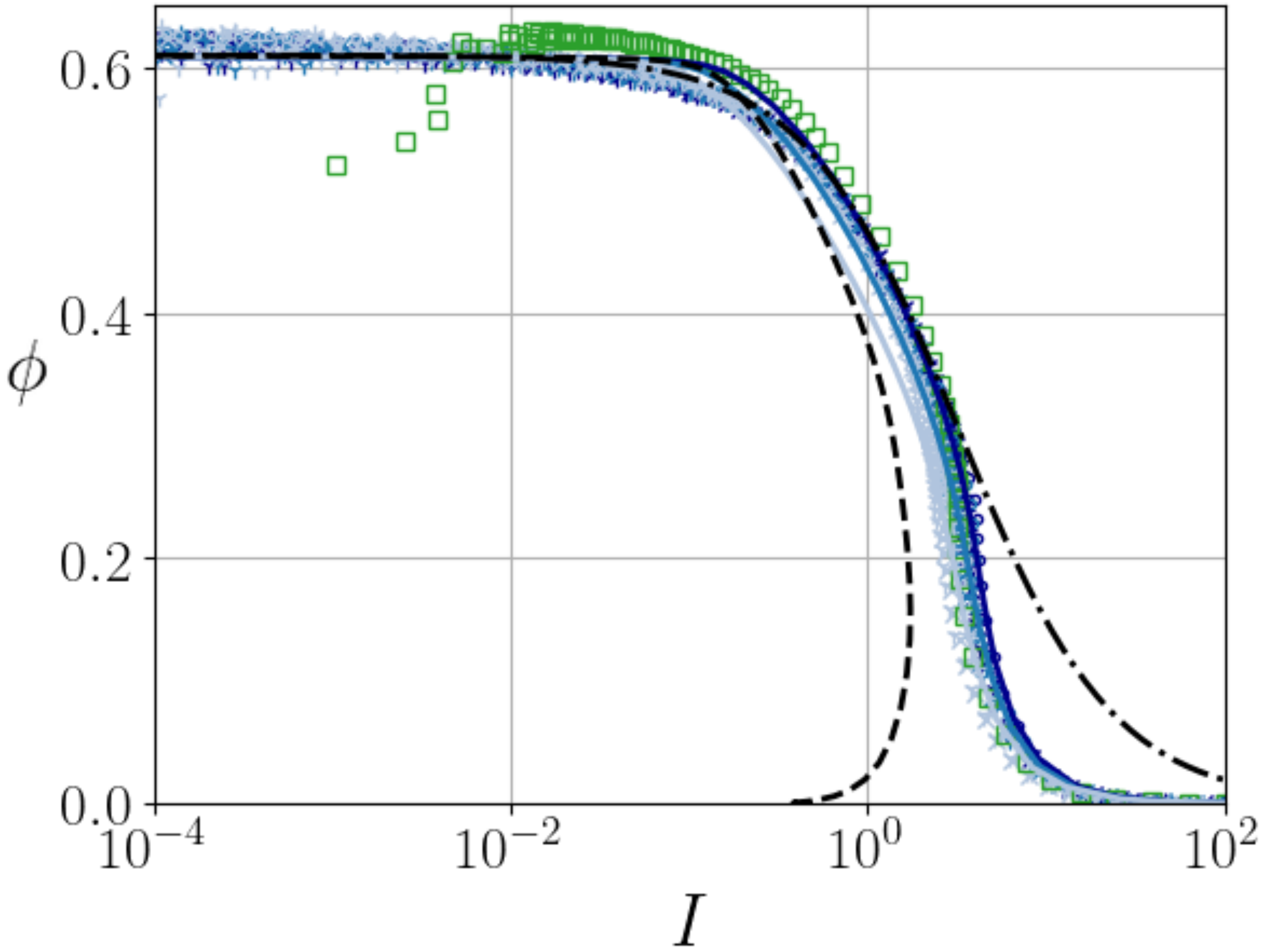

Eulerian-Eulerian model derivation

Local mass & momentum conservation for a fluid-particle mixture

$$\nabla.\vec{u} = 0 \quad \text{and} \quad \frac{d\rho\vec{u}}{dt} + \nabla.(\rho\vec{u}\otimes\vec{u}) = \nabla.\overline{\overline{\sigma}} + \rho\vec{g}$$

Local spatial averaging

Jackson (2000)

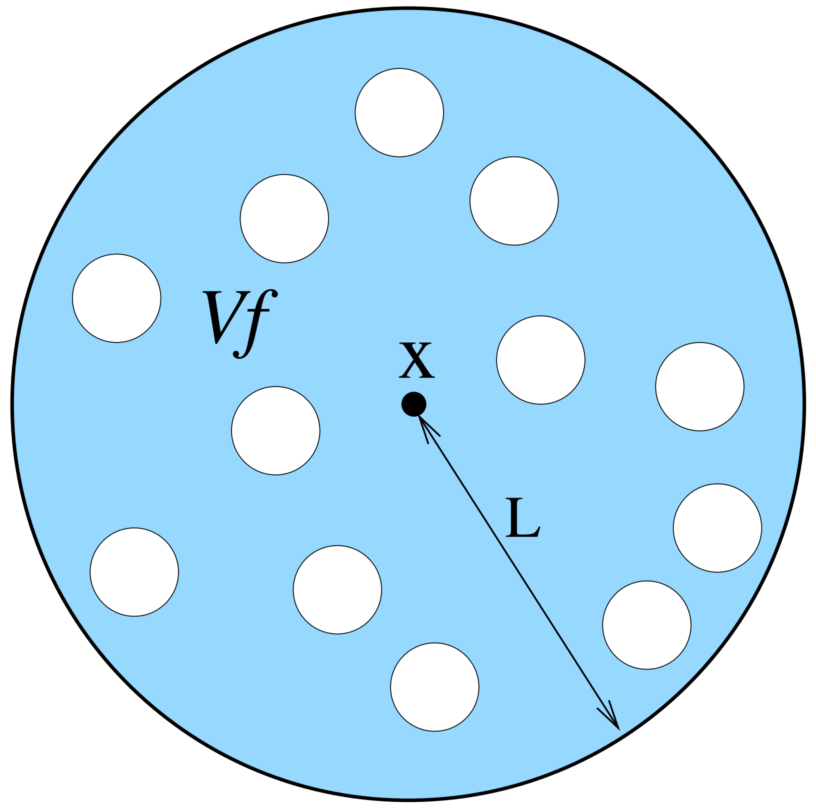

$$\langle f\rangle^f(\vec{x},t) = \frac{1}{\epsilon}\int_{V_f(t)} f(\vec{y},t)G_L(|\vec{x}-\vec{y}|)dV_y$$

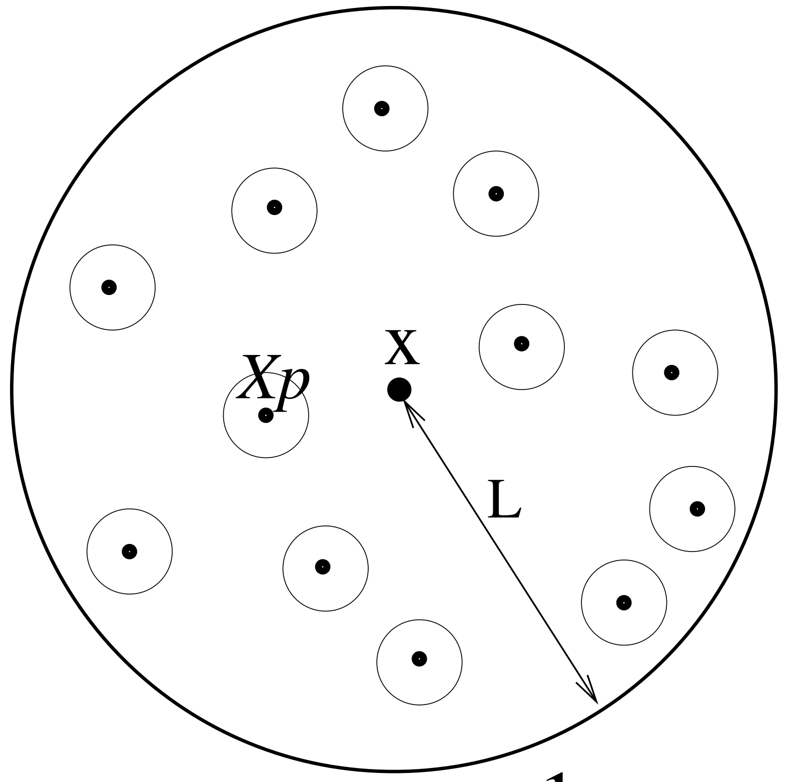

$$n(\vec{x},t)\,\frac{\pi d_p^3}{6} = \phi(\vec{x},t)$$

$$\langle f\rangle^p(\vec{x},t) = \frac{1}{n(\vec{x},t)}\sum_p f^p G(|\vec{x}-\vec{x}_p|)$$

Fluid phase mass and momentum equations

$$\frac{\partial\epsilon}{\partial t} + \nabla\left(\epsilon\langle\vec{u}\rangle^f\right) = 0$$

$$\rho^f\left[\frac{\partial\epsilon\langle\vec{u}\rangle^f}{\partial t} + \nabla\left(\epsilon\langle\vec{u}\rangle^f\otimes\langle\vec{u}\rangle^f\right)\right] = \nabla\sigma^f - n\vec{f} + \epsilon\rho^f g$$

Solid phase mass and momentum equations

$$\frac{\partial\phi}{\partial t} + \nabla\left(\phi\langle\vec{u}\rangle^p\right) = 0$$

$$\rho^p\left[\frac{\partial\phi\langle\vec{u}\rangle^p}{\partial t} + \nabla\left(\phi\langle\vec{u}\rangle^p\otimes\langle\vec{u}\rangle^p\right)\right] = \nabla\sigma^p + n\vec{f} + \phi\rho^p g$$

Two-phase flow « two-fluid » equations

$$\frac{\partial \epsilon}{\partial t} + \nabla \left(\epsilon \langle \overrightarrow{u} \rangle^f \right) = 0$$

$$\rho^f \left[\frac{\partial \epsilon \langle \overrightarrow{u} \rangle^f}{\partial t} + \nabla \left(\epsilon \langle \overrightarrow{u} \otimes \overrightarrow{u} \rangle^f \right) \right] = - \nabla p^f + \nabla \tau^f - n \langle \overrightarrow{f}^p \rangle^p + \epsilon \rho^f \overrightarrow{g}$$

Effective fluid stress

Viscous effects

Fluid-particle interactions

Drag + Buoyancy

$$\frac{\partial \phi}{\partial t} + \nabla \left(\phi \langle \overrightarrow{u} \rangle^p \right) = 0$$

$$\rho^p \left[\frac{\partial \phi \langle \overrightarrow{u} \rangle^p}{\partial t} + \nabla \left(\phi \overrightarrow{u} \rangle^p \otimes \overrightarrow{u} \rangle^p \right) \right] = - \nabla p^p + \nabla \tau^p + n \langle \overrightarrow{f}^p \rangle^p + \phi \rho^p \overrightarrow{g}$$

Granular stresses

μ(I) or Kinetic theory of granular flows

sedFoam: 3D two-phase numerical model for sediment transport

- Based on twoPhaseEulerFoam from H. Rusche (2002) and sedFoam-1.0 from Cheng & Hsu (2014)
- **Finite Volume Method** 2nd order accuracy in space and time
- **PISO algorithm** for pressure-velocity coupling
- **Publically available** on github: *https://github.com/SedFoam/sedfoam*

Collaboration Univ. Delaware
Prof. T.-J. Hsu

Chauchat *et al. (2017) - Geoscientific Model Development*

Geoscientific Model Development
An interactive open-access journal of the European Geosciences Union
| EGU.eu | EGU Journals | EGU Highlight Articles | Contact | Imprint |

https://doi.org/10.5194/gmd-2017-101
© Author(s) 2017. This work is distributed under the Creative Commons Attribution 3.0 License.

Discussion papers

Model description paper — 07 Jun 2017

SedFoam-2.0: a 3D two-phase flow numerical model for sediment transport

Julien Chauchat[1], Zhen Cheng[2,a], Tim Nagel[1], Cyrille Bonamy[1], and Tian-Jian Hsu[2]
[1]University of Grenoble Alpes, LEGI, G-INP, CNRS, F-38000 Grenoble, France
[2]Civil and Environmental Engineering, Center for Applied Coastal Research, University of Delaware, Newark, DE 19711, USA
[a]now at: Applied Ocean Physics & Engineering, Woods Hole Oceanographic Institution, Woods Hole, MA 02543, USA

Received: 22 Apr 2017 – Accepted for review: 05 Jun 2017 – Discussion started: 07 Jun 2017

Abstract. In this paper, a three-dimensional two-phase flow solver, SedFoam-2.0, is presented for sediment transport applications. The solver is extended upon twoPhaseEulerFoam available in the 2.1.0 release of the open-source CFD toolbox OpenFOAM. In this approach the sediment phase is modeled as a continuum, and constitutive laws have to be prescribed for the sediment stresses. In the proposed solver, two different inter-granular stress models are implemented: the kinetic theory of granular flows and the dense granular flow rheology $\mu(I)$. For the fluid stress, laminar or turbulent flow regimes can be simulated and three different turbulence models are available for sediment transport: a simple mixing length model (one-dimensional configuration only), a k-ϵ and a k-ω model. The numerical implementation is first demonstrated by two validation test cases, sedimentation of suspended particles and laminar bed-load. Two applications are then investigated to illustrate the capabilities of SedFoam-2.0 to deal with complex turbulent sediment transport problems with different combinations of inter-granular stress and turbulence models.

Citation: Chauchat, J., Cheng, Z., Nagel, T., Bonamy, C., and Hsu, T.-J.: SedFoam-2.0: a 3D two-phase flow numerical model for sediment transport, Geosci. Model Dev. Discuss., https://doi.org/10.5194/gmd-2017-101, in review, 2017.

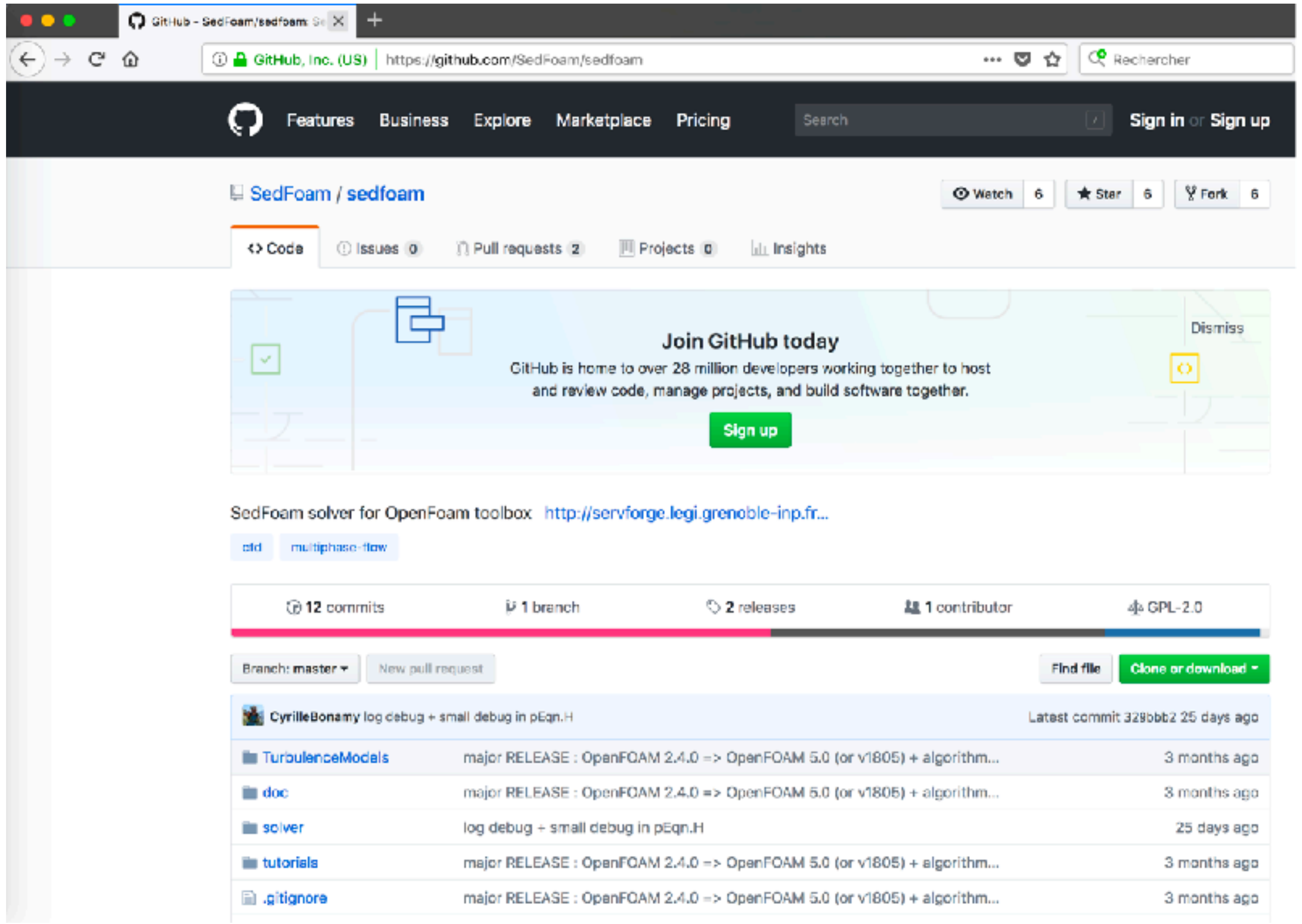

Sedimentation of polystyrene particles in silicon oil

Physical parameters: LMSGC experiment - MRI measurements

Pham Van Bang et al. (2006)

Fluid phase:

- $\eta_f = 20.10^{-3}$ Pa s (200 x water)
- $\rho_f = 0.95$ kg m^{-3}

Solid phase:

- $d = 0.29 \pm 0.03$ mm
- $\rho_p = 1.05$ kg m^{-3}
- $\phi^0 = 0.48$

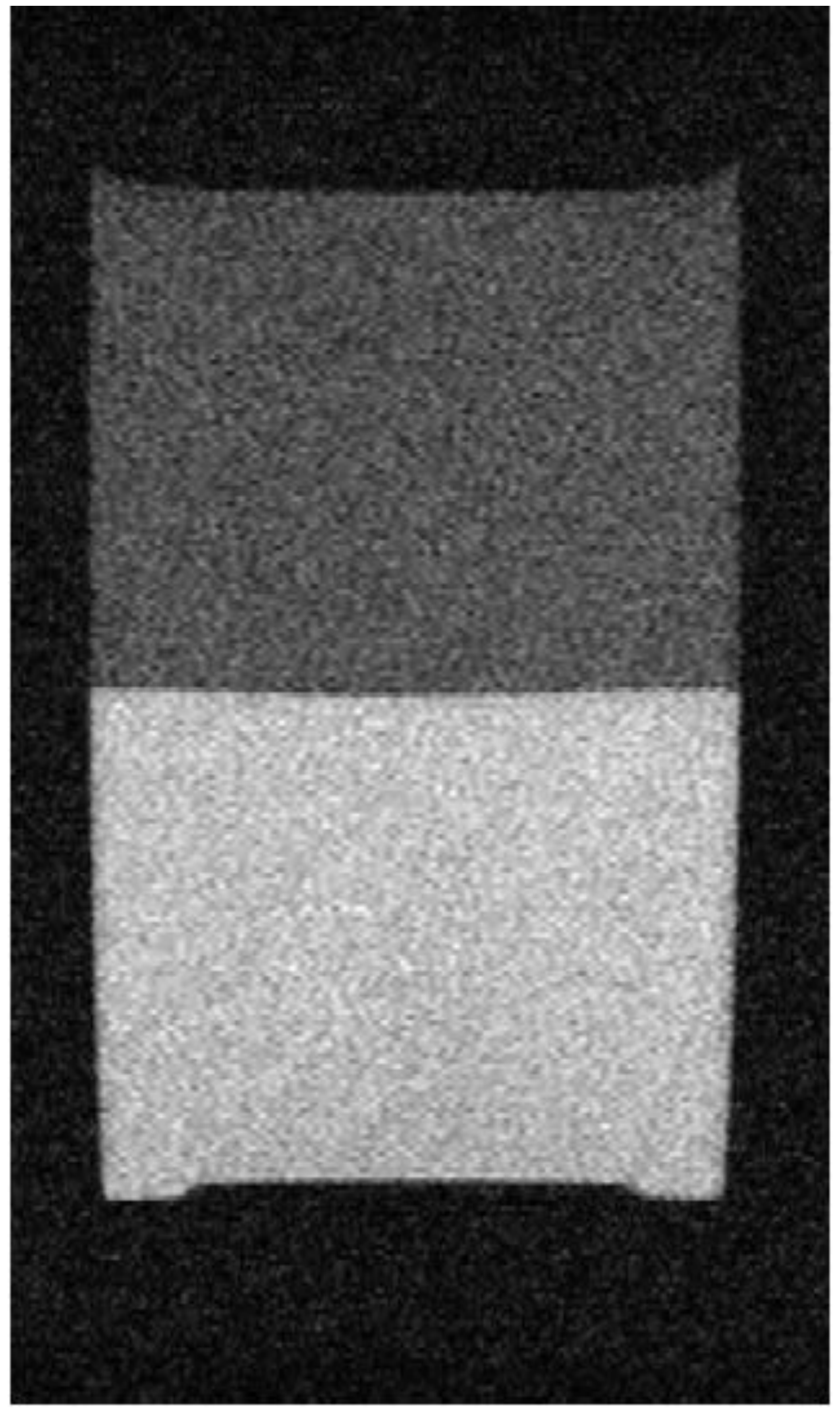

Model ingredients:

- Stokes drag + hindrance function
- Particle pressure due to enduring contacts:

$$p_e^p = \Pi_0 \frac{\left(\max(\phi - \phi_{rlp}; 0)\right)^3}{(\phi_m - \phi)^5}$$

Johnson & Jackson (1987)

where Π_0 is a modulus (in Pa) and ϕ_{rlp} is the random loose packing fraction

Numerical parameters:

- Δy=3 10^{-4} m; Δt=2 10^{-1}s first order upwind scheme for advection - Euler scheme in time

Sedimentation of polystyrene particles in silicon oil

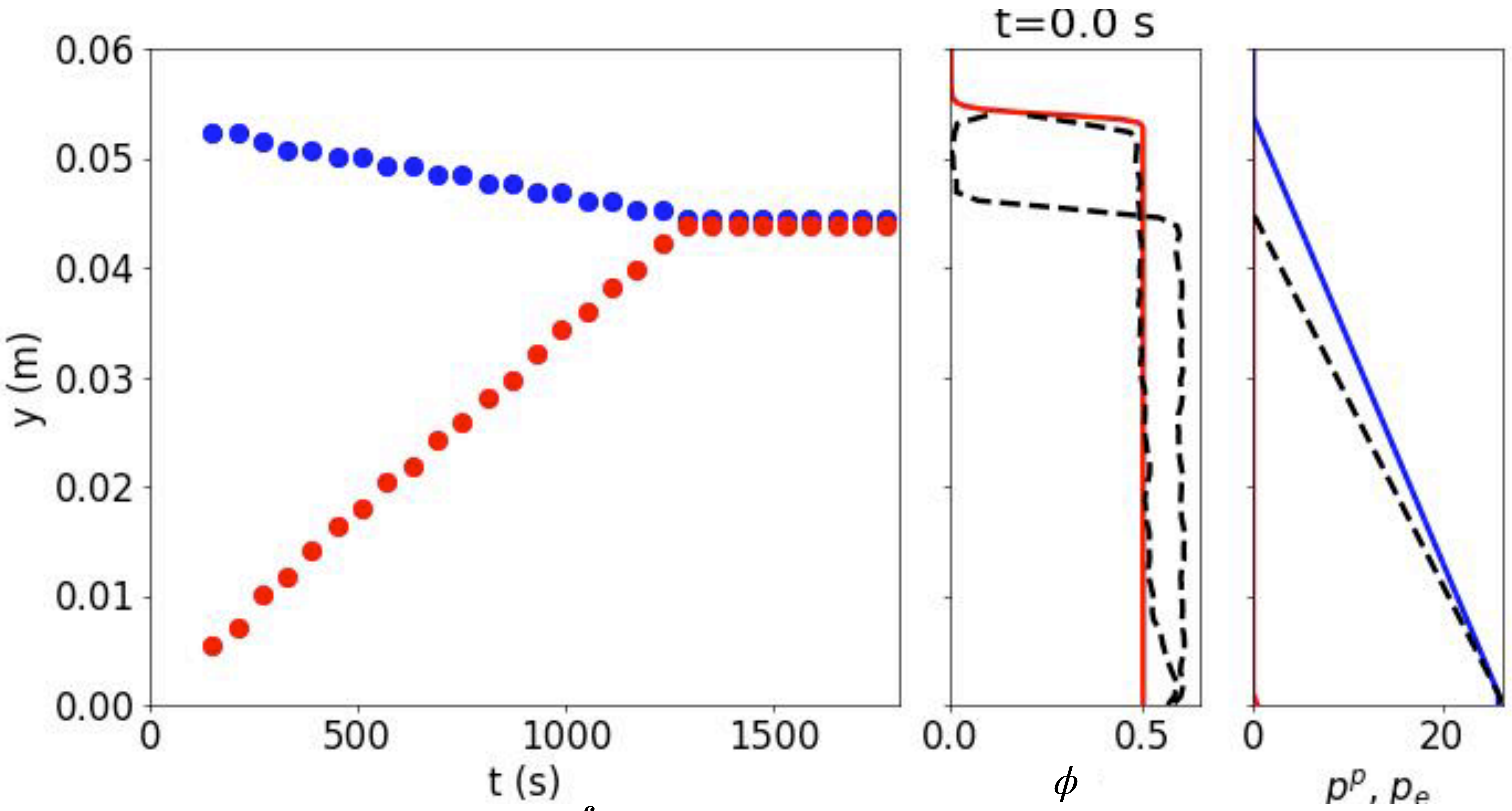

Excess pore pressure: $p_e = p^f - \rho_f \; g \; y$

Mixture momentum balance: $\dfrac{D\rho_m w_m}{Dt} = -\dfrac{dp^f}{dy} - \rho_m g - \dfrac{dp^p}{dy}$

Stability condition : $C_{FL} = \dfrac{\max || v^p - v^f || \Delta t}{\Delta y} < 0.7$ (empirical)

Chauchat et al. GMD (2017)

2nd open question

The two-fluid model is ill-posed for certain parameter values

Stewart (JCP 1979) :

The conclusions seem to suggest using the two-fluid model when coarse modeling is appropriate, in spite of ill-posedness**. However, there are reservations. [...] Furthermore, our analysis merely suggests reasonable physical limits on the applicability of [the two-fluid equations]. **Whether they, in fact, model reality is a question for confrontation with experiments

Dinh et al. (2003) :

***Mathematical awkwardness of the two-fluid formulation has led mathematically-minded researchers to caution the utility of the two-fluid model** [...]. In the contrary, **another camp of engineering researchers sees intrinsic values of the two-fluid transport equations** […]. **They regard ill-posedness as a minor artifact, which should be dealt with on a fitness-for-purpose basis**. Consequently, researchers in this group focused their effort on developing sets of constitutive laws that allow simulation of practical two-phase processes.*

Bresch et al. (2018) : Multi-Fluid Models Including Compressible Fluids

Stewart, H. (1979). Stability of two-phase flow calculation using two-fluid models. Journal of Computational Physics, 33(2):259–270.

Dinh, T. N., Nourgaliev, R. R., & Theofanous, T. G. (2003). Understanding of the Ill-posed two-fluid model. Proceedings of the tenth international topical meeting on nuclear reactor thermal hydraulics, (pp. 1CD-ROM). Korea, Republic of: KNS.

Bresch D., Desjardins B., Ghidaglia JM., Grenier E., Hillairet M. (2018) Multi-Fluid Models Including Compressible Fluids. In: Giga Y., Novotný A. (eds) Handbook of Mathematical Analysis in Mechanics of Viscous Fluids. Springer, Cham.

Laminar bed-load

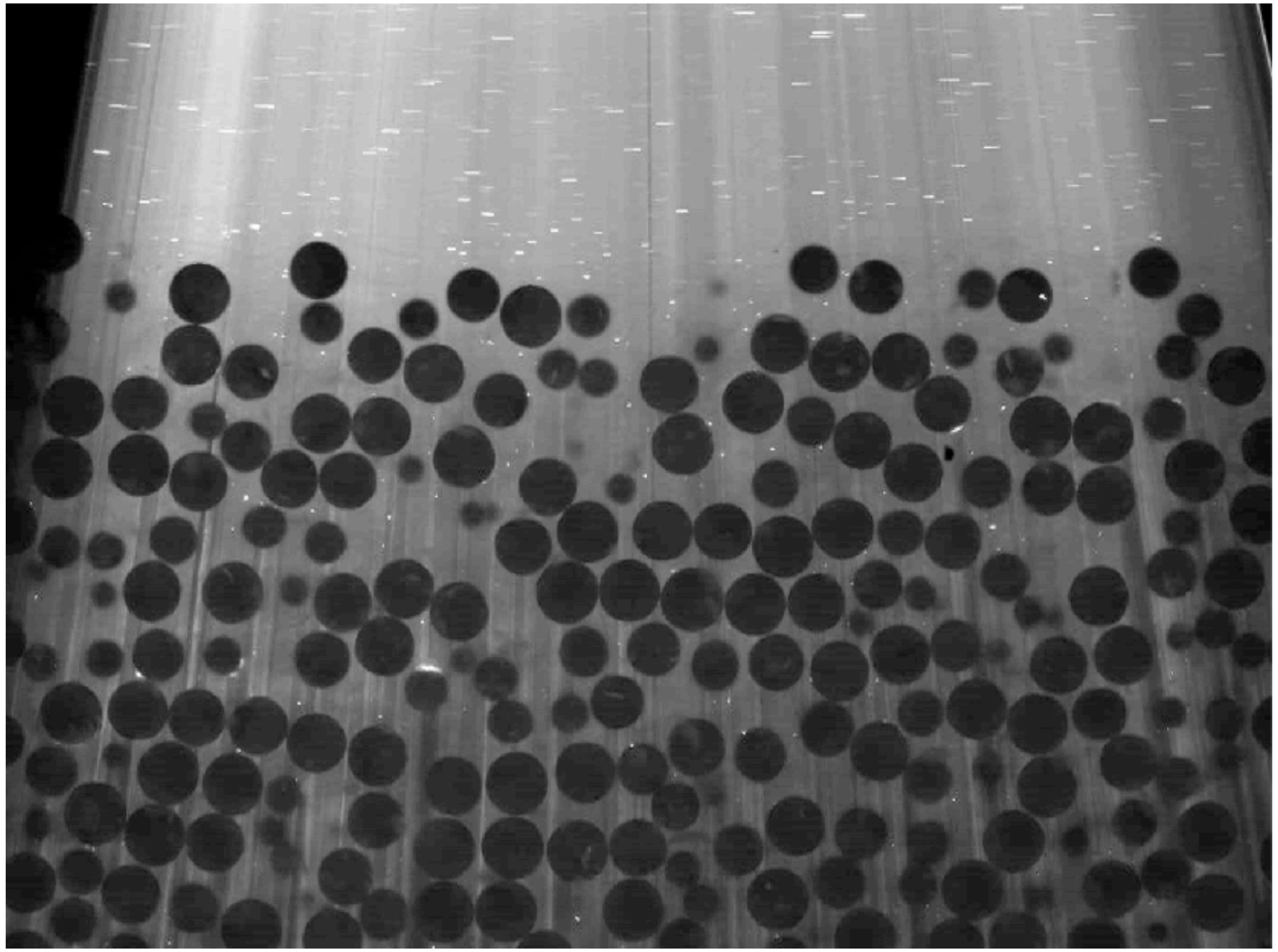

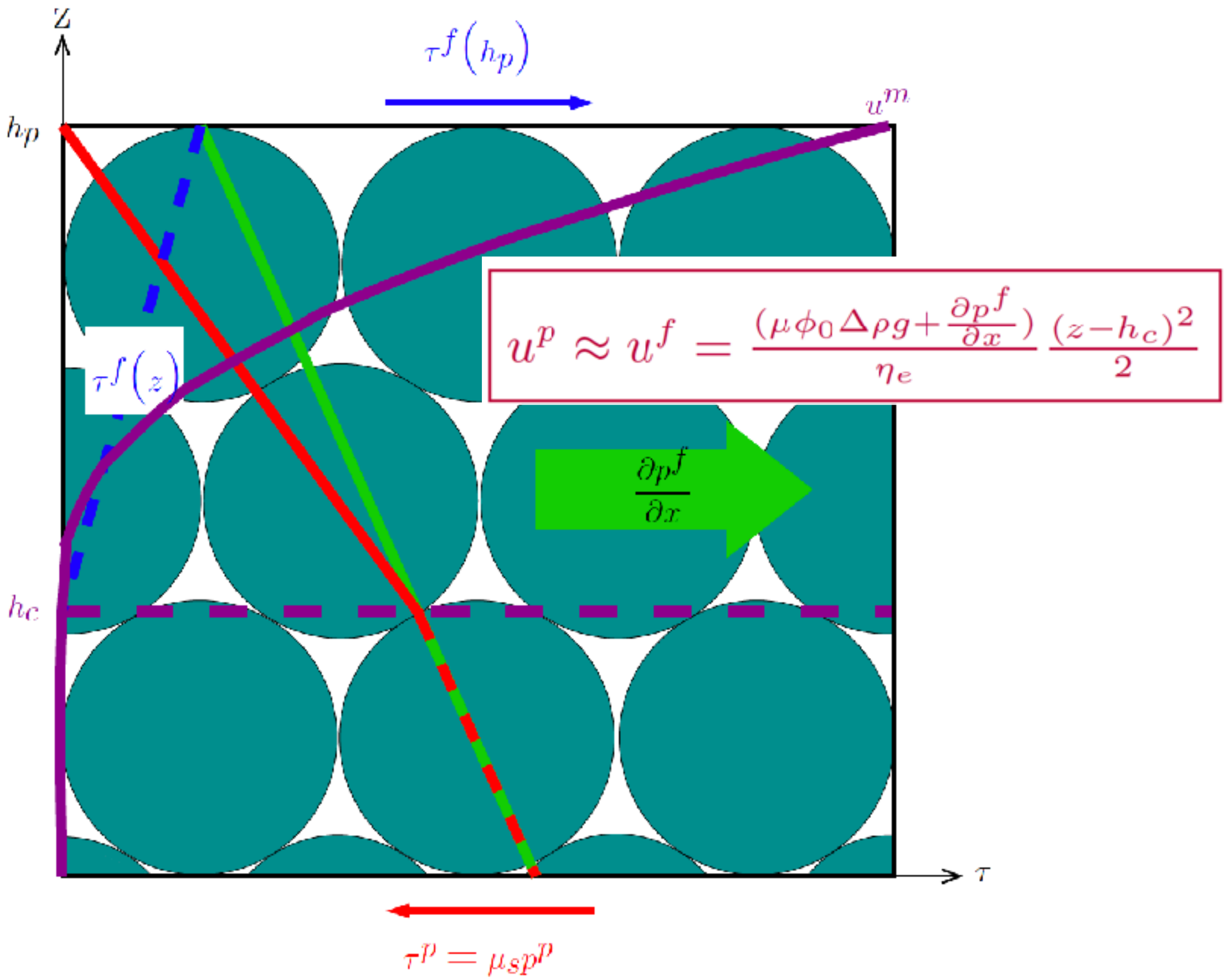

Index-matching experiments

- Particles: d_p=2mm PMMA ; $\rho_p/\rho_f = 1.2$
- Fluid: Triton X-100
- Re ~ 1

(Aussillous et al., JFM 2013)

Analytical solution

- Einstein viscosity: $\nu_{eff} = \nu^f(1 + 2.5\phi)$
- Coulomb friction: μ = constant
- Parabolic velocity profile

(Ouriemi et al., JFM 2009)

Granular stresses: particle-particle interactions

Dense granular flow rheology: μ(I) *(GDR Midi, 2004)*

Represent frictional-collisional interactions in dense granular flows

- **Shear stress**

$$\overline{\overline{\tau^p}} = \mu(I) p^p \frac{\overline{\overline{S^p}}}{||\overline{\overline{S^p}}||}$$

(Jop et al., 2006)

with $\overline{\overline{S^p}} = \nabla \overrightarrow{u^p} + \nabla \overrightarrow{u^p}^T - \frac{2}{3} tr(\nabla . \overrightarrow{u^p})$

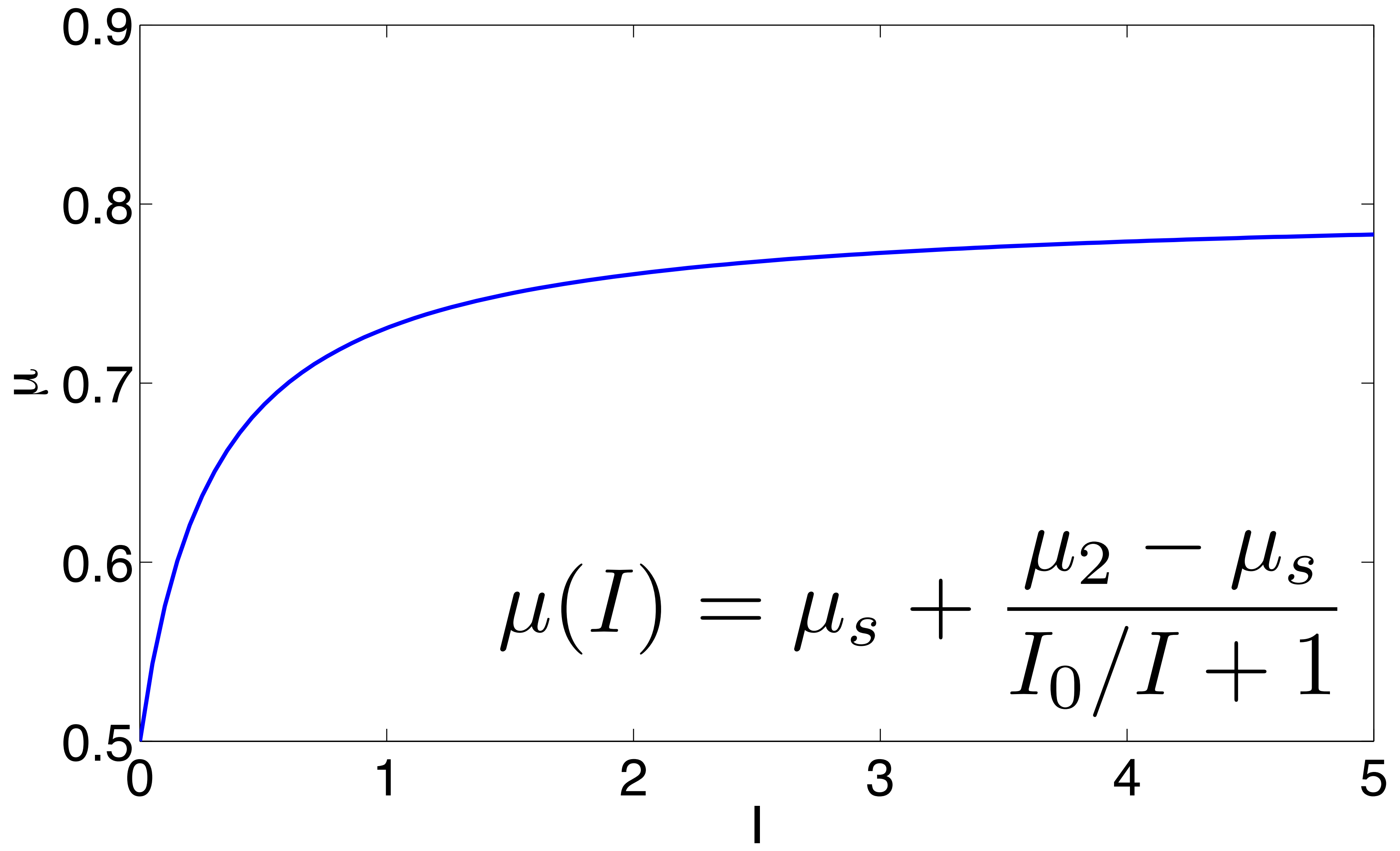

Visco-plastic rheology: contain a yield stress (need regularization) and a non-linear viscous term

Viscosity regularization (Chauchat and Médale, JCP 2014)

By definition: $\overline{\overline{\tau^p}} = \eta_p \overline{\overline{S^p}} \quad \rightarrow \quad \eta_p = \frac{\mu_s p^p}{||\overline{\overline{S^p}}||}$

$$\boxed{\eta_p = \frac{\mu(I) p^p}{\left(||\overline{\overline{S^p}}||^2 + \lambda^2\right)^{1/2}}}$$

where λ is a small parameter

Control parameter = Inertial number: $I = \frac{||\overline{\overline{S^p}}|| d}{\sqrt{p^p/\rho^p}}$

Plastic transition is approximated by a very viscous fluid rheology controlled by λ

Granular stresses: particle-particle interactions

Particle pressure: $p^p = p_e^p + p_s^p$ **2 contributions**

- **Rate independent:**

$$p_e^p = \Pi_0 \frac{\left(\phi - \phi_{rlp}\right)^3}{\left(\phi_m - \phi\right)^5}$$

pressure due to enduring contact *(Johnson & Jackson, 1987)*

- **Shear induced:**

$$p_s^p = \left(\frac{b\ \phi}{\phi_m - \phi}\right)^2 \rho^p\ d^2\ ||\overline{\overline{S^p}}||^2$$

Shear-induced pressure: lead to bed decompaction *(Maurin et al., 2016)*

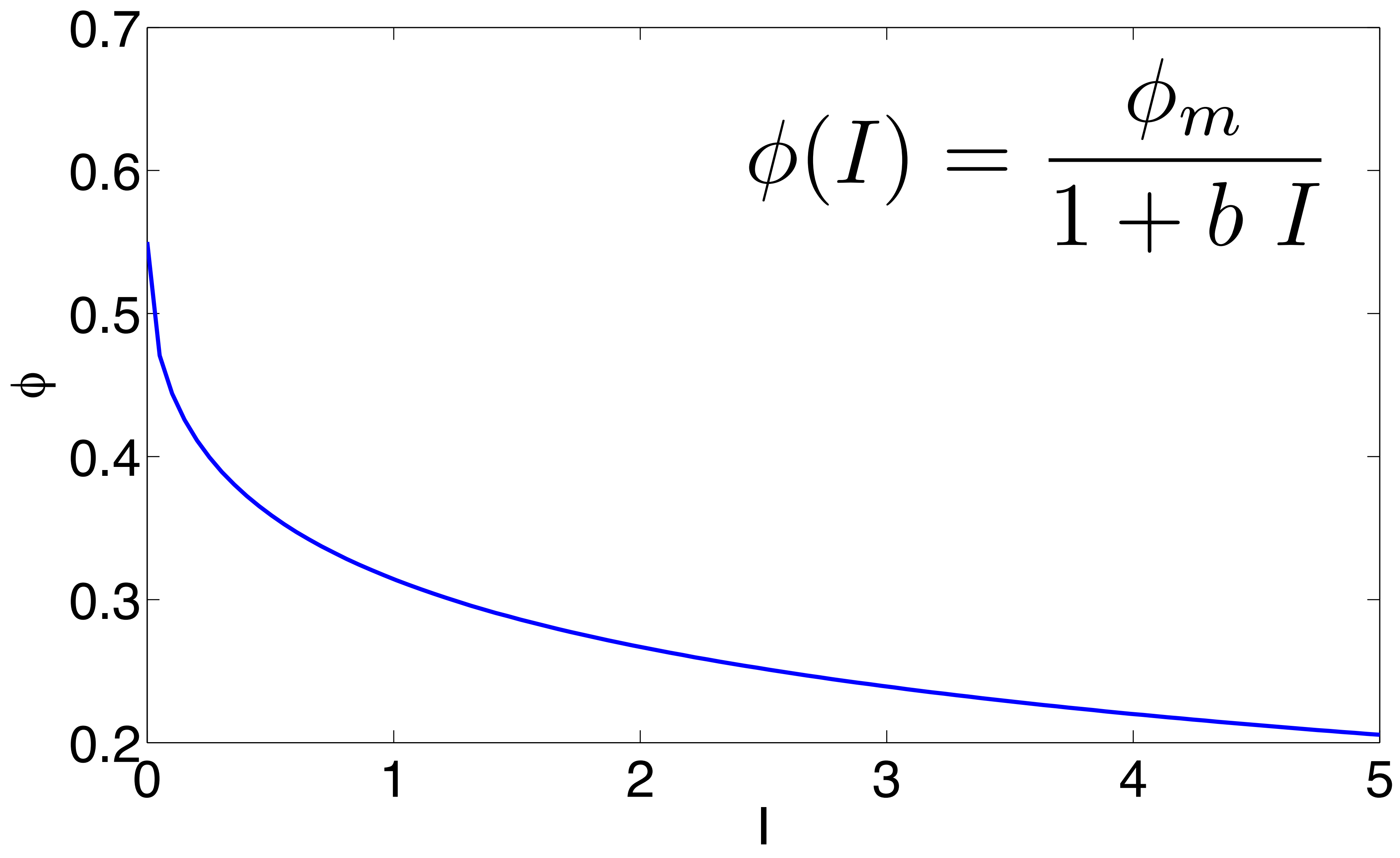

Laminar bed-load

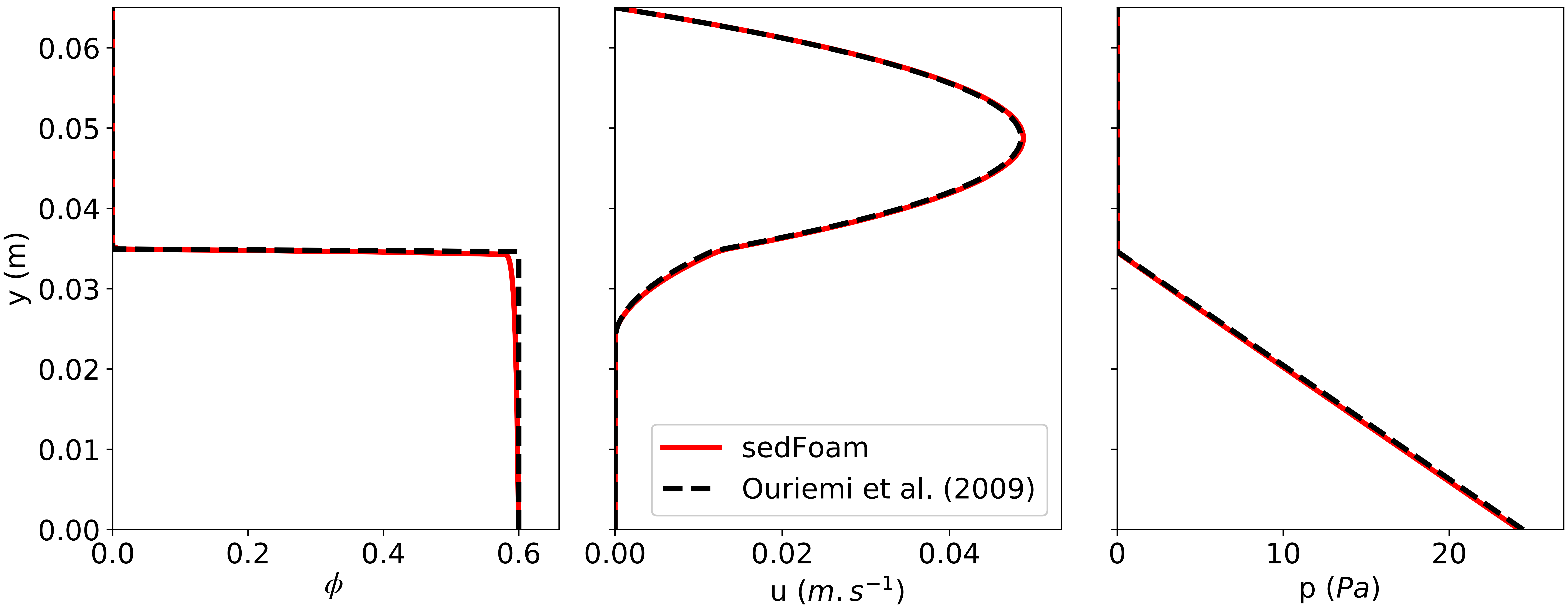

- Comparison with analytical solution: Coulomb rheology + Einstein viscosity model
  - Numerical implementation of granular flow rheology is validated

- Numerical parameters: $\Delta y = 3\ 10^{-4}$ m

Chauchat et al. GMD (2017)

Laminar bed-load

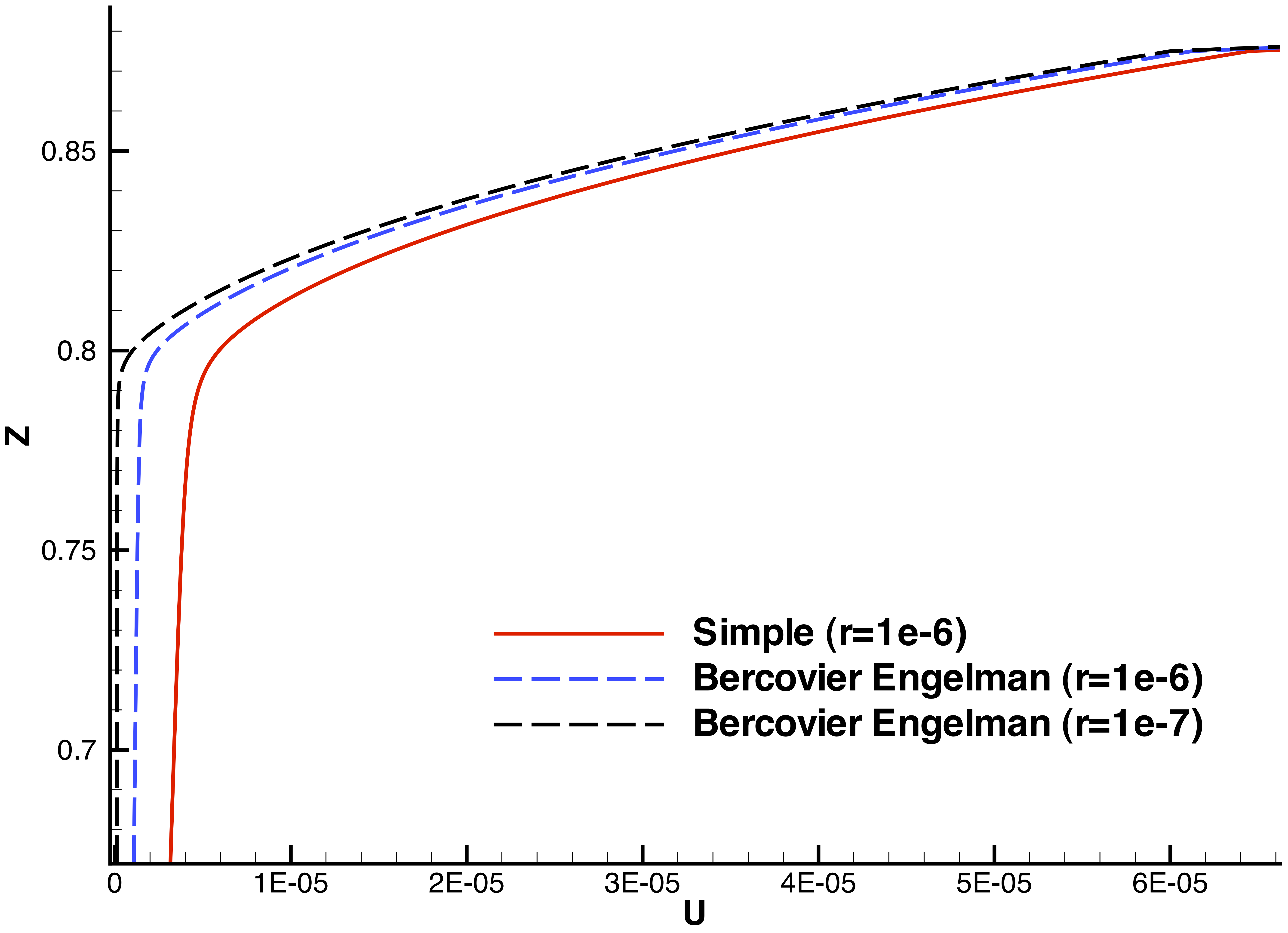

Sensitivity to regularization parameter

Simple: $\eta_p = \dfrac{\mu(I)p^p}{||\overline{\overline{S^p}}|| + r}$

Bercovier-Engelman: $\eta_p = \dfrac{\mu(I)p^p}{\left(||\overline{\overline{S^p}}||^2 + r^2\right)^{1/2}}$

Chauchat and Médale (2010)

Laminar bed-load

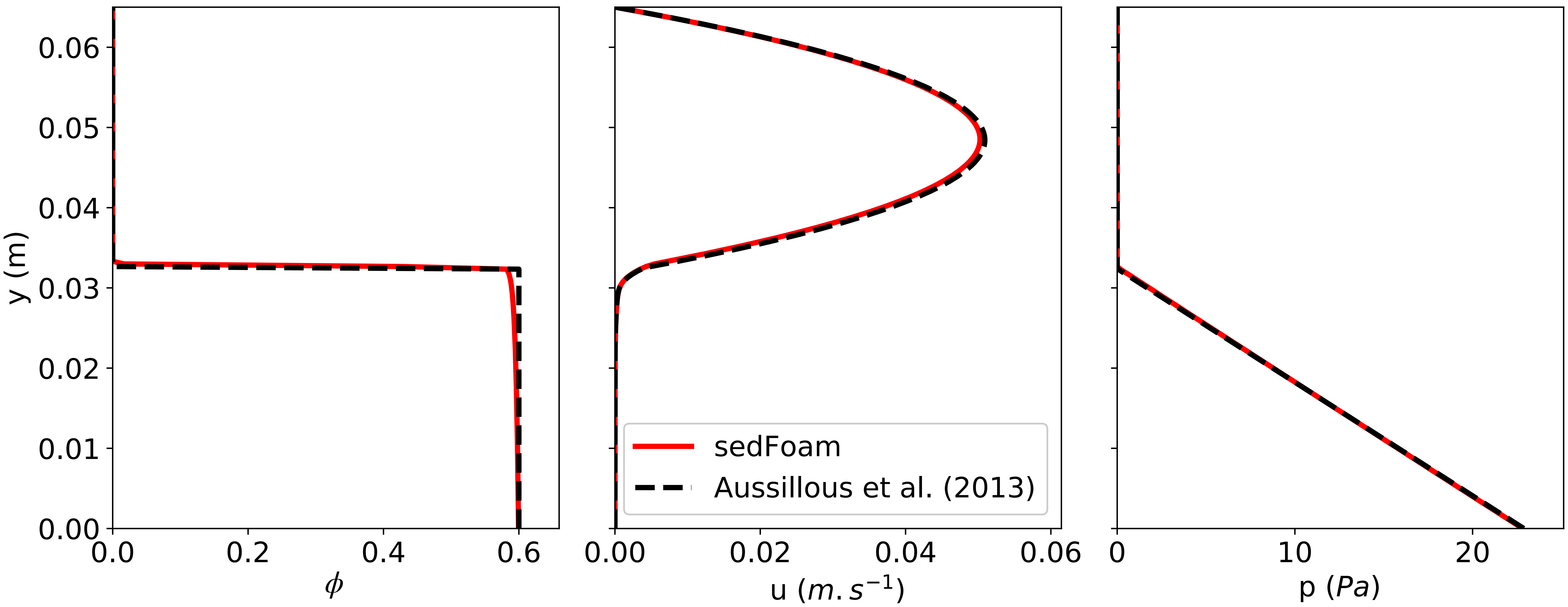

- Comparison with numerical solution: µ(I) rheology + Einstein viscosity model
  - Numerical implementation of granular flow rheology is validated

- Numerical parameters: $\Delta y = 3\ 10^{-4}$ m

Chauchat et al. GMD (2017)

3rd open question

The μ(I) rheology is ill-posed for certain parameter values and inertial numbers

Barker, T., Schaeffer, D. G., Bohorquez, P., and Gray, J. M. N. T. (2015). Well-posed and ill-posed behaviour of the mu(i) rheology for granular flow. Journal of Fluid Mechanics, 779:794–818

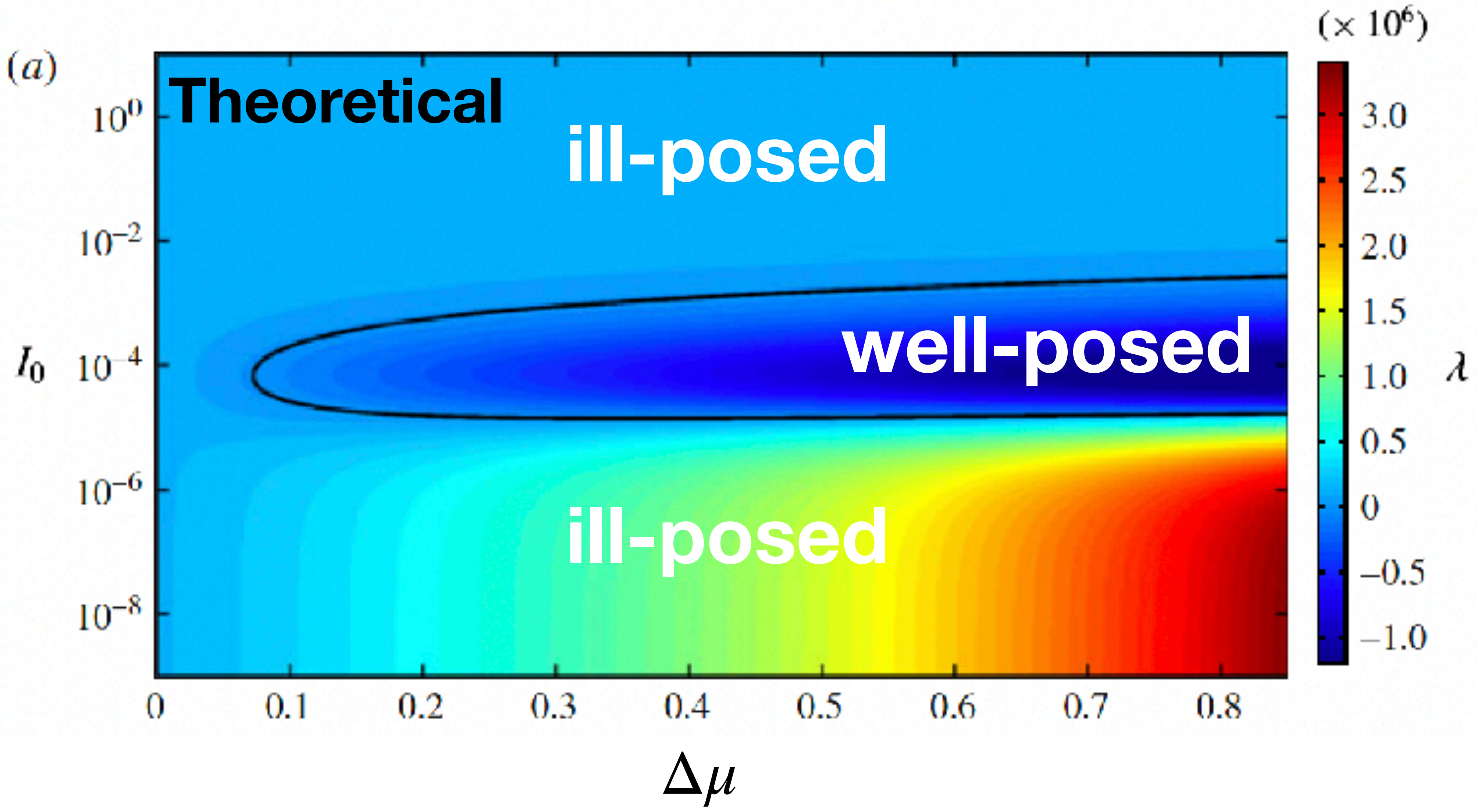

Perturbation analysis :

$$\begin{bmatrix} \hat{\boldsymbol{u}}(\boldsymbol{x}, t) \\ \hat{p}(\boldsymbol{x}, t) \end{bmatrix} = \exp(\mathrm{i}\boldsymbol{\xi} \cdot \boldsymbol{x} + \lambda t) \begin{bmatrix} \tilde{\boldsymbol{u}} \\ \tilde{p} \end{bmatrix}$$

$$\mu = \mu(I) = \mu_s + \frac{\Delta\mu}{I_0/I + 1}$$

2 options discussed in the literature:

- Develop a compressible μ(I) rheology

  - Heyman, J., Delannay, R., Tabuteau, H., & Valance, A. (2017). Compressibility regularizes the μ(I)-rheology for dense granular flows. *Journal of Fluid Mechanics, 830*, 553-568.
  - Barker, T., Schaeffer, D. G., Shearer, M., and Gray, J. M. N. T. (2017). Well-posed continuum equations for granular flow with compressibility and mu(i) rheology. Proceedings of the Royal Society A: Mathematical, Physical and Engineering Sciences, 473(2201):20160846.
  - Schaeffer, D., Barker, T., Tsuji, D., Gremaud, P., Shearer, M., & Gray, J. (2019). Constitutive relations for compressible granular flow in the inertial regime. *Journal of Fluid Mechanics, 874*, 926-951. doi:10.1017/jfm.2019.476
  - …

- Use a modified kinetic theory of granular flows to account for friction

  - Chialvo, S. and Sundaresan, S. (2013). A modified kinetic theory for frictional granular flows in dense and dilute regimes. Physics of Fluids, 25(7):070603.
  - Chassagne, R., Chauchat, J., and Bonamy, C. (submitted to PRF). A modified kinetic theory for frictional-collisional bedload transport valid from dense to dilute regime.

Turbulence-particle interactions

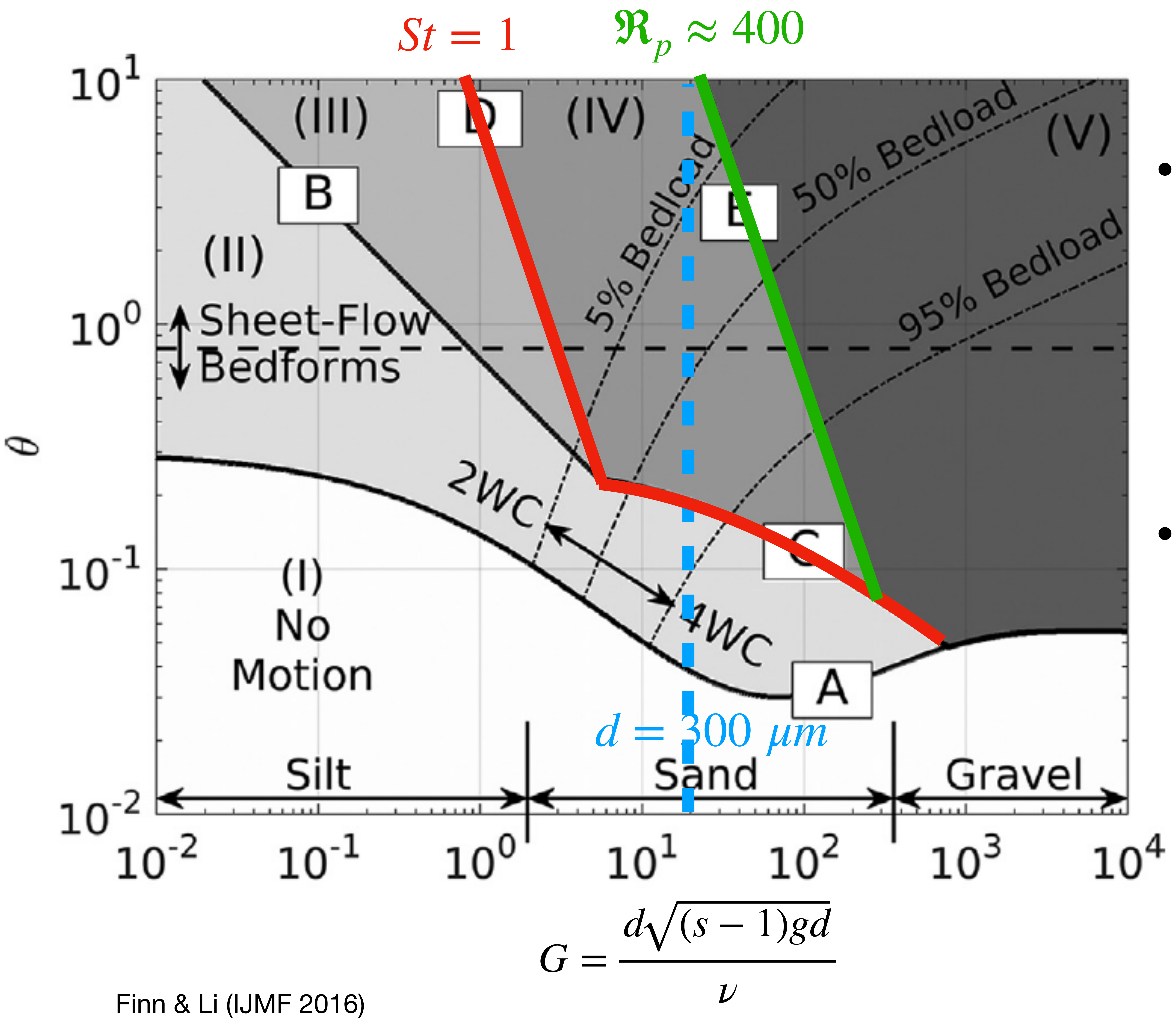

Finn & Li (IJMF 2016)

Balachandar (IJMF 2009)

- **Stokes number:** $St = \tau_p / \tau_\eta > 1$
  - Particle response time: τ_p ; Kolmogorov time scale τ_η
  - **Inertial effects**: particles do not respond instantaneously to all turbulent flow scales
- **Particulate Reynolds number:** $\mathfrak{R}_p = \frac{|u_r| d_p}{\nu^f} > \mathfrak{R}_p^c \approx 400$
  - **Vortex shedding in the wake** of particles is generated = produce turbulence at the particle scale

Regimes:

(II) Gravitational settling

(III) Kolmogorov Interactions

(IV) Inertial range dissipation

(V) Inertial range production

Favre-averaged two-phase flow equations

- Ensemble averaging: $\langle \phi \rangle = \lim_{N \to \infty} \sum_{k=1}^{N} \phi_k$ Favre-averaged velocities $\widetilde{\overrightarrow{u^f}} = \dfrac{\langle (1-\phi)\overrightarrow{u^f} \rangle}{1 - \langle \phi \rangle}$ $\widetilde{\overrightarrow{u^p}} = \dfrac{\langle \phi\, \overrightarrow{u^p} \rangle}{\langle \phi \rangle}$
- Favre-averaged two-phase flow equations:

$$\frac{\partial \langle \epsilon \rangle}{\partial t} + \nabla \left(\langle \epsilon \rangle \widetilde{\langle \vec{u} \rangle^f} \right) = 0$$

$$\rho^f \left[\frac{\partial \langle \epsilon \rangle \widetilde{\langle \vec{u} \rangle^f}}{\partial t} + \nabla \left(\langle \epsilon \rangle \widetilde{\langle \vec{u} \rangle^f} \otimes \widetilde{\langle \vec{u} \rangle^f} \right) \right] = -\rho^f \nabla \left(\langle \epsilon \rangle \widetilde{\Delta u^f \otimes \Delta u^f} \right) + \nabla \sigma^f - \langle n \langle \vec{f^p} \rangle \rangle + \langle \epsilon \rangle \rho^f \vec{g}$$

$$\frac{\partial \langle \phi \rangle}{\partial t} + \nabla \left(\langle \phi \rangle \widetilde{\langle \vec{u} \rangle^p} \right) = 0$$

$$\rho^p \left[\frac{\partial \langle \phi \rangle \widetilde{\langle \vec{u} \rangle^p}}{\partial t} + \nabla \left(\langle \phi \rangle \widetilde{\langle \vec{u} \rangle^p} \otimes \widetilde{\langle \vec{u} \rangle^p} \right) \right] = -\rho^p \nabla \left(\langle \phi \rangle \widetilde{\Delta u^p \otimes \Delta u^p} \right) + \nabla \sigma^p + \langle n \langle \vec{f^p} \rangle \rangle + \langle \phi \rangle \rho^p \vec{g}$$

Effective fluid stress

Viscous effects ~ negligible

Reynolds-like stresses

Mixing length, k-ε or LES

Fluid-particle interactions

Drag + Buoyancy

Granular stresses

µ(I) or Kinetic theory of granular flows

Fluid turbulence modeling

Reynolds shear stress: $\sigma_{ij}^{f\Delta} = -\rho^f \langle \epsilon \rangle \widetilde{\Delta u^f \otimes \Delta u^f}$ **and** $\sigma_{ij}^{p\Delta} = -\rho^p \langle \phi \rangle \widetilde{\Delta u^p \otimes \Delta u^p}$

Large Eddy Simulation: Dynamic Smagorinsky

Subgrid stresses

$$\left| \begin{array}{l} \sigma_{ij}^{f\Delta} = 2\rho^f \langle \epsilon \rangle \Delta^2 || \overline{\overline{S^f}} || \left(C_1^f S_{ij}^f - C_2^f \frac{1}{3} S_{kk}^f \delta_{ij} \right) \\ \sigma_{ij}^{p\Delta} = 2\rho^p \langle \phi \rangle \Delta^2 || \overline{\overline{S^p}} || \left(C_1^p S_{ij}^p - C_2^p \frac{1}{3} S_{kk}^p \delta_{ij} \right) \end{array} \right.$$

$$\overline{\overline{S^f}} = \nabla \overrightarrow{u^f} + \nabla \overrightarrow{u^f}^T - \frac{2}{3} tr(\nabla . \overrightarrow{u^f})$$

Coefficients C_n^k are computed using a dynamical procedure by assuming invariance of turbulent kinetic energy dissipation between the resolved and the sub grid scales

Sheet flow lab experiments (Revil-Baudard PhD, 2014)

- **Tilting flume:**
  - L = 10m ; W = 0.35m ; Slope = 0.5% ; Q = 30 L/s

- **PMMA particles:**
  - d_p = 3 mm
  - ρ^p/ρ^f=1.19
  - μ_s = 0.7

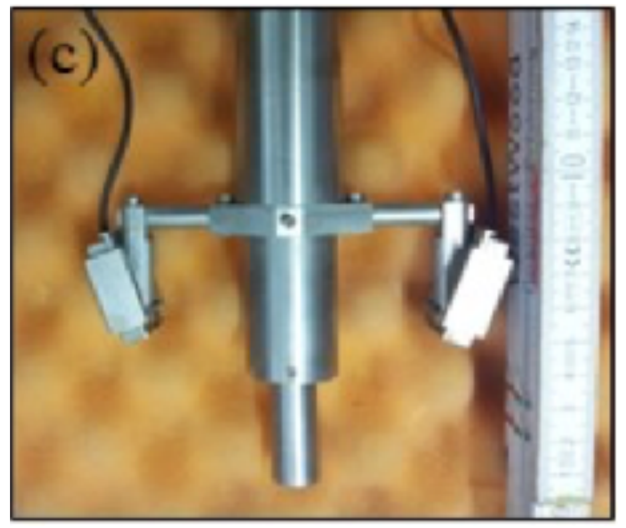

- **Acoustic Concentration and Velocity Profiler (Hurther et al., 2011)**
  - 2C Velocity (u and w) : Fs=75 Hz and Z = 3 mm
  - Concentration (ϕ) : Fs=4.9 Hz and Z = 3 mm
  - Fixed-bed interface (zc) : Fs=7.5 Hz and Z = 3 mm

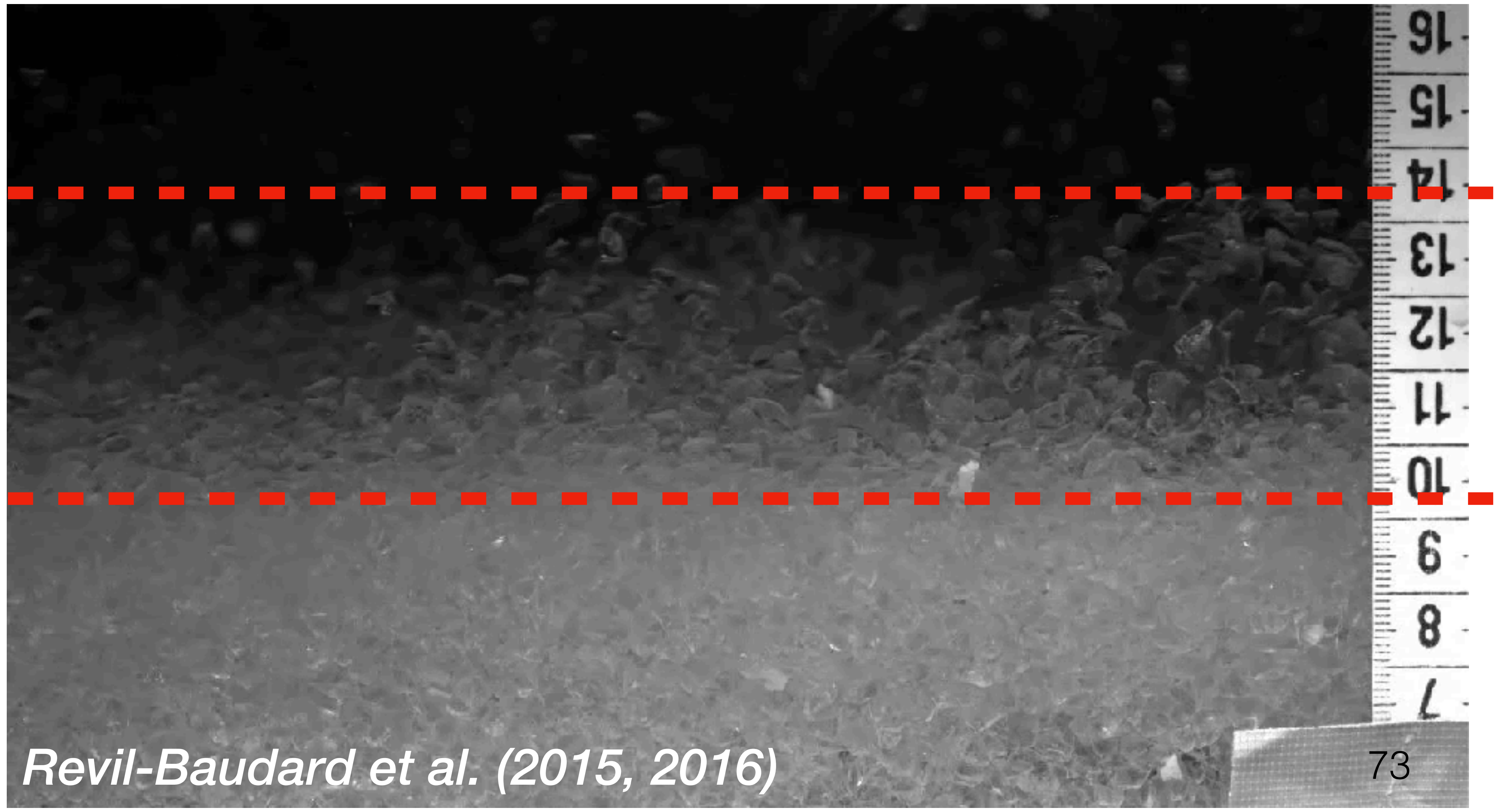

Revil-Baudard et al. (2015, 2016)

$$\tau^m = \rho^m g S_f (H_f - z)$$

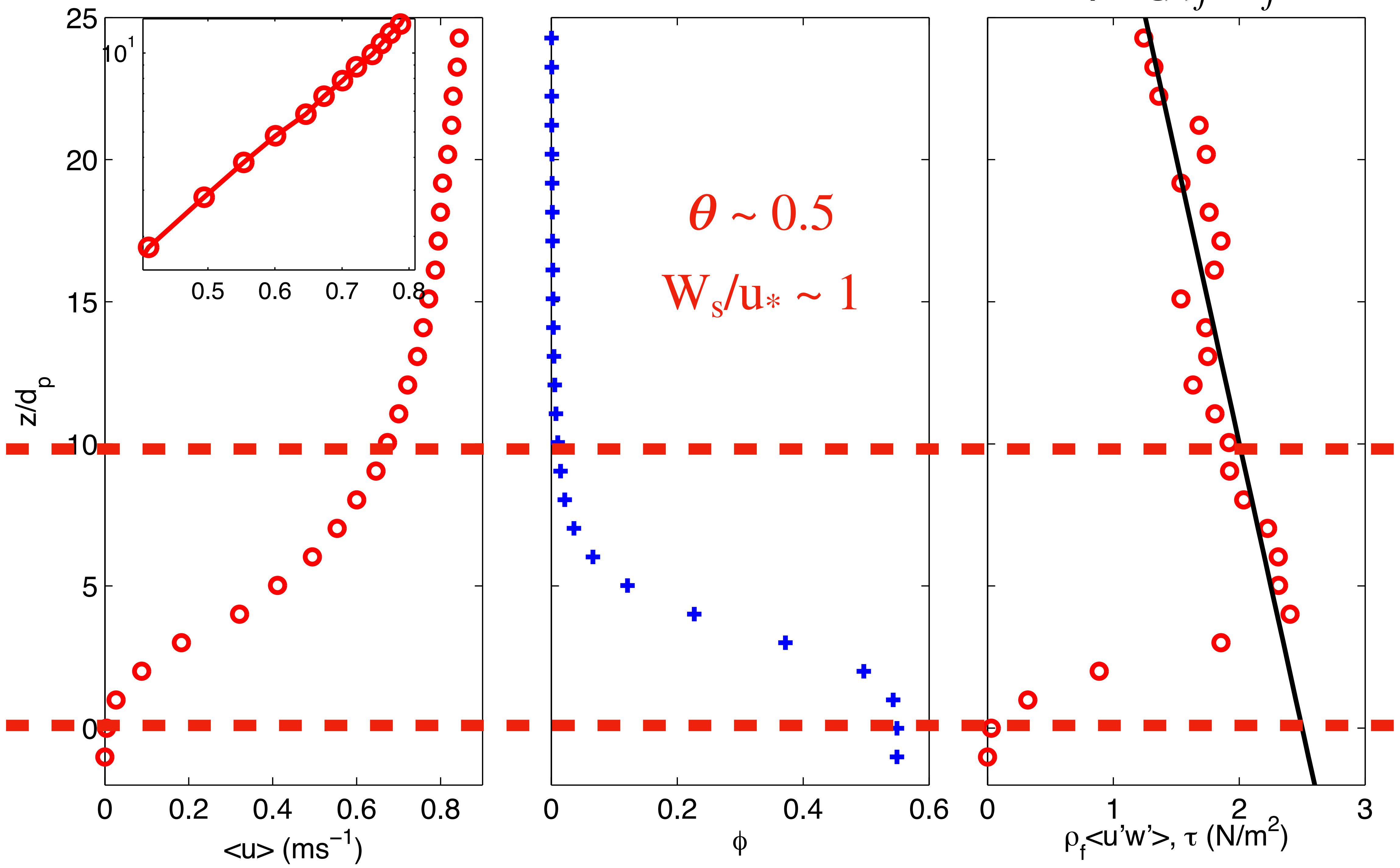

Bed friction velocity: $u_* = \sqrt{\langle u'w' \rangle |_{z=0}}$ =0.05 m/s

Two-phase flow LES of sheet flow (Cheng PhD, 2016)

Kinetic Theory of Granular Flows

Dynamic Smagorinsky model:

$$\nu^t = C_s^f \Delta^2 \, || \, \overline{\overline{S^f}} \, || \quad \text{where } C_s^f = \frac{< L_{ij} L_{ij}^d >}{< L_{ij}^d L_{ij}^d >}$$

Drift velocity model: $\vec{u^d} = \widehat{\phi C_D \, \vec{u^r}} - \widehat{\phi}\widehat{C_D}\widehat{\vec{u^r}}$

corresponds to the unresolved drag force (Ozel et al., 2013)

Mesh:

30M cells (Δx=Δy=1.65 mm ; Δz = 0.4 - 2.2 mm)

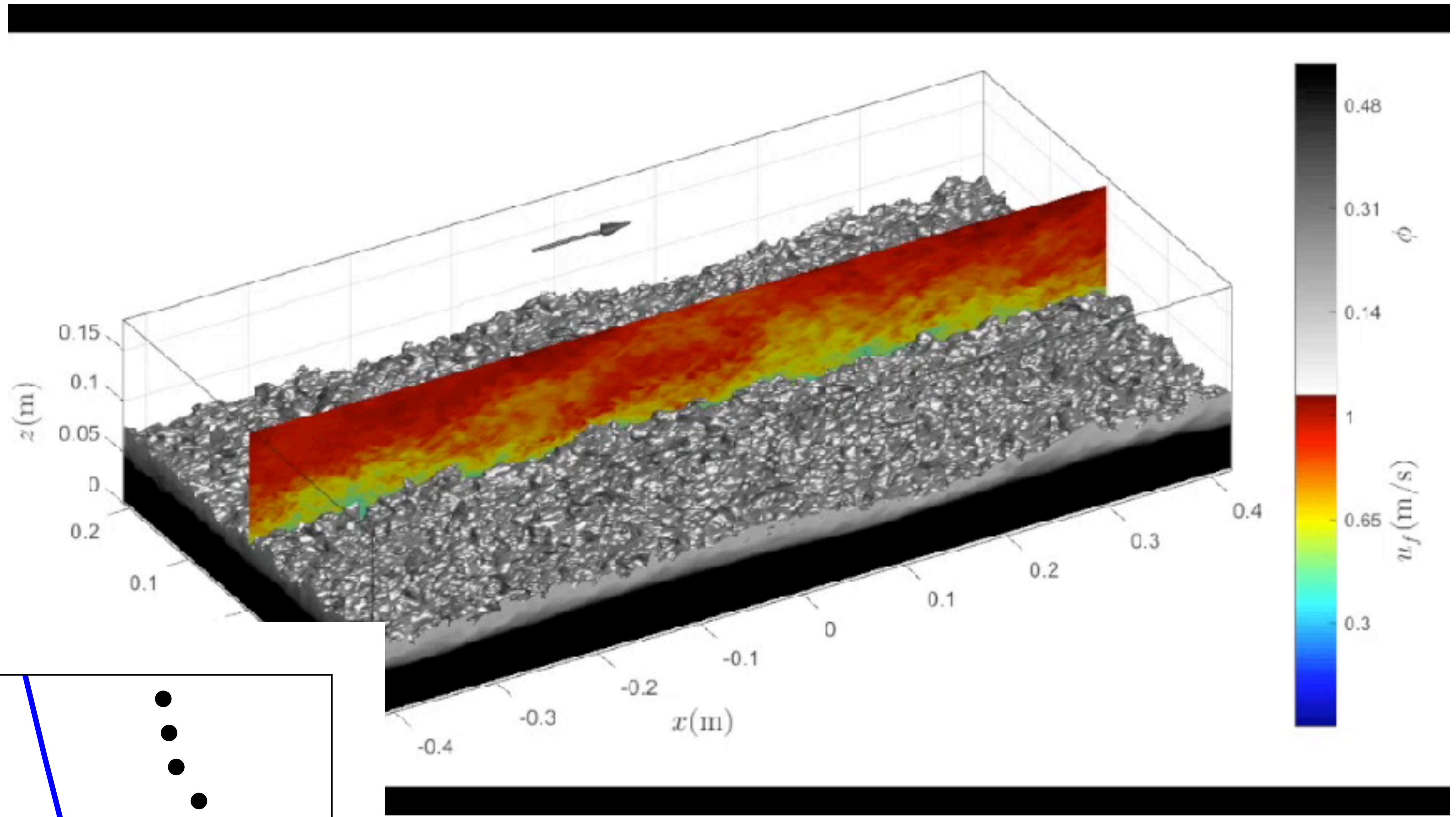

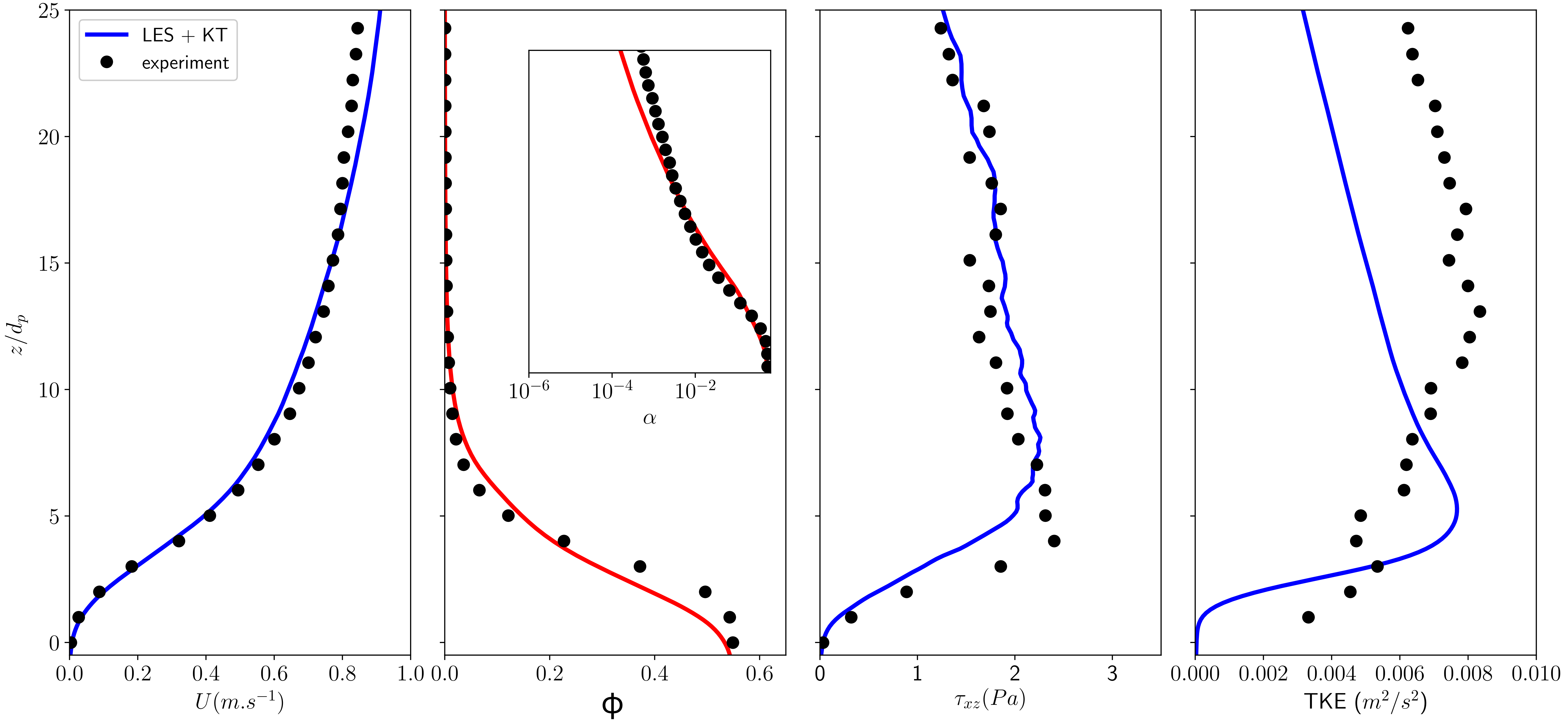

- Good agreement with experiments
- No tuning parameter (almost…)

Cheng et al. (2018)

Conclusion on sediment transport modeling at the grain-scale

- **Eulerian-Lagrangian modeling $\Rightarrow$ granular rheology in bed-load transport**
  - ➡ µ(I) rheology is accurate in the dense region (ϕ>0.3)
  - ➡ Frictional kinetic theory : works reasonably well over the full range of ϕ

- **Eulerian-Eulerian modeling**
  - ➡ µ(I) rheology successfully implemented using a regularization technique
  - ➡ Two-fluid LES: resolve turbulence-particle interactions

- **Opens new perspectives for upscaling and application to complex flow configurations**

Open question: Is it possible to derive a well-posed two-fluid model?

Open question: How to develop a well-posed granular rheology ? µ(I) or kinetic theory?

Outline

1. Coastal modeling at « large scale »

2. Sediment transport modeling at the grain scale : turbulent and granular processes

3. Upscaling of fine-scale processes at intermediate scales

Sand transport by waves: unsteady effects

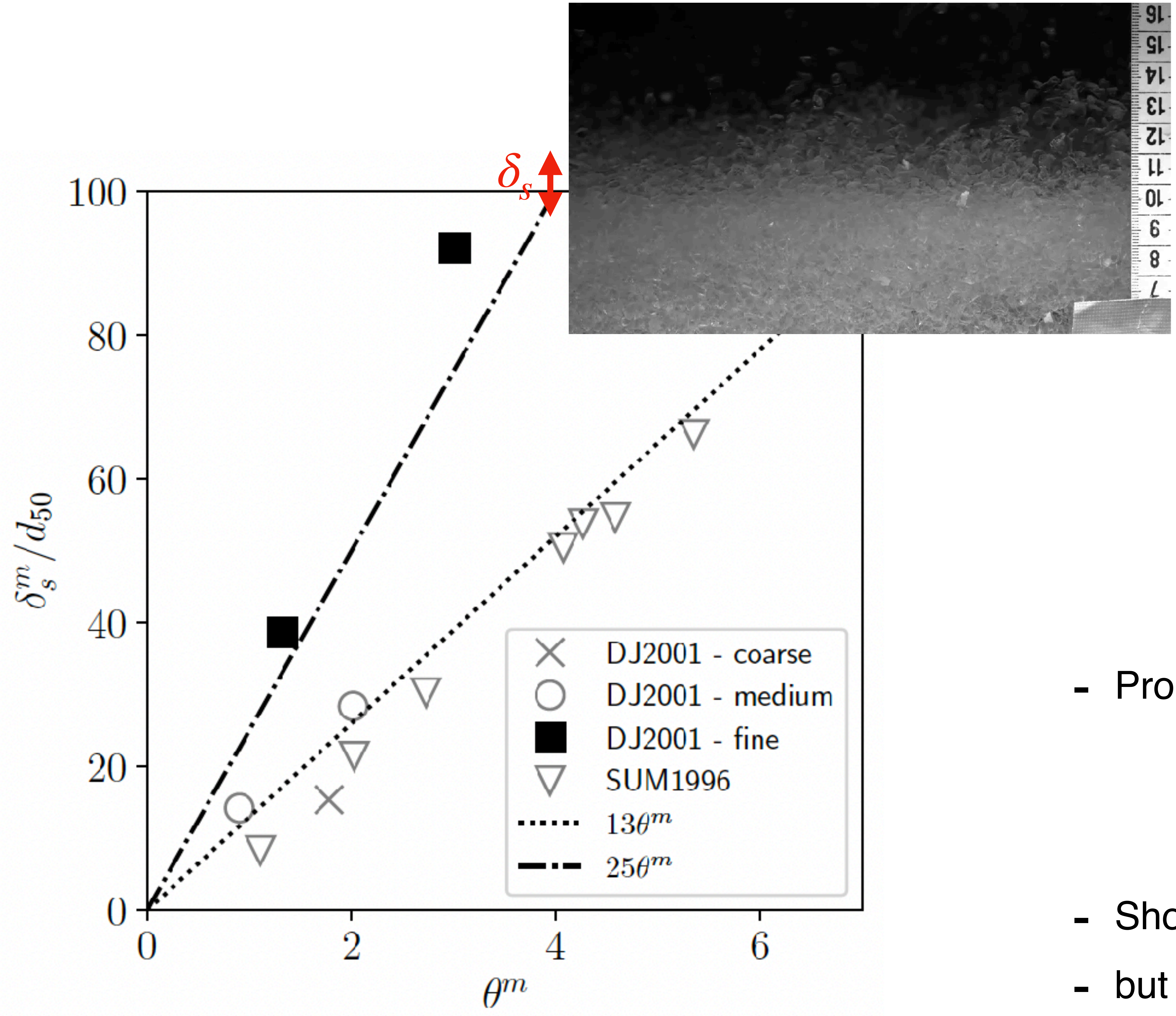

Waves: Dohmen-Janssen *et al.* (2002)
Current: Sumer *et al.* (1996)

Oscillating Water Tunnel - O'Donoghue & Wright (2004)

Sheet-flow layer thickness

- Proportional to Shields number:

$$\frac{\delta_s^m}{d_p} = \alpha\ \theta \qquad \text{with } \alpha = 10 - 13$$

- Should not depend on particle size
- but thicker sheet-flow layer observed for fine sand

Why ?

A. Mathieu PhD (2021)

Two-phase flow LES of oscillatory sheet flow

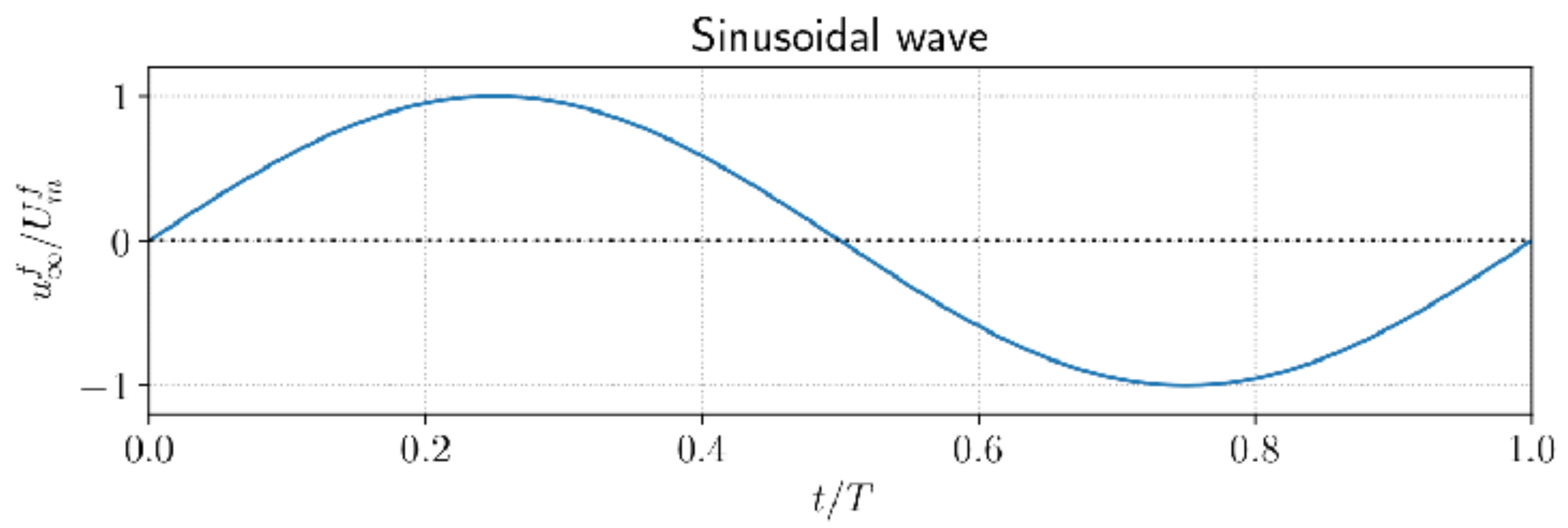

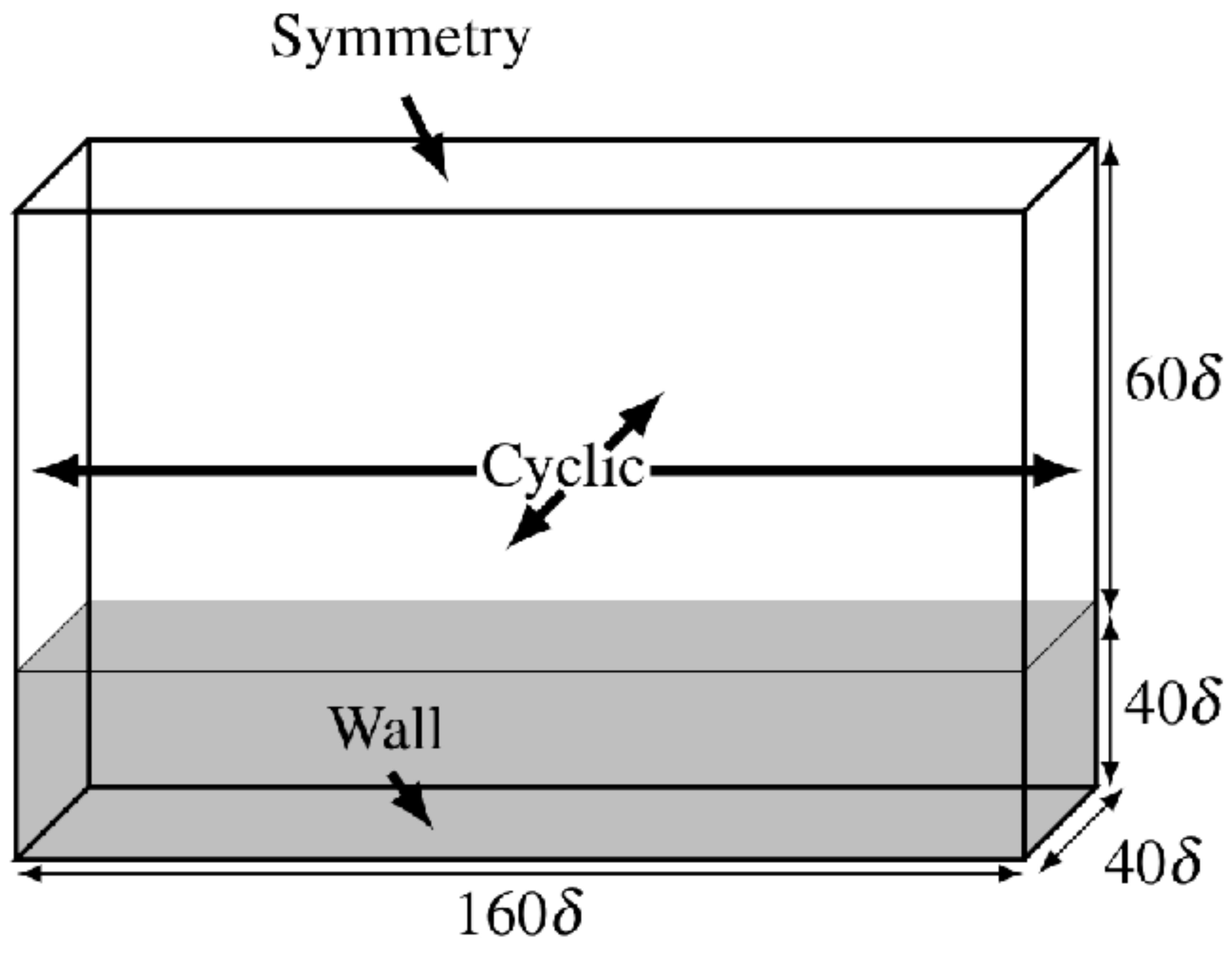

Mesh	Number of cells	Δ_x^+	Δ_z^+	Δ_y^+ (bed)
$200 \times 260 \times 92$	4,784,000	110	60	25

Configuration

O'Donoghue & Wright (2004)

Sine wave:

- $T = 5$ s
- $U_m^f = 1.5$ m/s
- Stokes layer thickness $\delta = 1.26 \times 10^{-3}$ m

Particles:

- $\rho^p = 2650\ kg\,.\,m^{-3}$ s

	Medium sand	Fine sand
d_p (μm)	280	150
V_s (cm/s)	4	1.6

$$\Delta^+ = \frac{\Delta\ u_*}{\nu^f}$$

A. Mathieu PhD (2021)

Two-phase flow LES of oscillatory sheet flow

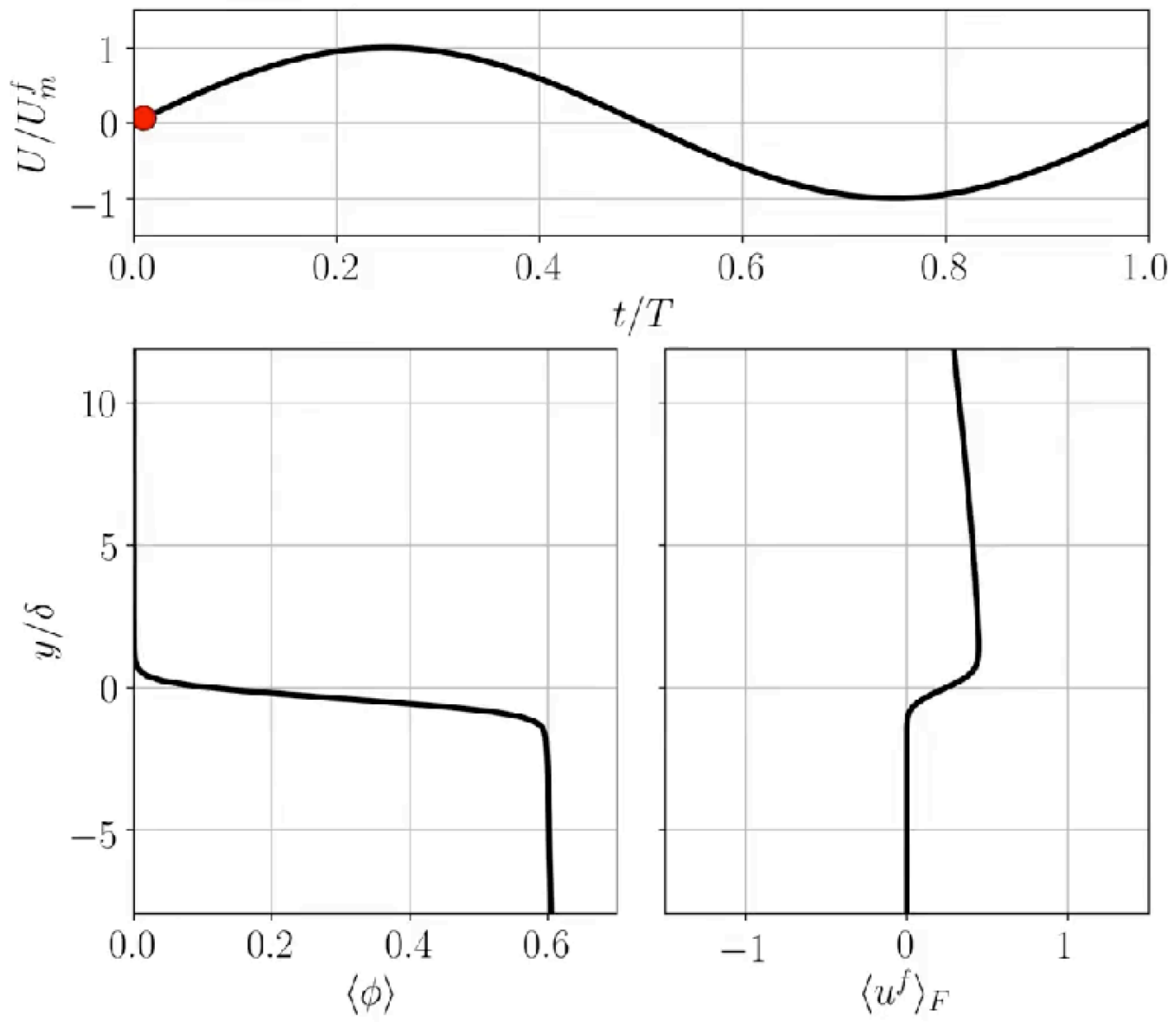

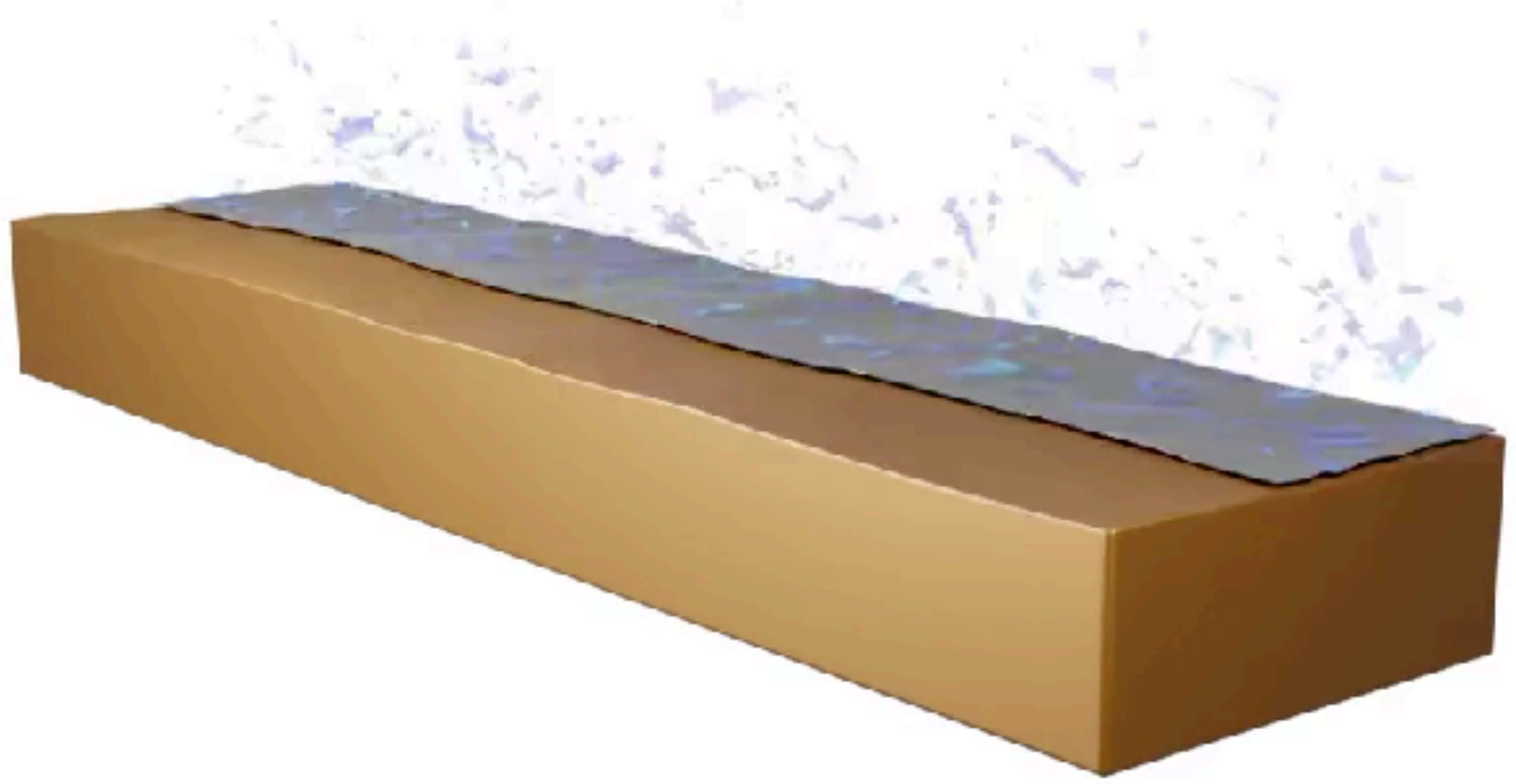

Medium sand

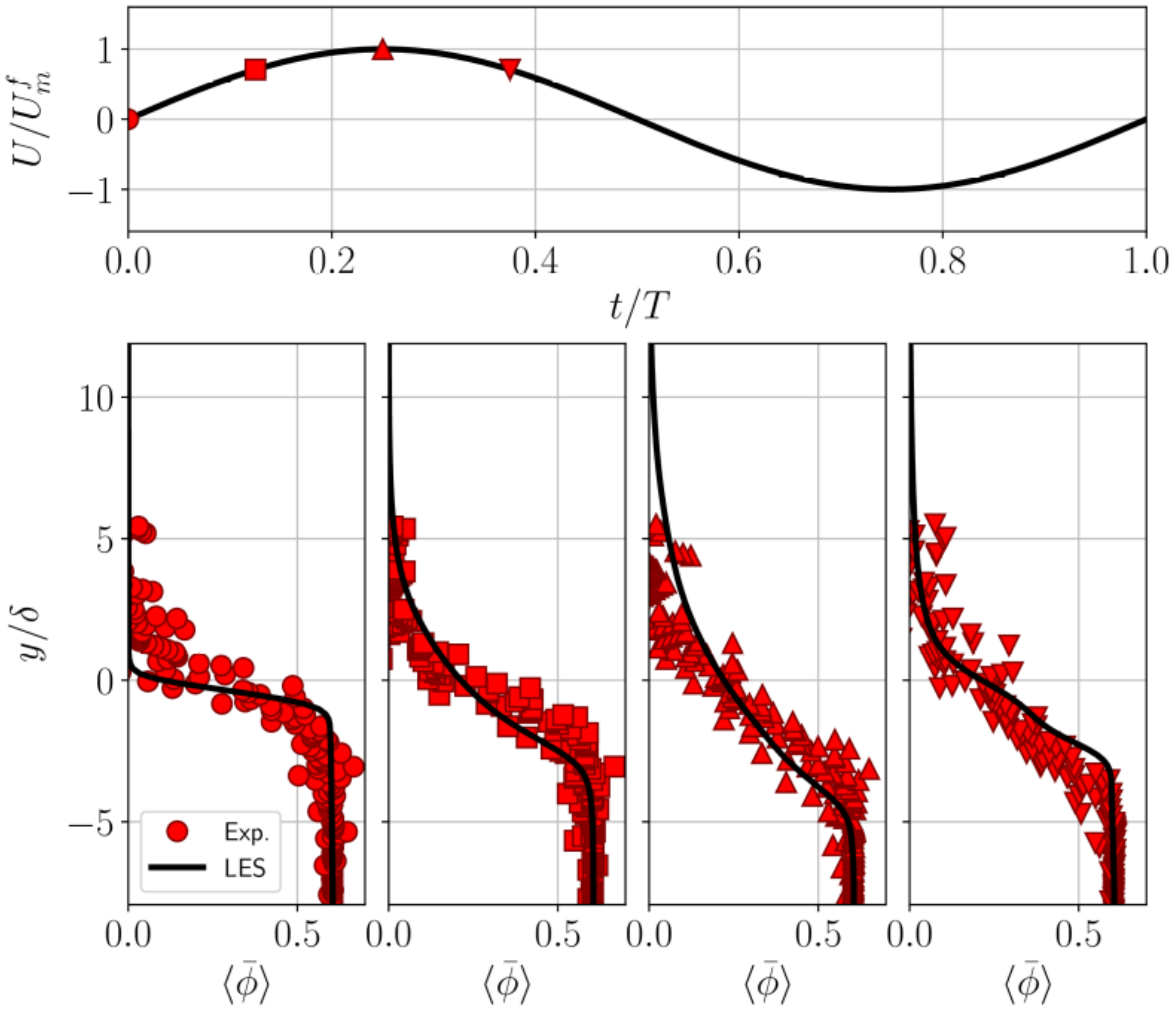

Isocontours of concentration : $\overline{\phi} = 0.5$ (brown) and $\overline{\phi} = 0.08$ (silver)

Turbulent coherent structures : Q criterion

A. Mathieu PhD (2021)

Two-phase flow LES of oscillatory sheet flow

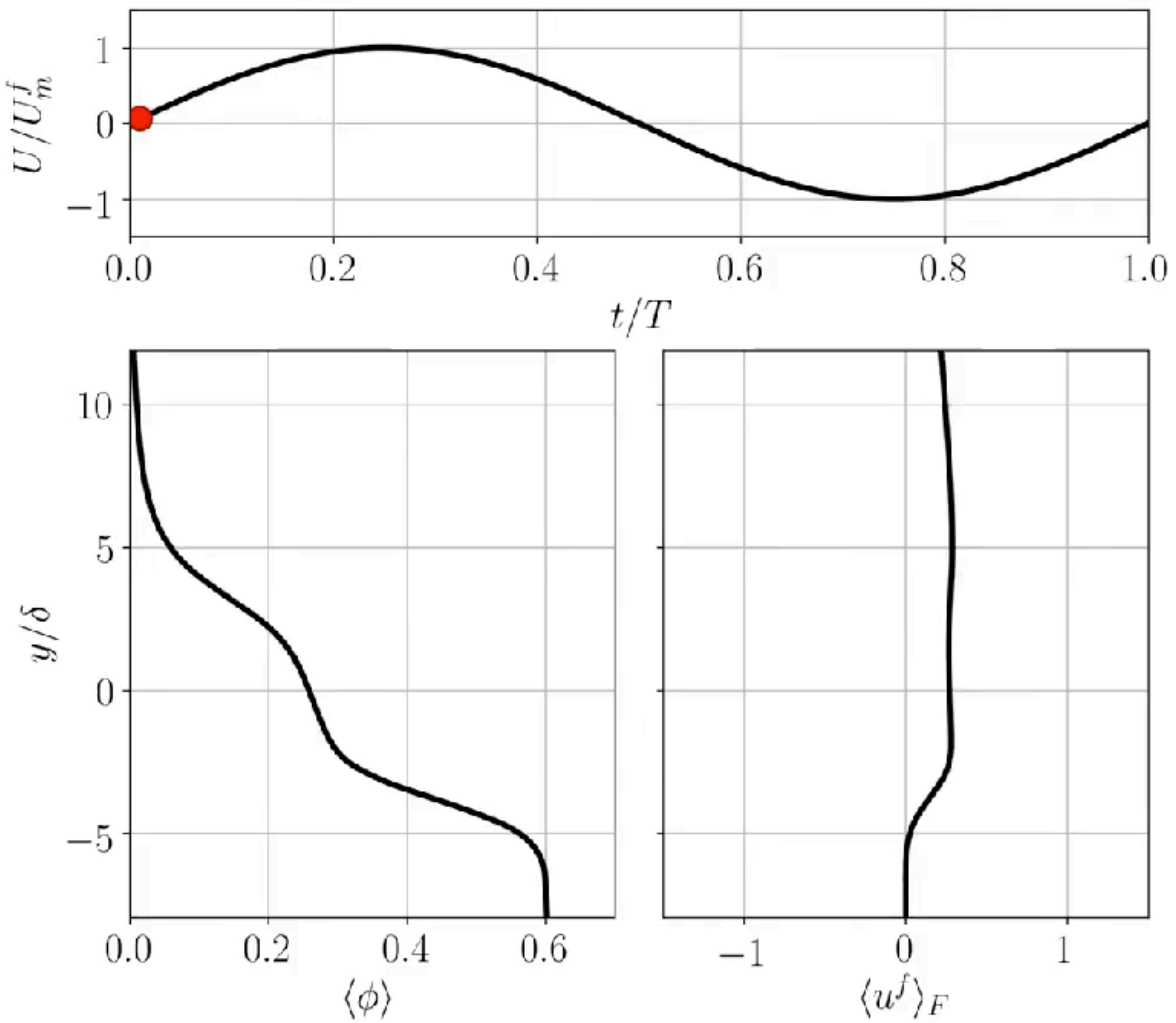

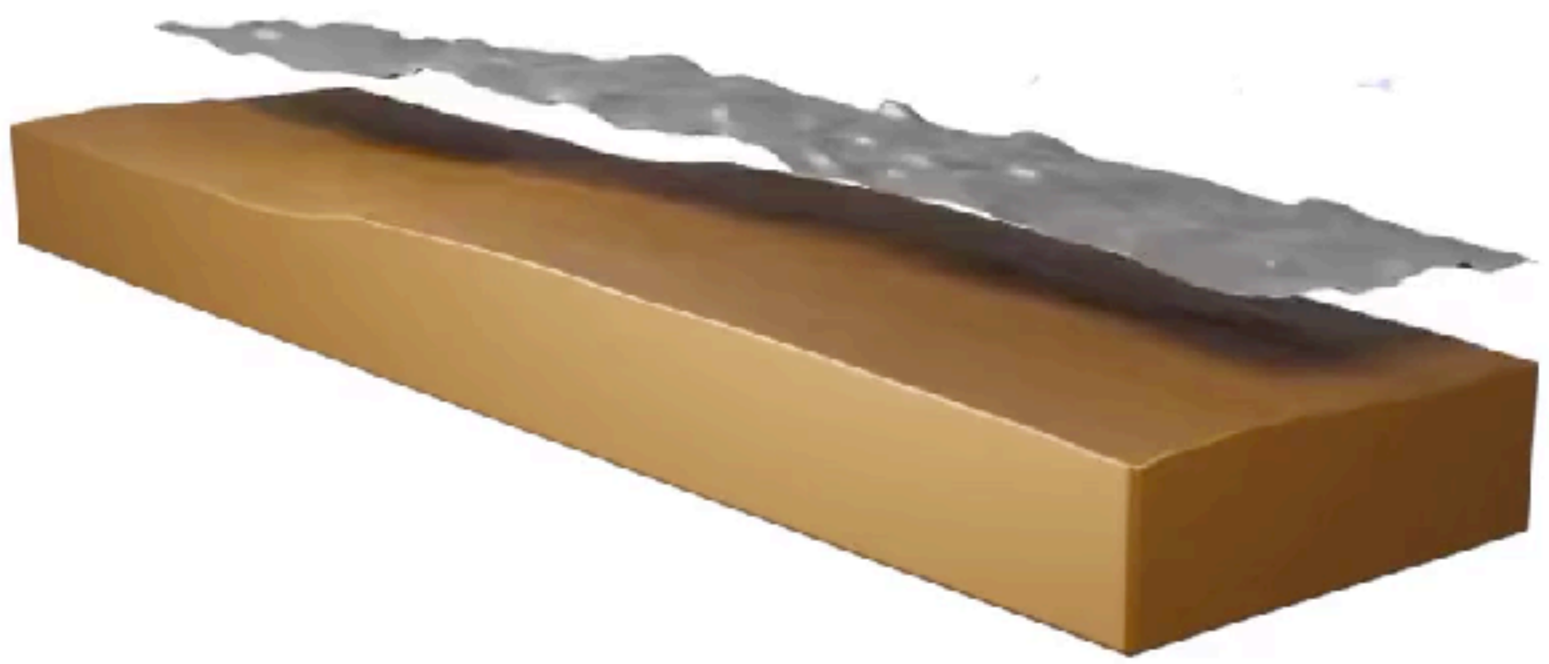

Fine sand

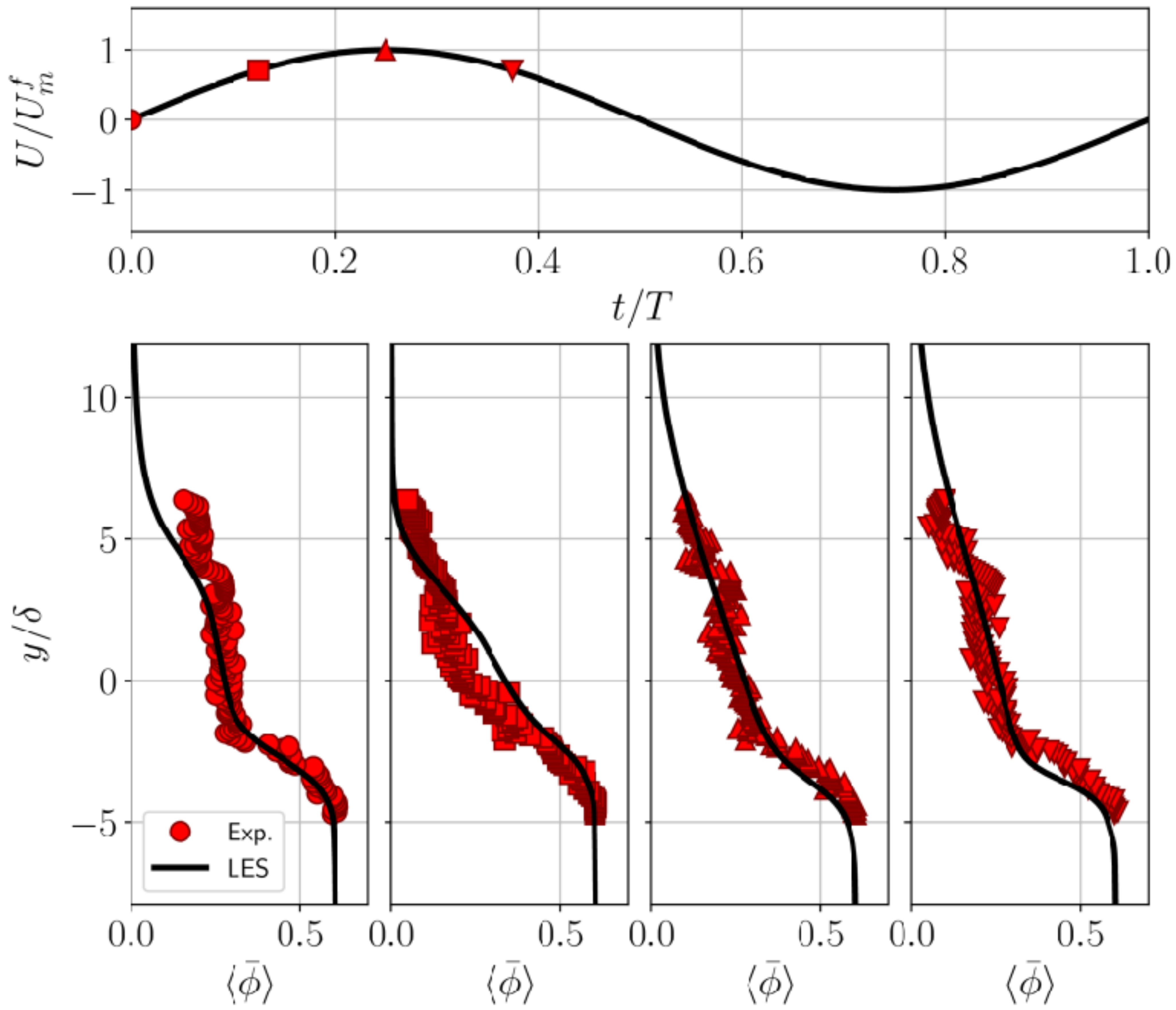

Behavior is different between medium and fine sand

Isocontours of concentration : $\overline{\phi} = 0.5$ (brown) and $\overline{\phi} = 0.08$ (silver)

Turbulent coherent structures : Q criterion

A. Mathieu PhD (2021)

Two-phase flow LES of oscillatory sheet flow

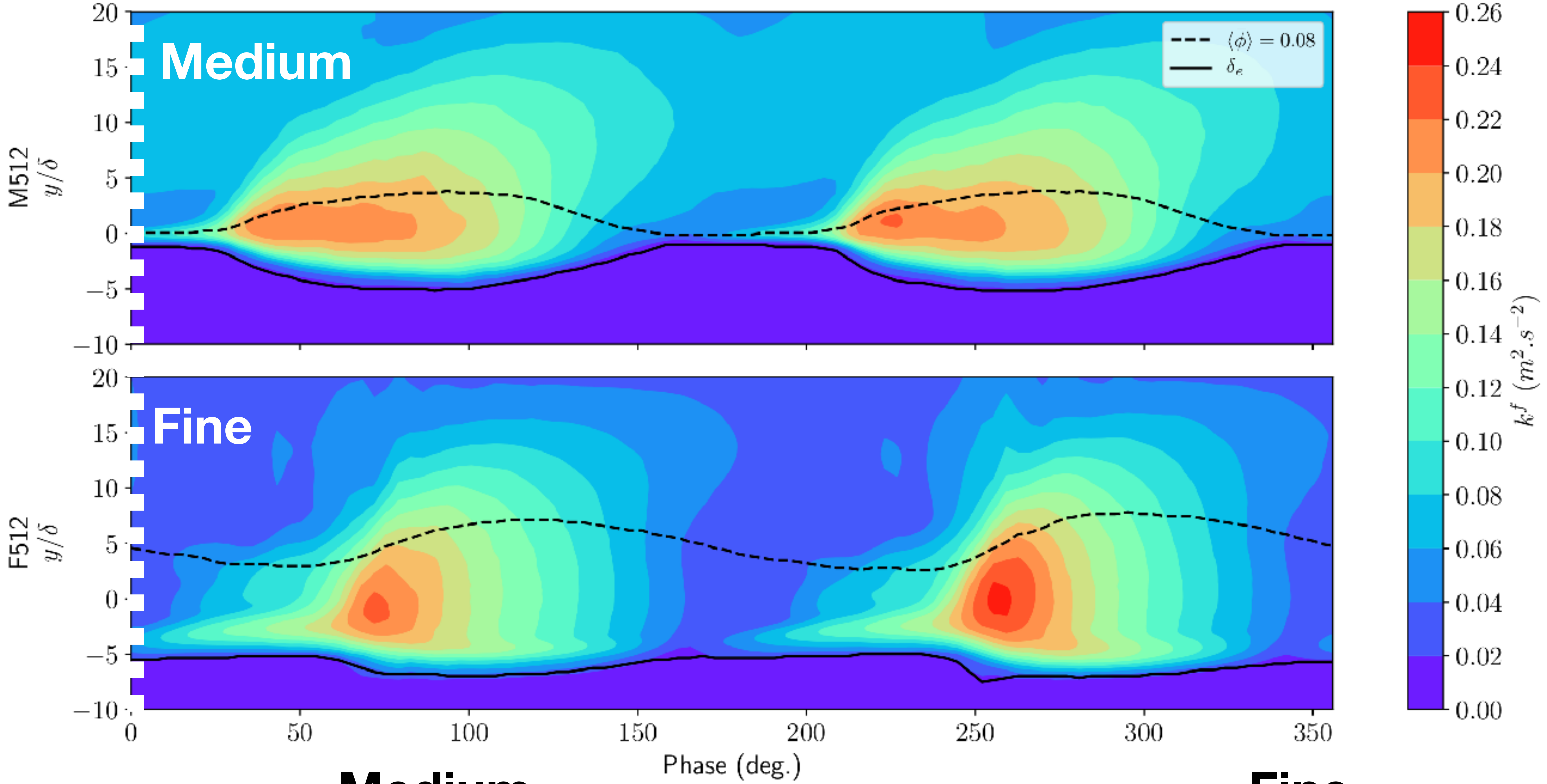

Flow reversal

- Medium sand deposited
- Fine sand still suspended

➡ Sheet-fow layer thickness not in phase with free stream velocity

Medium

Fine

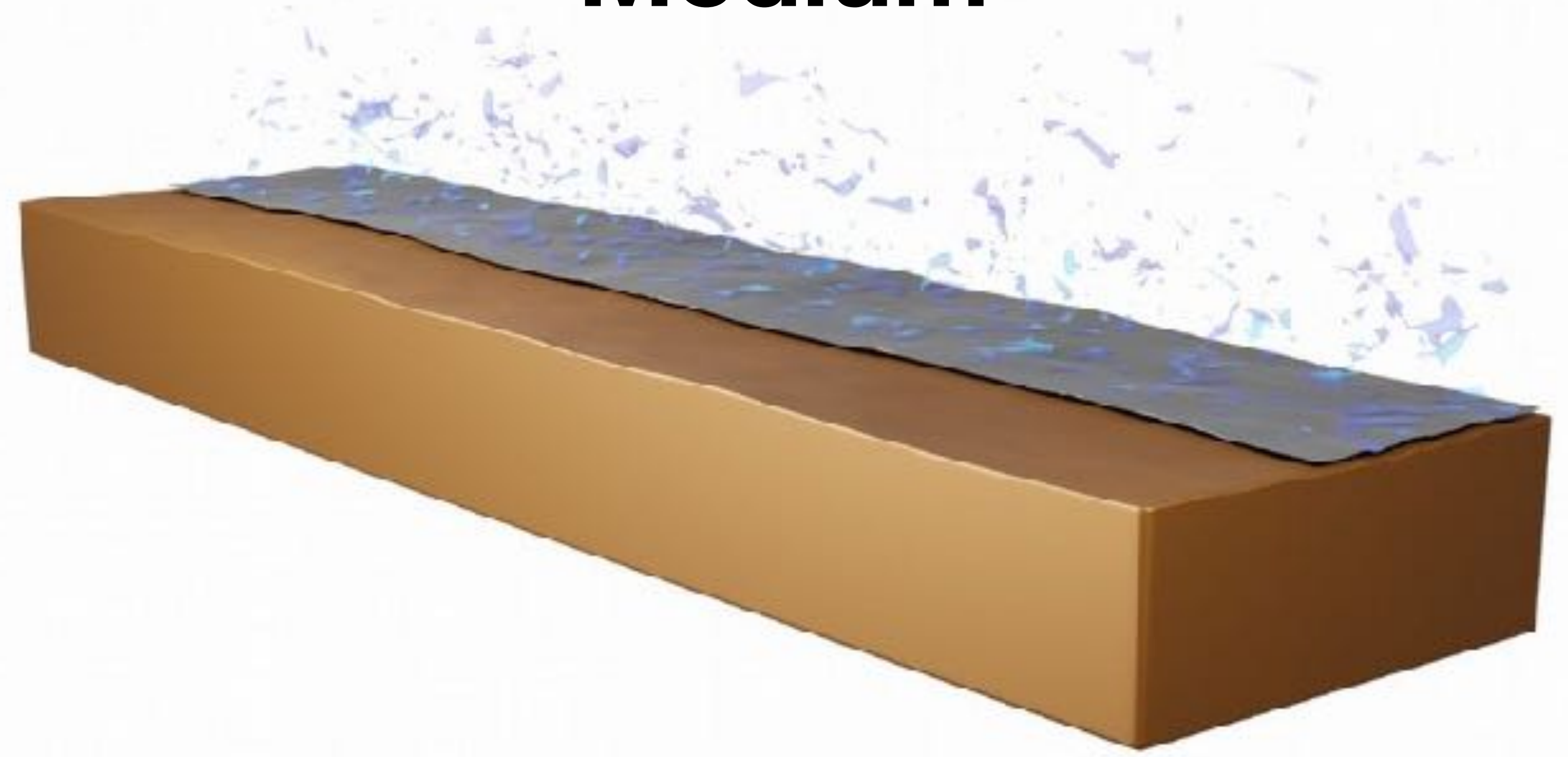

0°

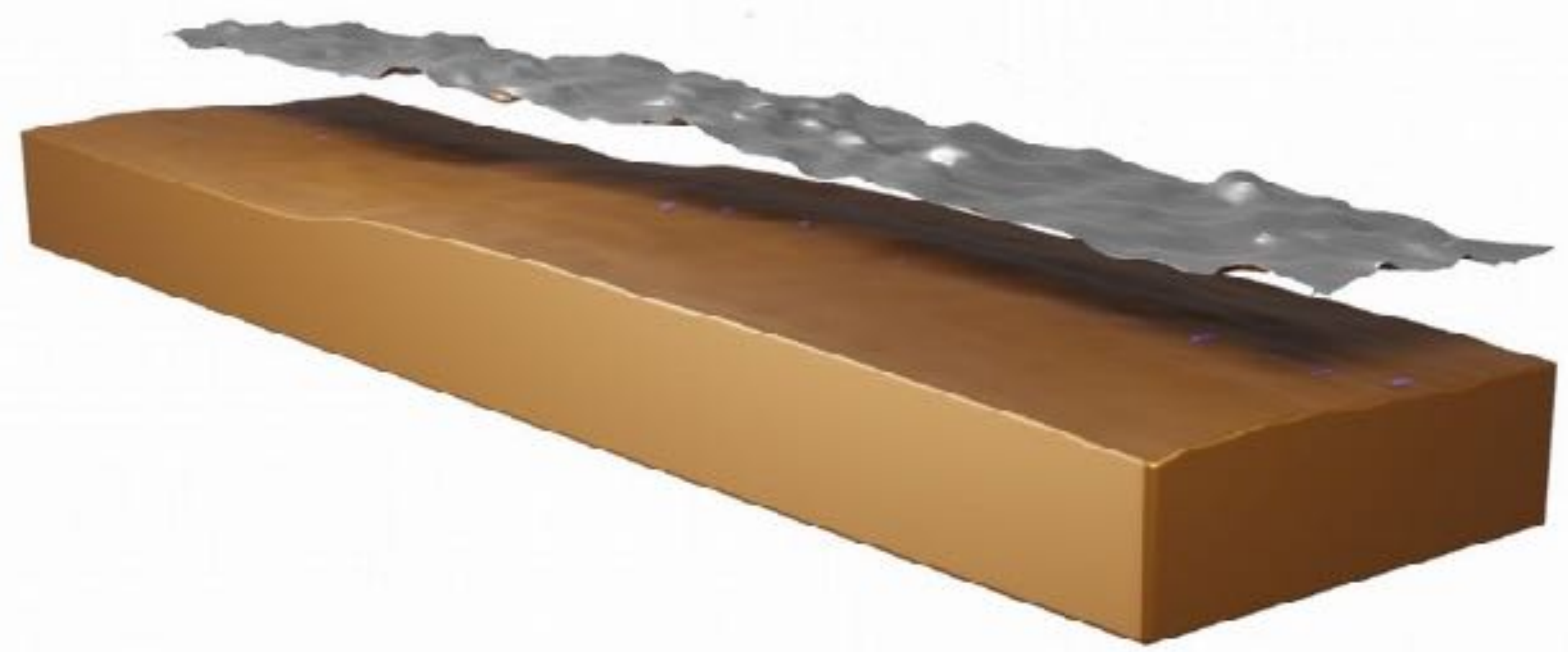

A. Mathieu PhD (2021)

Two-phase flow LES of oscillatory sheet flow

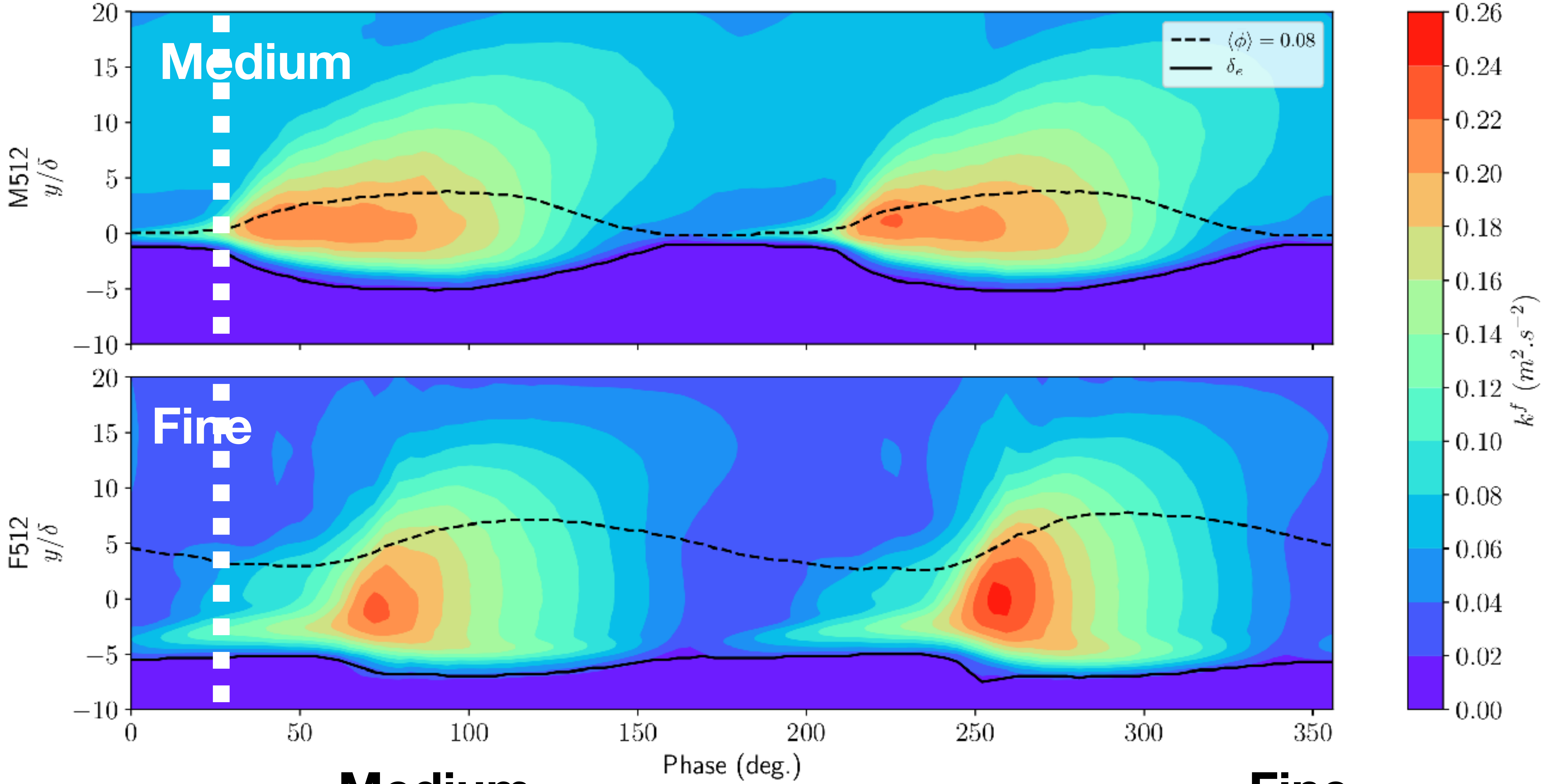

Acceleration phase

- Flow instabilities are triggered
- Stronger for medium sand

Medium **Fine**

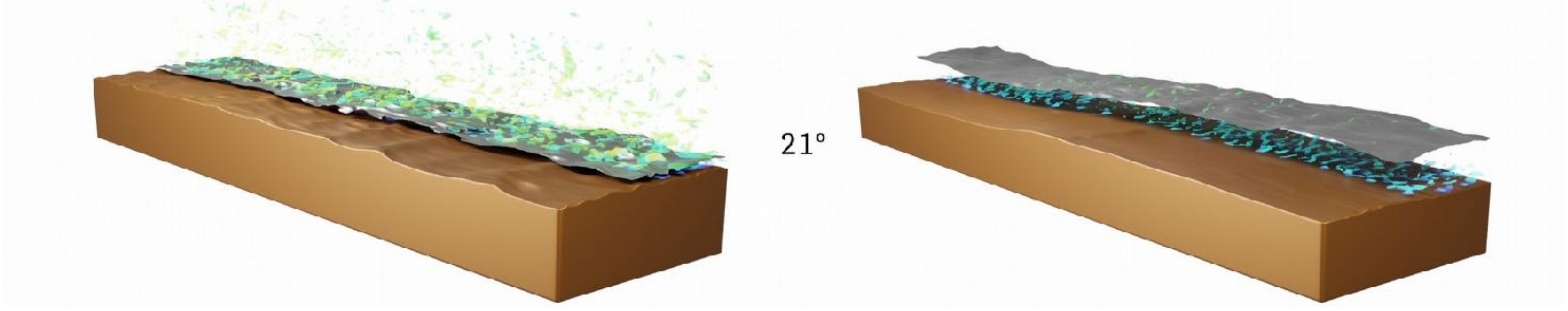

A. Mathieu PhD (2021)

Two-phase flow LES of oscillatory sheet flow

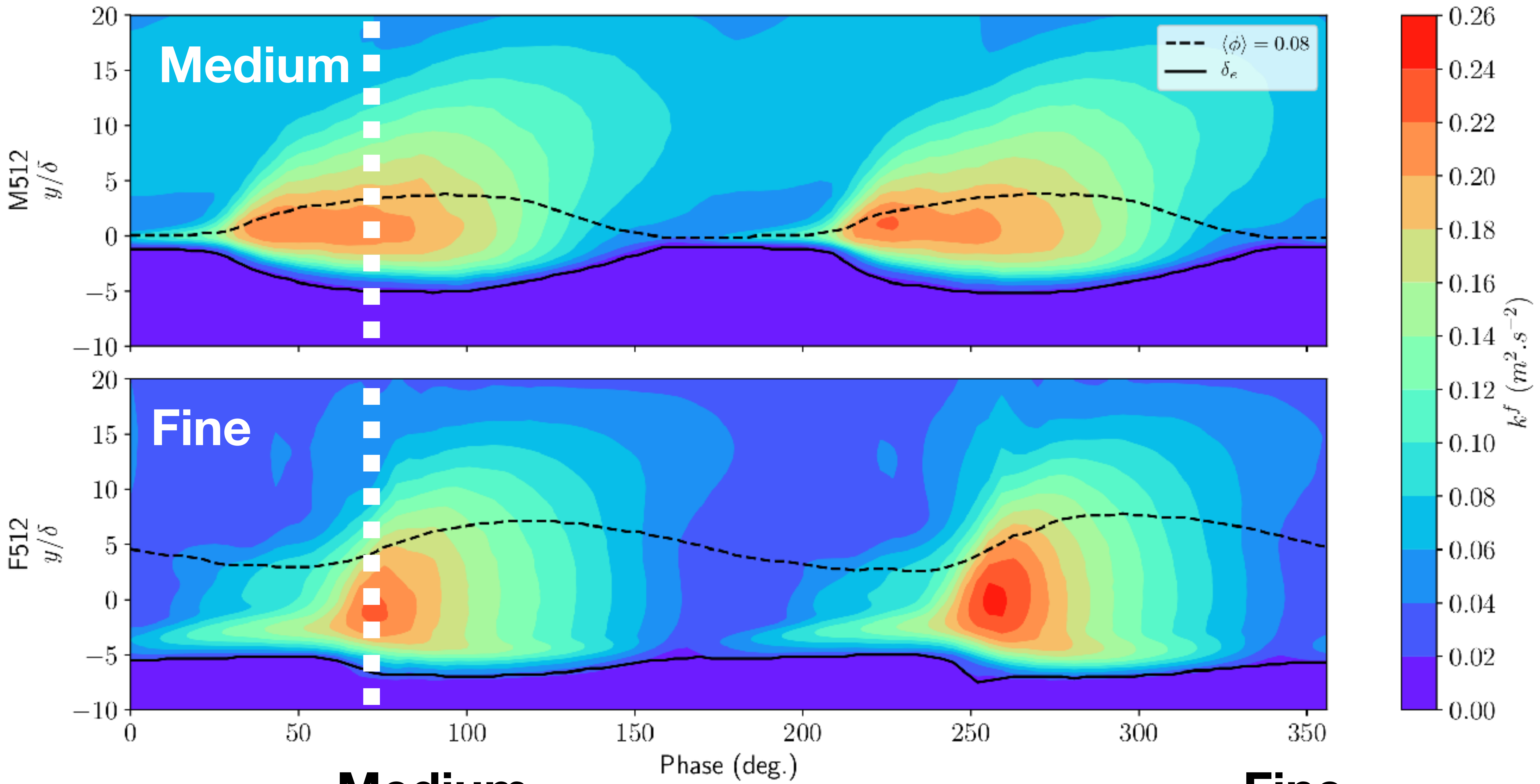

Medium

Fine

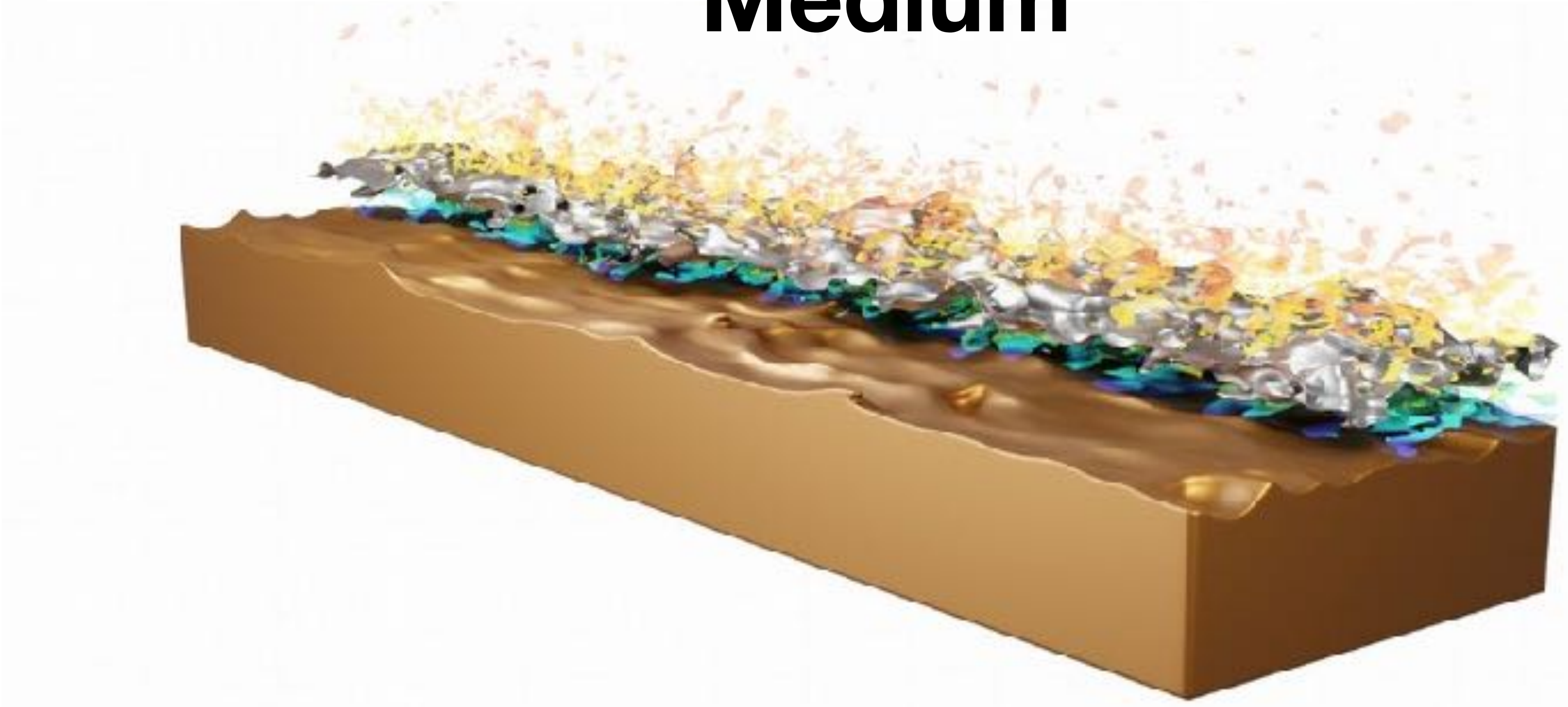

58°

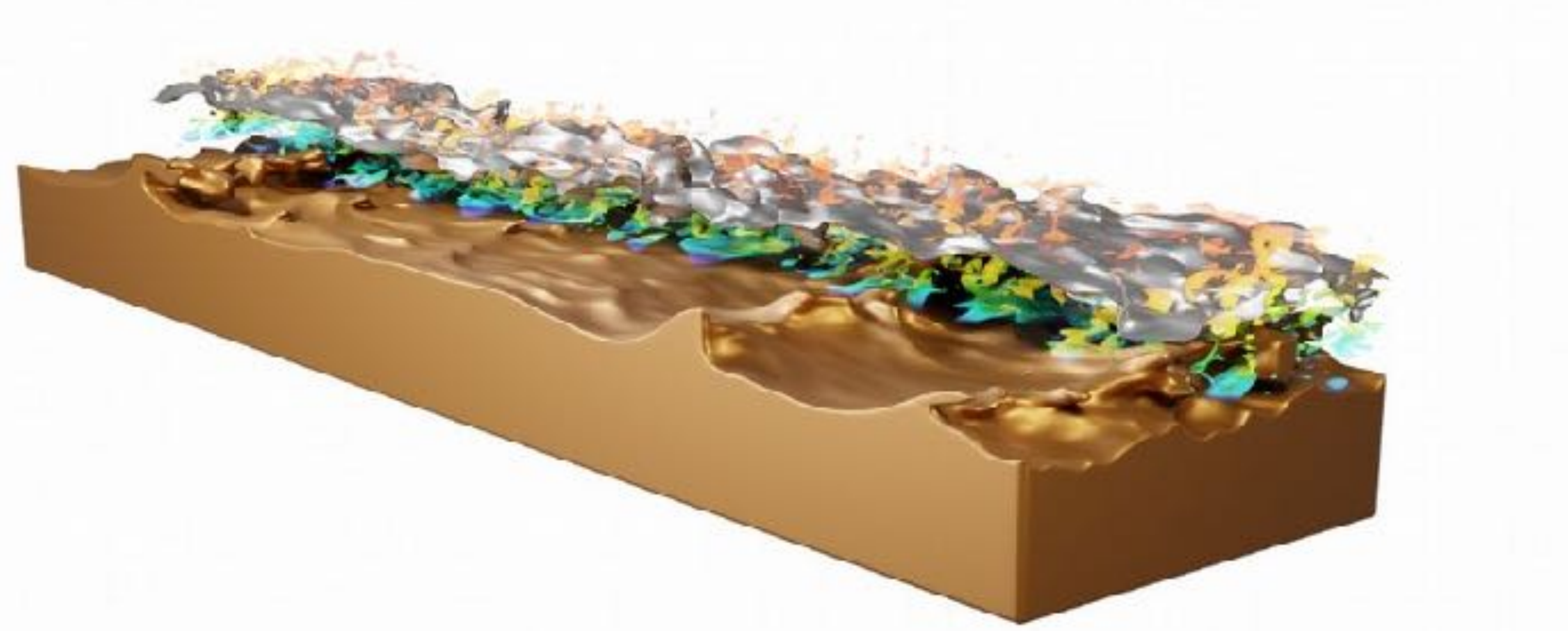

Flow peak

- Flow instabilities are well-developped
    - stronger for fine sand
- Sheet-flow layer thickness
    - in-phase for medium sand
    - phase-lag for fine sand

A. Mathieu PhD (2021)

Two-phase flow LES of oscillatory sheet flow

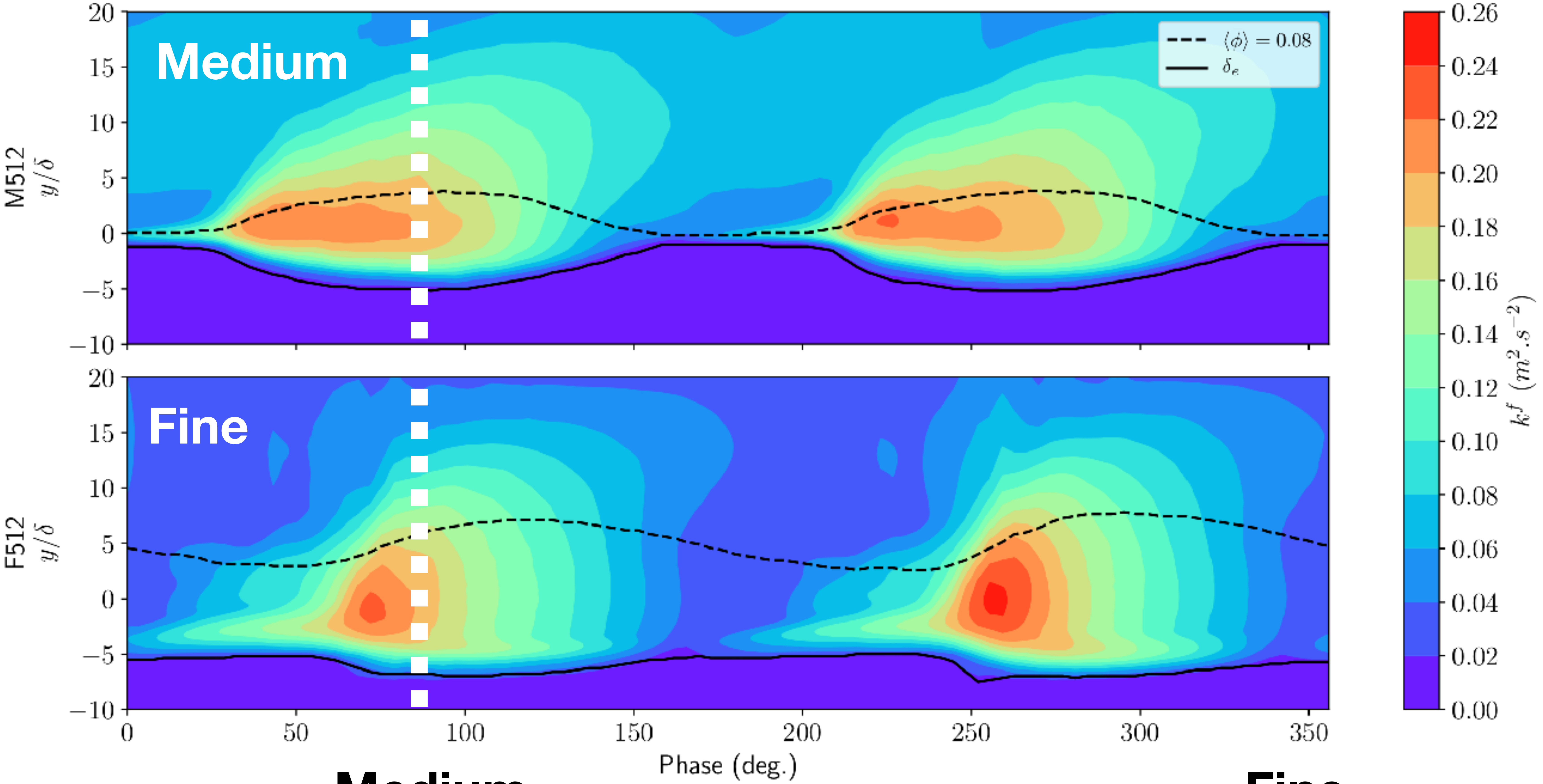

Medium **Fine**

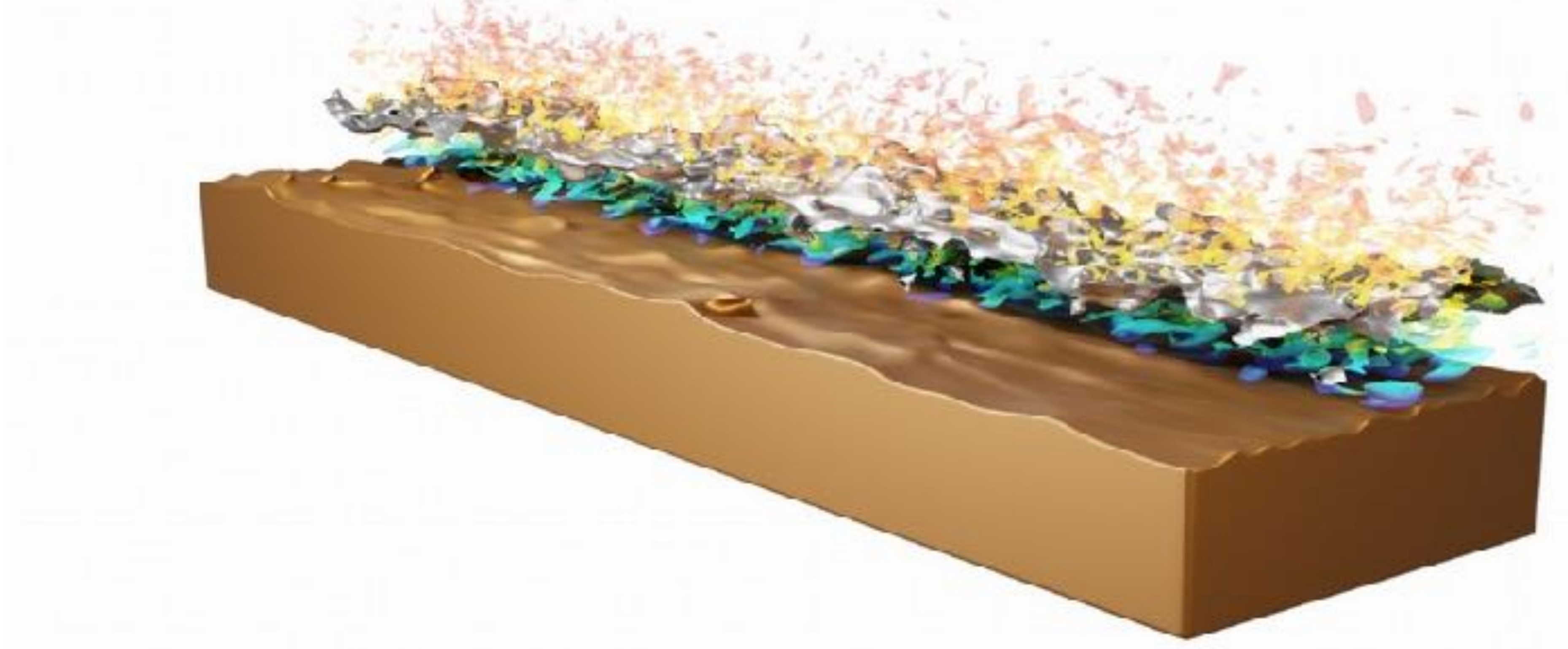

90°

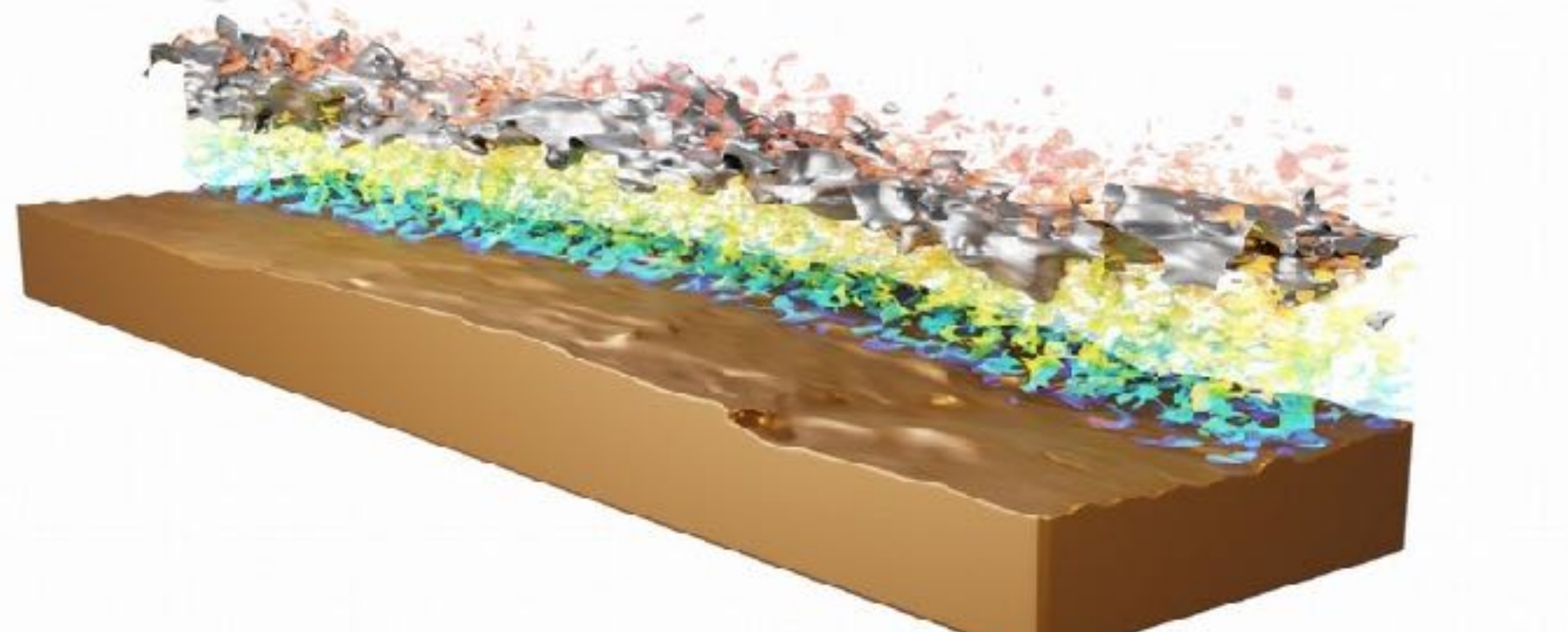

Deceleration phase

- Flow instabilities are well-developped
  - stronger for fine sand

- Sheet-flow layer thickness
  - in-phase for medium sand
  - phase-lag for fine sand

A. Mathieu PhD (2021)

Two-phase flow LES of oscillatory sheet flow

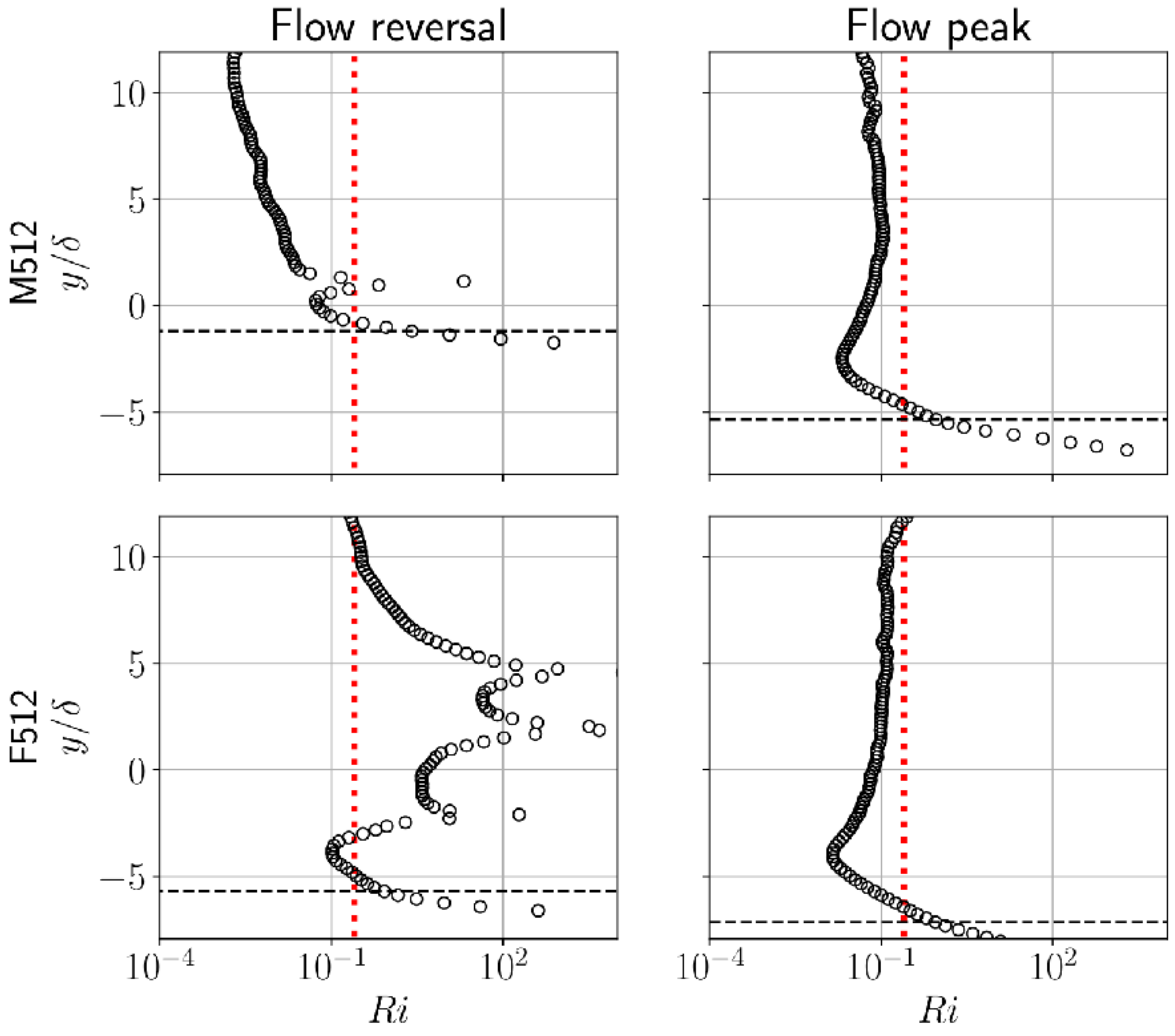

Density stratification

Richardson number: $$Ri = \frac{g}{\rho^m} \frac{\partial \rho^m / \partial y}{(\partial u^f / \partial y)^2}$$

Buoyancy dissipation / production of TKE

➡ Flow reversal

- For medium sand:
  - Density stratification is strong enough to damp turbulence
- For fine sand:
  - Density stratification overcome turbulence production
  - The flow is laminarized by the presence of the particles

➡ Flow peak

- always unstable = no effect of particles on turbulence

A. Mathieu PhD (2021)

Two-phase flow LES of oscillatory sheet flow

Sediment fluxes

Reynolds-averaged sediment mass conservation

$$\frac{\partial \overline{\phi}}{\partial t} + \frac{\partial}{\partial y} \underbrace{\left(\overline{\phi}\, \overline{\langle v \rangle^p} + \overline{\phi' \langle v \rangle^{p'}} \right)}_{= \overline{\phi \langle v \rangle^p}} = 0$$

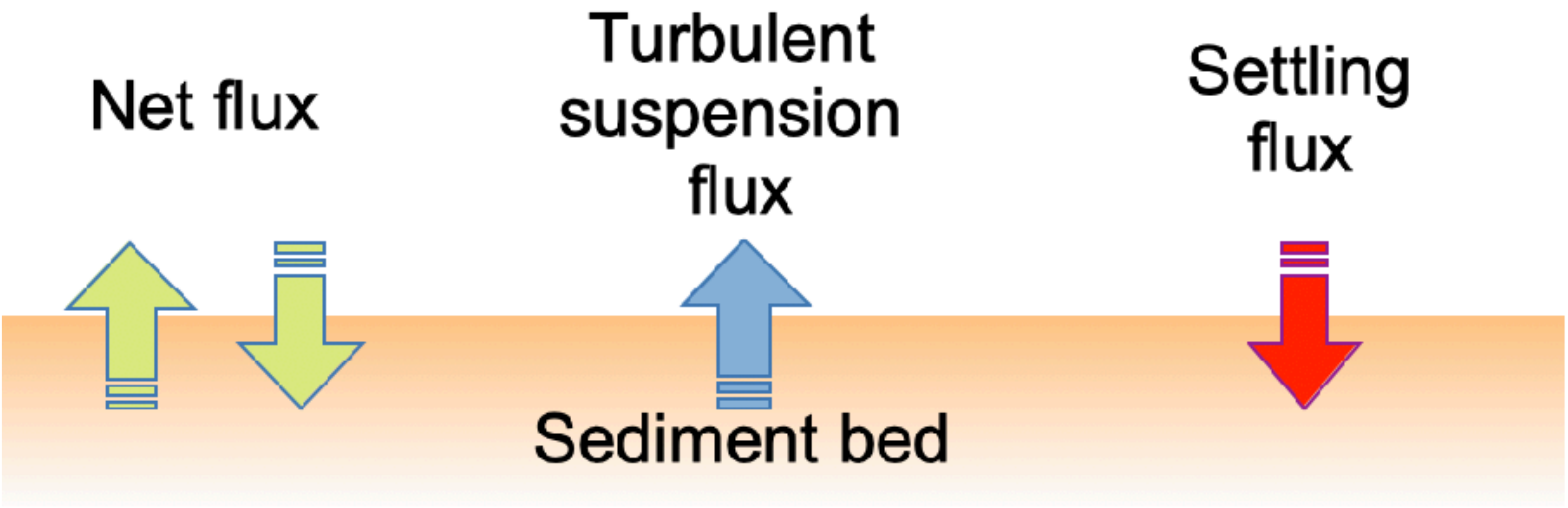

Turbulent flux = erosion

Settling flux = deposition

A. Mathieu PhD (2021)

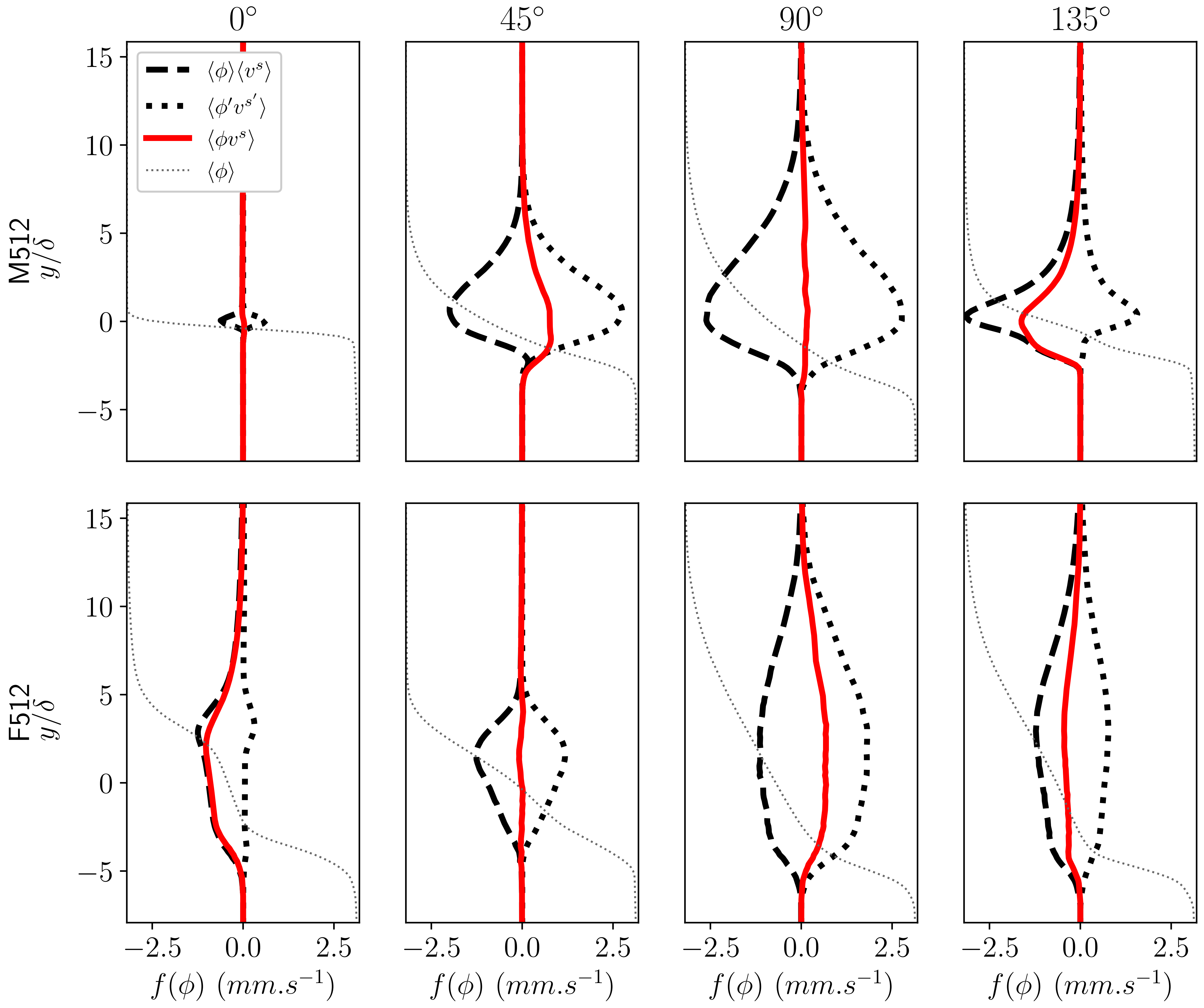

➡Flow reversal

- Essentially stable for medium sand
- Stable for fine sand => strong turbulence reduction

➡Flow peak

- always unstable = no effect on turbulence

Two-phase flow LES of oscillatory sheet flow

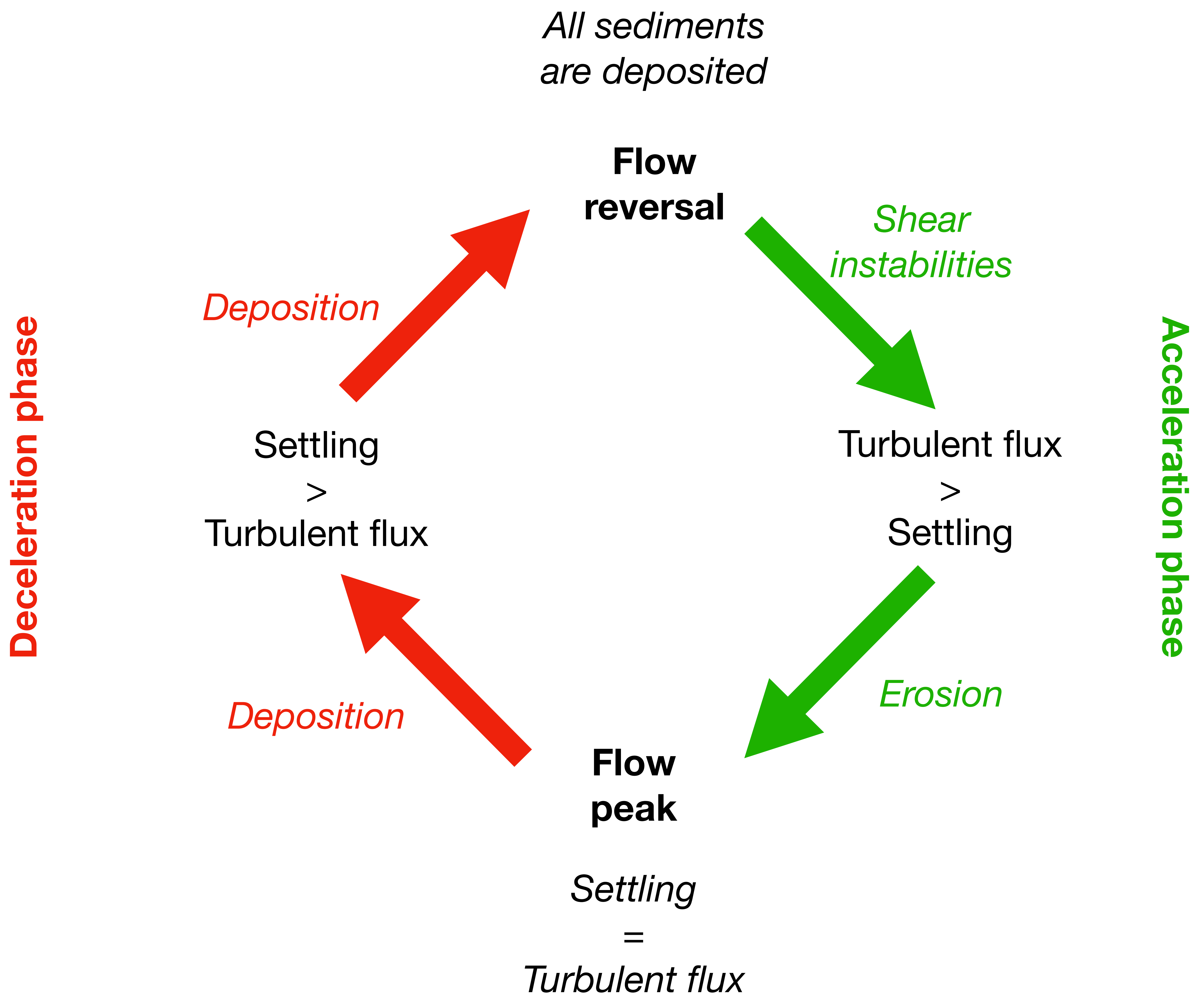

Medium sand

- Acceleration phase:
  - Flow instabilities generates strong turbulence & erosion
- Flow peak:
  - Equilibrium between settling and erosion
- Deceleration phase:
  - Gravitational settling dominates
- Flow reversal:
  - Sediments have settled back to the bed

A. Mathieu PhD (2021)

Two-phase flow LES of oscillatory sheet flow

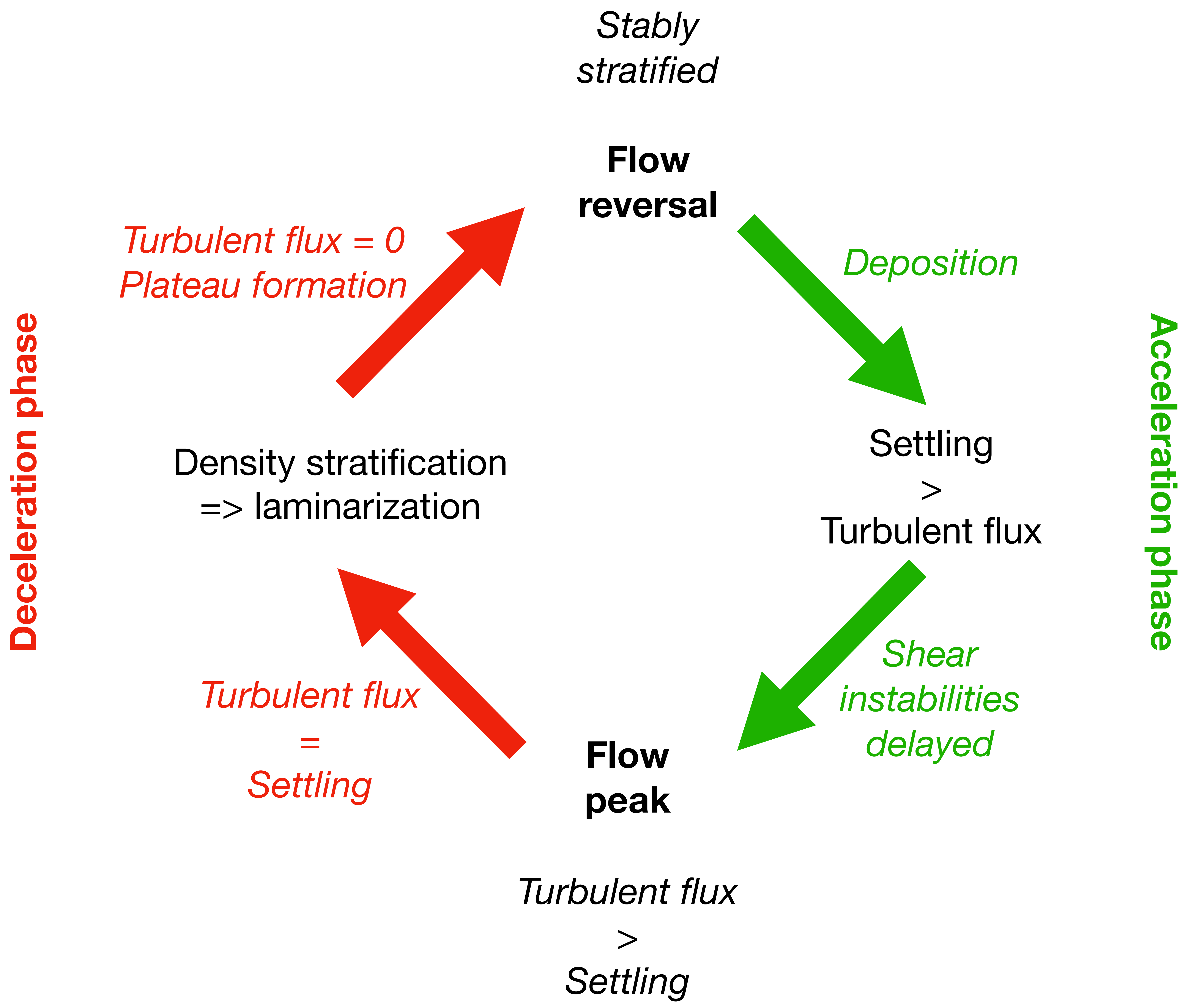

Fine sand

- Acceleration phase:
  - Stably stratified flow: still deposition
  - Shear instabilities delayed
- Flow peak:
  - Still net erosion
- Deceleration phase:
  - Delayed settling phase
  - Density stratification => laminarization
  - Formation of concentration plateau
- Flow reversal:
  - Stably stratified flow
  - Reminiscent suspended sediments from previous half-wave cycle

A. Mathieu PhD (2021)

Conclusion on upscaling of fine-scale processes

- **Two-phase flow simulations allows to study complex sediment-flow interactions such as sediment transport under waves with a process-based approach**

- **Physical explanation for the phase-lag or unsteady effect associated with fine sand**
  - Stratification => turbulence damping
  - Reduced turbulent fluxes/erosion
  - Non-linear sedimentation

- **Perspectives**
  - Characterize regime transitions
    - ➡ Controlling dimensionless numbers?
  - Infer sediment transport parametrization
    - ➡ Upscaling

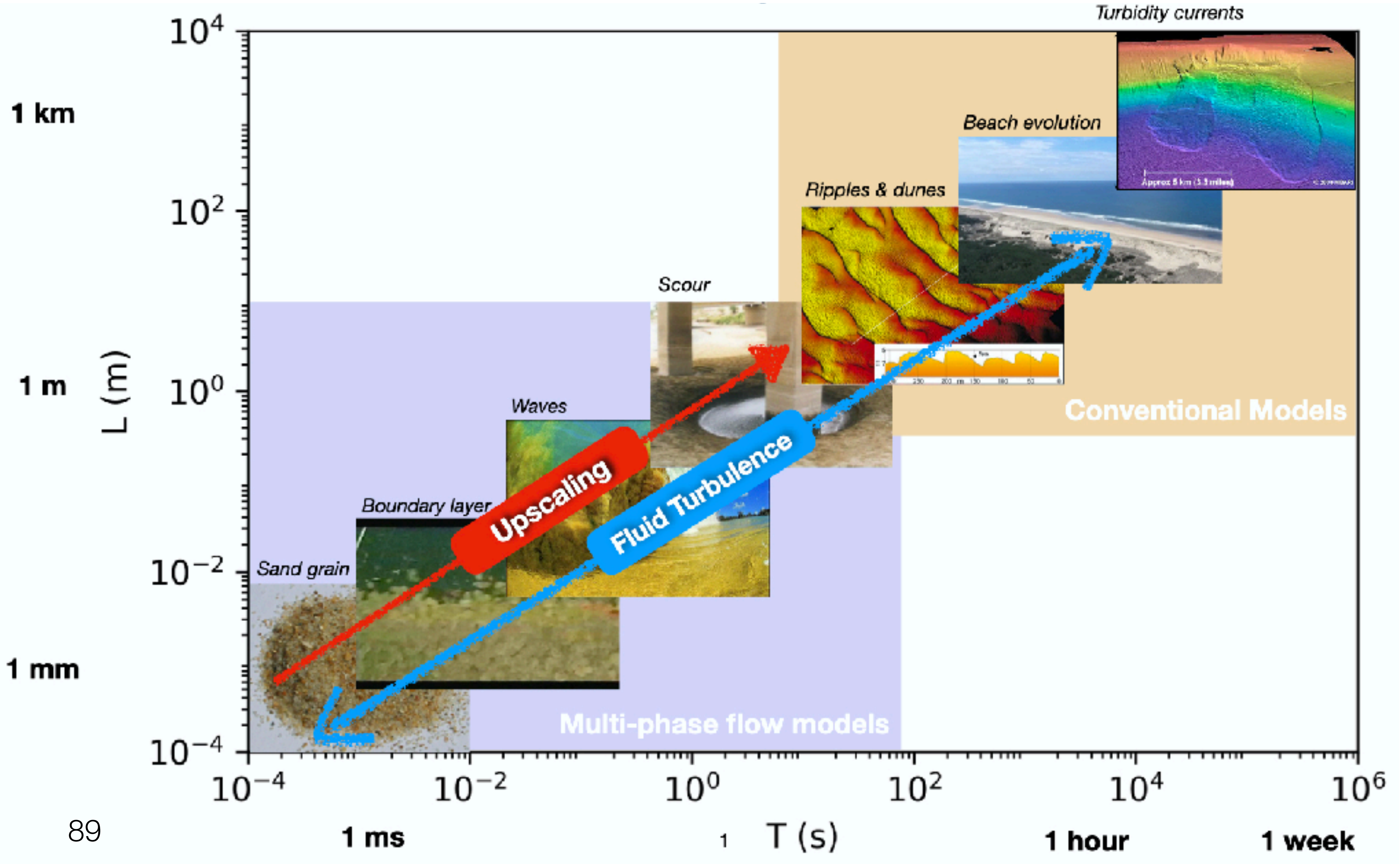

General conclusion & perspectives

Open question 1:

What are the stability conditions for the coupled system of equations wave-current-sediment ?

Open question 2:

How to develop a well-posed granular rheology ? $\mu(I)$ or kinetic theory ?

Open question 3:

Is it possible to derive a well-posed two-fluid model ?

Job opportunity

18 months postdoc is available to work on a coastal morphodynamic at LEGI (MEPELS project - SHOM)

- develop a mid term (1 to 24 months) hierarchical model
- combine process-based models with reduced complexity approach potentially using AI…